

**STRUCTURAL MODELLING OF ADHESIVE JOINTS IN
AUTOMOTIVE BODIES**

By

SILVANA M STEIDLER

A thesis submitted in partial fulfilment of the requirements of Oxford Brookes University
for the Degree of Doctor of Philosophy

June 2000



IMAGING SERVICES NORTH

Boston Spa, Wetherby
West Yorkshire, LS23 7BQ
www.bl.uk

The following have been redacted at the request of the university:

Fig 2.5 – page 20

Fig 2.6 – page 21

Fig 2.7 – page 23

Fig 4.5 – page 55

Fig 4.10 –page 77

Figs 4.11 & 4.12 – page 78

Fig 4.14 – page 80

Fig 4.15 – page 81

Fig 4.16 – page 82

Appendix II

Please contact the awarding university for further information.

ABSTRACT

The behaviour of a vehicle is dependent on the stiffness of the joints between the sheet components in the body shell. Although spot-welding is the predominant joining method for the construction of steel bodies in the automotive industry, other alternatives are now being considered. Adhesive bonding offers the best potential because the uniform load distribution in the joint reduces the stress concentrations produced when using spot-welding. It is generally observed that adhesive bonded structures are stiffer than assemblies fabricated with mechanical fasteners or spot-welds. The use of adhesives, either as an alternative or a supplement to spot-welding, is of interest because of the potential improvements in joint stiffness and in the overall behaviour of the structure.

The effective stiffness of an adhesively bonded joint may be difficult to quantify, as it is dependent on many design variables of the actual joint. Finite element models have been developed to study the effects of various design parameters, such as different joining techniques, on car body characteristics. However, finite element models of large vehicle structures involve large numbers of elements which as a result can impose excessive demands in computer capacity. Because of this, approximations are commonly made in the model to reduce the number of elements consequently resulting in inaccuracies. The main inaccuracy develops from the lack of geometric details within local joints which may lead to some uncertainty in local joint stiffness. As a consequence, this may introduce errors in the prediction of global vehicle stiffness.

In this project, the errors which result from the inaccuracies in macro modelling methods have been addressed through a parallel study of detailed micro models. Various adhesive joint configurations have been analysed using finite element methods to predict joint stiffness; comparative results were obtained through experimental testing of similar joints. A primary objective was to obtain characteristics of smaller joint structures and compare these to results from macro models of similar joints which could then be translated into larger-scale structure models for improved accuracy.

A methodology has been developed to translate micro model joint characteristics into large-scale structures through an undercut element technique. When applied to macro models which lack geometric details of joints, the undercut element method enables more accurate predictions of behaviour, particularly stiffness performance, to be made. The method has been shown to be applicable to a number of typical joints and also for different loading conditions. Validation of the method has been demonstrated by its application to progressively larger substructures, from which experimental test data was available for comparison. Because of the ease of use of the undercut method it may be conveniently applied to automotive bodies. The method provides a more accurate finite element model resulting in less computational time for analysis than other existing solutions.

ACKNOWLEDGEMENTS

I would like to express my gratitude to everyone who has helped me in the completion of this thesis. Particular thanks goes to my director of studies, Professor Alec Beever for his support and guidance throughout these past years and particularly, through his first years of retirement. I would also like to thank Dr. John Durodola for his advice and supervision and my colleagues at the Joining Technology Research Centre (JTRC).

I would like to thank the Engineering and Physics Research Council (EPSRC) for providing me with a research grant, and to all the industrial partners of the LIVEMAN project involved with Project 3. In particular I would like to acknowledge the assistance to the following working group partners for their significant technical contributions and for supplying materials: British Steel AEG, Ford Research, Hawtal Whiting and Jaguar Cars.

Specific aspects of the work contributed by colleagues and industrial partners are as follows,

- Fabrication of box beams and plenum chambers - JTRC , Ford and TWI
- Experimental testing of box beams and plenum chambers - JTRC
- Numerical modelling of plenum chamber and body-in-white - Hawtal Whiting

Most importantly, I would like to thank my parents for their support and love through both my engineering degrees; you have always pushed me for the best and I think WE have finally got there. Thank you to all my other family members for their patience. Dimitri, efkaristo gia ola – panta tha eimai konta sou opws esy stin kardia mou...

I would like to dedicate this thesis to my grandfather and grandmother, George and Rinoula Andreadis. You will always be in my heart.

LIST OF FIGURES

1.1	Programme of research activity	4
2.1	The ULSAB vehicle body parts [Anon (1997)]	16
2.2	The ULSAB vehicle body frame [Anon (1997)]	16
2.3	The ULSAB vehicle concept [Anon (1997)]	17
2.4	Audi A8 aluminium space-frame [Anon (2000e)]	19
2.5	The hydroforming process [Fenton (1998)]	20
2.6	Side panel of a vehicle with tailored blanks [Fenton (1998)]	21
2.7	Space-frame design consisting of extruded sections and cast nodes [Ostermann et al. (1993)]	23
2.8	Schematic representation of the clinching technique	24
2.9	Schematic representation of the self-pierce riveting technique	25
2.10	Schematic representation of the principles of resistance spot-welding process	28
2.11	Resistance spot-welding of a full vehicle body of a vehicle [Anon (1994d)] ..	29
2.12	Schematic representation of the weld-bonding process	33
3.1	Typical loads found in adhesive bonded joints	44
4.1	Deformation of single lap joint with the assumption that the adherends are rigid	50
4.2	Deformation of single lap joint with the assumption that the adherends are elastic	50
4.3	Volkersen's shear lag analysis (1938) showing (a) undeformed lap joint and (b) section through deformed joint with assumed forces	51
4.4	Schematic representation of Goland and Reissner's bending moment factor theory	53
4.5	Schematic representation of the peak/peel transverse stresses due to component loading at the left of the overlap [Bigwood & Crocombe	

	(1989)].....	55
4.6	Schematic representation showing the loading conditions used by Li, Blunt Stout (1997).....	69
4.7	Super-element representation in a lap joint.....	74
4.8	Spring-line element representation.....	74
4.9	Inclusion of the joint-line element method in a coach joint.....	75
4.10	Detailed FE model of a T-peel joint using solid elements [Nardini et al. (1990)].....	77
4.11	Definition of adhesive fillet size [McGregor et al. (1992)].....	78
4.12	Distribution of normal stresses along the mid-line of the bondline [McGregor et al. (1992)].....	78
4.13	Alternative methods for compensating joint details in FE models.....	79
4.14	Four methods of modelling a flange-type joint [Nardini & Hall (1995)].....	80
4.15	Example of the use of the Joint-Line Generator [McGregor et al. (1992)].....	81
4.16	Representation of the modifications studied in the FE analysis [Sharman & Al-Hammoud (1987)].....	82
5.1	Geometry of initial lap joint configuration.....	87
5.2	Testometrics 10 kN testing machine.....	89
5.3	LVDT extensometer of 50 mm gauge length.....	89
5.4	Typical load-displacement curves obtained from the experimental tests.....	89
5.5	FE model of lap joint showing two-way biased mesh elements along the overlap length.....	90
5.6	Boundary conditions of single lap joints in tensile loading.....	91
5.7	Comparison between experimental tests and FE results for single lap joints using (a) TEROSTAT 3218F and (b) CIBA XB5315 adhesives.....	93
5.8	Variation of joint stiffness with sheet thickness and overlap length for single lap joints using (a) TEROSTAT 3218F and (b) CIBA XB5315 adhesives.....	94

5.9	Variation of joint stiffness with sheet thickness and bondline thickness for single lap joints using (a) TEROSTAT 3218F and (b) CIBA XB5315 adhesives.....	95
5.10	Variation of joint stiffness with change in adhesive modulus for single lap joints	96
5.11	Solid element model of single lap joint.....	96
5.12	Shell-solid element model of single lap joint.....	97
5.13	Further results of FE modelling analysis on lap joints using (a) TEROSTAT 3218F and (b) CIBA XB5315 adhesives	100
5.14	Effect of adhesive modulus on joint stiffness of lap joints	102
5.15	Geometry of initial coach (T-peel) joint configuration	106
5.16	Coach (T-peel) joint details and definition of fillet ratio	106
5.17	Experimental set-up of tensile testing of coach joints.....	109
5.18	Schematic of gauge length.....	109
5.19	Representative load-displacement curves from experimental tests – CIBA XB5315 adhesive.....	109
5.20	Experimental set-up of coach joints in bending mode	110
5.21	Graphical representation of experimental tests showing 4-point bending	111
5.22	Solid half model of coach joint with (a) 0% and (b) 100% adhesive fillet ratios	112
5.23	Comparison between experimental tests and FE model results using CIBA XB5315 adhesive and for different sheet thicknesses: (a) 0.8mm, (b) 1.0mm and (c) 1.2mm.....	113
5.24	Variation of joint stiffness with bend radius and adhesive fillet ratio using (a) TEROSTAT 3218F and (b) CIBA XB5315 adhesives	114
5.25	Effect of adhesive modulus on joint stiffness for coach joints with (a) 0% and (b) 100% adhesive fillet ratios.....	115
5.26	Comparison between experimental tests and FE results for four-point bending analysis	116
5.27	Shell-solid models - equivalent (a) 100% (macro model) and (b) 0% fillet	

	ratios	117
5.28	Radiused shell-solid model - equivalent (a) 100% and (b) 0% fillet ratios.....	118
5.29	Stiffness results from extensive FE modelling of coach joints in tension – CIBA XB5315	119
5.30	Stiffness results from coach joints subjected to four-point loading – CIBA XB5315	119
6.1	Representation of solid element model with all geometric details.....	126
6.2	Shell-solid element model representing macro model with fully bonded flanges.....	127
6.3	Application of the undercut element method in shell-solid models.....	127
6.4	Comparison of experimental and FE modelling results with the inclusion of the undercut element method	128
6.5	Characteristic correction curve for determining the undercut distance for various fillet ratios.....	129
6.6	Application of the undercut element method to lap joints using different design techniques.....	131
6.7	Prediction of stiffness using the undercut element method in single lap joints for (a) TEROSTAT 3218F and (b) CIBA XB5315 adhesives.....	132
6.8	Various non-uniform geometric configurations	133
6.9	Application of loads and constraints to non-uniform geometric joints	134
7.1	Typical box beam configurations	138
7.2	Schematic of the idealised box structure	138
7.3	Torsional loading.....	139
7.4	Tensile loading	139
7.5	Flexural loading.....	139
7.6	FE solid element models with (a) 0% and (b) 100% adhesive fillet ratios	141
7.7	Shell-solid element models with (a) the implementation of the undercut element and (b) representing macro models with fully filled adhesive flanges.....	141

7.8	Resultant box structure with the application of torsional loading through nodal displacements.....	142
7.9	Schematic representation showing the arrangement of the box beams in the testing machine.....	144
7.10a	Experimental set-up of the box beams in the torsion testing machine.....	145
7.10b	Typical torque-rotation curve obtained from experimental tests.....	146
7.11	FE model of box structure with a central aperture	147
7.12	Experimental set-up of box beam with a central aperture for torsional loading	148
7.13	Dimensions of box structure in transverse tensile loading.....	150
7.14	Solid element (micro) model with 0% adhesive fillet ratio.....	150
7.15	Shell-solid (macro) element model with 5.5mm adhesive undercut	150
7.16	Experimental set-up of box beams for transverse tensile tests.....	151
7.17	Cross-section of experimental box structure and measurements of angles	152
7.18	FE model of box structure for flexural loading with the inclusion of a centre plug.....	153
7.19	FE results of box structure in flexure with the application of the undercut element	154
8.1	FE model of half the Jaguar X300 plenum chamber.....	158
8.2	Schematic representation of the plenum chamber cross-section showing the flange joints	158
8.3	Full FE model of the Jaguar X300 plenum chamber.....	159
8.4	Original FE macro model with a two-element bondline	159
8.5	Modified FE model with a three-element bondline and a 5.5mm undercut.....	159
8.6	Original FE model of a spot-welded joint.....	160
8.7	Original FE model of a weld-bonded joint.....	160
8.8	Modified FE model of a weld-bonded joint with a 5.5mm undercut.....	160

8.9	Jaguar X300 plenum chamber used in experimental tests.....	162
8.10	Experimental set-up of plenum chamber showing the position of the LVDT transducers	162
8.11	FE model of half the Jaguar X300 body-in-white	165
9.1	Basic configuration of the idealised box structure	171
9.2	Solid element model of a box structure with 0.2mm bondline thickness.....	172
9.3	Shell model derived from centre-lines of solid structure taking into account the bondline	172
9.4	FE solid element model with a 0% adhesive fillet ratio	172
9.5	Approximation of the plug in solid models to accommodate a 100% adhesive fillet	172
9.6	Applied displacements at inner 4 nodes	174
9.7	Applied displacements at outer 4 nodes	174
9.8	Application of rotation displacements on all nodes around a circular path.....	174
9.9	Variation of tensile stiffness with adhesive modulus for typical joint configurations	176

LIST OF TABLES

4.1	Summary of finite element analysis work on single lap joints.....	67
5.1	Basic material properties of the single lap joint configuration	87
5.2	Variables of parametric study on single lap joints.....	92
5.3	Variables of parametric study on coach joints – tensile and flexural loads.....	112
6.1	Stiffness results from FE analysis on non-uniform geometries with the application of the undercut	134
7.1	Comparison of numerical modelling methods with other published work on box structures in torsional loading	143
7.2	Comparison of torsional stiffness values from experimental tests and FE modelling methods	146
7.3	Torsional stiffness results of box structure for various size apertures	148
7.4	Comparison of torsional stiffness results from experimental and FE modelling methods for box beams with a large central aperture (26%).....	149
7.5	Comparison between FE and experimental test results for box structures in tension.....	152
7.6	FE results from analysis on out-of-square box beams in tensile loading	153
7.7	Comparison between FE and experimental results with the undercut element method - flexural loading.....	155
8.1	Torsional stiffness results from the FE analysis of the Jaguar X300 plenum chamber	161
8.2	Comparison of torsional stiffness results from FE and experimental tests of the plenum chamber	164
8.3	Torsional stiffness results from the FE analysis of the Jaguar X300 body-in-white	165

LIST OF NOTATIONS

E	-	elastic modulus
G	-	shear modulus
ν	-	Poisson's ratio
F	-	applied force
P	-	load
P_x	-	tensile load
P_y	-	loading in y-direction
V	-	shear force per unit width
T	-	tensile force per unit width
M	-	bending moment per unit width
α_1, α_2	-	shear compliance factors of adhesive and adherend 1 and 2
β_1, β_2	-	peel compliance factors of adhesive and adherends 1 and 2
I	-	second moment of inertia
τ	-	average shear stress
$\bar{\tau}$	-	adhesive shear stress distribution
$\bar{\tau}_{\max}$	-	maximum adhesive shear stress
k_{GR}	-	Goland and Reissner's bending moment factor solution
k_{HS}	-	Hart-Smith's bending moment factor solution
k_Z	-	Zhao, Adams and Pavier bending moment factor solution
S.F.	-	stress concentration factor
T	-	applied torque
L	-	length of beam
A	-	cross sectional area
k	-	stiffness
t_1, t_2	-	adherend 1 and 2 thickness
t_3	-	adhesive thickness
t_s	-	sheet thickness
t_b	-	bondline thickness
t_m	-	modified bondline thickness
t_a	-	actual adhesive thickness

E_a	-	actual adhesive modulus
E_m	-	modified adhesive modulus
δ	-	undercut distance
R_o	-	external bend radius
FR	-	adhesive fillet ratio
f	-	adhesive fill
x_o	-	distance along overlap length
x	-	distance from beginning of forming radius
b	-	joint width
d	-	distance between outer supports
l	-	overlap length

TABLE OF CONTENTS

1. INTRODUCTION

1.1	Design for Light-Weight Vehicles.....	1
1.2	Finite Element Modelling of Vehicle Structures.....	2
1.3	Outline of Work.....	3

2. DEVELOPMENTS IN MANUFACTURING METHODS IN THE AUTOMOTIVE INDUSTRY

2.1	Introduction	5
2.2	Materials	5
	2.2.1 Composites and Plastics	6
	2.2.2 Aluminium.....	9
	2.2.3 Steel	13
2.3	Construction Techniques	17
	2.3.1 Monocoque	17
	2.3.2 Space-frame	18
	2.3.3 Hydroform Intensive Body Structure (HIBS) Hydroforming ...	20
	2.3.4 Tailored Blanks.....	21
	2.3.5 Extrusions	22
2.4	Joining Techniques in the Automotive Industry.....	23
	2.4.1 Mechanical Fastening	24
	2.4.2 Welding Techniques	25
	2.4.3 Adhesive Bonding	31
	2.4.4 Hybrid Joining	32
2.5	Summary.....	34

3. ADHESIVE TECHNOLOGY

3.1	Introduction	38
3.2	Principles and Mechanisms of Adhesion.....	38
3.3	Generic Types of Adhesives.....	41
	3.3.1 Acrylics.....	41

3.3.2	Epoxies	42
3.3.3	Phenolics.....	43
3.3.4	Plastisols	43
3.3.5	Polyurethanes.....	43
3.3.6	Polybutidienes.....	44
3.4	Adhesive Joint Stress States	44
3.4.1	Joint Strength.....	45
3.5	Bonding in Vehicle Structures.....	46
3.5.1	Prediction of Behaviour of Vehicle Structures	46
3.5.2	Automotive Requirements for Stiffness	47
3.6	Joint Durability.....	47
3.7	Summary.....	48

4. REVIEW OF ANALYSIS OF BONDED JOINTS

4.1	Introduction	49
4.2	Analytical Approach.....	49
4.2.1	Linear-Elastic Approach	49
4.2.2	Non-Linear Approach	58
4.3	Experimental Visualisation Methods	59
4.4	Numerical Methods – Modelling of Adhesive Bonded Structures.....	60
4.4.1	Finite Element Analysis of Single Lap Joints.....	62
4.4.2	Finite Element Analysis of Coach Joints.....	68
4.4.3	Prediction of Stiffness.....	70
4.5	Extended Applications of Numerical Modelling	72
4.5.1	Problems Associated with Micro to Macro Modelling.....	73
4.5.2	ALCAN Approaches to FE Modelling Methods of Car Body Structures.....	75
4.5.3	Other FE Modelling Approaches.....	82
4.6	Summary.....	84

5. ANALYSIS OF ADHESIVE JOINT BEHAVIOUR

5.1	Introduction	86
5.2	Single Lap Joints	86
5.2.1	Joint Definition.....	87
5.2.2	Experimental Testing.....	88

5.2.3	Numerical Modelling.....	90
5.2.4	Initial Results	92
5.2.5	Further Refinements of Modelling Methods	96
5.2.6	Further Results of Modelling Methods.....	99
5.2.7	Discussion	101
5.3	Coach Joints.....	105
5.3.1	Joint Definition	105
5.3.2	Experimental Testing.....	107
5.3.3	Numerical Modelling.....	111
5.3.4	Initial Results	112
5.3.5	Further Refinements of Modelling Methods	116
5.3.6	Further Results of Modelling Methods.....	118
5.3.7	Discussion	120
5.4	Summary.....	123

6. DEVELOPMENTS OF MICRO TO MACRO MODELLING AND THE UNDERCUT ELEMENT CONCEPT

6.1	Introduction	125
6.2	The Undercut Element Concept	126
6.3	Validation of the Undercut Element Method for Other Adhesive Joints	130
6.3.1	Single Lap Joints.....	130
6.3.2	Non-Uniform Geometries	133
6.4	Summary.....	135

7. APPLICATION OF THE UNDERCUT ELEMENT METHOD TO IDEALISED BEAM STRUCTURES

7.1	Introduction	137
7.2	Idealised Box Beam Structures.....	137
7.3	Finite Element Modelling of Beams.....	140
7.4	Torsional Loading of Box Structures	142
7.4.1	Validation with Experimental Work.....	143
7.4.2	Effects of Apertures in Beam Walls	147
7.5	Transverse Tensile Loading of Box Structures	149
7.5.2	Validation with Experimental Tests	151
7.6	Flexural Loading of Box Structures	153

7.6.1	Validation with Experimental Work.....	155
7.7	Summary.....	156
8.	APPLICATION OF THE UNDERCUT ELEMENT METHOD TO VEHICLE STRUCTURES	
8.1	Introduction	157
8.2	Application of the Undercut Element Method to a X300 Plenum Chamber....	157
8.2.1	Validation with Experimental Work.....	161
8.3	Application of the Undercut Element Method to a X300 Body-in-White.....	164
8.4	Summary.....	166
9.	DISCUSSION	
9.1	Introduction	167
9.2	Requirements for Stiffness	168
9.3	Numerical Modelling of Adhesive Joints.....	168
9.4	Problems Encountered with FE Modelling Methods	170
9.4.1	Mesh Convergence	170
9.4.2	Geometric Representations.....	170
9.4.3	Application of Boundary and Loading Conditions.....	173
9.4.4	Other Sources of Inaccuracies	175
9.4.5	Introduction of Apertures into FE Models.....	177
9.5	The Undercut Element Method	178
10.	CONCLUSIONS	
10.1	Finite Element Analysis.....	179
10.2	The Undercut Element Method	180
10.3	Experimental Tests	180
10.4	Further Findings	180
10.5	Recommendations for Future Work	181
	REFERENCES	183

APPENDIX I 196

APPENDIX II 202

1. INTRODUCTION

1.1 Design for Light-Weight Vehicles

In the past decade, the automotive industry has aimed to produce lighter yet safer vehicles through various technological innovations. This is also being accomplished through novel design concepts and with the use of new and light-weight materials with advanced joining techniques.

Spot-welding has been the main joining method in the automotive industry and is still used extensively in areas, such as the main body shell and in components of a vehicle, where it provides structural integrity. This is primarily due to the ability of the process to make high strength reliable joints very rapidly and at relatively low costs. Because of the introduction of new materials for light-weight construction, the spot-welding technique has shown some disadvantages due to its limitations in joining materials such as aluminium, composites and dissimilar material combinations. As a result, the automotive industry has turned towards new and advanced joining methods, which might be appropriate and applicable to many of the new and existing materials for light-weight vehicles.

Adhesive bonding is one of the most acceptable solutions to joining for light-weight construction. One of the main advantages of this method is the capability of joining dissimilar and/or light-weight materials. Also, bonded joints are known generally to result in stiffer structures because of the uniform distribution of the loads transferred across the wider bondline area; in spot-welded structures, all loads and stresses are concentrated at the spot-weld area. The use of adhesives is not only limited to structural joints; different types of adhesives can serve different purposes such as for reinforcements, dampers to reduce noise/vibrations and as sealants for oils/water.

Despite recent developments in 'new' and 'advanced' materials, steel continues to be the primary material in car body structures and adhesive bonding is being investigated as an

improved joining method for body shells. The mechanical properties of steel are known to exceed those of most metals in strength and stiffness, and because both of these qualities are essential and required factors for a safe and comfortable vehicle, steel still continues to offer considerable potential as a cost effective material in car bodies.

Combining steel with adhesive bonding has resulted in significantly stronger and stiffer components and structures. By using adhesive bonding or complementing spot-welding with adhesive, the gauge thickness of steel can be reduced by approximately 20% [Lowe (1994)]. Therefore not only a stiffer body can be achieved, but also a light-weight vehicle can be produced. Various projects have been funded by the automotive industry to pursue the use of steel in body structures, and still produce a lighter vehicle through novel and advanced joining technologies.

1.2 Finite Element Modelling of Vehicle Structures

Finite element (FE) methods and other computer simulation/design packages have been extensively used in the automotive industry to try to predict the performance of vehicle bodies. In particular, finite element modelling of spot-welded vehicle structures has been widely used and well accepted [McGregor et al. (1993), Gilchrist & Smith (1993), Wang & Ewing (1991), Gumpinger et al. (1997)]. Results from numerical analyses seem to be very comparable with experimental testing of similar structures.

In contrast however, the analysis of the behaviour of adhesive bonded vehicle structures is less advanced; most of the literature reviewed has been restricted to smaller and more typical joints such as lap shear and peel joints. In order to understand the behaviour and performance of larger adhesive bonded structures found in vehicle bodies, it is necessary to extend the FE modelling capabilities to include adhesive joint characteristics in full body models.

The main problem with FE models of vehicle structures is the fact that essential approximations lead to a lack of geometric details and hence, the local joint stiffnesses are not accurately represented. As a result, current methods may not give an accurate prediction of the global vehicle stiffness. While these approximations have been acceptable when modelling spot-welds in vehicle structures, adhesive bonding introduces

additional details such as adhesive fillet, modulus, thickness and flange bend radius all of which affect the accuracy of the prediction of joint stiffness. It is therefore desirable to include these joint features in some way in the finite element models.

While it is possible to establish numerical models for parametric analyses of these adhesive joint variables from small-scale joints, there remains the problem of translating these joint characteristics into full body models. Direct inclusion of such joint details would demand excessive computer resource and programming/design time. It is therefore necessary to develop an alternative approach to translate micro joint characteristics into larger-scale models of vehicle bodies.

1.3 Outline of Work

The two main objectives of this study were to develop accurate predictions of joint behaviour using high resolution micro models and to determine a method of translating these micro model results into larger-scale models. These objectives were achieved primarily through the development and application of different finite element modelling approaches and validation by experimental testing of similar structures. Figure 1.1 shows a schematic outline of the work carried out in the study.

In order to derive a method of micro to macro translation, initial work was carried out to understand the behaviour of typical adhesive joints, such as single lap joints and T-peel or coach joints, through FE modelling and experimental methods (Chapter 5). Some of the experimental work used for the validation of the FE modelling methods was carried out by colleagues in the Joining Technology Research Centre, as part of the wider LIVEMAN project (EPSRC Grant Ref. GR/L03811). Various finite element methods were studied to compare the results obtained from a larger-scale model with those of a smaller and more detailed joint. In Chapter 6, the undercut element method is presented as a tool for translating micro to macro stiffness details to improve the accuracy of FE models. The method was applied to typical lap and coach joint configurations, to non-ideal geometries and to larger and more representative of vehicle substructures such as the idealised box beam (Chapter 7). The application of the undercut method to typical vehicle structures, such as the plenum chamber and the body frame, are discussed in Chapter 8, and a general discussion of the project is presented in Chapter 9.

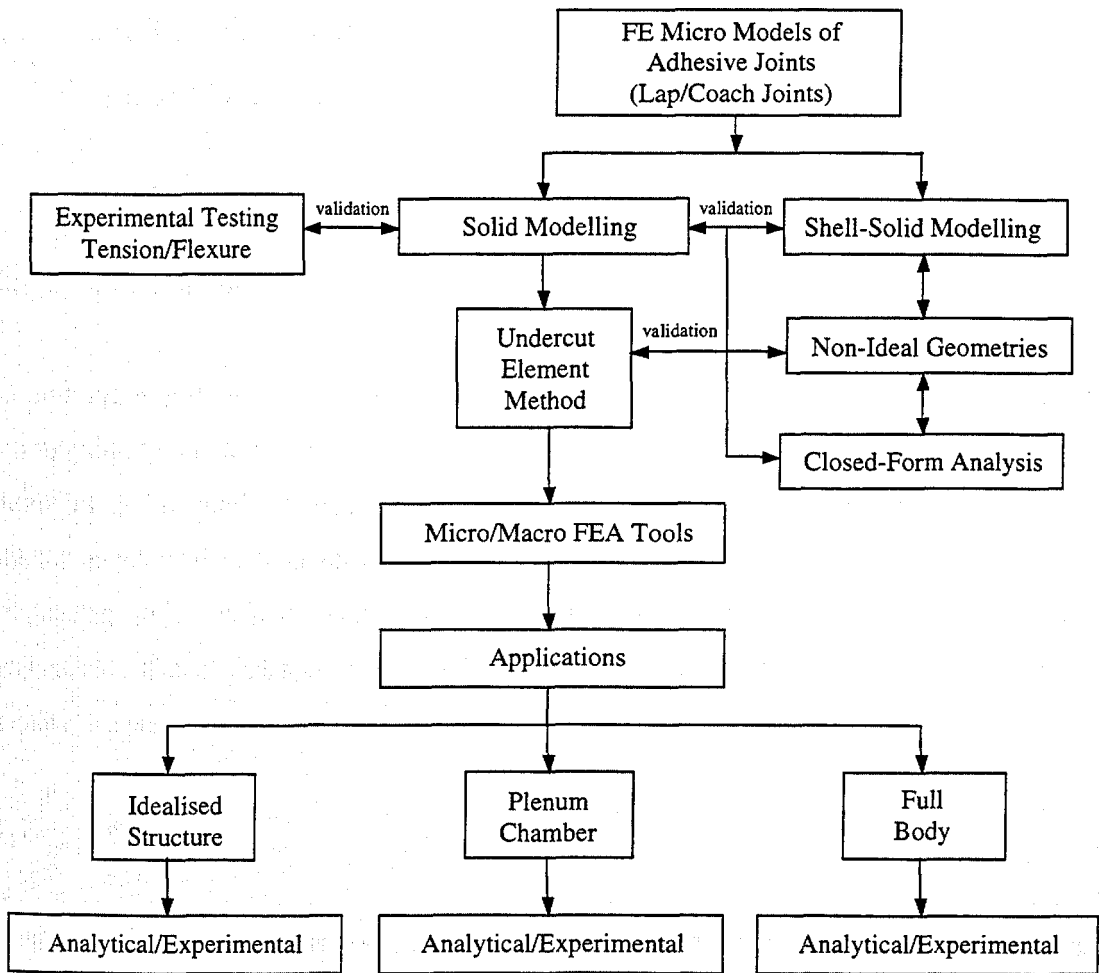


Figure 1.1 Programme of research activity

2. DEVELOPMENTS IN MANUFACTURING METHODS IN THE AUTOMOTIVE INDUSTRY

2.1 Introduction

In the past decade there has been a large demand for the production of safer, more economical and more environmentally considerate vehicles. A solution to produce such vehicles is through weight reduction. The automotive industry has developed and investigated challenging ideas for the production of lighter vehicles which have proven to be successful. Reduction in the overall weight of existing vehicles can result in a reduction of fuel consumption, leading to greater economy in running costs and lower exhaust emissions.

2.2 Materials

Over the years, materials used in vehicle body construction have developed in parallel with technology. The history of automotive materials ranges from steel, being the oldest yet most recognised material, to composites and aluminium alloy materials which represent the newer and lighter materials. At present, a primary objective of the automotive industry is to produce vehicles with significant weight reduction through thinner gauge sheets and cross-sections, stronger materials and by using materials with lower specific weight, such as plastics and aluminium alloys. As a result, vehicle performance and handleability will be improved as will the reduction in fuel consumption and consequently, improvements in environmental impact.

One of the most important aspects in the design of a light-weight vehicle is the requirement of a stiff chassis or body structure, in order to maintain good handling, comfort and lessen noise and vibrations. Steel, for example, has been widely used in vehicle structures because of its high strength, low costs and good workability. In fact, statistics show that the average amount of steel used in a vehicle today accounts for up to 60% (400 kg) of the total vehicle weight; this percentage has been similar for the past 14

years as steel dominates the high volume production of cars. However, with the demand for light-weight vehicles, new materials are being introduced. Statistics in 1994 [Lowe (1994)], showed that an average European car contained 70 kg of aluminium and 120 kg of plastics almost doubling the figures measured in 1980. It has been predicted that the use of light-weight materials in future vehicles will grow significantly. In this section various materials are considered in the context of their potential contributions for the production of light-weight vehicles.

2.2.1 Composites and Plastics

There has been an increase in the use of plastics and composites in the automotive industry in the last decade. In the 1980s, these materials were used primarily in limited applications such as the body panels of vehicles; in the 1990s, the use of composites and plastics extended to other areas and components in vehicle structures. In 1988, statistics predicted that there would be an expected increase in the use of plastics and composite materials from 5% to 70% by the year 2000 [Simon (1988)]. Although this predicted figure has actually not been obtained, the application of composites and plastics in vehicle structures is expanding. One of the main limitations in the use of composites in larger areas of vehicle structures has been the materials cost. A composite body would be 24% lighter than a comparable steel body even though the total cost would be more than twice as high [Anon (1996d)]. Even today, with the possible exception of high performance sports cars, the majority of polymer/composite applications in automotive products are essentially non-structural.

Composites are attractive primarily due to their extreme light-weight and strength; they can provide the same stiffness of steel yet at a lower weight. As a result, the light structure of composite materials ensures a reduction in fuel consumption to provide an efficient vehicle. However, one of the main drawbacks with the use of composite materials in vehicle structures is the fact that they are not suitable for mass production and for recycling.

An understanding of the physical properties of composites is important for the effective design and exploitation of characteristics of composite structures. For example, a 45° bi-directional lay up of fibres can give a shear modulus which is ten times greater than one

made from uni-directional fibres [Anon (1985)]. When used in sandwich panels and honeycomb structures, various fibre/cell sizes can be used to give different strengths and densities. In fact, such composites are particularly good when dealing with flexural rigidity and buckling stresses of structures. These composites are designed to withstand a number of failure modes and fatigue performances [Anon (1985)].

High performance fibre reinforced plastic composites appear to be potential materials for the construction of light-weight vehicles. Although the materials are expensive and manufacturing processes not complete, composites show very high performance and are indeed, light-weight. High-speed resin transfer moulding processes allow the capability to construct large-scale structures, even the size of a front end of a vehicle [Beardmore (1988)].

Sheet moulding compounds (SMC) are among the most common types of plastics used primarily in the exterior production of vehicles, e.g. roof, panels, bonnet. The main advantages of these materials are associated with their light-weight, good stiffness and improved resistance to damage. SMC has been widely used in the plastic outer skin panels of various cars such as the Corvette and Renault Espace vehicles, and in the isolated panels in the Aerostar, Bronco II and heavy truck vehicles [Beardmore (1988)].

Although the use of plastics is advantageous for the production of lighter vehicles, one of the main disadvantages are the costs, surface quality, paintability and most importantly the recyclability of SMC [Anon (1990a)]. Consequently, these drawbacks have limited the use of plastics and composite materials to smaller structures in the exterior parts of the vehicle, such as in the body panels. Today, many concept cars have been designed with composites in the main body frame however, the costs of production are very high.

Applications

In the early 1990s, Ford created a concept car based on the existing Taurus model [Anon (1990b)]. The vehicle was made of only five composite sections through the resin transfer moulding (RTM) process and replaced more than 400 steel parts; thus reducing the overall number of joining techniques required, e.g. bolting, welding, bonding. The use of composites gave the overall vehicle a weight saving of approximately 30% and a reduction in manufacturing and assembly costs.

In 1977, Ford formed a project with the intention to create a concept car in which most areas in the body frame and chassis would be replaced by carbon fibre reinforced plastics (CFRP) [Sigman et al. (1983)]. The main objective of the project was to use CFRP in the body frame of the car. This was achieved by using basic sections and geometries, similar to those previously used, while reducing the overall number of parts; thus, minimising the overall weight of the vehicle. Results showed that a 27% weight reduction could be achieved through the use of CFRP in the main body frame compared with its steel counterpart. However, strength and durability tests which were carried out on the vehicle proved to be unsatisfactory. Nevertheless, the stiffness and vibration behaviour of the vehicle were very promising, and results showed that CFRP is ideal, if properly designed, to meet most structural rigidity requirements.

In 1986, Citroen launched its ECO 2000 concept vehicle with the aim to achieve a more environmentally acceptable vehicle through lower fuel consumption [Anon (1985)]. The weight of the body, including closure panels, was 20% less than the average production hatchback. This was accomplished by using mainly composite and plastic parts, while steel was used only in those areas where it was essentially needed.

The main objective of the project involving the Viking VIII concept car was to create a light-weight monocoque chassis by using composite materials based on fibreglass, Kevlar and carbon fibres [Seal et al. (1981)]. The overall aim was to design a chassis which would have a high degree of torsional rigidity, essential to obtain better handleability and ride comfort. The completed vehicle was a safe, light-weight and high performance low cost sports car.

The Treser-1 sports car was constructed with an extruded aluminium space-frame weighing only 64 kg and fibreglass-reinforced honeycomb plastic panels [Pennington (1998)]. The light-weight and easy formability of aluminium, combined with the moulded carbon fibre reinforced plastic for the panels, resulted in an integrated structure with a high specific stiffness. The sandwich panels were bonded to the aluminium frame while 75% of the frame was joined through rivet-bonding and the remaining 25% through welding.

More recent projects on the use of composites in vehicle bodies were set up by the United States Council for Automotive Research (USCAR), based on the PNGV (Partnership for a

New Generation of Vehicles) requirements to reduce fuel consumption through weight savings [Anon (2000a)]. Initial research showed that composites and plastics could be used in vehicle bodies to obtain a 50-70% weight reduction compared to a steel body, however at a cost penalty. The continuing phase of the project is aimed towards improving the manufacturing, design, materials and joining technologies of composites to obtain a more cost effective solution.

2.2.2 Aluminium

The potential for the use of aluminium in the automotive industry appears to be high due to the low density and good mechanical properties of the material. It has been recognised that the greatest weight saving of the body shell can be obtained when a light material, such as aluminium, is used for the frame or structure [Powell (1994)]. Further reductions in weight can be achieved by expanding the use of these light-weight materials to other areas of the vehicle, such as the skin panels or closures. Although the density of aluminium is approximately 1/3 that of mild steel, it can give weight reductions up to about 45% while still maintaining an equivalent car performance [Lowe (1994)]. It should be noted however, that there is considerable opportunity for weight reduction also in steel bodies and this will be discussed in section 2.2.3.

The use of aluminium in the automotive industry is not too unfamiliar as it has been used in cast, extruded and forged forms in the production of car components. Engine component parts, such as cylinder heads and blocks, pistons, oil pumps and clutch housings, are typical applications for aluminium, primarily because of the light-weight and corrosion resistance of the metal [Anon (1995b)]. However, the use of aluminium in primary structures of cars is still a fairly new concept. There are some initial problems associated with substituting aluminium for steel in areas such as the chassis or body frame, as aluminium requires different design, production, processing and manufacturing technologies compared with those currently used [Anon (1995b)]. Although the main advantage in using aluminium is its light-weight properties, it also has benefits such as fewer component parts through space-frame construction [Lowe (1994)]; this technology will be discussed in section 2.3.2.

Also, although the cost of aluminium is relatively expensive, the recyclability of the metal proves to be advantageous when considering environmental issues. The potential of

creating a new car from recyclable parts of an old vehicle, is both environmentally beneficial and could be cost saving. There are however, some issues which must be taken into account when considering the recyclability of scrap material. Because various types of aluminium alloys are used in many vehicle constructions, it would be necessary to identify, separate and sort each form of alloy, before recycling the scrap. Several techniques have been developed to overcome these initial problems associated with the recycling of aluminium.

In addition to the recyclability and lightness of aluminium, there are other advantages when used in vehicle bodies. In particular, the fuel consumption of the vehicle is 70% dependent on the body weight of the car. Hence, reductions in the overall weight of a vehicle would also give improvements in fuel economy and exhaust emissions [Wheeler (1997), Grant (1994)]. Statistics show that for every 1% weight saving there can be a resultant 0.6% fuel saving [Anon (1995b)]. The reduction in fuel consumption also reduces the amount of CO₂ released into the atmosphere.

The main disadvantage in using aluminium is the cost; aluminium costs five times as much as mild steel in weight [Lowe (1994)]. In addition, the resistance to noise and vibrations in aluminium structures is only one third that of an identical steel body. Solutions to vibration and noise problems have been found through insulation and alternative designs; the consequence however, is in additional costs for materials and additional weight to the vehicle. Also, in order to achieve an equivalent stiffness to that of a steel body, thicker gauge material must be used. In terms of joining of the material, aluminium is metallurgically less tolerant and thus more difficult to weld than steel. Hence, alternative methods of joining aluminium such as clinching, riveting and bonding must be adopted.

Applications

In the late 1970s, BL Technology began a project to develop three experimental vehicles which would be light-weight and energy efficient through the use of stamped aluminium sheets, adhesive bonding and spot-welding to form an integral structure [Selwood et al. (1987)]. This programme culminated in the development of the Energy Conservation Vehicle 3 (ECV3) which was made out of an aluminium structure and mostly plastic skin panels [Powell (1994)]. Through light-weight materials and advanced technologies, the

concept vehicle was 35% lighter than similar sized vehicles and consequently the fuel consumption was also significantly reduced. Although the vehicle never went into production, the programme showed that large weight savings in the vehicle body was easily obtainable through light-weight materials, and that further reductions in weight could be obtained through the use of aluminium in closures and skin panels.

The Aluminium Intensive Vehicle (AIV) project was initiated by Alcan International and Gaydon Technology (formerly BL Technology), with the intention to create low, medium and high mass production vehicles through aluminium construction [Wheeler et al. (1987)]. Several cars were released under the AIV programme, including the mid-sized saloon Dyna-Panhard of the mid 1950s. The Dyna-Panhard vehicle was made from stamped and spot-welded, medium strength aluminium-magnesium sheet alloy and weighed approximately 714 kg. Another project under the AIV programme, was the series production of the Porsche 928S. The steel unibody structure of the 928S vehicle was replaced with aluminium stampings and was joined with spot-welding and weld-bonding methods. The resultant vehicle showed an average weight reduction in the body frame of 47%.

In the 1980s, Alcan developed its own technique called the aluminium structured vehicle technology (ASVT) system [Wheeler et al. (1987)]. The main objective was to improve on earlier works carried out in the AIV programmes by investigating new designs and manufacturing approaches for aluminium structures. Because of the use of aluminium, there was a great interest in using adhesive bonding technologies. Bonding or weld-bonding as joining methods were expected to increase joint stiffness by providing a more uniform load distribution over the bondline area. As a result, any stress concentrations which were previously existent when using spot-welds/rivets would be minimised thus reducing material weight, sheet gauge and costs. A significant drawback in spot-welding aluminium is that the process requires higher power and current in order to induce a weld across an aluminium plate. It is therefore a difficult technique for high volume production of vehicles. Consequently, advanced technologies would be needed to spot-weld aluminium and this would then increase costs in production. The technology of the ASVT programme was incorporated in many vehicle replicas, such as the Austin Rover metro, the BMW 3 series and the experimental Ferrari 408. However, the first production vehicle using the ASVT technology was the all-aluminium Jaguar XJ220. Other vehicle

programmes to adopt the ASVT technology were included in the Ford AIV based on the DN5 Taurus/Sable model, the GM EV1 electric vehicle and in the P2000.

After the success of the AIV programme, the US Federal Government and the American automotive industries joined forces to establish a leadership for the development and production of affordable, low emission, fuel-efficient cars. The programme called the Partnership for a New Generation of Vehicles (PNGV) was established in September 1993 [Anon (2000a)]. The main aim of the PNGV programme was to develop mid-sized saloon cars which would produce lower fuel emissions to achieve up to 80 mpg, and still maintain the same structural rigidity and costs as conventional cars [Wheeler (1997)]. This would be achieved by constructing a vehicle using advanced light-weight materials such as aluminium, using advanced joining techniques. The objective of the PNGV programme was to obtain an overall weight reduction of 40% compared to other conventional vehicles.

In 1993, Audi launched the A8 which was the first full production vehicle made solely out of aluminium [Lowe (1994)]. Its design was based on an aluminium extruded space-frame and cast nodes which were used to join these extruded sections together. The maximum weight saving was achieved by using stressed aluminium body panels, and accounted for approximately 150 kg reduction relative to its steel body counterpart [Anon (1995b), Drewes et al. (1994), Birch (1999)]. In addition, a range of novel joining techniques was used in the construction and these included shielded arc welding, resistance welding, punch riveting, clinching and adhesive bonding techniques. The performance of the A8 vehicle proved to be superior in crash test performances and gave a resultant torsional stiffness 40% greater than that of the previous Audi 100 series (C4) [Anon (1995b)].

After the success of the A8, Audi will be launching the all-aluminium bodied A2, in the summer of 2000 [Birch (1999)]. The A2 vehicle will be the first aluminium car to be mass produced. Using Audi's aluminium space-frame technology, the weight of the body of the A2 will be approximately 895 kg, or 43% less than if it were built using steel and conventional manufacturing processes.

In 1996, Lotus introduced the Elise; an all-aluminium vehicle joined through adhesive bonding. The chassis of the vehicle was mostly made from complex-shaped aluminium

extrusions which created a space-frame that was only 68 kg hence, only half the weight of an equivalent steel body [Kochan (1996)]. The aluminium chassis of the Lotus Elise was composed of thirty-five extruded components and three sheet metal parts. All extrusions were made from 6063-aluminium magnesium silicon alloy while the body panels, which were bonded to the space-frame, were made from various grades of aluminium alloys. With the use of adhesive bonding, distortions, which resulted from welding methods, were minimised and loads were spread across a greater area hence, providing strength advantages [Kochan (1996)]. Additional fasteners were also used to provide increased resistance to impact loading and peel forces during crash; in fact over 130 rivets were used. Although the Lotus Elise represents an innovative vehicle using novel joining and construction techniques with light-weight materials, one of the main concerns is associated with the maintenance and repair of the aluminium-bonded extrusions. Unlike the efficient repairs made to steel bodies, aluminium extruded vehicles would require more time and advanced skills. However, some areas within the vehicle, such as the body, have been constructed so that if damage occurs, the components can be separated and then replaced, if not repaired. Nevertheless, Lotus has been successful in developing the light-weight Elise through new materials and advanced joining techniques.

After the success of the Elise, Lotus launched the V6 M250 in 1999 [Birch (1999)]. The chassis of the M250 was made using bonded-aluminium technology making the overall mass of the vehicle less than 1000 kg. The remaining body parts were constructed primarily using aluminium and composite materials.

At the North American International Auto Show held in Detroit early in 2000, Ford Motor Company and General Motors introduced their two hybrid concept cars called the Prodigy and the Precept vehicles, respectively [Anon (2000b)]. Both concept cars were based on the PNGV requirements for weight reduction and lower fuel consumption. The Precept vehicle used aluminium and aluminium metal matrix composites in the body and chassis. The Prodigy also used aluminium and other light-weight materials throughout the vehicle, to obtain a weight reduction of 450 kg, compared to a conventional sedan vehicle.

2.2.3 Steel

Steel is still the most widely used metal in the automotive industry. The knowledge on the processing, handling and manufacturing techniques of steel is very familiar and quite

advanced. Not only is steel cheaper than most metals, but it also meets the standard requirements for the production of a large-scale vehicle in terms of strength, stiffness, formability, joinability, paintability and weldability [Anon (1995a), Drewes (1994)]. The material properties of steel make it ideal for use in the automotive industry particularly because of its high modulus of elasticity and yield point, which ensure good strength and stiff bodies. Although corrosion may be a problem with steels, coatings are being used for prevention or delay of rusting. Steel is an ideal material for car bodies as it is easy to repair and can be recycled repeatedly without compromising its quality.

High-strength low alloy steels are being increasingly used in the production of skin panels, suspension components and other structural parts within a vehicle. The cost of high-strength steels, in comparison to other materials such as aluminium and composites is low and because of their advanced mechanical properties, they can be used in thinner sections to reduce weight.

Zinc-coated steels have also been used in the development of light-weight vehicles [Matthews et al. (1997)]. In particular, there has been a great demand for zinc-coated steels for the monocoque as well as the closure panels. Replacing traditional steels with medium strength alloy steels is thought to give a 10% reduction in weight, and an even greater reduction can be achieved with the use of high strength alloy steels [Anon (1996a)]. Pre-coated steels are also being used primarily to prevent structural corrosion through moisture entry. Similar to other steels, this material can be easily recycled and because of its good mechanical properties is ideal to obtain stiff structures.

Applications

Steel is widely used in vehicle production by most of the world's largest car manufacturers. Steel is applied in many different areas in vehicles particularly in the body frame where stiffness is essential. In the last decade new technologies of steel are being developed to create light-weight vehicles. With the development of aluminium space-frames and extrusions, steel industries are researching into newer technologies for light-weight production which are more cost competitive than aluminium constructions. For example, following the launch of the all-aluminium Audi A8, Volvo launched its all-steel 850 vehicle whose main joining technology was its extensive use of laser-welding [Irving (1995)].

The Ultra Light Steel Auto Body (ULSAB) Project

The American Iron and Steel Institute (AISI), in collaboration with Porsche Engineering Services and other 35 worldwide industrial manufacturers, developed a \$22 million project called the Ultra Light Steel Auto Body (ULSAB). The main objective of the consortium was to demonstrate the potential of steel as a light-weight material by creating a sedan/saloon concept vehicle [Anon (1995d), Wells & Rawlinson (1997), Koehr (1997), Lowe (1997)]. The vehicle was to have a lighter and yet safer steel body structure which could be produced at low costs and high volumes. The ULSAB project aimed to obtain a 25% weight reduction in the vehicle body, an 80% increase in static torsional rigidity and a 52% increase in static bending rigidity.

The ULSAB project began in 1994 and was divided into 2 sections: Phase I and Phase II. Phase I involved designing the main body structure by using new technologies with advanced materials and manufacturing processes [Anon (1995c)]. The development was based on the principle of a holistic design where the body was treated as an integrated system rather than individual components assembled together. The materials used in the ULSAB concept vehicle were primarily high strength steels. Laser welding (continuous and spot) was the principal method of joining with only one area bonded (rear spare tyre cavity structure); however, tailored blanks and hydroforming methods were also used in the construction. Consequently, this resulted in a reduction in the overall parts required to 94 large components (158 including brackets) in the body [Koehr (1997)].

Hydroforming technology was used to create structures within vehicle bodies of improved structural performance and reduced weight. Complex structures can also be easily produced with this method resulting in time saving in the manufacturing process (see section 2.3.3). In the ULSAB concept vehicle, the main structures produced through the hydroforming process were the A-pillar and the side roof rail. The roof rails were selected as they represent the main structure of the body and because they must provide a strong structural connection between the A-pillar, B-pillar, C-Pillar and rear shock tower. By hydroforming the roof rails, there was a reduction in the number of parts thus reducing weight whilst maximising structural performance. Also, because the roof rail has a number of different shapes, sizes and cross sections, hydroforming provides the ability to easily create such complex structures.

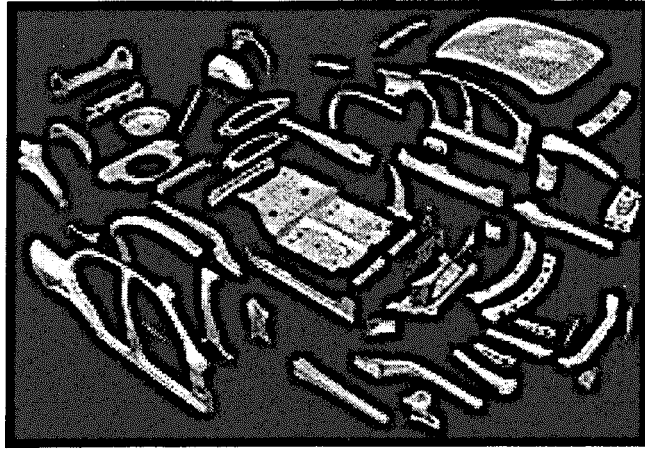


Figure 2.1 The ULSAB vehicle body parts [Anon (1997)]

Tailored blanks were also used to create almost 50% of the ULSAB's mass content. The use of tailored blanks in body structures was carried out by combining a number of different grades, material thicknesses and surface qualities of sheet materials together, but without compromising on weight. Combining various types of steels and thicknesses together provides stronger areas within a structure, thus eliminating the need for any additional reinforcements. In the ULSAB vehicle, tailored blanks are extensively used in the side of the body where five different grades and thicknesses of steel are used.

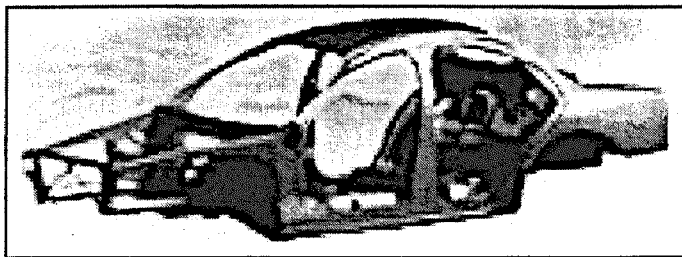


Figure 2.2 The ULSAB vehicle body frame [Anon (1997)]

After the completion of Phase I in 1995, Phase II involved the validation of the ULSAB concept body structure designed in the earlier stage and the completion of the exterior styling of the vehicle [Anon (1995e)]. With the actual construction of the body, final verifications on the design for weight, performance and ease of production were tested. The finished steel body weighed 25% less than an average steel body vehicle and was claimed to be the only body structure concept which provided substantial weight reduction at a potential cost saving [Anon (1998)].

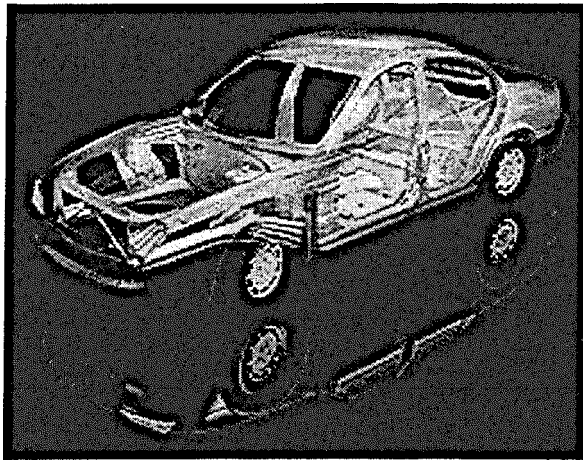


Figure 2.3 The ULSAB vehicle concept [Anon (1997)]

After the success of the ULSAB project, a new consortium including many of the same steel producing companies was formed in 1999 [Anon (1999)]. The program called ULSAB-AVC (Advanced Vehicle Concepts) aimed to pursue the development of steel-based solutions in vehicle bodies through new and advanced vehicle architecture and to extend the technology to other vehicle structures.

2.3 Construction Techniques

New and advanced construction techniques are being developed to work in parallel with advancements in joining methods and new materials for light-weight vehicle construction. In this section, various construction are considered in the context of how these methods can be used to provide stiffer, yet lighter vehicle structures.

2.3.1 Monocoque

A monocoque or integral body construction is a method of building a unitary vehicle body which carries all loads and stresses. There is no need for a separate chassis as the engine, transmission and suspensions are all attached directly to the body creating one structural unit. In this construction technique only the panels are considered part of the body frame, as they contribute significantly to the torsional and bending stiffness of the vehicle. The body is designed so that in the areas where the stresses are highest, there is considerable localised strengthening. The main advantage of using the monocoque construction is the cost and the resultant weight reduction [Matthews & Davies (1997)]. The monocoque

provides structural integrity, strength and rigidity thus, providing a safer car in case of impact. Monocoque construction has been used in a number of different projects and for different materials including aluminium (AIV), steel (ULSAB) and composite materials. In the 1980s, ALCAN developed the aluminium vehicle technology (AVT) in which stamped sheet monocoque was used and joined through adhesive bonding [Wheeler (1997)].

2.3.2 Space-frame

Although space-frame design developed from traditional coach building principles, recent interests in this method have been driven by new demands for light bodies and the use of aluminium. The space-frame concept provides a skeleton-like structure to which panels, i.e. floor pans, dash panels and exterior panels, can be mechanically fastened or attached to the structural frame through adhesive bonding, welding or riveting. The principle behind the space-frame is that beams, usually hollow sections and extrusions in the case of aluminium bodies, are joined together by nodal connections and that the rigidity of the vehicle is determined by the frame, rather than the panels. As the panels do not contribute to the frame stiffness they can be made from either metallic or polymeric materials, while the frame is usually metallic [Han & Clark (1995)].

There are various methods and techniques which can be used in producing space-frames. For steel bodies, an emerging technique consists of constructing the frame from hydroformed struts and tubes which are then connected through thin nodal connections [Dieffenbach (1996)]. Joining techniques used in the production of the space-frames include laser welding, metal inert gas (MIG) welding, spot-welding, mechanical fasteners and/or adhesive bonding. For aluminium bodies, Audi has proved to be one of the leaders in the use of the space-frame technology.

In 1993, Audi developed the A8 sedan vehicle based on an all-aluminium space-frame. The body structure consisted of aluminium beams formed by extrusions and high-pressure die casting nodes joined by MIG welding and adhesive bonding [Dieffenbach (1996)]. Sheet aluminium is used throughout the outer skin and various interior parts of the vehicle such as the plenum chamber, the wheel housing and the floor [Gugisch (1993)]. The main joining techniques used in the vehicle included MIG welding, punch riveting, spot-welding, clinching and adhesive bonding. It has been estimated that an all-aluminium

body is approximately 150 kg lighter than a comparable all-steel one of 300 kg hence, giving an approximate 50% weight saving on the body or 10% of the total vehicle weight [Anon (1995a), Drewes et al. (1994)]. The complete body of the Audi A8 actually weighed about 245 kg and contained 60 parts fewer than what would be required in a comparable steel body. Figure 2.4 shows the Audi A8 space-frame using all-aluminium extruded components.

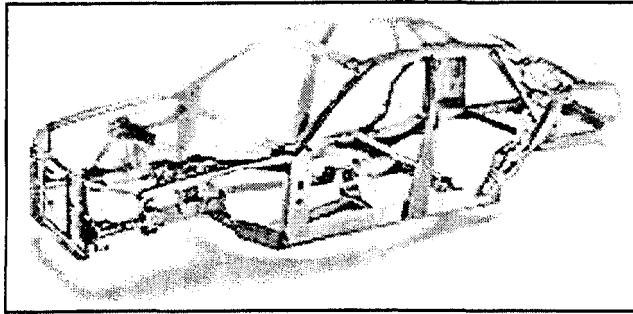


Figure 2.4 Audi A8 aluminium space-frame [Anon (2000e)]

Since the success of the Audi A8, there have been other manufacturers which have also produced light-weight aluminium vehicles through space-frame technology. The Aluminium-based Concept of a CO₂ Emissions Saving Subcompact (ACCESS) car for example, was developed in 1996 by NedCar Product Design & Engineering and in collaboration with twenty European automotive suppliers. The main objective in the development of this vehicle was to reduce the CO₂ emissions by 40%. Other aims that were addressed within the project were to reduce exterior noises and to enhance active and passive safety. The ACCESS vehicle mainly consisted of an aluminium extruded space-frame with thermoplastic body panels and aluminium sandwich panels [Frielink (1997)]. Panels and sandwich structures were joined to the space-frame by means of adhesive bonding which provided additional stiffness to the vehicle.

FE models representing the ACCESS car were used to study the torsional rigidity of the vehicle and the maximum stresses in the adhesive layers for various loading conditions. Results from the analyses showed that the roof contributed only minimally to the overall bending rigidity and hence any variants of adhesive properties in that area would not alter significantly the flexural stiffness. However, torsional rigidity was significantly affected by adhesive properties and the bondline thickness. Results from the study showed a significant reduction in torsional stiffness as the bondline thickness in the roof was gradually increased. However, for an adhesive thickness above 4 mm, the roof did not

contribute significantly to the rigidity, as the adhesive would bear all distortions [Frielink (1997)].

2.3.3 Hydroform Intensive Body Structure (HIBS) / Hydroforming

Although hydroforming is a relatively old process, its application in the automotive industry is new. Sometimes known as the Hydroform Intensive Body Structure (HIBS) process, this construction method is used to create strong structures in vehicle bodies such as engine cradles and body rails. Hydroforming is advantageous because it can reduce tooling costs, improve dimensional accuracy and reduce component weight through the use of less material, while increasing the strength and stiffness of the structures.

The process consists of creating closed box hollow sections to improve structural performance through high-pressure hydroforming. The technique involves placing a hollow tube, usually steel or aluminium, into the die of a hydraulic press. When the die is closed, high-pressure water is injected into the tube, stretching and deforming it into the shape of the die, as shown in Figure 2.5.

Because of the simplicity of the process, complex structures of high quality can be easily produced thus eliminating additional welds and flanges. Consequently, this will also reduce the overall number of parts required which in turn will result in lower production costs. The finished hydroformed part is a single component of high strength, excellent

surface quality and with a possible weight reduction in the range of 10-15% [Fenton (1998), Kochan (1996)].

The automotive industry is already using the hydroforming technique to substitute fundamental parts in body frames of vehicles. In the ULSAB project for example, the roof rails of the concept car were hydroformed and by doing so, they not only reduced the overall number of parts in the body, but also achieved reductions in weight and in time for assembling the main structure. Another example of hydroforming in the automotive industry was with the Opel system developed in 1997 which involved using hydroformed engine cradles. Other typical applications of hydroforming are in smaller structures found in vehicle bodies, such as exhaust manifolds, dashboard cross-members and other structural parts for roll-over protection [Kochan (1996)].

2.3.4 Tailored Blanks

Tailored blank technology is a construction technique used in vehicle bodies to provide different material properties and thicknesses most efficiently in areas of the vehicle where they are needed, as shown in Figure 2.6.

Different grades, material thicknesses and surface qualities are selected and placed within the area of the structure to create a resultant component of variant thickness and offer better weight saving compared with other conventionally uniform sheet thicknesses. The main advantage in using tailored blanks is the flexibility of selecting different and appropriate material properties to develop optimised structures with specific characteristics.

Tailored blanks are also advantageous in vehicle structures for improvements in fatigue strength, corrosion resistance and enhanced stiffness, as well as for cost and weight reductions [Drewes et al. (1994)]. In the automotive industry, high strength materials and mild steel sheets of different thicknesses, usually ranging between 0.8 mm for panels to 1.5 mm for local pillar reinforcements, are joined through laser welding.

With tailored blanks, the overall number of parts can be reduced and the need for any reinforcements in structures can be eliminated; this can be achieved by locally increasing the sheet thickness in those critical areas of the vehicle, such as in the pillars, where additional reinforcement is required. Consequently, the weight saving of a side unit of a vehicle, such as the one shown in Figure 2.6, can reach approximately 15% of the overall body weight.

The manufacturing process involved in tailored blanks results in fewer subassemblies and thus less material and scrap, and fewer moulds/die sets [Anon (1995a)]. The resultant outcome of a body part formed through laser-welded tailored blanks is a structure of increased stiffness, improved fatigue and corrosion resistance and better crash performance [Fenton (1998)]. Typical applications for tailored blanks in vehicles include the body side frames, the inner door panels as well as the motor compartment rails.

2.3.5 Extrusions

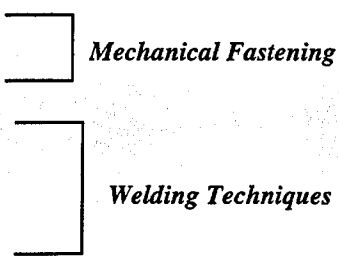
The extrusion process is one of the most common manufacturing techniques used in light-weight construction, being particularly advantageous for aluminium products. This is primarily due to the high ductility and 'styling freedom' of aluminium whose material properties are suitable for the manufacturing of thin-walled sections obtainable through extrusions.

Extrusion is a typical hot-forming process where the desired cross-sectional shape is produced in single forming stage. The process of extrusion involves heating the material in the form of cast billets at approximately 500°C. A hydraulic press is then used to force the material to flow through the die opening to form the component. Solid, semi-hollow and hollow sections of various shapes can be obtained with the use of different dies [Ostermann et al. (1993)].

There are some limitations in using extruded sections in smaller vehicle components primarily because of the costs associated with the process. However, the process is used effectively in the manufacture of sections in larger vehicle structures. Audi and Alcoa for example, have developed extruded space-frame structures consisting of extruded sections and cast nodes, as shown in Figure 2.7.

2.4 Joining Techniques in the Automotive Industry

Reducing the overall weight of a vehicle is possible through light-weight materials and new joining techniques. Advanced joining technologies are being developed and used to join new lightweight and/or dissimilar materials together. The following joining methods are commonly used processes for the fabrication of vehicles, in particular to the production of light-weight vehicles [Lucas (1995)]:

- Clinching
 - Self-Pierce Riveting
 - Laser Welding
 - Resistance Spot-Welding
 - Arc Welding
 - Adhesive Bonding
 - Hybrid Joining
- 
- The diagram consists of two vertical brackets on the right side of the list. The top bracket groups 'Clinching' and 'Self-Pierce Riveting' under the label 'Mechanical Fastening'. The bottom bracket groups 'Laser Welding', 'Resistance Spot-Welding', and 'Arc Welding' under the label 'Welding Techniques'. 'Adhesive Bonding' and 'Hybrid Joining' are listed below the second bracket but are not grouped by it.

Hybrid joining methods are generally combinations of processes for example, riveting with adhesives (riv-bonding), spot-welding with adhesives (weld-bonding) or mechanical clinching with adhesives (clinch-bonding).

2.4.1 Mechanical Fastening

This almost 'primitive' method of joining involves connecting/joining different components together by means of some kind of mechanical fastener. There are no limitations to which kinds of materials can be joined as there are no physico-chemical reactions involved when using mechanical fasteners. Components joined with threaded fasteners, such as screws and bolts, can be easily assembled and disassembled. Some of the most common mechanical joining processes, which are typically used in the automotive industry, are described in the following section.

Clinching or Press-Joining

The clinching or press-joining process is a technique of joining sheets by mechanically fastening or interlocking them together. A punch is used to indent or pierce the sheets into a lower die and as a result a permanent joint is formed, as shown in Figure 2.8. The strength of the joint depends on the tool size particularly the diameter of the punch, i.e. the larger the punch size, the greater the strength of the joint.

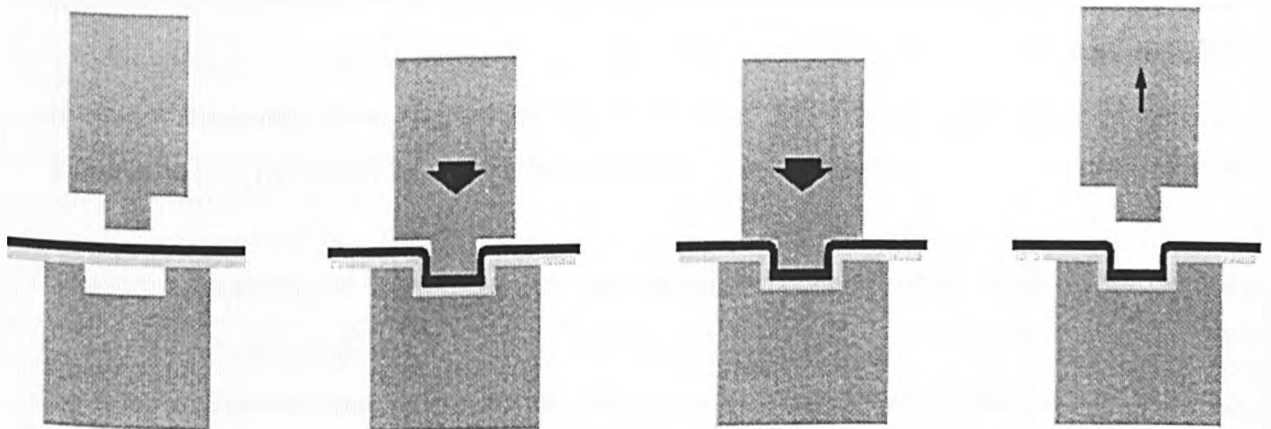


Figure 2.8 Schematic representation of the clinching technique

The permanent joints created by clinching have properties which are generally lower than those obtained through spot-welding. However, unlike spot-welding, this technique allows dissimilar and unweldable, e.g. pre-painted, materials to be joined together. The press-joining process is quite efficient as it requires minimum time and energy, and does

not need any consumable joining materials. However, as with spot-welding, it does require access to both sides of the joint and thus restricts joining to easy accessible components, such as lap or flange type joints.

Self-Pierce Riveting

Riveting is a traditional and practical joining method still used today in the automotive industry. The self-pierce variant is a one-step joining process which involves punching a rivet through two sheets, as shown in Figure 2.9.

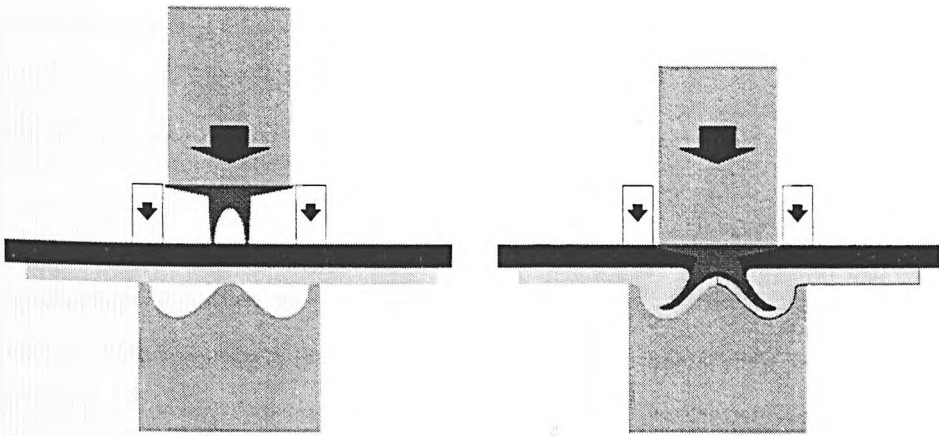


Figure 2.9 Schematic representation of the self-pierce riveting technique

Limitations arise due to the length and size of the riveting jaws which will have an influence on the overall strength of the joint. Furthermore, similar to spot-welding and clinching methods, riveting requires access to both sides of the joint thus making it impossible to join a number of vehicle structures.

Generally, mechanical fastening such as self-pierce riveting, can result in problems associated with the sealing of the joint; this is caused by the holes which are created when the rivet is punched through the sheet. However, some of the advantages in this joining technique include the fact that there is no heat and only low energy input required, no pre-drilled holes necessary, and the process is generally very simple, fast and automatic.

2.4.2 Welding Techniques

The definition of welding is given as *the process where a localised coalescence of metals or non-metals is produced either by heating the materials to the welding temperature, with or without the application of pressure, or by the application of pressure alone, with or*

without the use of a filler metal [Anon (1987)]. Welding methods may be classified according to the actual process involved. They are generally classified into three groups known as fusion welding, solid-phase welding and brazing/soldering. Fusion welding is characterised by the melting or fusion of the base metal and the filler material, if the filler is used, through a heat source which generates enough heat to maintain a molten pool of metal of the required size [Anon (2000d)]. Typical fusion welding processes include gas metal arc welding (MIG/MAG), gas tungsten arc welding (TIG), plasma welding and laser welding. Solid-phase welding produces welds without melting the base material and without the addition of a filler metal through pressure and generally with some heat [Anon (2000d)]. Some examples of this process are friction welding and cold pressure welding. The third welding group is brazing and soldering where only the filler metal is melted and not the base materials.

Welding is often a preferred joining process as it provides bonds of extremely high structural integrity. Continuously welded joints are equally if not more, strong than the base materials. Probably the greatest disadvantage with all welding processes is the fact that the process is irreversible and disassembly of the welded component is impossible. However, this can also be seen as an advantage if one seeks permanency in the bond. Other disadvantages in the process are the distortions which are created because of welding, and metallurgical damage due to the heat caused by welding; this is most commonly associated with welding of aluminium structures [Kochan (1996)].

One of the main drawbacks of welding techniques, particularly with respect to light-weight vehicle construction, is the limitations and restrictions in the types of materials to be joined. Because the welding process usually involves the fusion of the metals, problems arise with the use of certain metals/alloys and dissimilar materials combinations. Laser, resistance spot- and arc-welding are the three most commonly used welding techniques in the automotive industry. The advantages and limitations of each of these processes will be discussed in detail in the following section.

Laser Welding

Laser welding is defined as the process where light energy emitted from a laser source is focused upon a workpiece to fuse materials together [Anon (2000d)]. The advantages of laser welding are mainly associated with the fact that the welds produced are continuous

seams throughout the joint. As a result of the continuous connection, the weld provides better structural stiffness and seals the joint for corrosion resistance. Laser welding operates at high speeds and the outcome is a fine weld with reduced distortions and thermal damage thus requiring minimum finishing [Norrish (1992)]. Joints can be made with a single side access and therefore a wide range of joint configurations is possible. One of the main disadvantages in laser welding processes is the associated high capital costs. However, for high volume mass productions, laser welding is efficient and cost effective and hence is gradually being introduced into vehicle body manufacturing.

The principal types of lasers used in welding are CO₂ gas and Nd:YAG lasers.

(i) CO₂ Lasers

The lasing medium consists of a mixture of gases which include carbon dioxide, nitrogen and helium at a ratio of approximately 80:15:5 [Lucas (1995)]. The combination of these three gases, when confined within a glass tube, produces a beam of light well within the infrared region and has a wavelength of approximately 10.6 micrometers. The CO₂ laser operates in a constant wave mode giving a continuous beam at a given averaged power, rather than as a series of discrete, pulsed emissions [Lucas (1995)]. Typical power capacities of CO₂ lasers for welding equipment is about 12 kW.

(ii) Nd:YAG Lasers

Nd:YAG lasers use a solid crystal of yttrium aluminium garnet doped with neodymium as their medium. The crystal is excited by an external flash of light which creates an infrared beam of 1.06 micrometers wavelength. The radiation can be transmitted through optical fibres as well as through air and conventional glass optics. Recent Nd:YAG lasers can operate at an average power of up to 4 kW; however, extensive work is being carried out to create higher output powers. These lasers can operate in a continuous wave mode or in a pulsed mode depending on the selected source of power.

Resistance Spot-Welding

Spot-welding is a highly automated and well-established process commonly used in the automotive industry to join various components in vehicle bodies. The knowledge and experience of the process combined with modern control systems provide high confidence in the quality of spot-welded joints. The flexibility and the relatively low costs make

resistance spot-welding a significant joining process in the manufacture of light-weight vehicles.

In the spot-welding process, materials are joined at a localised area by electrical resistance heating under a forging pressure. The heating of the material creates a molten pool at the interface between the sheets and when cooled, the fused area solidifies to produce a weld nugget. Figure 2.10 shows a schematic representation of the spot-welding process.

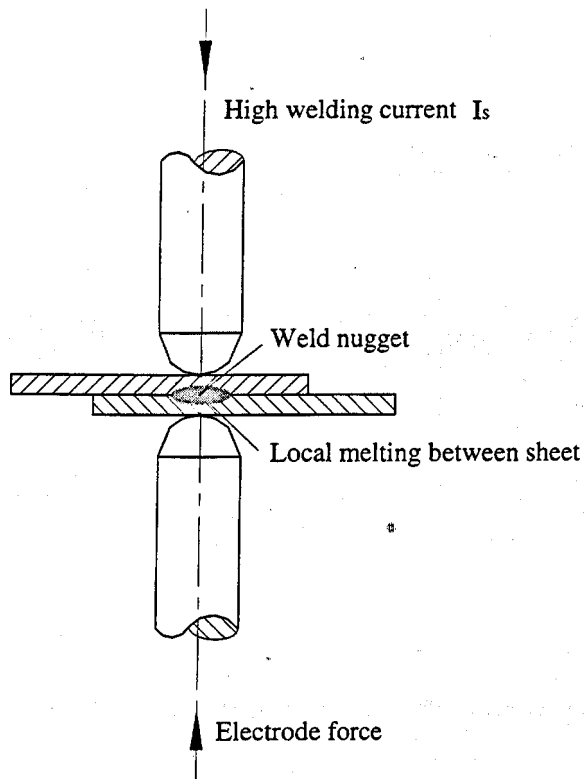


Figure 2.10 Schematic of the principles of resistance spot-welding process

The geometry of the welded area depends on the shape and diameter of the electrode and the process parameters. This contact area produced by the weld is critical since this is where the greatest stress concentration will occur. A resistance spot-welded joint is usually considered to be approximately 20% less stiff than a continuous joint [Lucas (1995)].

Spot-welding is suitable to join relatively thin sheets, typically within the range 0.5 to 5 mm thickness. In general, the welding time is short, nominally 0.2 seconds, to minimise heat loss into the electrode and into the bulk of the material being joined [Lucas (1995)]. Hence, the advantages of this process include the high application speed and the relatively

low costs. Spot-welding can be used for a limited range of materials and in the automotive industry these include low alloy steels, mild steel and zinc-coated steel. Figure 2.11 shows the resistance spot-welding process in a vehicle body.

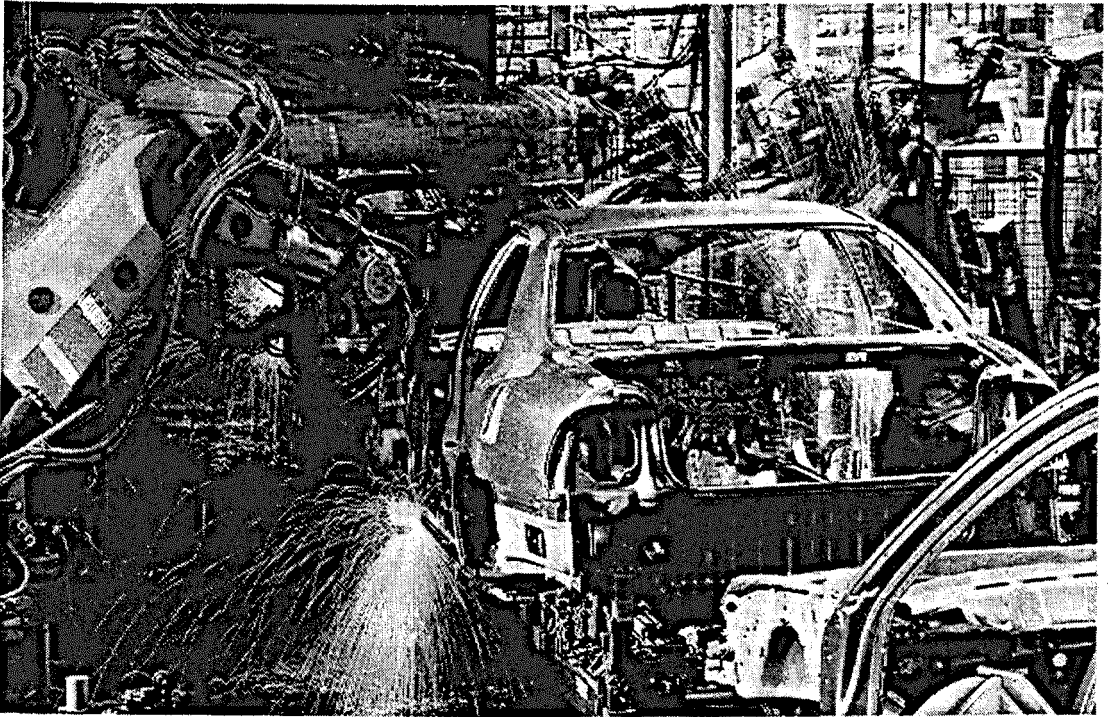


Figure 2.11 Resistance spot-welding of a full vehicle body [Anon (1994d)]

One disadvantage with resistance spot-welding is the fact that the process requires access to both sides of the joint and thus restricts a number of joint designs; tubular sections, for example, cannot be joined. Therefore, spot-welding is generally limited to lap and flange type joints which are typically 12 to 15 mm wide. Also, the spacing between the welds should be at least eight to ten times greater than the combined sheet thickness; if not the nugget size will normally decrease due to current shunting. Another problem that arises from the welding method is the surface damage of the sheet. This tends to be more of a problem particularly in those areas where aesthetics is required.

Arc Welding

The arc welding processes involve the use of a high energy heat source generated by an electric arc to melt the edge of the base material thus forming a weld pool which when solidifies, creates a weld. The high heat input may however, cause distortions in the components and this may affect the properties of the joint. The advantages associated with most arc welding processes include the high productivity rate for both manual and

mechanised operations. For manual welding, it is necessary to have a highly skilled welder but for readily automated processes, welding is carried out robotically. Maintenance and monitoring of the welding equipment are essential factors in order to avoid defects and to obtain consistent welding quality. Most modern techniques associated with vehicle fabrication are based on gas shielded arc processes.

(i) Metal Inert Gas (MIG)/Metal Active Gas (MAG)

Gas-shielded arc welding was first introduced in the early 1950s and is a commonly used process for the joining of ferrous sheet, plates and tubular sections [Lancaster (1992)]. The two primary gas shielded processes are MIG and MAG, depending whether the gases used during the process are inert e.g. argon/helium, or active e.g. carbon dioxide gases; generally MAG welding is commonly used for welding steel. The main advantage of shielded gas metal arc welding is that the equipment requirements are simple and the operating efficiency is high. However, some of the disadvantages include the fact that the process is often labour intensive and problems of thermal distortions have to be controlled.

(ii) Tungsten Inert Gas (TIG) Process

TIG is commonly used to produce high quality and precision welding, especially in areas of a workpiece where access is restricted. The arc is formed between a pointed tip of a non-consumable tungsten electrode and the base material to fuse the joint area. The arc is sustained by an inert gas, such as argon and helium, which is used to protect the weld pool and the electrode from atmospheric contaminations [Norrish (1992)]. The main advantage with TIG welding is that the process is very controllable and the joint quality is usually high. Generally, the process is commonly used for welding thin sheets; for thicker base materials, a separate filler material may be required. TIG welding is specifically suitable for aluminium alloys and has been applied in the fabrication of the Audi A8 body shell.

(iii) Plasma Arc Welding (PAW)

The plasma arc welding process was derived from the TIG process, where the arc is formed between the tip of a non-consumable tungsten electrode and the base material. The difference with TIG welding is that for PAW processes a range of shielding and cutting gases are used, depending on the application required for. The convergence of the shield gas and plasma gases at the orifice through a nozzle constricts the arc thus, giving improved arc stability and better quality with less contaminated welds. Other features of

the plasma arc welding process are the higher energy density and heat content, deeper penetration capabilities and that higher welding speeds can be obtained [Messler (1993)].

2.4.3 Adhesive Bonding

There has been an increasing interest in the use of adhesive bonding in the assembly of automotive structures in recent years, particularly with the demand for light-weight vehicles. Adhesive bonding offers many advantages compared with other joining methods such as welding and mechanical fasteners. Firstly, with adhesive bonding it is possible to join dissimilar materials such as plastics with metals and/or aluminium and steel, all of which are considered for light-weight construction. Secondly, adhesive bonds are made over larger joint areas than other conventional joining methods and consequently, the load is distributed over the bondline providing a more uniform stress distribution and potentially giving strength advantages. In addition to their use as a joining medium, adhesives can also be used as insulation materials to improve vibration damping, reduce noises, or they can be used as a sealant to form leak-proof seals. Adhesives can also act as excellent electrical and thermal insulators.

Another advantage associated with adhesive bonding is that no additional holes are made to the components and therefore, smooth external surfaces are created which are aesthetically pleasing and improve aerodynamic performances. The ability to join more complex shapes is also a benefit when using adhesive bonding and therefore, the overall number of parts in a car body can be reduced significantly, as well as the overall manufacturing costs. Bonded structures are generally more torsionally rigid than structures joined through spot-welding methods, for example. This is primarily due to the even distribution of the loads from one surface to the other, through the glue-line.

One of the main advantages of adhesive bonding, and of prime interest to the automotive industry, is the fact that thinner gauge, low alloy steel materials can be joined together, while maintaining the structural stiffness and integrity of the joint. Adhesive bonding offers the best potential compared to other joining techniques and is applicable to a number of materials such as steel as well as light-weight materials e.g. aluminium. Various studies showed that it was possible to reduce the thickness of an aluminium sheet in typical model structures from approximately 1.3 to 0.51 mm with adhesive joints and still maintain the same characteristics and mechanical behaviour [Anon (1994a)].

However there are some disadvantages in the adhesive bonding process. For example, one of them is the need for good process control during the joint fabrication and hence, the lengthy time associated to obtain a required bond strength. Also, both the quality and the strength of the bond will depend on the adherend geometry and on the bonding procedures, i.e. surface preparation, mixing of constituent material, wetting of surface, service temperature, humidity and other environmental conditions. Another weak point in the joining process is the fact that bonded components are difficult to disassemble or dismantle for in-service repairs. Manufacturers are continually developing new and improved materials to overcome some of these limitations, and adhesive bonding is becoming more widely accepted by the automotive industry for vehicle body assembly. A more detailed description of the adhesive bonding process, materials and joint characteristics are presented and discussed in Chapter 3.

2.4.4 Hybrid Joining

The combination of different joining techniques, such as adhesive bonding with spot-welding or mechanical fasteners, can provide improved effectiveness of joint characteristics. The advantages of the individual processes seem to compensate for the weaknesses of the other process, resulting in a stronger joint. For example the welds confer the peel strength that the adhesives lack and in turn, the adhesive protects the spot-welds from fatigue failure. The combination of these two techniques has been shown to improve torsional strength and rigidity of the completed structure [Anon (1995b)].

Weld-Bonding

This joining process consists in a combination of adhesive bonding and welding, usually spot-welding, to create a strong bond. The main advantage of hybrid bonding is the resultant improvements in fatigue life, durability, stress distributions, rigidity, sealing, stiffening and generally a better performance of the joint strength both statically and dynamically. The presence of adhesive also helps dampen noises and vibrations as well as minimise corrosion. The overall energy absorption of weld-bonded joints is greater due to the synergistic effects of the combined processes.

The weld-bonding process is fairly simple. Initially, the surfaces of the components to be joined should be cleaned and pre-treated as required, then the adhesive can be applied. After the components have been assembled, they can be spot-welded and then depending

on the type of adhesive used, they can be cured. Figure 2.12 shows a single lap joint which has been joined through the weld-bonding process.

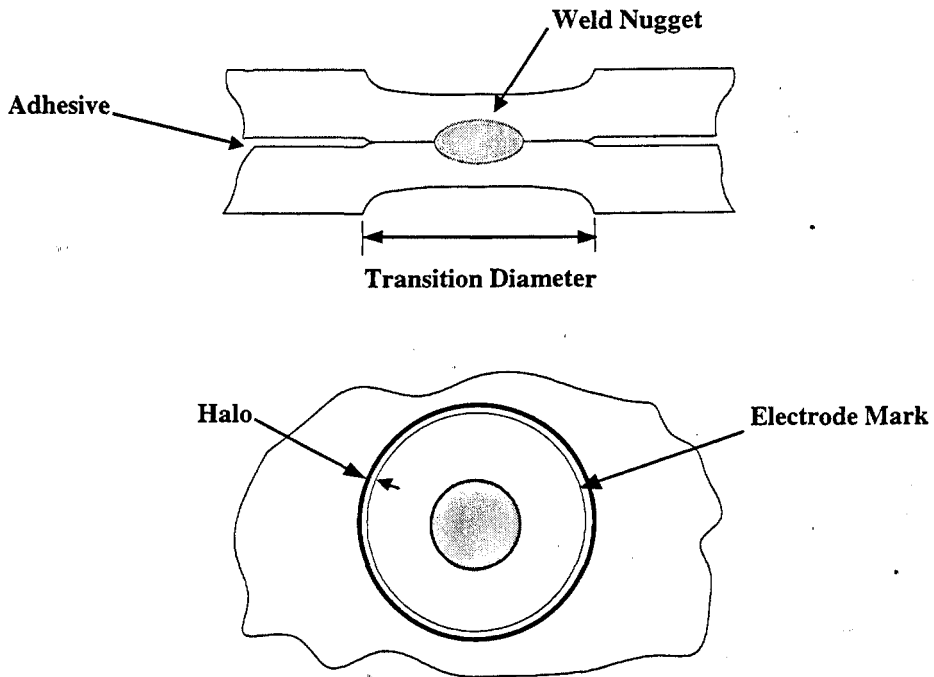


Figure 2.12 Schematic representation of the weld-bonding process

The inner circle represents the diameter of the weld nugget while the area between the two circles is referred to as the *halo*. The area outside the halo region is uniformly bonded with adhesive. However, the area enclosed within the halo represents the region where the two sheet components are not actually bonded together due to the displacement of the adhesive and the heating effects which result from the spot-weld. The selection of appropriate adhesives is fundamental for weld-bonding. The most commonly used adhesives are those with a low viscosity; this is so any excess adhesive can squeeze out between the sheets when the electrode force is applied. The weld-bonding process does limit the types of joints that can be joined to lap and flange type structures. Ideally to obtain a better performance from a weld-bonded joint, surfaces should be treated prior to the application of the adhesive. However, in the automotive industry for example, where weld-bonding is widely used, surface preparations are not used and the adhesive is simply applied to the sheets.

The use of adhesive bonding and spot-welding is being widely investigated in the automotive industry as a solution to increase the torsional stiffness and rigidity of vehicles

while reducing material gauge, the number of welds required and consequently the overall weight. Another advantage with weld-bonding, particularly related to the automotive industry, is the impact resistance. The body of a vehicle must be strong enough to withstand crash/impact and hence, have sufficient energy absorption capacity. In the weld-bonding process, the adhesive allows the transfer of loads from sheet to sheet, while spot-welds provide strength; thus making the process ideal for impact. Typical applications of weld-bonding in vehicle structures include joining stiffeners to boot lids, bonnets and roofs to increase rigidity and reduce vibrations.

Adhesives with Mechanical Fasteners

Adhesives are sometimes combined with mechanical fastening methods, such as self-pierce riveting or clinching, for improved performance. The main advantage is that both adhesive bonding and fasteners are potential methods of joining dissimilar materials. Additionally, the mechanical fastener will provide additional strength to the bonded joint. Adhesives, such as epoxies and PVC plastisols, combined with mechanical fasteners are often used in the automotive industry. For example, a representative application of clinch-bonding is the joint around the door window aperture between the aluminium outer skin and a steel inner shell [Lucas (1995)].

2.5 Summary

The evolution of the design of the vehicle has been driven primarily by the demand for light-weight vehicles. The production of light-weight vehicles will result in less fuel consumption and hence, exhaust emissions and pollution. As a consequence, light-weight vehicles will not only be more economical, but also more environmentally friendly.

Because of the high customer demands for improved passenger safety, larger vehicle sizes and possibly even because of the demand for more luxuries and technologies within a car, it has been difficult to reduce the weight of vehicles. However, with today's new and advanced technologies it is possible to construct a vehicle meeting both customer demands and manufacturer requirements. Light-weight vehicles can be produced through various design concepts which involve new developments in materials, construction techniques and joining technologies. Each of these areas has its own advantages and the combination of all three has provided a valuable route to light-weight vehicle construction.

- *Materials*

Many 'new' and 'old' materials are being looked at as potential for light-weight vehicle construction. For example, aluminium is considered a 'new' material for applications in vehicle bodies and has proved to be suitable for the construction of lighter vehicle bodies. Typical aluminium vehicles currently in production show weight reductions of approximately 45% than that of a conventional steel vehicle body. However, even though aluminium is considered one of the more suitable materials for light-weight construction, the cost of the material is high compared to that of say, steel. Furthermore because of its relative novelty for vehicle bodies, new knowledge and understanding of the behaviour and applicability of aluminium is required. New and advanced technologies must be adopted since some of the existing manufacturing and joining processes are not applicable to aluminium; consequently, the overall cost of aluminium vehicles is high.

On the other hand, steel represents an 'old' material since it has been used in vehicles since the early 1920s. Not only is steel a relatively low cost material but its manufacturing techniques are very well known, making both the joining and processing of steel, also cheap. The material properties and characteristics of steel have proven to be suitable for strong structures; however, it has a density three times heavier than aluminium. Because of the wide experience and knowledge in steel, novel design concepts and joining technologies are being pursued to reduce the gauge of steel in vehicles, and recent developments have demonstrated the potential for a 25% weight reduction and a 75% improvement in stiffness on steel body constructions.

- *Construction Techniques*

New construction techniques have been developed to meet the requirements for light-weight vehicles and the use of new materials. Space-frame, hydroforming, extrusion and tailored-blank constructions are some of the novel manufacturing techniques for automotive applications and which offer advantages in the reduction of body weight. For example, the space-frame technique for example, has been used in many new vehicle designs particularly in the Audi A8, as it provides rigidity for the frame structure through hollow sections. The overall number of parts required is reduced as is the weight of the vehicle body. The extrusion process is also important for the manufacture of components for space-frame constructions. In the extrusion process, beams of thin-walled sections can

be formed and the process is particularly suitable for aluminium alloys. The hydroforming process also reduces the overall number of parts in the vehicle body by producing a single structure of high strength and with excellent surface quality.

Tailored blanks have been used particularly in areas of the vehicle where different strengths are required and where reinforcements may have been needed previously. Traditional panels, for example, are made with uniform sheet thicknesses and additional reinforcements are placed in those areas which are most critical. One of the main advantages with tailored blanks is that different grades and thicknesses of materials can be placed efficiently to create a light-weight structure of high strength.

- *Joining Methods*

Spot-welding has been the main joining technique in vehicle body constructions. However, with the requirements for lighter vehicles, new materials are being used and spot-welding is often not suitable to join such materials. The use of adhesive bonding in the automotive industry is increasing rapidly, primarily due to the need to join new and/or dissimilar materials for light-weight construction. The main advantages of adhesive bonding are that dissimilar materials can be joined and that bonded joints can provide an increase in stiffness and rigidity. Because of the enhancement in joint stiffness it is possible to reduce the gauge thickness of the material resulting in light-weight construction. When used in combination with point joining methods such as fastening, clinching or spot-welding, the joints have greater peel strength, impact resistance and energy absorption. These hybrid processes are often preferred because of the additional joint integrity and are likely to be most widely adopted in light-weight vehicle construction.

With the combination of material selection, new construction techniques and joining methods, there have been many novel vehicle designs which give significant weight reductions. Aluminium has proven to be an excellent material for light-weight vehicle manufacturing however, it is still quite expensive. Adhesive bonding offers considerable potential for future light-weight vehicles as it allows the bonding of different and light-weight materials to each other and at the same time increases significantly the stiffness. The application of adhesives in steel bodies also offers potential for weight reduction,

through the possible use of thinner materials, and enhanced joint characteristics which can lead to improved stiffness.

3. ADHESIVE TECHNOLOGY

3.1 Introduction

Adhesive joints are typically formed by placing a pasty or liquid adhesive material between the surface components to be joined (adherends), so that they wet the surfaces. Solidification of the adhesive then provides cohesive strength to form a structural connection between the adherends. Compared with most other joining methods, adhesive bonding allows the joining of component pieces over a larger surface area where the loads are evenly distributed and hence, stress concentrations are reduced.

Adhesives and adhesive joints are commonly sub-divided into two distinct classes - structural and non-structural. In non-structural applications, the adhesive is used for purposes other than that of structural strength, e.g. dampening, sealing, insulation, noise reduction, packaging and labelling. However, in engineering assembly most joints are load-bearing and if adhesives are to be used, they must have a structural capability. Structural adhesives are used to assemble load-carrying components and structures so they must have sufficient strength to transmit any applied loads and stresses from one surface to the other, without losing integrity within the desired design limits. The following sections describe various aspects of structural adhesives and their use in engineering applications.

3.2 Principles and Mechanisms of Adhesion

As adhesive bonding relies on interfacial attachment, it is evident that surface properties of the adherends have an important effect on the structural behaviour of the joined components. Surface preparation of the adherend is therefore very important when dealing with major load-bearing structures which might be subjected to severe environmental conditions.

Surface analysis and characterisation has become a major area of research to explain the behaviour of adhesive joints. However, the theory behind the nature of adhesion and the mechanism of the formation of the bond, between the substance of the adhesive and the material of the adherends, is still not well defined. Various theories have been suggested throughout the years and are described in the section below.

Mechanical Theory

The mechanical theory is the oldest and simplest explanation for the adhesion between two surfaces by suggesting mechanical interlocking. In most cases, the adhesive is applied in a liquidy state so that it can penetrate into the pores of the surface of the substrate; mechanical interlocking will result as the adhesive solidifies. It is generally observed that rougher and porous surfaces may provide better adhesion and enhancement in joint strengths, through the embedding of fibres with the adhesive.

Diffusion Theory

The diffusion theory, proposed by Russian chemists Voyutskii and Vasenin, states that one end of the polymer molecule chain from one surface diffuses into the structure of the second surface, resulting in the formation of a strong bond across the interface. The theory proves to be quite valid for adhesion between two similar polymers to themselves (autohesion) or to each other, as it is based on the theory of diffusion and polymer structures where chain structures of molecules are capable of micro-Brownian movement [Lees (1984), Semerdjiev (1970), Allen (1992a)]. However, the theory is not applicable when considering adhesion between smooth and rigid materials where the molecules are in practice fixed and not mobile [Allen (1992b)].

Electrostatic Theory

The Russian Deryaguin proposed the concept of electrostatic theory in 1969. The theory suggested the existence of an electrical layer between the adhesive and adherend interface. This contact at the interface is developed by the attractive forces between the molecules of the surfaces, which contribute to the adhesive bond strength.

Adsorption Theory

The adsorption theory explains the theory of adhesion between two surfaces due to intermolecular attractions known as Van der Waal's forces and London dispersion forces [Semerdjiev (1970)]. In practice, if the molecules of the adhesive and adherend are brought close enough to each other then the Van der Waals forces will give rise to physical adsorption [Lees (1984)]. This is usually observed as wetting, which is dependent on the surface tension of the liquid (adhesive) and the surface energy of the solid (adherend). Wetting is a prerequisite for good adhesion and can only occur if the surface tension of the adhesive is lower than the surface energy of the adherend. Some polymers, particularly polyolefins and PTFE, have relatively low surface energies and because of this, are quite difficult to bond.

The only requirement to the theory of adsorption is that the surfaces of the two materials to be bonded are in sufficiently close and intimate contact so that Van der Waal's forces may be established across the interface. The dispersion forces are probably the most significant in providing the necessary strength and durability to the joint.

Chemical Bonding

It is sometimes speculated that chemical reactions occur across the interface to form chemical links between the adhesive and the adherend. In principle, chemical bonds should be much stronger and more durable than the physical adhesion mechanisms discussed previously. Coupling agents and adhesive promoters are sometimes used to stimulate chemical bonding. For example, silanes have been demonstrated to be very effective in enhancing joint durability.

There is some evidence to suggest that, in certain circumstances, each of the above theories of adhesion may be valid and in typical applications more than one mechanism may exist. However, for most metal-to-metal structural adhesive bonding, it is believed that physical adhesion based on the adsorption theory is the main provider of joint strength.

3.3 Generic Types of Adhesives

From the physical mechanisms of adhesion, it is clear that the bonding process requires the adhesive to be liquid at some stage during application to wet the substrates and then subsequently, to solidify to provide the strength or cohesion across the joint. Adhesives are sometimes classified by the solidification mechanisms for example, by solvent evaporation, or by cooling from above the melting point (hot melts) or by a chemical curing reaction (thermosetting). For engineering applications in which joints with high structural integrity between metal components are required, the thermosetting adhesive groups are most widely developed and applied. In the automotive industry the thermosetting adhesive types include acrylics, epoxies, phenolics, plastisols and polyurethanes. In the following section, these adhesives will be briefly described stating the advantages and disadvantages of each and their common uses in automotive applications.

3.3.1 Acrylics

Acrylics are generally cold-curing adhesives which are applied in thin-film forms and are classified according to the curing mechanisms. The three main types of acrylics are: anaerobics which cure with the absence of oxygen, cyanoacrylates which cure only when applied as a thin-film and when in contact with moisture/water, and toughened acrylics, which need some agent/hardener in order to cure.

Anaerobic

Anaerobic adhesives are acrylic-based adhesives which set only in the presence of metal ions and in the absence of atmospheric oxygen. Hence, anaerobics remain in a liquid state in the presence of oxygen but automatically cure once enclosed in a joint [Watson (1992a)]. One of the main advantages with anaerobic adhesives is that there is greater joint manipulation prior to curing; as curing only occurs with the lack of oxygen, i.e. when the joint is closed. Anaerobic adhesives come in a wide range of strength and viscosity variations. They are commonly used in the automotive industry for assembling components and for sealing, locking, threaded parts, gaskets, fasteners and any other fitted mechanical components.

Cyanoacrylates

Cyanoacrylates are highly reactive, one-part acrylic resin-based adhesives of very low viscosity. Commonly known as 'superglues', these adhesives can cure at very high speeds and provide high bond strengths. However, in order to obtain rapid curing of cyanoacrylates, the adhesives must be applied in thin-film form, so that they come in contact with residual surface moisture and as a result, may cure within seconds. Some of the disadvantages with cyanoacrylates include the fact that they have poor gap filling capabilities, poor thermal resistance and they are very susceptible to moisture. Typical applications of cyanoacrylates in automotive assembly are to bond small plastic and rubber components which require high speed assembly [Watson (1992b)].

Toughened Reactive Acrylics

Toughened reactive acrylics are two-part systems which are formed by a combination of a resin/adhesive mixture which is applied to one surface, and a liquid initiator applied to the other. Curing time depends primarily on the hardener and the initiator used; however, in practice a completely cured joint can be obtained within minutes. The main advantages in toughened reactive acrylics are that they offer excellent peel and impact resistances, and are also tolerant to oily surfaces. These adhesives are primarily used in large structures where surface treatment is minimal and in bonding plastics, rubbers, sheet metal, coatings and thus, provide some potential for vehicle bodies.

3.3.2 Epoxies

Epoxies are probably one of the most popular adhesive groups used today in engineering applications. Because of the high strength of these adhesives, epoxies are usually used in the bonding of larger structures and components.

Epoxies are reaction products of acetone and phenol. They can be either cured with heat (in one-part systems) or through the addition of a hardener (in two-part systems), or sometimes with a combination of the two. A whole range of hardeners can be used to give rise to a wide and versatile variety of epoxy adhesives with different properties. The adhesive modulus of epoxy adhesives can range typically from 10 MPa – 5 GPa. High strength epoxy adhesives can give ultimate shear strengths in excess of 50 MPa but in general, they have relatively low peel and impact strengths. Newer epoxy formulations

have been developed to improve peel and impact characteristics for example, through rubber toughening.

3.3.3 Phenolics

Phenolics were one of the first structural adhesives to have been developed. The combination of phenolic resins with natural or synthetic rubbers offers a large variety of adhesives with good flexibility and vibration absorption [Semerdjiev (1970)], yet prove to be complicated to use. This is primarily due to the water release during curing which requires high pressure and elevated temperatures in order to maintain contact between the two surfaces being bonded [Lees (1984)]. The main advantage with these adhesives is their excellent durability to moisture and their performance in severe environments. Phenolics also have major benefits due to their high strength and adhesion properties. Phenolics are widely used in the aircraft industry and in the automotive industry for friction and clutch linings.

3.3.4 Plastisols

Plastisols are viscous adhesives made from PVC particles suspended in a combination of liquids known as plasticizers. Plastisols are usually applied in paste-like form onto the component to be bonded. When heat is applied, the solubility of the polymer within the plasticizer begins to increase thus, increasing the viscosity. With elevated temperatures, i.e. 140°C, most of the plasticizer will be absorbed into the particles and which will toughen; this is when the adhesive is fully cured. The toughness and good ageing characteristics of plastisols make them suitable for use in bodies such as for underbody protection and sealing. Other typical applications are in bonding large metal components, such as lightly stressed panels in vehicles, e.g. bonnets, boot lids.

3.3.5 Polyurethanes

Polyurethanes are very versatile adhesives and can be formulated to meet a wide range of requirements. The main advantages associated with polyurethanes are their ductility/toughness and their fast curing. However, because of their fast curing rate, polyurethanes prove to be difficult to handle and usually demand special equipment to manage. They are also very sensitive to moisture during curing, have poor durability and give low strengths at elevated temperatures. Polyurethanes are used widely in load-bearing

applications in particular in dry conditions as they are easily affected by moisture. They are also typically used in the bonding of sandwich panel sections, as gap fillers (as foam), in bonding door trims and head linings in vehicles.

3.3.6 Polybutadienes

Polybutadienes are low modulus adhesives made from synthetic rubber. Generally rubber based adhesives are more flexible and have higher impact strengths than other structural adhesives such as epoxies and phenolics, although their specific strengths are much lower [Watts (1992)]. Polybutadienes are typically used both to join component pieces and as a method to improve noise/vibration absorption within vehicle bodies.

3.4 Adhesive Joint Stress States

The use of adhesives for structural assembly requires a careful consideration of joint configuration and design. Depending on the components' geometries and directions of applied forces, adhesive joints may be subjected to a number of different modes of loading. These are usually described as peel, cleavage, shear and tension/compression, and are shown schematically in Figure 3.1.

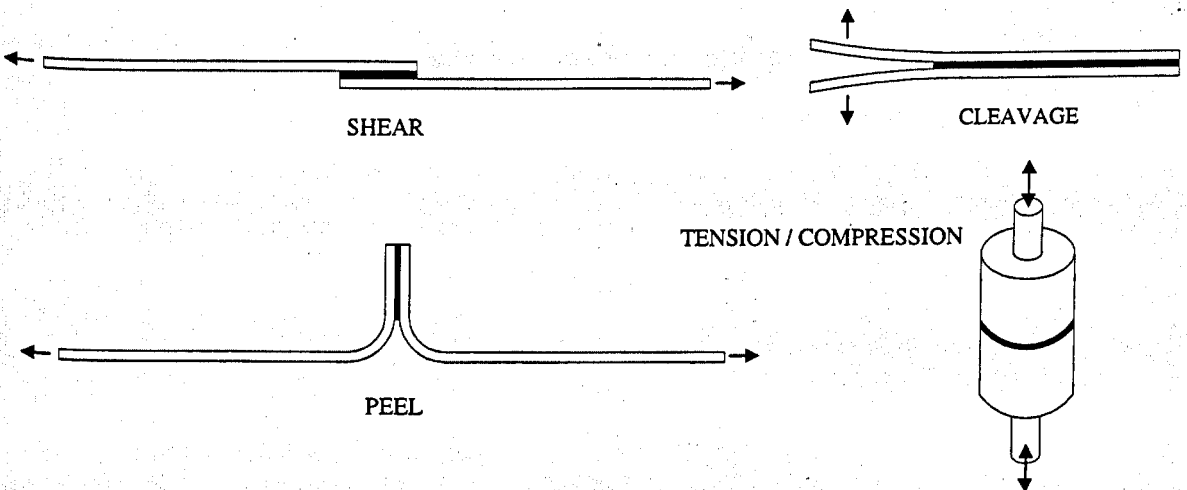


Figure 3.1 Typical loads found in adhesive bonded joints

Typically, adhesive joints subjected to tensile and shear loading provide the strongest joints and those most resistant to bond failure; this is because of the more uniform distributions of the stresses over the total bonded area. However, if misalignments or eccentricities are introduced into the load path, high peel and/or cleavage stresses are

developed. The stress concentrations resulting from peel and cleavage forces may be reduced by using lower modulus adhesives.

The resistance of adhesive bonded joints to peel/cleavage loads is still a major limitation. Particular attention should therefore be made during joint design to avoid or minimise peel stresses. In practice however, this design guideline is not always applied as peel joint configurations are still widely used in the form of flange joints, especially in the automotive industry. This is due to the fact that the flanges in coach joints are most suitable for manufacturing processes such as spot-welding and fastening techniques. With the more recent advent of adhesives, manufacturers continue to employ the same joint configurations for adhesive assembly as the joints are usually supplemented by spot-welds.

3.4.1 Joint Strength

The mechanical strength of an adhesively bonded joint depends on a number of factors including joint configuration, geometry, bond area, materials and the sheet/bondline thicknesses. By appropriate design, it is possible to obtain adhesive joints which are stronger than the components themselves. For example, increasing the overlap length of a lap joint to a certain extent can result in an increase in joint strength. On the other hand for peel joints, joint strength is more dependent on configurations and dimensions such as the sheet thickness, forming bend radius, adhesive fillet and substrate flexibility. Adhesive joint strength may be also sensitive to the bondline thickness even if failure occurs cohesively through the adhesive. This sensitivity arises from complex interactive effects of stress distribution, bending moments and in the case of dynamic loading, the ability of the adhesive to absorb impact energy. In general thicker bondlines will lead to less stiff joints.

Other factors which are often considered in joint design and analysis include the modulus of the adhesive, tapering of the joint edges, the thickness of the bondline and the presence of adhesive fillet. In the case of T-peel joints as used in car bodies, the flange bend radius is also an important parameter which has a critical interaction with the adhesive fillet. In addition to the geometric design details, the characteristics and behaviour of the joint clearly depends on the adhesive type and it is essential to specify an appropriate adhesive

to meet the design requirements. These aspects are discussed in more detail in Chapters 4 and 5.

3.5 Bonding in Vehicle Structures

Adhesives have been used in car bodies for many years but most applications have been non-structural to provide sealing and damping properties. More recently the potential for structural adhesive joints has been recognised in novel forms of construction and in conventional body structures. In most current applications adhesives are used in conjunction with spot-welding or mechanical fasteners, e.g. clinching, to form hybrid joints. This effectively determines the joint configurations as traditional monocoque bodies are fabricated with lap and flange/coach joints. Major research programmes have addressed various aspects of adhesive bonding in vehicle structures particularly in areas such as durability, impact behaviour and process tolerances. Another primary area of study is the effectiveness of adhesives on structural stiffness of car bodies.

3.5.1 Prediction of Behaviour of Vehicle Structures

The capability to predict the structural behaviour of vehicle body parts is possible primarily due to the advances in numerical modelling. Theoretical calculations are also commonly used; however, for larger and more complex shapes, such as vehicle body structures, the calculations may require a number of approximations. These approximations may give a general estimate of the behaviour of a structure neglecting geometric details and specific material properties. In general, most modelling methods rely on additional experimental testing to validate the accuracy of the theoretical predictions.

Testing of structures through experimental procedures represents the actual behaviour without approximations and although finite element models can also represent real conditions, there are some limitations. Nevertheless, finite element methods are being increasingly used in the development of structures with enhanced behaviour. One of the main advantages with numerical modelling methods is that it is possible to design new structures and predict their behaviour without actually manufacturing the structure. Consequently, both costs and manufacturing time are significantly reduced.

3.5.2 Automotive Requirements for Stiffness

There are many design criteria that must be satisfied in order to produce a light, yet structurally safe vehicle. In addition to joint strength and integrity, required to ensure driver and passenger safety, rigidity and stiffness of the body frame is essential to maintain accurate handling as well as to reduce noise and vibrations from the motor and the ground surfaces. The overall stiffness of the body frame will contribute to the overall performance of the vehicle and therefore, is an important factor in the design for light-weight vehicles. While light-weight materials, new joining technologies and new design concepts for the construction of the main body frame are being developed to meet objectives of weight reduction and efficiency, it is essential that mechanical characteristics of the body, particularly stiffness, are not compromised.

3.6 Joint Durability

It is relatively easy to obtain good initial strength of a joint however, it is more difficult to obtain a good durability of a bonded joint. There are many factors which influence the durability of a joint. Most significantly, adhesive bonded joints may degrade primarily due to their sensitivity/susceptibility to their operating environment. Operating conditions for cars can be very demanding as they include extreme temperature ranges, humidity and wetness, and other aspects such as the presence of aggressive chemicals. These have a damaging effect on the joint which when combined with dynamic loading, can lead to rapid degradation.

Many methods have been investigated to improve joint durability through the selection of different adhesives and through attentive surface preparation. For example, if the operating conditions of the joint are known, then a suitable adhesive that can withstand such temperatures might be used. Similarly, the surface pre-treatment of the joint through methods such as the application of primers, might be used to improve durability.

Nevertheless, in the fabrication of joints for car structures, joint durability is only partly considered. While ideally surface treatments such as degreasing, abrasion and the application of silanes, would improve the strength of adhesive joints, the automotive

industry do not use such treatments primarily because of the nature and limitations of their manufacturing processes.

3.7 Summary

- Adhesive bonding offers considerable potential for light-weight vehicle construction, particularly as it allows joining of many and dissimilar materials.
- The selection of the appropriate adhesive is important and depends on the specifications of the joint design.
- A number of adhesive systems can be used for structural assembly. The most commonly used structural adhesives include epoxies, phenolics, acrylics, plastisols, polyurethanes and polybutadienes.
- There are several design parameters which can be altered in order to improve the strength of an adhesive joint; these include geometric parameters such as sheet thickness, type of adhesive, bondline thickness, sheet bend radius, overlap length, etc.
- Although there are preferred joint configurations for adhesively bonded joints, e.g. lap shear, rather than T-peel, their application in the automotive industry is limited by manufacturing and production constraints.
- Degradation is usually caused by environmental and operating conditions to which the adhesive joint is exposed. These conditions might include elevated temperatures, moisture, wetness, aggressive chemical, etc. Such factors should be known prior to the design of a bonded structure so that an appropriate adhesive system can be specified.

4. REVIEW OF ANALYSES OF BONDED JOINTS

4.1 Introduction

The analyses of bonded joints and the prediction of joint characteristics have been subjects of research effort for many years and many theories and equations have been derived to calculate the behaviour of joints. Experimental testing has also been widely used to compare with results obtained from theoretical calculations. The development of finite element methods provided a powerful tool for the prediction of joint behaviour and in early applications, simple FE models of joints gave comparable results to experimental and theoretical analyses. As a result of continuing refinements and better understanding, FE methods are now most widely used in the analyses of joint behaviour.

Most of the analytical, experimental and numerical studies have been developed for the stress analysis of adhesive joints. However, the main intent of this thesis is to study and understand the stiffness characteristics of adhesive joints. In section 4.2-4.4 an overview on the work carried out on stress analyses of lap and coach joints is reviewed. This will provide a better understanding of the behaviour of adhesive joints and an insight to how the performance of the joint is influenced by changes in geometric design parameters. In section 4.5, typical finite element modelling techniques, used by the automotive industry to predict vehicle behaviour including stiffness, are discussed in detail. Finally, the limited published work on predicting the stiffness behaviour of structural joints, representative of vehicle structures, is also reviewed.

4.2 Analytical Approaches

4.2.1 Linear-Elastic Approach

The closed-form approach is based on fundamental continuum mechanics. This method involves solving equations of force, stress and displacements for given boundary conditions. The approach is a valuable way to understand the mechanics of joints such as single lap joints, in particular using simple, linear elastic analysis. However, the analysis

becomes quite complex when non-linearities and/or complicated geometries are introduced.

The simplest analysis on single lap joints, shown in Figure 4.1, assumes that the adherends are perfectly rigid and that the adhesive layer deforms only in shear. For rigid adherends, the adherend tensile stress will decrease linearly to zero over the joint length from A to B.

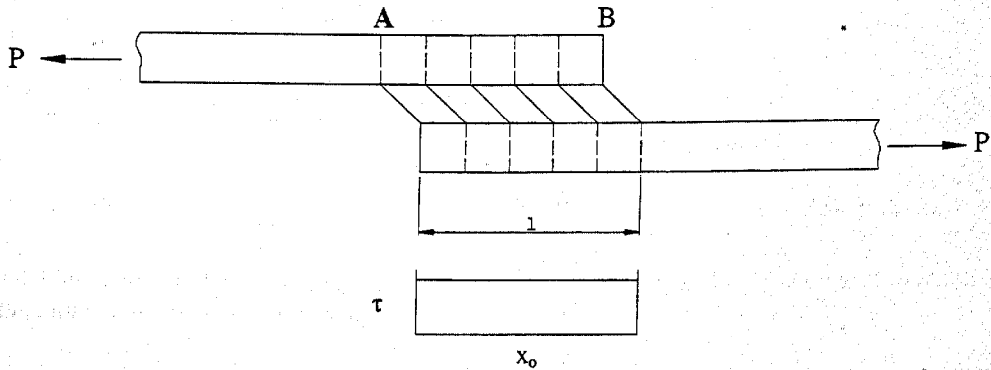


Figure 4.1 Deformation of single lap joint with the assumption that the adherends are rigid

Consequently, the average shear stress (τ) is given by the equation,

$$\tau = P / b l \quad (4.1)$$

Where P is the applied load, b is the width and l is the overlap length of the joint.

In Figure 4.2 a similar joint is considered; however in this case, the adherends are assumed to be elastic. Consequently there will be deformation in the adherends, such that in the upper adherend the maximum tensile stresses occur at A and tends to zero at point B; the inverse holds true for the lower adherend. The adhesive is assumed to act only in shear and because of the differential strains in the adherends, the deformation in the elements of the bondline results in a shear stress distribution, as shown in Figure 4.2.

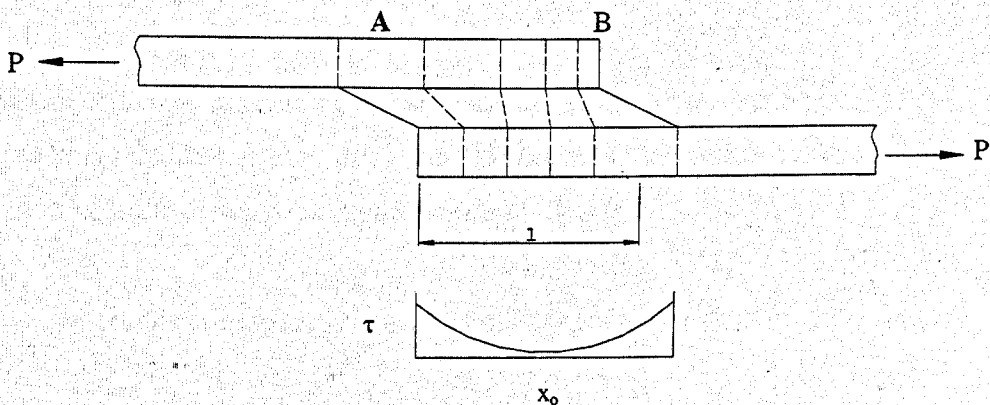


Figure 4.2 Deformation of single lap joint with the assumption that the adherends are elastic

The analysis of adhesively bonded lap shear joints has been studied for over 60 years with the first major investigation being carried out by Volkersen in 1938. Volkersen (1938) developed an equation to describe the distribution of stresses in the adhesive layer based on the assumption that the adhesive deforms only in shear while the adherends deform only in tension, as illustrated in Figure 4.3.

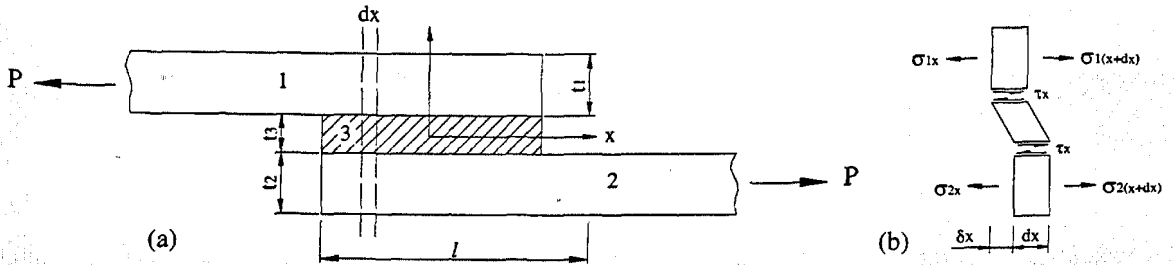


Figure 4.3 Volkersen's shear lag analysis (1938) showing (a) undeformed lap joint and (b) section through deformed joint with the assumed forces

The principal observation from Volkersen's *shear lag analysis* study was that the shear stresses along the bondline were distributed non-uniformly, with sharp peaks at the ends of the bondline; this phenomenon is known as *differential shear*. The theoretical longitudinal and transverse shear-stress distributions ($\bar{\tau}$) in the adhesive layer were given by the expression,

$$\bar{\tau} = \frac{\omega}{2} \frac{\cosh \omega X}{\sinh \omega/2} + \left[\frac{\psi - 1}{\psi + 1} \right] \frac{\omega}{2} \frac{\sinh \omega X}{\cosh \omega/2} \quad (4.2)$$

Where,

$$\omega^2 = (1 + \psi) \phi$$

$$\psi = t_1 / t_2$$

$$\phi = \frac{G l^2}{E t_1 t_3}$$

$$X = x_0 / l$$

And where t_1 and t_2 are the adherend thicknesses, t_3 is the adhesive thickness, G is the adhesive shear modulus, E is the adherend Young's (tensile) modulus, l is the overlap length and x_0 is the distance along the overlap.

For cases where the adherends are of equal thickness i.e. $t_1 = t_2$, then $\psi = 1$ and $\omega = \sqrt{2\phi}$

The maximum adhesive shear stress occurs at the ends of the joint and is given by,

$$\bar{\tau}_{\max} = \sqrt{\frac{\phi}{2}} \coth \sqrt{\frac{\phi}{2}} \quad (4.3)$$

Volkersen predicted that the stress concentration factor (S.F.) of an adhesively bonded joint with equal thickness adherends was given by the expression,

$$\text{S.F.} \propto \sqrt{\frac{G l^2}{2 E t_1 t_2}} \quad (4.4)$$

Where G is the shear modulus of the adhesive, l the overlap length, E is the adherend Young's modulus, and t_2 and t_1 are the adhesive and adherend sheet thicknesses, respectively.

Volkersen's theory suggested that the shear-stress concentration factor in the adhesive layer of a lap joint could be minimised through appropriate choice of design variables; the stress concentration factor could be reduced by changing the overlap length, the shear modulus or the bondline thickness, sheet thickness and its modulus. The theory predicted that the maximum shear stresses in the adhesive would occur at the ends of the overlap, where in fact the shear stresses should be zero due to the free surfaces at the ends of the overlap [Kinloch (1986), Zhao (1991), Adams et al. (1997)].

Volkersen did not take into account two important factors in his theory. The first arises from the fact that the applied loads are actually not collinear and the eccentricity results in rotational effects within the joint. These bending moments will cause high peel stresses and the effects of these were included in later studies [Goland & Reissner (1944), Zhao (1991)]. The second factor that was not accounted for in the analysis was that adherends will actually bend when a load is applied. Thus the joint will distort and as a result, the joint displacements are not proportional to the applied loads giving rise to geometric non-linear problems. Although Volkersen's work was based on very general and simple concepts, it provided a foundation for many further analyses.

Goland and Reissner (1944) improved the theory suggested by Volkersen by providing a solution for peel and shear stresses by including the rotational effects of the load path. In the analysis, they used a bending moment factor k which related the bending moment on

the adherend at the end of the overlap M_o to the in-plane loading. Once the bending moments were calculated, these were used as boundary conditions to analyse the overlap region. Two solutions were suggested to determine the stresses within the adhesive and both were applicable only to equal thickness adherends; the first solution was for very stiff adhesives while the second for flexible adhesives. For stiffer adhesives, the stiffness of the adhesive was assumed to be the same as that of the adherends. For flexible adhesives on the other hand, the adherends were assumed as plates and the adhesive as tension-shear springs, hence neglecting the bondline thickness. Results from their analyses showed that the maximum shear stresses occurred at the edges of the adhesive layer and large peel stresses occurred within the adhesive layer. Figure 4.4 shows the schematic representation of Goland and Reissner's proposed deformation.

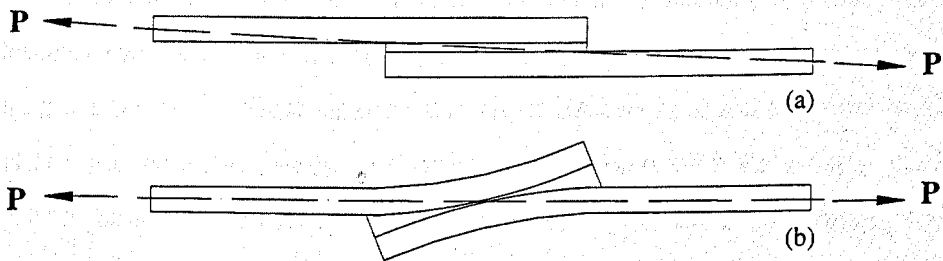


Figure 4.4 Schematic representation of Goland and Reissner's bending moment factor theory

In practice, if the applied loads are small then it is assumed that no rotation occurs in the overlaps; thus the line of action of the load will be as in Figure 4.4 (a) where it passes through the edges of the overlap and adherend. In this case, the bending moment factor k is approximately equal to unity and hence, the bending moment on the adherend is given by,

$$M_o \approx P t / 2 \quad (4.5)$$

Where P is the applied load and t is the adherend thickness.

However if the magnitude of the applied load increases, the rotation of the overlap will also increase, as illustrated in Figure 4.4 (b). In this case, the line of action of the load will act closer to the centre-line of the adherends and thus, the value of the bending moment factor will be reduced and the bending moment will be given by equation 4.6.

$$M_o = k_{GR} P t / 2 \quad (4.6)$$

Where k_{GR} is the bending moment factor suggested by Goland and Reissner and is given by,

$$k_{GR} = [1 + 2\sqrt{2} \tanh (\theta/2\sqrt{2})]^{-1} \quad (4.7)$$

And where,

$$\theta = 1 \sqrt{\frac{3 P (1 - \nu^2)}{b E t^3}}$$

Most of the earlier work by Volkersen and Goland and Reissner was of limited accuracy due to the restricted boundary conditions used. In their solutions, they assumed that the peel and shear stresses across the adhesive thickness were constant, that the maximum shear stresses occurred at the end of the overlap and neglected any shear deformations of the adherends [Adams et al. (1997)]. However, because the ends of the adhesive are free surfaces, there cannot be any shear stresses and consequently the shear stresses at the ends of the joint must be zero. Most of the later work looked at improving the analyses of stresses within the adhesive while still following Goland and Reissner's method for calculating the bending moments at the overlap. Some of the more significant developments were investigated by Sneddon (1961), Hart-Smith (1973), Renton and Vinson (1975), Allman (1977).

Hart-Smith (1973) improved on Goland and Reissner's method by developing a new bending moment factor which however, involved complicated mathematics. Hart-Smith believed that Goland and Reissner's predictions overestimated the bending moment at the edges of the overlap and hence, his theory took into account the effects of large deformations in the adhesive but disregarded any large deformations in the overlap. Equation 4.8 shows Hart-Smith's solution for predicting the bending factor moment, for equal thickness adherends.

$$k_{HS} = [1 + \theta + (\theta^2/6)]^{-1} \quad (4.8)$$

Hart Smith's solution proved limited as it was only applicable to joints with similar adherends. Eventually, Bigwood and Crocombe (1989, 1990) investigated adhesive bonded structures formed by two different adherends and developed an analytical solution for these. Finite element methods were also used to compare with the theoretical calculations. The generalised closed-form solution was derived for a simplified elastic

analysis of the adhesive/adherend sandwich subject to a combination of loads: shear, tensile and moment loads which were applied to the ends of the adherends. Equations to calculate peak stresses due to shear, tensile and bending loads (Figure 4.5) were derived and are given in equations 4.9-4.10 and 4.11-4.13 for simplified peel and shear analyses.

The solutions for the simplified peel analysis are given in equations 4.9 and 4.10. For a shear force per unit width, the compressive transverse stress is given by,

$$\sigma_V = \frac{-2^{1/2} \beta_1 V}{(\beta_1 + \beta_2)^{3/4}} \quad (4.9)$$

For a bending moment, the transverse stress is given by,

$$\sigma_M = \frac{-\beta_1 M}{(\beta_1 + \beta_2)^{1/2}} \quad (4.10)$$

Where the peel compliance factors for adherend 1 and 2 are given by β_1 and β_2 , respectively;

$$\beta_1 = \frac{12 E_a (1 - \mu_1^2)}{E_1 h_1^3 t} \quad \beta_2 = \frac{12 E_a (1 - \mu_2^2)}{E_2 h_2^3 t}$$

The solutions to the simplified shear stress analysis are defined in equations 4.11-4.13 for tensile loads, shear loads and bending moments. For a tensile force load, the shear stress is given by,

$$\tau_T = \frac{-\alpha_1 T}{2(\alpha_1 + \alpha_2)^{1/2}} \quad (4.11)$$

For a unit width shear load, the shear stress is defined as,

$$\tau_V = \frac{3V}{4h_1} \quad (4.12)$$

And for a unit width bending moment, the shear stress is calculated using,

$$\tau_M = \frac{3 \alpha_1 M}{h_1 (\alpha_1 + \alpha_2)^{1/2}} \quad (4.13)$$

Where the shear compliance factors α_1 and α_2 are a measure the relative shear stiffness of the adhesive and of the adherends and is given by,

$$\alpha_1 = \frac{G_a (1 - \mu_1^2)}{E_1 h_1 t} \quad \alpha_2 = \frac{G_a (1 - \mu_2^2)}{E_2 h_2 t}$$

These solutions can be applied to joints with different or similar adherends where in the latter case; $E_1 = E_2$, $\alpha_1 = \alpha_2$, $\beta_1 = \beta_2$ and $h_1 = h_2$.

Zhao (1991) developed a simpler solution to that suggested by Hart-Smith, for the bending moment factor and is given in equation 4.14. He also proposed a solution for both different adherends and identical adherends and assumed that the overlap area did not deform during loading and hence, was rigid; thus only the adherends were analysed (Hart-Smith's solution included the adhesive). The solution was proved accurate for predicting stresses in single lap joints provided that the overlaps were greater than 6 mm. The method gave good solutions for stiffer and thicker adherends and was simple to use.

$$k_z = [1 + \theta]^{-1} \quad (4.14)$$

Adams and Peppiat (1973) studied the Poisson strain effects on shear stresses in the adhesive layer, and the longitudinal stresses in the adherends acting at right angles to the applied load. The results from their investigation showed that the maximum longitudinal shear stresses occurred at the edges of the overlap and that Poisson's ratio did have a significant effect on the stresses in the adhesive. Although their analyses was intended for lap joints, it neglected any effects due to bending and hence, was more applicable to double lap joints. They also treated the adhesive as an infinite number of springs and thus peel and normal stresses within the adhesive were ignored. However, their analysis did take into account shear stresses in the adherend by using Demarkles' approach (1955); the latter however, neglected bending moments which caused peel stresses within the adhesive. Adams and Peppiat's provided an analytical solution which could be used to calculate tensile stresses in the adherends and the shear stresses in the adhesive caused by Poisson strain effects.

Probably some of the most significant analytical work was carried out by Renton and Vinson (1975) and Allman (1977), who took into account the effects of bending, shear and normal stresses of the adherend to provide more accurate solutions. In both studies, they assumed that the adhesive shear stress was zero at the overlap ends. Allman's analysis is thought to be one of the most detailed and thorough solutions as it included bending, shearing and stretching of the adherend and also accounted for shearing and peeling in the adhesive. He assumed a linear variation of the peel stress across the adhesive thickness, and accounted for shear stresses at the free ends however, the shear stresses across the adhesive thickness remained constant. Allman's study investigated joint behaviour using stress functions in an approximate numerical method which is similar to the known finite element method.

Mallick (1989) extended the work carried out by Allman to accommodate thermal stresses and to account for longitudinal stresses along the overlap. His analysis was applicable to a large range of material properties including isotropic and anisotropic adherends as well as elasto-plastic adhesives.

Ojalvo and Eidinoff (1978) studied the influence of bondline thickness on the stress distribution in lap joints based on Goland and Reissner's work. Most previous studies ignored the bondline in their stress analyses solutions and hence, Ojalvo and Eidinoff proposed a solution which would allow the prediction of the shear stress variation across the bondline thickness. By including the effects of the bondline thickness in the analyses, results showed an increase in the predicted shear stresses and a reduction in the peel stresses. Greater effects would exist for joints with shorter overlaps, thicker adherends and stiffer adhesives.

Oplinger (1994) studied the effects of adherend deflection in lap joints based on Goland and Reissner's earlier solutions. The aim was to develop an analytical solution that would decouple the adherends and treat them as two separate beams; this allowed individual boundary conditions to be applied to each adherend as required, and at the same time provide bending deflections of the joint. The study gave a general overview on Goland and Reissner's and Hart-Smith's solutions and aimed toward developing an analytical method by maintaining the simplicity of Goland and Reissner's solution but taking into

account additional details such as adhesive fillet and shear deformations within the adherend, which were previously unaccounted for.

4.2.2 Non-Linear Approach

Dickson et al. (1972) included material non-linearities in the study of single lap joints by using a two-stage approach. In the analysis the bondline area was divided into elastic and plastic zones, each of which were then analysed separately. The stresses within the plastic zones, which were calculated based on a von Mises criterion, were assumed constant and equalled to the maximum stress obtained from a uniaxial stress-strain curve. The stress-strain relationship of the adhesive within the elastic area was assumed to be perfectly linear. An iterative method was then used to calculate the stresses in the elastic and plastic zones of the adhesive layer.

Grant and Taig (1976) introduced material non-linearities into Volkersen's (1938) shear lag solution. Although a more realistic stress-strain curve was used in the approach, it proved limited as it only accounted for shear stresses and strains caused by tensile loading of the adherend; thus, it neglected peel stresses due to bending of the adherends. Therefore, although the analysis was derived for lap joints, it was actually applicable to double lap joints, where bending is restricted.

Hart-Smith (1981) also included non-linear adhesive properties and took full account of the effects of bending moments into his analytical solution. In the approach, he assumed a degree of adhesive plasticity in the shear component of stress based on bi-linear, elasto-plastic characteristics. The adhesive layer was divided into three regions; the outer two represented the plastic region while the central zone the elastic region. The principle behind an elasto-plastic model is that the adhesive behaves elastically until the yield point where it becomes plastic at the same stress until failure. A bi-linear model will give a closer representation to the true adhesive characteristic over the entire load range. However, in both models the areas under the stress-strain curves are equal to that under the true stress-strain curve; and the failure stresses and strains are equivalent for the curves. It must be noted that Hart-Smith's solution assumed only the elasto-plastic shear properties of the adhesive while the adherends are still considered elastic.

Bigwood and Crocombe (1990) assumed that the adhesive layer behaved as a non-linear layer between the linear elastic adherends. The approach was similar to that used in their previous linear analysis study [Bigwood & Crocombe (1989)] where an adhesive/adherend sandwich panel was used; thus making the analysis applicable to a number of joint configurations. While previous work divided the adhesive layer into elastic and plastic zones for the analysis, Bigwood and Crocombe considered the adhesive as a continuous layer. Stress-strain curves for the adhesive layer were calculated, based on a von Mises criterion, over the entire overlap length giving more accurate results.

4.3 Experimental Visualisation Methods

To further understand the behaviour of adhesive joints, work was carried out, not only using analytical and numerical solutions but also through experimental visualisation methods. A brief review of some significant works is discussed in this section.

Demarkles (1955) studied rubber lap joints through an analogue photoelastic technique by using foam rubber as the adherends and an adhesive layer of similar mechanical properties as the rubber. The study showed that because of the similarity between the adherend and the adhesive properties, the strain distributions were quite similar to those obtained in their study of welded joints. The photoelastic analysis was used by others and proved a valuable approach in determining the areas of highest stresses such as those measured at the ends of the overlap. However, the method proved limited in measuring quantitatively the stresses and strains within the adhesive.

Adams et al. (1973) studied the behaviour of models of adhesive joints by using a hard rubber as the adherends and a relatively soft foam rubber as the adhesive. The results from the study gave more realistic stress-strain distribution curves for the adhesive layer than those indicated by Demarkles. Two of the more significant observations from the investigation were the high stress concentrations at the adherend corners and that the directions of maximum principal stresses were about 45° to the applied load. Experimental results gave good agreement with finite element (FE) models representing similar joints. Theoretical calculations using Volkersen's approach were also determined; however, because the theoretical calculations do not take into account the shear strains in

the adherend, the maximum shear stresses predicted in the adhesive layer at the ends of the joints were higher than those obtained experimentally.

After the attempt to calculate stresses within the adhesive using photoelastic methods, another optical technique called Moiré interferometry was developed. The Moiré technique is used to obtain surface deformations in the adherend and adhesive by means of gratings. Although this method allows the entire bondline to be studied, one of its main limitations is that the measurements can be made only at the faces of the joint surfaces. More recent approaches to this method have been devised. Tsai et al. (1995), for example, investigated geometric non-linear deformations and adhesive stress distributions in single lap joints using Moiré interferometry. Results were compared with non-linear two-dimensional finite element modelling methods and theoretical calculations. The measurements of longitudinal strain in the tested joints gave similar values to those calculated from numerical models. However, because of the three-dimensional effects caused by bending-twisting and by the free edges, FE models using a three-dimensional analysis would be more appropriate. Also the Moiré technique limits the analysis to only the faces of the joints. Measured shear stresses proved very similar to those found using numerical analysis when the adhesive spew fillet was taken into account.

4.4 Numerical Methods – Modelling of Adhesive Bonding Joints

One of the most significant methods for the prediction of joint behaviour is through numerical modelling techniques. Although continuum mechanics and basic analytical approaches give a foundation for the general understanding of the behaviour of adhesive bonded joints, there is a limitation to the amount of accuracy that can be achieved. In particular, complex shapes and geometric details such as adhesive fillets for example, cannot be accounted for in closed form solutions. Numerical methods have been developed to provide a versatile analytical tool for a wide range of engineering applications. Finite element analysis allows hypothetical joint designs to be analysed and the behaviour to be predicted. With numerical methods, it is possible to predict the joint behaviour and if necessary, improve the joint design prior to joint fabrication.

The limitations brought through theoretical methods are minimised through numerical modelling and the accuracy of the joint model is significantly improved. Through finite

element modelling the stress distributions, not only in the adhesive layer but also in the adherends, can be determined for a number of different loading conditions. In the following sections, significant findings using numerical techniques are discussed for two typical adhesive joint configurations; the single lap joint and the T-peel or coach joint.

Background

Many computer codes have been developed to implement the finite element method proposed over 60 years ago for the solution of engineering problems. The concept behind finite element methods is based on the analysis of a body, or a continuum, which is divided into smaller bodies or units; the solutions are then obtained for each unit rather than of the entire body. The subdivisions of a structure are also known as finite elements; these elements are interconnected at the joints by nodes. By minimising the total energy of the system, displacements could be calculated in various regions in the structure and from these, the stresses and strains could be derived [Zienkiewicz (1971), Crocombe & Mout (1988)]

In the late 1950s, the aircraft industry was the primary user of the initial finite element codes to solve structural problems. Extensive research was carried out by Turner et al. (1956) to improve and expand the boundaries of finite element methods. Bending elements, curved shell elements and the isoparametric concept were also introduced soon after.

In 1971, Zienkiewicz used the finite element concept to determine the stresses in a wide variety of structures with different geometric shapes and loading conditions. The finite element method was recognised as a general method of problems normally formulated as partial differential equations, and gave more accurate solutions than previously used closed-form theories which were derived by Volkersen (1938) and Goland & Reissner (1944). Finite element methods were used extensively in the analyses of non-linear and dynamic structural problems in many different fields, e.g. soil and fluid mechanics, thermodynamics, etc.

Later in the 1970s, finite element methods were adopted by Japanese car manufacturers who used the techniques to predict the behaviour of concept vehicles. They believed it

was safer and more economic to analyse a numerical model of the vehicle before actually building it.

4.4.1 Finite Element Analysis of Single Lap Joints

The single lap joint represents one of the simplest joint configurations and because of the understanding of the behaviour from theoretical methods, single lap shear joints were the first adhesive bonded joint geometries to be studied using finite element methods. Much work has been done to predict the stresses within adhesive bonded lap joints and how different design parameters, such as the joint geometry and adherend/adhesive material properties, influence the stresses in joints. In this section, only some aspects on the stress prediction of lap joints are reviewed using numerical methods. It is hoped that this will give a general understanding of the effectiveness of modelling methods.

As early as 1971, Wooley and Carver (1971) were among the first to apply finite element methods for predicting stresses in single lap joints. Their research considered geometrically linear analysis and the effect of a range of design parameters such as adhesive modulus, bondline thickness and overlap lengths with adhesive square-ends. The modelling work was carried out using plane-stress analysis and succeeded in obtaining similar results to those obtained by Goland and Reissner in their theoretical study of lap joints. However, no attempt was made in refining the mesh distributions in the model at the most critical areas within the joint, i.e. overlap ends.

Wang et al. (1976) carried out a parametric study on single lap joints similar to Wooley and Carver's study, but refined the mesh at the edges of the bondline and the interface with the adherend sheet. The results from their studies showed how such mesh refinements could allow one to observe the variation of stresses across the bondline thickness, which previously were not noticeable with a coarse mesh. Wang also included a spew fillet in his joint analyses; however, the size of the spew was restricted to the thickness of the adhesive layer.

Cooper and Sawyer (1979) studied lap joints using both linear and non-linear finite element analyses. Results from their study showed that the maximum shear stress occurred at the edges of the overlap. Experimental tests were also carried out on similar joints using photo-elastic methods and results proved comparable with FE results and

theoretical calculations based on Goland and Reissner's method; which from the investigation, proved to be sufficient in predicting mid-surface stresses.

Adams and Peppiatt (1973) used a two-dimensional analysis, using plane-strain, triangular elements, to calculate the shear stresses in the adhesive layer and the stresses in the adherends acting at right angles to the direction of the applied load. Although their method was initially designed for lap joints, it was actually only valid for double lap joints, as they did not consider the large rotations involved in single lap joints. The method was one of the first to consider transverse shear stresses and proved valid in predicting tensile stresses in the adherends along the overlap for both single and double lap joints; where stresses are calculated at the centre-line across the adherend thickness.

Wang and Rose (1997) expanded on earlier work carried out by Adams and Peppiatt (1973) by investigating triaxial stresses of a thin adhesive bondline, i.e. shear, peel and transverse shear. Wang and Rose based their investigation on Adam and Peppiatt's work and developed an analytical solution to include such stresses; the analytical work was also validated through finite element methods. Results from the analysis showed the importance of taking into account longitudinal and lateral stresses as well as peel stresses in adhesive bonded joints. By taking into account these triaxial stress effects, peel stresses will be higher than the previous predictions.

Adams et al. (1978) were among the first to study the effect of adhesive spew on stresses in lap joints. In their investigation, they compared the effect of square-edges in the adhesive with spew adhesive fillets and how these affected the stresses. Hildebrand (1994a/b) was one of many workers to pursue the investigations carried out earlier by Adams et al. He studied the design and shape of the adhesive in lap and T-peel joints particularly for composite/metal structure using non-linear finite element methods. In his analysis, both lap and peel joints were optimised by modifying the geometry of the joint ends to give improved joint strength. Results from the study showed that composite/metal joint strength can be increased by 90-250% for lap and 200% for peel joints, with careful design of the joint end, e.g. tapering of the adherend/adhesive fillet.

Harris and Adams (1984) and Hart-Smith (1985) studied the effect of non-linear material properties using finite element analyses of adhesive joints. Harris and Adams' approach

took into account large displacements occurring in the joint and modelled both adhesive and adherends with elasto-plastic properties. The work was valuable as it showed the capability of finite element methods in predicting joint strength. Hart-Smith (1985) developed a numerical model which allowed for parametric investigations such as the effects of bondline thickness, joint length and adherend/adhesive material properties in order to reduce peel stresses within bonded joints.

Adams and Harris (1987) found that the fracture load was virtually unaffected by the presence of an adhesive fillet at the ends of the bondline if the adhesive layer was less than approximately 0.5 mm thick. The explanation to this concept was based on the fact that the fracture mechanism of adhesive joints often occurs due to the development and propagation of a 'damage zone'. This 'damage zone' may contain micro-cracks and hence does not fracture due to one single sharp crack but due to a collective number of cracks.

Aivazzedeh et al. (1987) carried out stress analyses on lap joints using different types of finite elements. The three finite elements included: 4-noded displacement elements (with 8 degrees of freedom and with 2 displacements at each node), 4-noded complete elements (with 20 degrees of freedom and with 2 displacements, 3 stresses at each node) and a mixed interface element (with 14 degrees of freedom and 2 displacements and 2 transverse stresses at each interface nodes). Results from the study showed that the more accurate analysis was carried out when mixed elements were used, and the displacement elements also gave good results as long as the model was refined.

Crocombe and Moulton (1988) used finite element methods to investigate the effects of changes in bondline thickness on the strength of lap joints. Experimental and theoretical methods were also carried out for comparison with the numerical analyses. Results showed that failure occurred within the joint and that it was influenced by the adhesive thickness. Experimental tests showed that thinner bondlines would give higher joint strength, thus failure load. However, results from the finite element elastic analysis predicted increases in stresses and thus, a decrease in the joint strength. Non-linear plastic analyses would provide more realistic predictions of joint strength. Later, Crocombe (1989) developed further his previous study by predicting failure of bonded joints through a global yielding criterion. Crocombe postulated that the lap joint would fail when the adhesive has yielded through the thickness of the joint, i.e. the whole overlap. His

criterion was applicable to lap joints when very ductile adhesives were used; however, the criterion was not accurate in predicting failure of other joint geometries.

Adams and Davies (1995) studied the effect of temperature on the behaviour of lap joints using a three-dimensional non-linear analysis. Different adhesive and adherend materials were used in the analysis to determine how variations in temperature would affect each one of them. Results from the analysis gave good comparison with actual joints and theoretical calculations. They also showed the importance of modelling the joint using a three-dimensional analysis, as the stresses were non-uniform across the joint width; this was partly attributed to transverse shrinkage and bending effects which will increase at elevated temperatures.

Work by Clark and McGregor (1993) suggested that joint strength could be predicted by evaluating the average stress over a finite area. This novel failure criterion was called 'ultimate tensile stress over a zone'. The main concept of the criterion is that *the maximum principal stress must exceed the ultimate tensile stresses of the adhesive material over a finite zone normal to the direction of the maximum principal stresses* [Clark & McGregor (1993)] and is independent of joint geometry. The size of the zone could be determined through a calibration process combining experimental and numerical analyses of joints.

Zhao (1991) proposed a two-step method for accurate stress analysis of a single lap joint and this was compared to initial theoretical work on bending moments. Hybrid elements were used in the analysis as these proved to be most suitable for bending problems; hybrid elements combine the displacement and stress elements giving a more accurate solution, in most cases. The method was proposed for non-linear stress analysis problems as it takes into account non-linear material properties.

Richardson et al. (1993) investigated the validity of modelling adhesive bonded joints using a two-dimensional and a three-dimensional finite element analyses. One of the main observations from their study was that the average load applied in the two-dimensional analysis did not simulate the loading conditions in the three-dimensional analysis. They observed that in order to correct the loading applied to the two-dimensional model, it was necessary to understand the load transfer between adherend/adhesive in the three-

dimensional analysis. In doing so, appropriate corrections could be done to reproduce the conditions of the three-dimensional joints at various positions across the joint width

Tsai and Morton (1994a) studied 2D geometrically non-linear finite element models of a single lap joint and compared their results to an improved theoretical analysis. They also investigated the three-dimensional state of deformation of single lap joints in linear elastic models allowing however, geometric non-linear effects in the boundary conditions. Results showed that 2D plane strain FE models are accurate for predicting the stress-state in areas away from the free surface. They also found that the introduction of small spew fillets reduces the maximum peel and shear stresses in the 2D and 3D models.

Sheppard et al. (1998) investigated the effects of singularities at the ends of adhesive joint by proposing a damage zone version based on a critical damage zone size; a modified version of the failure criterion was also proposed to predict failure load of the joint. The modified damage zone model was applicable to a number of various joint configurations and loading conditions.

Chiu and Jones (1992) studied the effect of stress distributions on lap and double lap joints by varying adherend and adhesive thickness. Results from their linear elastic analysis indicated that the shear stress distributions along the bondline were evenly distributed with higher stresses at the corners; these stresses could be reduced by increasing the thickness of the adherends. The normal (peel) stress distribution gave large peak stresses at the corners and these will have a significant influence on the failure of the joint. The region of high stress was noted to be less than 1.5 times the thickness of the adhesive. The peak stresses in the adhesive could also be reduced by increasing the adherend thickness; alternatively, different adhesives could be used.

Lang and Mallick (1998) studied adhesive spew using finite element methods and particularly, how spew geometry affected the peak stresses and stress distributions in single lap joints. Results from their study showed that by increasing the size of the spew, the peak stress concentration would be reduced when compared to square-end fillets (no spew); a similar characteristic was found by shaping the spew so that a smoother transformation between adhesive-adherend interface was obtained.

Lang and Mallick (1999) investigated the effects of adhesive voids on stresses in single lap joints using a linear plane strain numerical analysis. To simulate the voids, the middle region of adhesive within the overlap was removed. Lang and Mallick looked at the effects of various sizes of voids and compared these to joint with no adhesive defects. Stresses were measured in high stress concentration regions and therefore, the mesh definition around these singularity points was intensified. Results showed that larger voids did not increase the maximum stresses near the spew ends however, it created large localised stresses near the edges of the voids.

Wang and Rose (2000) studied corner singularities at the adhesive-adherend interface in bonded lap joints using finite element methods and developed an empirical equation for the distribution of stresses. Their main areas of interest were the adhesive corners particularly, whether the adhesive ends were square or had a spew fillet. The outcome of their study was an equation which gave a good representation of the stresses at the adhesive-adherend interfaces, for adhesives with square edge corners and spew fillet corners.

A summary of work on lap joints using finite element methods is reviewed above and is summarised in Table 4.1.

	3D Analysis	Non-Linear Analysis	Adherend/Bondline Thickness	Overlap Length	Adhesive/Adherend Modulus	Spew Fillet	Mesh Refinement at Overlap Edges	Voids and Defects	Element Study	Failure Criterion
Wooley & Carver (1971)			*	*	*					
Wang et al. (1976)			*	*	*	*	*			
Cooper & Sawyer (1979)		*		*			*			
Adams & Peppiat (1973)	*		*	*		*				
Wang & Rose (1997)	*									
Adams et al. (1978)						*				
Hildebrand (1994a/b)		*			*	*	*			
Harris & Adams (1984)		*			*					*
Hart-Smith (1985)		*	*		*					
Adams & Harris (1987)		*	*			*				*
Crocombe & Mout (1988)		*	*			*				*
Adams & Davies (1995)	*	*			*	*	*			
Clark & McGregor (1993)						*	*			*
Zhao (1991)		*							*	
Aivazdedeh (1987)							*		*	
Richardson et al. (1993)	*	*	*			*	*			*
Tsai & Morton (1994a)	*	*				*				
Sheppard et al. (1998)		*				*	*			*
Chiu & Jones (1992)			*		*		*			
Lang & Mallick (1998)						*	*			
Lang & Mallick (1999)						*	*	*		
Wang & Rose (2000)						*	*			

Table 4.1 Summary of finite element analysis work on single lap joints

4.4.2 Finite Element Analysis of Coach Joints

The T-peel joint, known as the coach joint in the automotive industry, is one of the common and most typically used joints found in a vehicle body structure. Most of the analytical studies of T-peel joints have been based on a stress analysis and in this section the literature is reviewed on modelling work carried out on coach joint configurations.

Crocombe and Adams (1981) used large elastic displacements in their finite element models to model rotations in peel joints. Such rotations proved to increase the stress concentrations within the adhesive and consequently resulted in a reduction of joint strength. The study showed the capability of finite element methods in predicting joint strength.

Work carried out by Ford Motor Company [Grant (1994)] studied the effect of adhesive fillet size, shearing burrs, substrate thickness, bondline thickness and bend radii on the strength of adherend lap shear and T-peel joints. The results from her study indicated that the shape of the spew fillet was very significant on the strength of the T-peel joint. The effect of bondline thickness on joint strength was not so significant except when there was no fillet. The effect of sheet bend radius was significant; as it was increased it caused a decrease in bond strength.

Gilchrist and Smith (1993) studied the behaviour of defects within the bondline on the joint strength for adhesive and spot-welded coach joints. Modelling was carried out based on a two- and three- dimensional plane strain analysis. Results showed that defects generally initiate within the adhesive fillet region and then propagate throughout the remaining bondline. Ideally, the maximum amount of adhesive should be used within the adhesive fillet area in order to increase the strength of a joint.

Fernlund et al. (1995) studied T-peel joints subjected to both tensile and three-point bending loads. The objective of the study was to predict the fracture load of adhesive bonded joints using FE models. Good agreement was found between the predicted loads and the actual loads obtained through numerical and experimental methods, respectively.

Many numerical studies have been carried out on the effect of design parameters on stresses. Apalak and Davies (1993) for example, studied the effect of varying the bondline

thickness on corner joints. Li et al. (1997) studied stresses in T-joints bonded to a rigid plate using linear elastic finite element analyses. The main aim of their study was to investigate the effect of different loading conditions, shown in Figure 4.6, and the effect of different design parameters, e.g. overlap length, bondline and adherend thickness, for similar loading conditions. Results from their analyses showed that when joints were subjected to a load in the negative x-direction (P_x) or to a bending load (M), then the maximum stresses occurred on the inside corner of the plate; stresses in the adherend were higher than those in the adhesive. For loading in the y-direction (P_y) results showed that the maximum stresses were concentrated at the left free end of the adhesive layer and this is where failure is expected to occur.

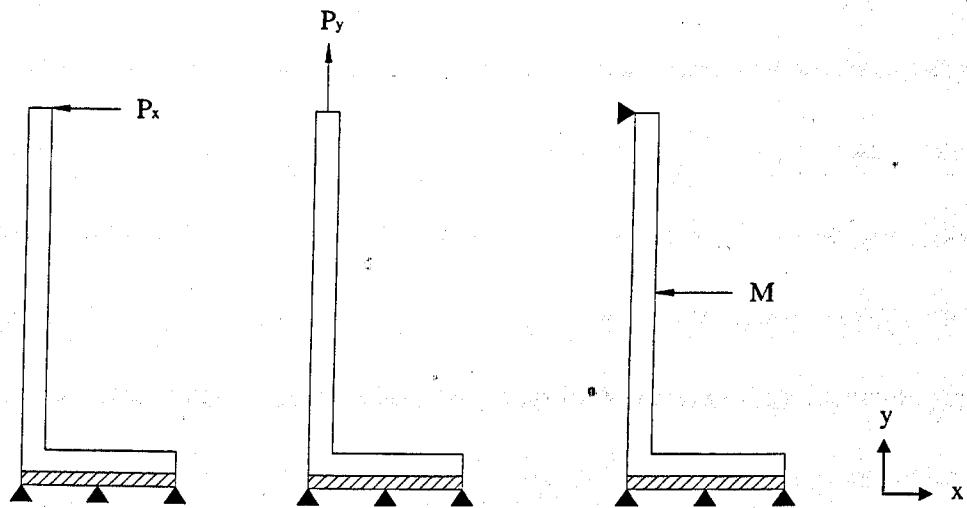


Figure 4.6 Schematic representation showing loading conditions used by Li, Blunt and Stout (1997)

The second investigation studied three design parameters for different loading conditions, namely: the effect of bondline length and the adhesive/adherend thickness. Results showed that increasing the overlap length of bondline would result in an increase in joint strength. Different loading conditions gave different effects generally, the results showed that increasing the bondline length would reduce the maximum stresses for a given load. The study on the effect of adhesive thickness showed similar trends in that by increasing the adhesive thickness would reduce the peak stresses along the adhesive layer for all loading conditions but increased the stresses at the free ends. By increasing the adherend thickness, the maximum stresses were also reduced, which for all load cases, occurred at the left free end of the adhesive layer. All three parameters were shown to significantly affect the stress distributions in adhesively bonded T-peel joints and emphasised the importance of joint design detail.

4.4.3 Prediction of Stiffness

The previous sections have reviewed the application of finite element methods to study stress distributions in adhesive joints. However, one of the key design parameters of particular interest to the automotive industry is the stiffness behaviour of body substructures and of the entire vehicle body. In this section, literature on the prediction of joint stiffness of bonded structures using finite element methods is reviewed.

Work by Eichhorn and Schmitz (1984) studied various joining techniques such as spot-welding, adhesive bonding and weld-bonding, and their effect on stiffness and strength performances of this sheet box structures. Three different box sections were considered and experimental tests were carried out to determine their performance to different joining methods. It was found that weld-bonding methods gave enhanced stiffness behaviour compared with equivalent spot-welded structures; to obtain an equally stiff structure, it would be necessary to double the number of spot-welds, i.e. halve the spot-welding pitch, in spot-welded structures.

Beevers and Kho (1983, 1984) also studied the effect of different joining methods on the stiffness of box structures. Various loading conditions were studied including torsion, flexure and compressive modes. Results indicated that bonded structures were significantly stiffer than beams formed by spot-welding and riveting. Also various types of adhesives were used and stiffer structures were obtained when using a higher modulus adhesive. Numerical models were used to investigate the effect of adhesive fillet size and forming bend radius on the overall performance of the structure. Results showed that ideally the bend radius should be zero and that the adhesive fillet size should be as large as possible for a stiffer structure.

Sakurai and Kamada (1988) investigated joint stiffness of automotive body structures using finite element techniques and compared the results with experimental tests. The main objective of the study was to use FE methods to predict the stiffness of structures as accurately as possible. A parametric study was carried out to investigate the effects of various design parameters on the bending and torsional stiffness of a complex vehicle structure, e.g. the rocker to centre pillar. The parameters investigated included the effects of various sized holes, different joining methods and changes in sheet thickness. Results showed that a reduction in stiffness was obtained when the apertures were positioned

closer to the joints, while increasing the number of spot-welds within the structure would increase the stiffness. One of the main outcomes of the study was that the modelling techniques used gave good predictions of stiffness.

Lee et al. (1997) investigated the potential of aluminium as a light-weight solution in vehicle bodies by means of finite element methods. The main purpose of the study was to understand how design variables, such as sheet thickness and joining techniques, i.e. weld-bonding, could influence the stiffness behaviour of aluminium structures to provide equivalent strength and stiffness to steel structures. Single lap and T-shaped joints were used in a linear static analysis to understand the effect of such design parameters on joint stiffness. Finite element models of weld-bonded joints were carried out using spring elements to represent the adhesive layer and shell elements for the adherends. Results showed that weld-bonded lap joints gave significantly greater shear stiffness compared to spot-welded joints and that as the spot-weld pitch increased, the enhancement of stiffness in weld-bonded joints is proportionally greater. Experimental tests of lap joints showed very similar results to the numerical models. Similar studies on T-shaped joints showed that joint stiffness was more affected by change in sheet thickness than with spot-weld pitch. Weld-bonded joints gave stiffness values that were approximately two times greater than equivalent spot-welded joints. Experimental tests confirmed the numerical predictions. A case study looked at investigating the stiffness behaviour of an actual vehicle substructure, i.e. the B-pillar. The sheet thickness and the spot-welding pitch were varied and the effects on stiffness were studied using FE analysis. Results confirmed the previous predictions from the analysis on typical joints, showing that weld-bonded aluminium structures would give greater stiffness values for larger spot-pitch and thicker sheets. The study showed that reinforcing sheets in needed areas could provide a lighter solution and a stiff structure. Another outcome from the investigation was that weld-bonding methods proved suitable for joining aluminium structures and provided structures with enhanced structural stiffness.

Pine et al. (1998, 1999) studied the torsional stiffness of box sections, commonly found in vehicle structures, through experimental methods. Spot-welded and bonded structures were analysed to explore how different design parameters such as sheet thickness, materials and sectional areas could be used to reduce the weight of structures while enhancing stiffness. Results showed that improvements in torsional stiffness could be

obtained through adhesive bonding methods without any significant increases in weight. Further enhancement in torsional stiffness was obtained by increasing the sheet thickness (from 0.8 to 1.16 mm) and the area of the box section (from 2500 to 3393 mm²). The resultant weight increase was 45% and 16%, respectively; thus, increasing the area of the section can enhance stiffness without significant weight gain.

Some of the latest finite element work on stiffness prediction was carried out by Hinopoulos and Broughton (1999) on T-peel joints. Finite element analyses were carried out to investigate the effects of environmental factors and geometric parameters on the performance of T-peel joints. Two-dimensional and three-dimensional numerical models were validated with experimental tests. The study showed that stress distributions and stiffness behaviour of T-peel joints are sensitive to changes in geometric design details e.g. adherend material properties, adhesive fillet, adherend thickness and the flange bend radius, and to changes in adhesive modulus arising from experimental exposure. An overall observation from the study was that results from the non-linear FE models gave stiffness results that were generally higher than those measured from the experimental tests. The departure between numerical results was mainly attributed to errors in the experimental tests such as manufacturing inaccuracies of the adhesive fillet ratio.

Most of the analyses for the prediction of stiffness are made on smaller joints using detailed numerical models. Because of the large sizes of vehicle models and the associated computational costs, simplified finite element models are typically used rather than detailed models. These simplified models facilitate design changes if required, yet they do restrict and limit the accuracy of the models in particular when bonded joints are being considered. Different modelling techniques have been used to represent these simplified models and these are presented in section 4.5.

4.5 Extended Applications of Numerical Modelling

The foregoing sections have highlighted the fact that finite element methods are now widely used to study and predict adhesive joint characteristics. With the recent rapid increase in computer capabilities, it is possible to develop joint models with large numbers of elements and high mesh densities to give fine resolution of stress distributions.

Finite element techniques are also used for the analyses of the mechanical behaviour of larger structures such as car bodies. However, because of the physical size of such structures it is necessary to use relatively coarse mesh densities which inevitably results in lower resolution of the analyses. The use of shell elements to represent the sheet panels in body structures combined with solid elements, which are mainly used to represent the adhesive bondline layer, gives greater computational efficiency but even with current computing capacity and sensible modelling, the size of these numerical models is limited. It is therefore still necessary to use approximations which introduce loss of accuracy in some structural details such as the effects of adhesive joint details. A number of attempts to reduce these inaccuracies have been considered by translating the characteristics of micro-models into larger macro-models [Nardini et al. (1990), McGregor et al. (1992), McGregor et al. (1993), Nardini & Hall (1995)].

4.5.1 Problems Associated with Micro to Macro Modelling

The main concern in macro models is the existent inaccuracy problems caused by assumptions and approximations in joint modelling. Approximations are generally made on the geometry of the joint such as the forming bend radius, the type of elements used in the model (shell-solid or solid element models) and modelling assumptions such as the inclusion or non-inclusion of geometric non-linearities.

Material property approximations are also made within the model due to the type of analysis used to represent the materials, i.e. linear elastic, non-linear etc. In addition, defects in the materials are usually neglected. Another important factor which significantly affects the accuracy of the FE model is the mesh density in large-scale models; the coarser the mesh, the less accurate are the solutions.

With the inclusion of adhesive bonding and weld-bonding methods in the vehicle bodies, there has been some concern over the validity and accuracy of the macro modelling techniques used, particularly in the combination of shell and solid elements. Some solutions have been devised to overcome these problems in macro models based on substitution elements, which can be inserted at appropriate points in the full model. The introduction of substitution elements, such as spring elements and joint-line elements, into the macro models has proved to be an effective technique to improve joint details and the

accuracy of large structure finite element models. Some of the existing solutions to macro modelling approximations are discussed in the following section.

Super-elements / Sub-structuring

Super-elements can be used as a solution to reduce inaccuracies of macro models. As illustrated in Figure 4.7, super-element number 2 can be modelled to include precise details of the joint and then coupled to the other super-elements 1 and 3.

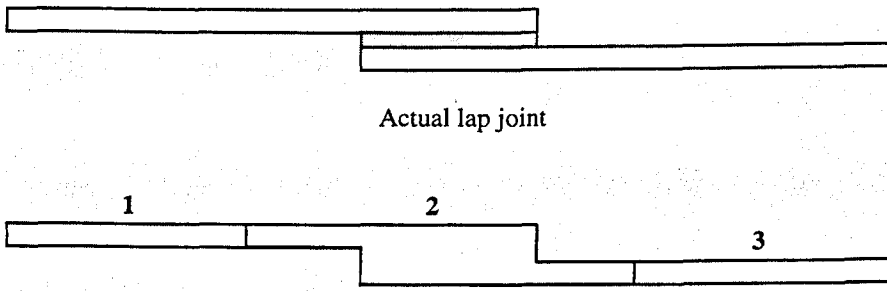


Figure 4.7 Super-element representation in a lap joint

The main advantage with introducing super-elements in large-scale models is that all geometric details can be accommodated and that localised redesign requires only partial re-analysis, consequently resulting in less processing time for large problems. One major disadvantage with this technique is the limitation of the total number of super-elements which can be written into models in some FE packages. They are also limited to linear elastic analyses.

Spring Elements

Spring elements have been considered as a means of including joint details in jointed structures [Nardini et al. (1990)]. In the approach, spring elements are placed between the nodes, creating a small separating distance between the nodes, as illustrated in Figure 4.8. Spring elements have six degrees of freedom; three in translation (u_x , u_y , u_z) and three in rotation (ϕ_x , ϕ_y , ϕ_z).

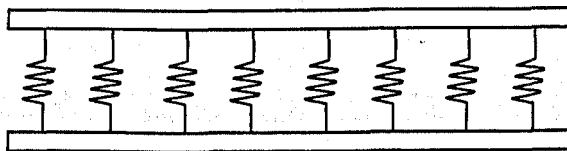


Figure 4.8 Spring-line element representation

The advantage with using spring elements is that these elements correct any geometrical approximations that exist in larger structure models. There are however, some disadvantages as there are no stress results and there are difficulties associated with defining local co-ordinates for their implementation.

Joint-Line Elements

The joint-line element method [McGregor et al. (1992), Nardini & Hall (1995)] has been developed as a method to overcome problems associated with large models or macro-modelling methods. Joint-line elements contain all the geometric and material properties of an actual joint; as for example, tensile and bending stiffnesses. These properties could also be determined through micro models of joint which include all geometric details, i.e. flange, bondline, etc. Figure 4.9 shows the actual joint configuration and the modified model with the inclusion of joint-line elements.

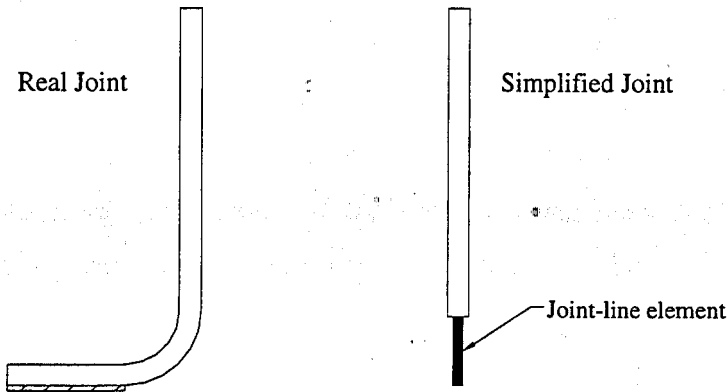


Figure 4.9 Inclusion of the joint-line element method in a coach joint

The joint-line element method is valid for equivalent orthotropic material models and proves to be quite appropriate as it maintains the physical properties of the structure to be modelled. The advantages of introducing joint-line elements include the availability of resultant stress outputs and the simplicity of the geometry to be modelled. One of the main disadvantages however, includes the fact that the geometry and the loading effects are still not accurately represented and a specialised pre-processing package is required.

4.5.2 Alcan Approaches to FE Modelling Methods of Car Body Structures

As a response to the motor industry's intent to use aluminium in car construction, Alcan, a primary aluminium material supplier, established a major research initiative to support this

new technology [Nardini et al. (1990), McGregor et al. (1994)]. A substantial group was formed to address problems associated with the joining of aluminium sheet components. The main scope of their work was to optimise joint design and performance through the application of appropriate analytical methods.

Parametric Study of Adhesive Bonded Joints

Initial work carried out by Alcan on adhesive bonding for joining aluminium structures was published in 1987 [Marwick & Sheasby (1987), Wheeler et al. (1987)]. The main objective of their study was to understand the limitations associated with large-scale modelling techniques, and to develop a modelling method that would incorporate adhesively bonded joint details for aluminium structures.

In the first stage, Alcan carried out an extensive parametric study of various adhesive joint configurations to investigate how different design details and joining techniques would affect the behaviour of aluminium joints. Some of geometric details studied in the parametric investigation were the effects of material thickness, forming radius, spot-welding pitch and fillet size on joint behaviour. The study was aimed to provide a better understanding of adhesive joint details and the need to compensate for their inadequate representation in large scale models; thus, better predictions of the joint behaviour could be derived.

Detailed FE models of coach joints (T-peel joints) were designed using solid elements to provide accurate analyses. It should be noted that because of size limitations, solid elements are not often used to represent large and complex structures. Also, because of the nature of solid elements, they are only typically used in cases where a structure is least subject to bending. Figure 4.10 shows a detailed model of a coach joint showing geometric details such as the forming bend radius and the adhesive spew fillet size. Finite element studies were carried out using a linear elastic analysis. The results from the analysis indicated that points A and B were the locations of the maximum principal stresses in the adhesive and in the aluminium sheet, respectively. Various joint details were then modelled with the aim to try to reduce the stress concentrations in the bondline. All results from the parametric study were calculated in terms of a stress ratio, which was the maximum stress per unit stress applied to the specimen.

This first study looked at the effect of the forming bend radius on stress. Results showed that when the size of the bend radius increased, the adherend stress ratio increased. However, the stress ratio within the adhesive bondline remained constant for various bend radii. The reason for the increase in the stress ratio of the aluminium adherend is due to the local bending occurring in the area of the forming radius; as the size of the forming radius increases so does the local bending resulting in higher stresses within the adherend.

The second parameter studied was the influence of the bondline thickness on the stress ratio. Results from the finite element analyses showed that for thinner bondlines, i.e. 0.2 mm, the stress ratios were high. As the thickness of the bondline increased to a value greater than say 0.8 mm, the stress ratio was at a constant value of approximately 1. This means that no further improvements in joint strength would be achieved by increasing the bondline thickness to a value greater than 0.8 mm. This is primarily because coach joints are subjected to peel stresses and hence, increasing the bondline thickness to a certain extent will improve the performance of the joint. Similar studies on lap joints indicated a reverse effect; as the bondline increased, the joint strength decreased. Thus thinner bondlines in single lap joints will result in a stronger structure since the joint is primarily subjected to shear stresses.

A third study looked at the effect of adhesive fillet size on joint behaviour. This study is of great importance because most FE models of vehicles ignore fillet size and simply

model a fully flanged adhesive. Before investigating the results from the parametric study, it is first important to define fillet size. ALCAN defined adhesive fillet size as *the distance from the start of the forming radius to the contact point between the adhesive fillet and adherend, as a percentage of the external forming radius* [McGregor et al. (1992)], and is represented schematically in Figure 4.11. Therefore, a 0% fillet ratio represents the condition where there is no adhesive beyond the start of the forming radius; and with a 100% adhesive fillet, the whole forming radius is filled with adhesive.

The study on the effect of adhesive fillet size (ratio) on the stress ratios and strengths of different joint geometries of aluminium bonded joints gave significant results. The stress ratio in both the adhesive and adherend was significantly reduced as the fillet size was increased. By examining the stress distribution along the bondline, shown in Figure 4.12, it can be seen that most of the load transfer and hence, greatest stress along the bondline occurs in the region of the fillet. A larger fillet will reduce the moment at the edges of the adhesive and also provides a greater area to reduce the stress.

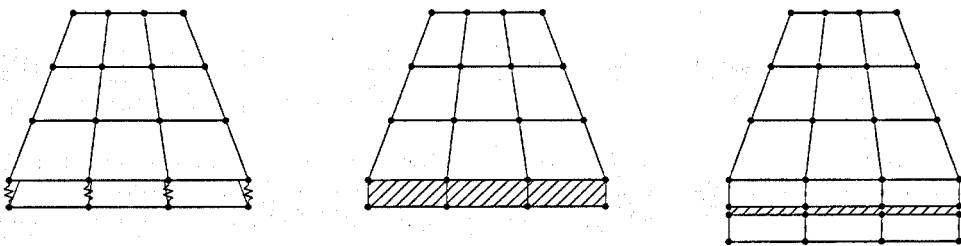
Results from the parametric study generally showed that the joint strength of T-peel joints is significantly influenced by the geometry of the structure such as the adhesive fillet ratio and the geometry of the sheet bend radius. Ideally, to obtain stronger joints, a flange fully filled with adhesive, i.e. 100% fillet ratio should be used. However, this is not always the case in actual joints where fillet size is variable primarily due to manufacturing effects.

Similar studies on lap joints do not show such a high sensitivity to fillets as in T-peel joints. It should be noted that coach joints are more representative of joints typically used in vehicle structures primarily because of the flanges which allow access for spot-welding. The general outcome from the investigation was the importance of including accurate geometric details of adhesive bonded joints in FE models in order to obtain more representative predictions of joint behaviour. Experimental tests were carried out on similar joints to confirm the validity of the numerical models.

Representation of Adhesive Bonded Joints in Large-Scale Models

The initial parametric study of adhesive bonded joints showed that geometric details such as the forming radius, the fillet size and the bondline thickness, have a significant influence on the behaviour of a bonded structure. The second stage of the work [Nardini et al. (1990), McGregor et al. (1992), Nardini & Hall (1995)] looked at improving current modelling techniques of bonded structures, which lacked such geometric details.

The study presented alternative ways of representing the bondline in finite element models, shown in Figures 4.13 (a)-(c) and 4.14 (a)-(d), to compensate for structural details such as forming bend radius, bondline thickness and adhesive fillet ratio.



(a) Thin plates & spring model (b) Thin plates & solid model (c) Thick plates & solid model

Figure 4.13 Alternative methods for compensating joint details in FE models

In the first model (a), the sheet is represented by thin plates (shell elements) and the adhesive layer by springs. When using this modelling technique, the stiffness of the joint is calculated in three co-ordinate directions: F_x , F_y and F_z . This model represents the actual adhesive joint quite well, even though the stresses within the adhesive cannot be determined. The second model (b) uses thin plates to represent the sheet, and solid elements to represent the adhesive layer. This method is commonly used in industrial FE models today. To accurately represent the bondline thickness and joint behaviour within the model, the distance between the plates must be adjusted and the material properties

modified. Another proposed method of modelling adhesive joints is to use thick plates and solid elements as shown in (c). In this model there are no approximations in geometry, i.e. thickness however, it is essential that thick shell elements (and not 3D solid elements) are used in order to represent flexural behaviour adequately; since solid elements have three degrees of freedom and are less accurate for representing bending.

Figure 4.14 (a)-(d) shows similar modelling methods to Figure 4.13; however, now these are applied to flange-type joints.

The first technique (a) disregards the flanges from the parts and thus represents a continuous connection between the sheets. With this model, any stiffness that would result from the presence of a flange is therefore neglected. As a result, the continuous joint provides an overestimated stiffness, while the lack of the flange causes a lack of stiffness. In effect the two counterbalance to some extent thus, providing a reasonable approximation of the overall structural stiffness even though this is just due to a cancellation of stiffness errors. Variant (b) represents a model where the flanges are included; however, the method does not take into account the variation of thickness of the two flanges and does not model the offset between the two sheets for the adhesive layer. Model (c) however, accounts for separate flanges which are connected between each other through nodes, but does not account for a bondline thickness. In figure (d) a model of a flange joint is represented showing individual flanges which take into account sheet and bondline thickness. This model is thought to be best representative of the actual joint.

From the work carried out, it has been shown that the absence of flanges in FE models significantly reduces the overall stiffness of the structure. Also, from the parametric work on detailed joints, it was clear that the performance of adhesive structures was significantly influenced by the geometric variables of the joint. Alcan therefore, developed a modelling methodology which could be used to provide a more accurate prediction of adhesively bonded structures in vehicles [McGregor et al. (1992)]. The main feature of their proposal was based on the joint-line element method, discussed earlier in section 4.5.1. The function of joint-line elements is to accurately represent the stiffness properties of the joints in order to enable accurate predictions of overall structural stiffness and dynamic responses [Nardini & Hall (1995)]. The principal stage in their methodology was to model the joint-line areas within the full-scale FE models of the structure.

A NASTRAN based software called the Joint-Line Generator was developed to simplify the implementation of the joint-line elements in FE models of shell element type structures. The code identifies the joints and connection lines between surfaces and inserts joint-line elements (shell elements) at the joint lines. The main loading conditions of each structure is investigated, and the stiffness values at those loads are used to derive the equivalent material properties for the joint-line elements; these properties approximate the details of the forming radius and joining system so that the stiffness corresponds to the actual stiffness of the real joint. The resultant FE structure is a model having original geometry and properties, complemented with the additional elements from the joint-line elements. Figure 4.15 shows an example of how the Joint-Line Generator creates joint-line elements at the interfaces of the four components in the structure.

The overall number of nodes and elements in the FE model will increase only slightly after joint-line elements are inserted. However, if joint-line elements were not used and actual joint geometries such as the flanges were modelled, then the total number of elements and nodes would be significantly larger.

4.5.3 Other FE Modelling Approaches

Work carried out by Sharman and Al-Hammoud (1987) studied the effect of local details on the stiffness of car body joints using FE modelling techniques and comparing them to experimental tests. The main aim of this investigation was to determine the accuracy of modelling techniques in the prediction of stiffness of vehicle structures. The study also aimed to show how joint details, which are inaccurately defined in vehicle models, would affect the overall stiffness results. Three structures within the body frame, mainly the A pillars, were considered in the investigation. Within each structure, various joints were identified and modifications were carried out on each one in order to determine their effects on stiffness. Figure 4.16 shows some of the modifications that were investigated in the FE analysis. The position of the nodes represents the spot-weld connections.

Results from the numerical analysis showed that increasing the spot-weld pitch in areas of high stresses would contribute to a significant loss in stiffness. The presence of the flanges had major contributions in stiffening the structure and this was dependent on the position and pitch of the joint (nodal) connections. Results also showed that variations in bondline thickness did not significantly affect the stiffness. One observation from the study was that finite element predictions were generally stiffer, by approximately 13%, than those measured from experimental tests of similar structures.

Wu and Crocombe (1996) used three different modelling techniques to analyse different adhesive joints including lap and T-peel joints. The first method represented a simplified model using different beam elements in the adherend and plane four-noded isoparametric elements in the adhesive layer. Because of the different element used, the nodes at adherend-adhesive interface were connected through rigid couplings. This simplified model did not take into account local deformations of the adherend and the displacements between the two different elements. The second modelling approach, called the two-dimensional continuum method, improved the simple first modelling approach. Both adherend and adhesive were modelled using similar elements, i.e. four-noded isoparametric elements, and mesh patterns. In these models, the adherend thickness was represented with four elements while only one element was used across the adhesive thickness. The third model, described as a hybrid version of the simplified modelling method, used quadrilateral elements in the adhesive layer and in critical areas within the adherends which gave high stresses, such as the corners of T-peel joints; the remaining adherend region was meshed using beam elements. The hybrid approach combined the first and second modelling techniques together to provide a method for obtaining reliable stress results at reduced computational time.

Kim et al. (1995) investigated the accuracy and applicability of current modelling techniques to represent vehicle structures. Simplified FE models of vehicle structures are usually represented using shell elements for the sheets and spring elements (rotational and translational) which have been primarily used to represent joints in vehicle structures as they accommodate for joint flexibility. This study emphasised the need to represent joints more carefully and accurately in FE models in order to correctly predict the static and dynamic behaviour of structures. The method included the use of short-beam elements instead of the conventional spring elements for joint modelling. One of the main

advantages in using short-beam elements is that sensitivity analyses can be carried out for a variety of commercial FE packages; such an analysis is not always available for non-structural elements such as spring elements. Preliminary results showed that the method was valid and applicable to vehicle structures.

4.6 Summary

The study of stresses in adhesive joints is an extensive area of research and much has been already published. The applications of analytical methods, numerical modelling and experimental techniques to typical adhesive joints prove valuable tools for providing an understanding of joint behaviour. In automotive vehicle structures, joint stiffness is an important characteristic as this determines the behaviour such as the drive, comfort and life of a vehicle. A stiff body also leads to reductions in noise and vibrations and thus, enhances passenger comfort. Because of the size and complexity of vehicle bodies, closed-form solutions are difficult to apply and require unacceptable approximations and assumptions. Numerical methods, such as finite element analyses, have proved to be more practical and applicable for the study of stiffness behaviour of larger vehicle structures and bodies.

The modelling of large structures, such as car bodies, involves many geometric approximations because of the large-size of the model and the associated computational costs, i.e. time, information, storage and staff. Finite element models are initially derived from CAD models which are directly supplied from car manufacturers. CAD models include a number of geometric approximations particularly when representing joint details such as the flange corners; these are represented with sharp edges rather than with radiused corners. Consequently the FE models also include such approximations. Another problem with FE models of large components is associated with the difficulties of combining different modes of analyses such as static and instability analyses, simultaneously. To reduce the overall number of elements and hence reduce the size of the model and the running time, geometric details such as sheet bend radii are simplified and represented using shell elements. Spot-welded joints are represented by rigid links while adhesive bonded areas can be either represented by rigid spring elements or by solid elements. As these techniques still involve a number of approximations, some uncertainties remain in the validity and accuracy of FE model predictions, and particularly

that the global vehicle stiffness predictions may not accurately represent the actual vehicle structural performance.

There is therefore, a need for efficient modelling techniques that will give more accurate predictions of bonded vehicle characteristics without exceeding computer capabilities. Several research groups have approached this micro to macro modelling problem by using various FE techniques. Most of these solutions accommodate corrections in full body analyses through the addition of substitute elements such as joint-line elements, spring elements and super-elements to represent the characteristics of the joints. However, in most cases the study of joint behaviour is initially carried out on small representative joints which enable all the joint details to be analysed on a high resolution micro model. This is because the accuracy of the micro models is much higher than the macro models used in larger FE analyses of structures. One of the problems remaining is the translation of joint stiffness characteristics from micro models to macro models for the analysis of larger and more complex structures. Some of the existing solutions are able to provide representative joint characteristics but they introduce problems in large-scale models particularly in terms of ease of use, limitations in convenient FE packages and processing time.

The aim of the micro to macro modelling concept is to provide a tool for translating joint properties, such as geometric details and material properties, into larger models which lack this accuracy. In Chapter 6, a novel concept has been devised to overcome these difficulties. Instead of adding a modified element to compensate for existing errors, an undercut element concept, which accounts for joint details often neglected in macro-models, is introduced. The concept and application of the undercut element method will be discussed in the following chapters.

5. ANALYSES OF ADHESIVE JOINT BEHAVIOUR

5.1 Introduction

It is necessary to study and understand joint characteristics and the behaviour of small-scale joints before trying to predict the behaviour of larger structures. Particular emphasis is made on predicting the stiffness of joints when subjected to various loading conditions, such as tensile and flexural loading. The analysis of stiffness in smaller joints provides a better understanding of the behaviour of such joints in service and should enable a more accurate prediction of the stiffness of larger structures such as car bodies, for example. The stiffness characteristics of joints in vehicle bodies are important to the design as they have a major influence on the noise, vibration, comfort and handling of the vehicle. In this chapter, various typical joint configurations are investigated through numerical modelling techniques and experimental testing methods.

5.2 Single Lap Joints

One of the most common types of adhesive joints is the single lap joint. Because of its simple and symmetric shape, this type of joint is used frequently in experimental studies to compare the effect of different adhesives, surface treatments and processing methods on joint properties. Lap joints are also used to compare adhesive bonded joint characteristics with other joining methods, such as spot welding, clinching and fastening. The lap joint is also relatively amenable to finite element analysis for the prediction of joint behaviour. In the automotive industry, lap joints are widely used to provide data for selection and specifications of adhesives and also, to investigate a range of different loading conditions, which may prove difficult to carry out on larger or more complex structures.

The main objective of the work described in this section was to develop finite element models of adhesively bonded lap joints, and to predict the behaviour of these joints in terms of stiffness. The results from these numerical models were also compared with other published work on similar lap joints, to provide confidence in the FE modelling

techniques that are currently used. Further validation was also established through experimental tests carried out on similar joint configurations. An extended parametric study was then carried out through FE models and experimental testing; these were used to evaluate the effects of certain design parameters including sheet thickness, bondline thickness and overlap lengths, on the performance and the overall stiffness of the joints.

5.2.1 Joint Definition

The basic geometric configurations of the lap joints were chosen to enable accurate experimental joints to be made and to provide the basis for the development of acceptable numerical models. Details of the lap joint configurations are illustrated in Figure 5.1 and with the following material properties (Table 5.1).

	Material	Tensile Modulus E (GPa)	Poisson's Ratio ν
Adherend	Mild Steel	207	0.29
Adhesive	TEROSTAT 3218F	0.006	0.4
	CIBA XB5315	1.8	0.4

Table 5.1 Basic material properties of single lap joint configuration

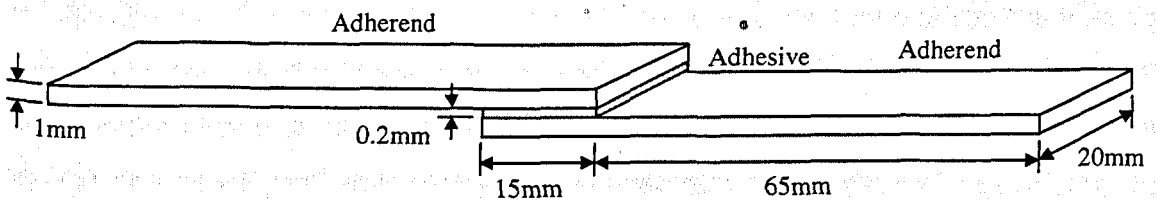


Figure 5.1 Geometry of initial lap joint configuration

Only the design variables under investigation, such as adherend/adhesive thickness, adhesive modulus and overlap length were changed to study their effects on joint stiffness. Peel and shear stresses of adhesive lap joints were also studied initially, and how different design parameters affected the stress distributions along the bondline.

The adhesives used in the experimental studies were a low modulus polybutadiene (TEROSTAT 3218F) and a high modulus epoxy (CIBA XB5315). The tensile moduli of the two adhesives were 0.006 GPa and 1.8 GPa, respectively. The bondline thickness was kept constant at 0.2 mm using ballotini, or glass beads, to maintain the desired thickness. The adherends were made out of mild steel sheets, ranging from 0.8 mm to 1.2 mm, with an increment of 0.2 mm.

5.2.2 Experimental Testing

Mild steel lap joints were prepared with TEROSTAT 3218F (polybutadiene) and CIBA XB5315 (epoxy) adhesives, for a range of overlap lengths and sheet thicknesses. Coupons of 20 mm width were degreased with methyl ethyl ketone (MEK), grit-blasted with 60- μ m alumina grit and then once again, degreased. The surface preparation was required to ensure that the adherend surfaces were uniform and free from any oils or grease contaminants. A small proportion of ballotini, approximately 1% of weight, was added to the adhesive to control the bondline thickness. The adhesive was then spread along the required bonded area on one of the adherend plates. Some initial problems were encountered when trying to apply the lower modulus adhesive (TEROSTAT 3218F) to the plates; this is associated with the high viscosity of the adhesive. Hence, it was necessary to use a heated gun to warm the adhesive until it reached an almost liquid state suitable for application.

The overlap lengths were accurately controlled and formed by means of a steel jig, which was adjustable to produce specimens of different overlap lengths. Surplus adhesive was scraped from the edge of the joint overlaps to minimise the adhesive spew fillet. The specimens were clamped with bulldog clips to ensure accurate fixture prior to and during the curing process, and the joints were then cured according to the adhesive specifications; the conditions for both adhesives were specified at 180°C for 30 minutes. Three joints were made for each parametric configuration investigated.

All lap joints were tested in a Testometrics 10 kN testing machine at an extension rate of 2 mm/min, shown in Figure 5.2. Joint specimens were placed into the testing machine, and 10 mm at each end of the specimen were tightly secured through wedge grip jaws. Packing pieces were included within the grip area to provide uniform alignment.

A linear variable differential transformer (LVDT) extensometer with a 50 mm gauge length was clipped symmetrically across the lap joints, as shown in Figure 5.3. The extensometer was calibrated and fully integrated with the testing machine operation, so that its signal could be digitally processed through an appropriate PC software package. The associated analytical code enabled accurate load-displacement curves and stiffness values to be generated automatically.

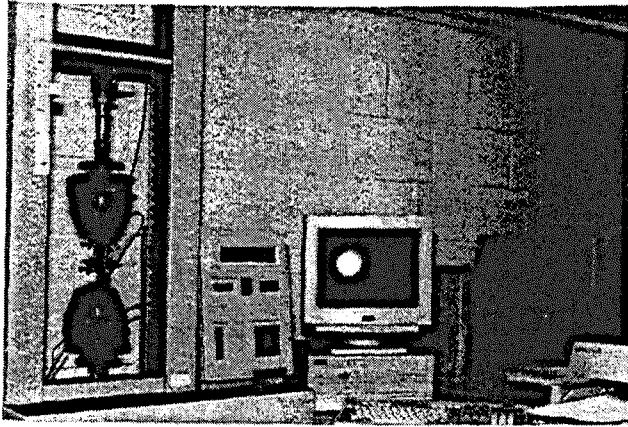


Figure 5.2 Testometric 10 kN testing machine

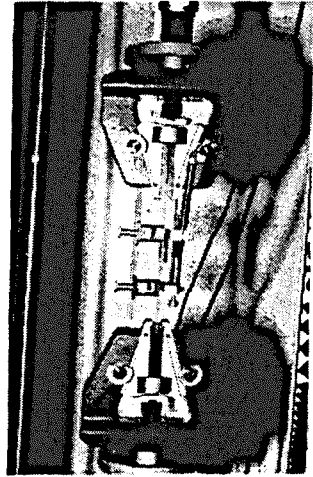


Figure 5.3 LVDT extensometer of 50 mm gauge length

Representative outputs are illustrated in Figure 5.4 which shows the resultant load-displacement curves of the extensometric measurements of lap joint specimen, with CIBA XB5315 and TEROSTAT 3218F adhesives. Stiffness values are calculated by obtaining the slope of the linear part of the curves.

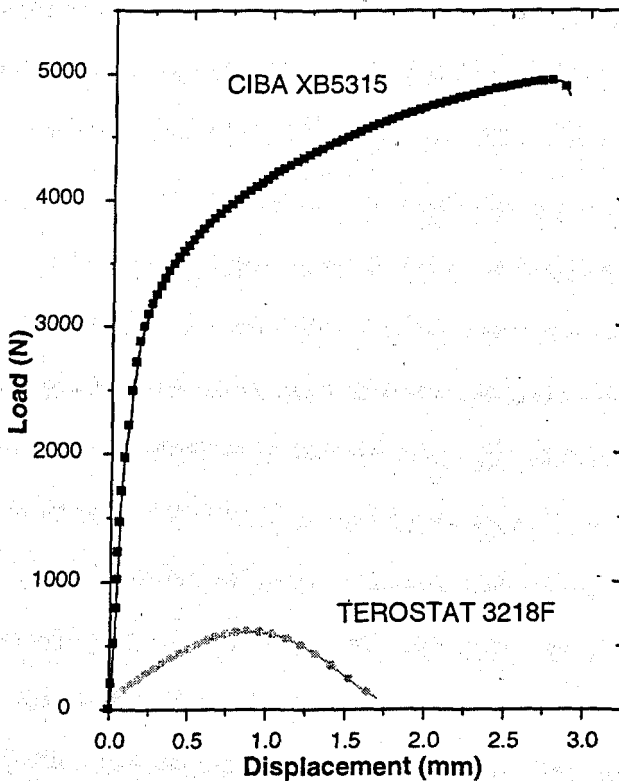


Figure 5.4 Typical load-displacement curves obtained from the experimental tests

Some of the load-displacement curves exhibit non-linearity at fairly low load levels, particularly for joints with short overlap lengths and polybutadiene adhesives. The stiffness values were therefore taken from the slope of a chord to a selected load level, where the departure from linearity was not excessive. In practice however, these values are slightly lower than the tangential slope at zero load. Results from the experimental tests are presented in section 5.2.4 and compared with FE model predictions described in section 5.2.3.

5.2.3 Numerical Modelling

Initial finite element modelling was carried out on single lap joints, similar to the configurations shown in Figure 5.1. ABAQUS Version 5.8 FE code [ABAQUS User's Manual (1998)] was used to study the effects of different parameters on the stiffness of adhesively bonded single lap joints, when subjected to tensile and four-point bending loads.

All of the work described for the parametric study of lap joints was based on 2D linear elastic models with solid elements. Plane strain analyses were used, since the adherend width was large with respect to the adherend thickness. Three were used to define the mesh across the bondline while six elements across the adherend thickness. Eight-noded quadrilateral elements gave an approximate total of 720 elements and 2365 nodes in each model; this was found to give an appropriate prediction of stiffness. Other modelling methods and techniques have been studied and these will be discussed later in section 5.2.5, on similar lap joint configurations.

Uniform and biased mesh seeds were used to define appropriately the mesh densities in high stress level regions, as shown in Figure 5.5. Because of the high stress concentration at the edges of the adhesive/adherend overlap, the meshing was progressively refined using two-way biased elements along the bondline; this provided improved resolution in critical areas. The remaining sheet material was meshed using uniformly spaced elements, as those areas were less significant to the performance of the overall structure.

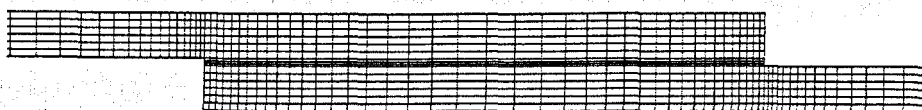


Figure 5.5 FE model of lap joint showing two-way biased mesh elements along the overlap length

All models were subjected to a tensile force at one end of the joint and constrained in the horizontal and vertical directions at the other end. A shear force of 300 N/mm was applied to each model, thus inducing an average shear load of $\tau_{av} = 20$ MPa along the bondline (for a 15 mm overlap). The adherend plates were constrained in the y-direction (normal to the plane) at both ends. Figure 5.6 represents the loading and boundary conditions used in the analyses.

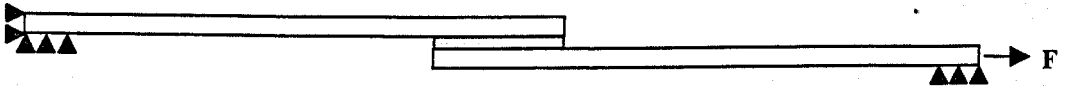


Figure 5.6 Boundary conditions of lap joint in tensile loading

Joint stiffness values were calculated for the geometric conditions used in the experimental tests, by determining the relative displacements of the elements located at 25 mm on each side of the joint centre line. The extension over this equivalent gauge length was obtained from the difference between the displacements in the x-direction, for an effective load of 300 N acting on a joint unit width of 1 mm. The stiffness was then calculated as the force required to produce a 1 mm extension in a joint of unit width of 1 mm, i.e. N/mm.mm.

FE Convergence Analysis

Before investigating the parametric FE study of single lap joints, a series of models were used to investigate convergence of results. In FE models, it is important to define a sufficient amount of nodes and elements in order to obtain accurate results. However, it is equally important not to exaggerate in the overall number of nodes/elements, as this will result in large computer processing time. In this study, the number of elements across the sheet and bondline thickness and length, were altered. Results showed that increasing the number of elements across the adhesive thickness to exceed four elements only altered the resultant stiffness by 1%. A parallel analysis was also carried out on similar joints using shell-solid element models and showed similar convergence results. All results presented are based on FE models which used the minimum amount of elements required to give accurate stiffness values.

Parametric Study

Once the basic model was established and sensible results were obtained, the joint dimensions and adhesive properties were varied to explore the effects of each variable on

joint stiffness. Table 5.2 shows a list of the variables used in the parametric study.

	Initial Joint Configuration	Variables						
Adherend Modulus (GPa)	207 GPa							
Adherend Thickness t_s (mm)	1.0 mm	0.8	1.2					
Overlap Length (mm)	15 mm	5	10	20	25	40		
Adhesive Thickness t_b (mm)	0.2 mm	0.1	0.5					
Adhesive Modulus (GPa)	1.8 GPa	0.006	0.02	0.1	0.2	1	2.5	

Table 5.2 Variables of parametric study on single lap joints

5.2.4 Initial Results

Experimental Testing

Initial results are shown in Figures 5.7 (a) and (b), where experimental and FE models results are compared to each other for low and high modulus adhesives, respectively.

Parametric Study

Figures 5.8 and 5.9 give the results obtained from the parametric study on various lap joint configurations. In Figures 5.8 (a) and (b), the effects of overlap length and sheet thickness (t_s) on joint stiffness are studied using TEROSTAT 3218F and CIBA XB5315 adhesives, respectively. The effects of the bondline thickness on joint stiffness are investigated for similar adhesives in Figures 5.9 (a) and (b). Figure 5.10 shows the results of the study on the effect of adhesive type on joint stiffness; this was carried out by modifying the value of the elastic modulus of the adhesive used in the FE analysis.

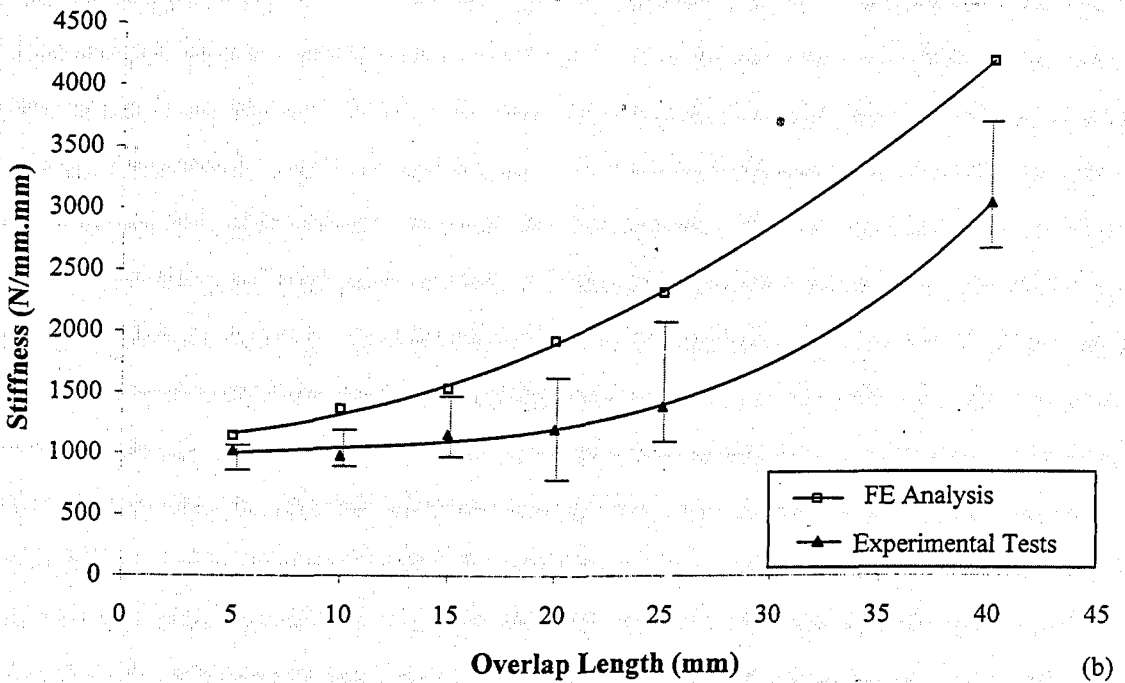
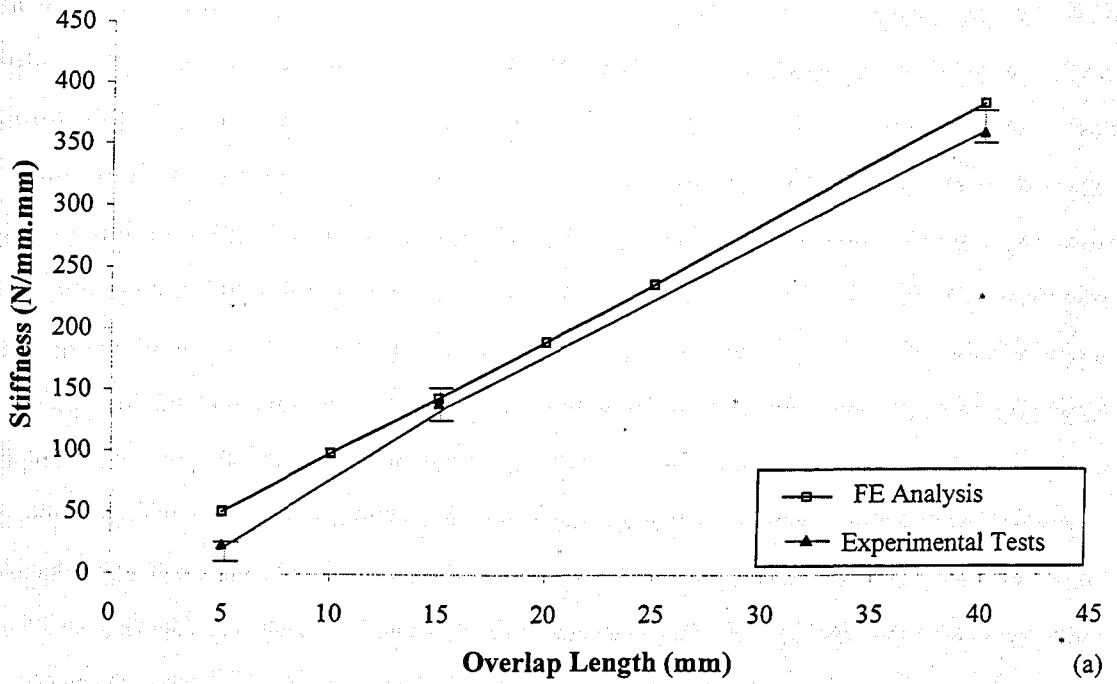


Figure 5.7 Comparison between experimental tests and FE results for single lap joints using a) TEROSTAT 3218F and b) CIBA XB5315 adhesives
(Error bars indicate the maximum and minimum values calculated from the experimental tests)

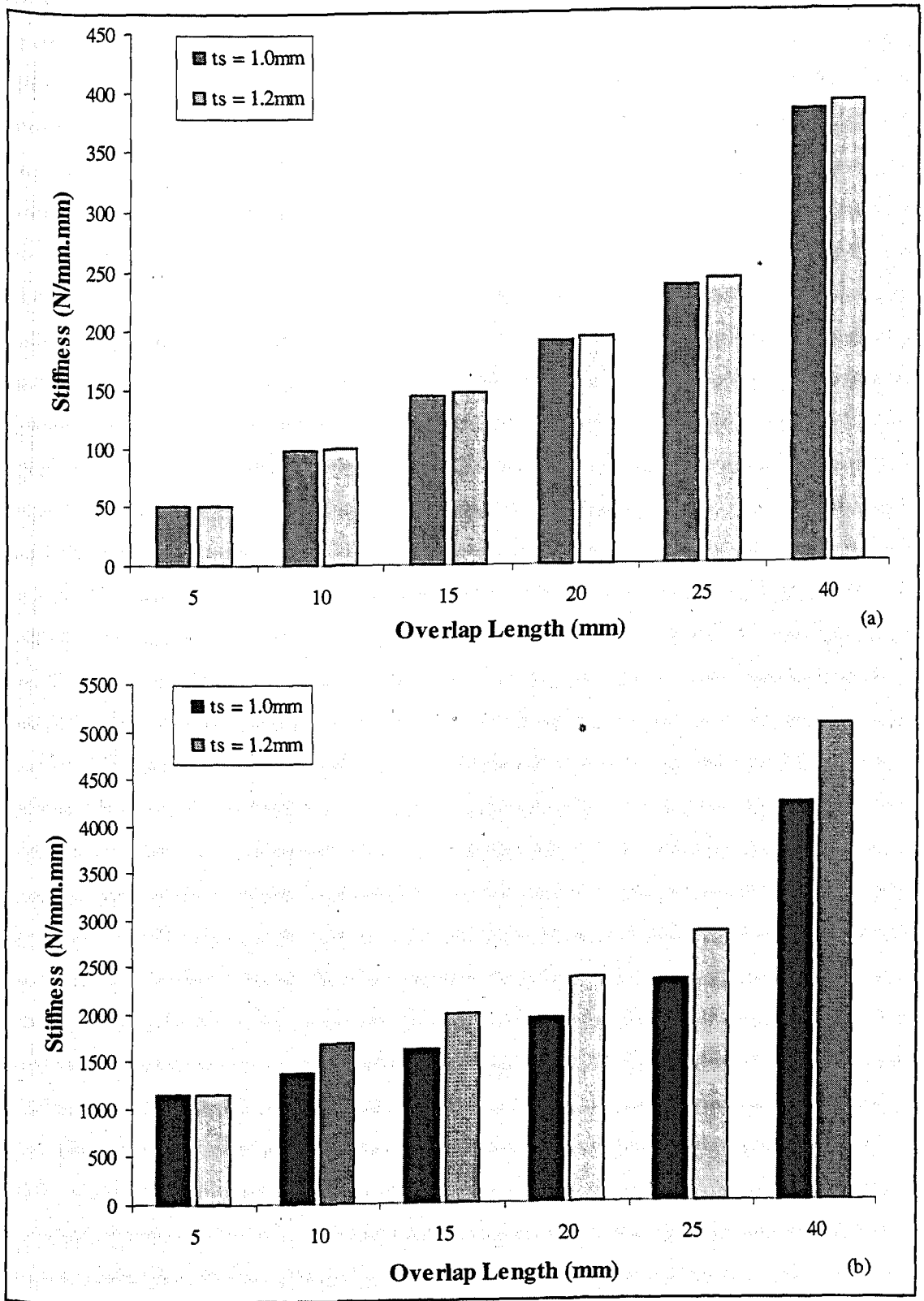


Figure 5.8 Variation of joint stiffness with sheet thickness and overlap length for single lap joints using (a) TEROSTAT 3218F and (b) CIBA XB5315 adhesives

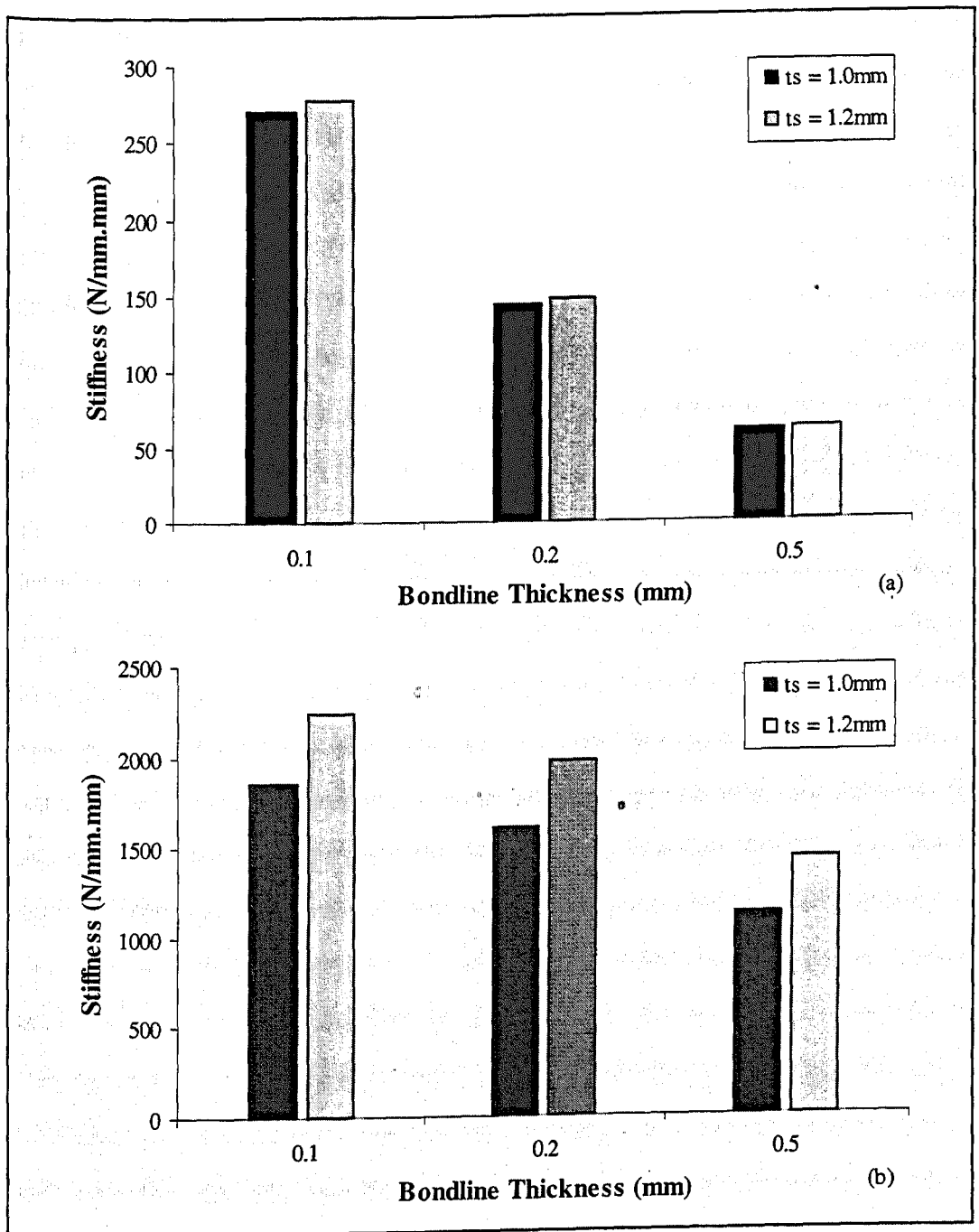


Figure 5.9 Variation of joint stiffness with sheet thickness and bondline thickness for single lap joints using (a) TEROSTAT 3218F and (b) CIBA XB5315 adhesives

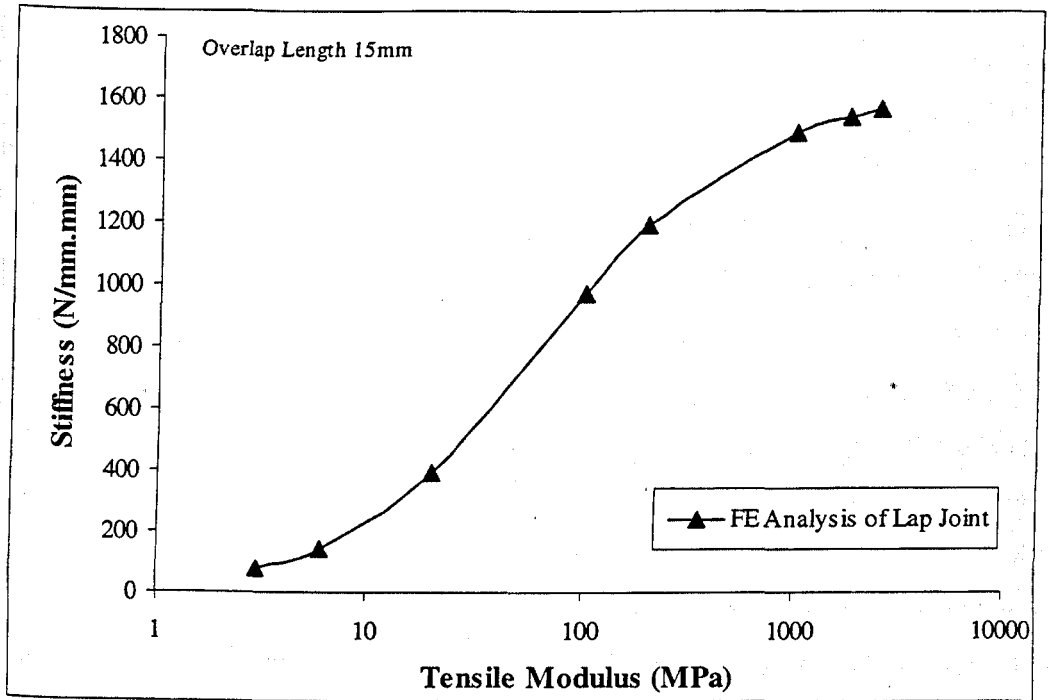


Figure 5.10 Variation of joint stiffness with change in adhesive modulus for single lap joints

5.2.5 Further Refinements of Modelling Methods

Initial modelling of lap joints was carried out using 2D solid elements, as discussed earlier in section 5.2.3. In this section, further refinements of finite element models were carried out in order to improve and validate the accuracy of the initial models. These will be discussed in detail.

3D Solid Element (Micro) Modelling

FE models of single lap joints were designed using solid elements on a three-dimensional basis, shown in Figure 5.11. Eight-noded elements were used to represent both the adherend and the adhesive layers. Three and six elements were used to define the mesh across the bondline and adherend thickness, respectively. The total number of nodes and elements used in this analysis were typically 16954 and 3310, respectively.

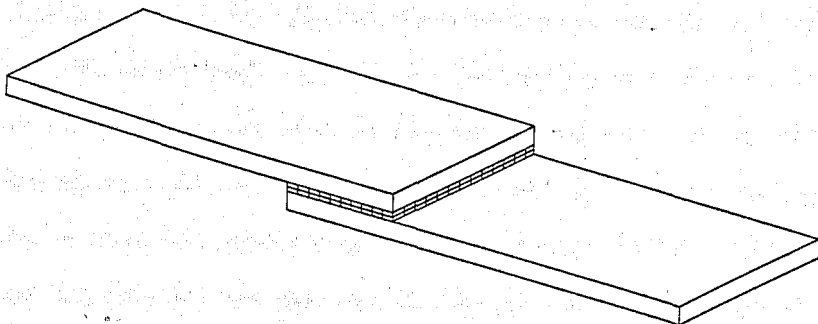


Figure 5.11 Solid element model of single lap joint

Shell-Solid (Macro) Modelling

Another FE modelling method combined shell elements with solid elements. This method was used to represent the modelling techniques used in large-scale models of vehicle structures, and is sometimes described as macro modelling. Figure 5.12 shows a schematic representation of a lap joint where the shell elements, using eight-noded quadrilateral elements, represent the centre-line of the sheet adherend and the solid elements, using twenty-noded hexagonal elements, represent the modified adhesive layer. The total number of nodes and elements used in this analysis was typically 4733 and 1320, respectively. Four elements were used to define the mesh across the bondline thickness.

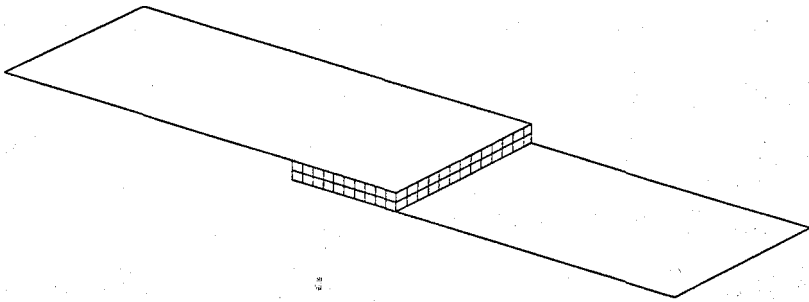


Figure 5.12 Shell-solid element model of single lap joint

When combining shell elements with solid elements, the bondline thickness must be modified to allow for the change in position of the shell and solid element interfaces. This is since the positions of the shell elements represent the mid-span of the actual sheet thickness. In a simple interpretation, the distance d between the shells representing the adherends is give by equation 5.1.

$$d = (t_1 + t_2) / 2 \quad (5.1)$$

Where t_1 and t_2 are the thickness of adherends 1 and 2, respectively.

For similar adherends of 1 mm thickness, this would result in a bondline thickness, or distance d between the shell plates, of 1 mm. Clearly, this would result in a much lower stiffness due to the greater compliance of the thicker adhesive. One method to compensate for this is to increase the effective adhesive modulus in the same ratio as the increase in bondline thickness, and this is given by the expression,

$$\text{Effective Modulus} = \text{True Modulus} \cdot \frac{(\text{Average Sheet Thickness})}{\text{Bondline Thickness}} \quad (5.2)$$

For example, for a lap joint having a bondline thickness of 0.2 mm and 1 mm thick adherends, the true modulus will be increased by a factor of 5. Hence, for a CIBA XB5315 adhesive which has a modulus of 1800 MPa, the calculated modified/effective modulus would be 9000 MPa; an increase of five times that of the original adhesive modulus. Similarly, for a TEROSTAT 3218F adhesive of 6 MPa modulus, the effective modulus would be 30 MPa.

This technique of 'correction' is used by the automotive industry for their full body analysis of vehicle structures which combine both shell with solid elements. In these macro models, the shell elements represent the steel sheets and panels, while the solid elements are now being used to represent the new adhesive layer. However, finite element models of vehicle structures are produced directly from computer aided design (CAD) models and because adhesive bonding is a fairly new technique in body structures, the bondline distance has not actually been included into most CAD drawings. Nevertheless, FE users would implement these solid elements, representing the adhesive layer, by simply applying the appropriate correction distance and the effective modulus into the models; this will ensure a more representative model for FE analysis.

On further inspection of the simple 'correction' method, it was noted that adjustments for the separating distance between the shell elements did not include the original bondline thickness. Thus, for a lap joint with two similar adherends of 1 mm thickness and 0.2 mm bondline, the corrected shell separation would be 1.2 mm rather than 1.0 mm, and the effective modulus would be calculated using,

$$\text{Effective Modulus} = \text{True Modulus} \cdot \frac{(\text{Bondline Thickness} + \text{Average Sheet Thickness})}{\text{Bondline Thickness}} \quad (5.3)$$

Substituting the variables into the equation, now gives an effective modulus of the solid elements representing the adhesive layer. Using this modified 'correction' method, the effective modulus for TEROSTAT 3218F and CIBA XB5315 adhesives would be 36 MPa and 10800 MPa, respectively.

In the automotive industry, this method is appropriate for new CAD designs which actually do include the bondline thickness into the drawings. However, to include such

modifications to CAD drawings of vehicle structures, which do not take into account the glue-line, would require extensive effort.

Various models representing lap joints have been designed using the current industrial method for modelling adhesive joints (macro model) and by implementing an additional correction factor to compensate for the glue-line. These are also compared to detailed solid (micro) models and experimental test results. Joint stiffness for all the models has been calculated over a 50 mm gauge length and the results are presented in the following section.

5.2.6 Further Results of Modelling Methods

The effectiveness of the refinements and corrections made to shell-solid modelling methods is shown in Figures 5.13 (a) and (b). Results from the shell-solid models are compared to experimental tests and detailed solid model results for TEROSTAT 3218F and CIBA XB5315 adhesives.

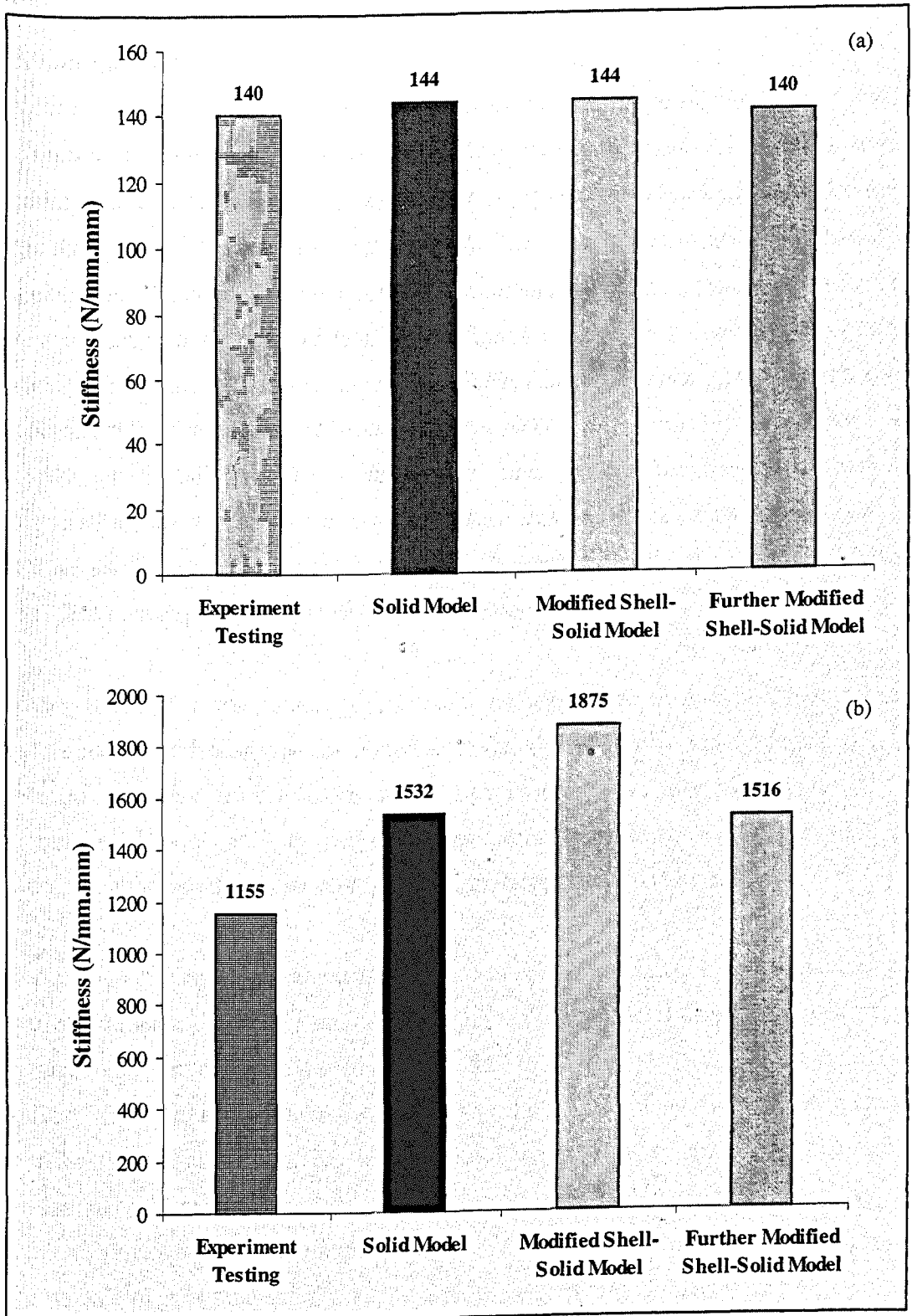


Figure 5.13 Further results of FE modelling analysis on lap joints using (a) TEROSTAT 3218F and (b) CIBA XB5315 adhesives

5.2.7 Discussion

Experimental Tests

Results from the experimental tests were compared with initial FE modelling results and are shown in Figures 5.7 (a) and (b). The measured values of stiffness from the experimental tests give fairly good agreement to the calculated values from the FE models, particularly for shorter overlap lengths and for the lower modulus adhesive. However, it was observed that generally, the experimental results were almost always lower than those obtained through numerical models. This might be caused by a combination of different factors. First of all, it should be noted that all FE analyses assume linear elastic behaviour in both the adhesive and the adherends. In the experimental tests, yield will occur in the adhesive, particularly in the areas at the ends of the bondline where the stress concentrations are at their highest. As a result, this will increase the shear strain in the bondline leading to lower stiffness values. The non-linearity of the load-displacement curves from the experimental tests (Figure 5.4) confirms that yield does occur in the joint.

Another reason for the lower experimental results might be due to the fact that the measurement of stiffness was calculated from the slope of a chord to a selected load level, where the departure from linearity was not excessive, rather than by a tangential slope. The tangential slope at very low loads may reflect the linear model behaviour more accurately, although it may be more difficult to determine [Steidler et al. (1997)].

A further possibility for lower experimental results may be caused by the variability in the experimental tests. This may include experimental inaccuracies caused due to slippage in the transducer mounting points or perhaps due to slight defects unaccounted for in the bondline. There is also some uncertainty as to the actual value of the elastic modulus of the adhesives assumed in the experimental tests, and whether they are actually representative of the adhesive conditions in the joint and thus, the FE models. The modulus values quoted by the manufacturers are thought to have been obtained from bulk specimens, and it is suggested that the condition of the glue-line may differ because of different curing conditions and test temperatures. Although the variability in the experimental results is not excessive for an average interpretation, it is likely that the possible sources of experimental inaccuracies, as described previously, might lead to slightly lower stiffness results. Nevertheless, the reasonable correlation between

experimental tests and similar FE models show that numerical analyses can give fairly accurate predictions of joint stiffness.

Parametric Study from FE Models of Lap Joints

Results from the parametric study on the effect of overlap length and sheet thickness are shown in Figures 5.8 (a) and (b) for TEROSTAT 3218F and CIBA XB5315 adhesives, respectively. Results confirm that increasing the overlap length gives stiffer joints; it appears that the joint stiffness is less affected by sheet thickness for low modulus adhesives compared to when using higher modulus adhesives.

Figures 5.9 (a) and (b) show that increasing the bondline thickness will result in a reduction in joint stiffness. Again, for a lower modulus adhesive, the stiffness of the joint is less affected by sheet thickness. The stiffness results of an adhesively bonded lap joint can be compared to the stiffness values of a solid lap specimen and of a plain sheet of similar dimensions (Figure 5.14); this will provide a better understanding of how and why the bondline affects joint stiffness.

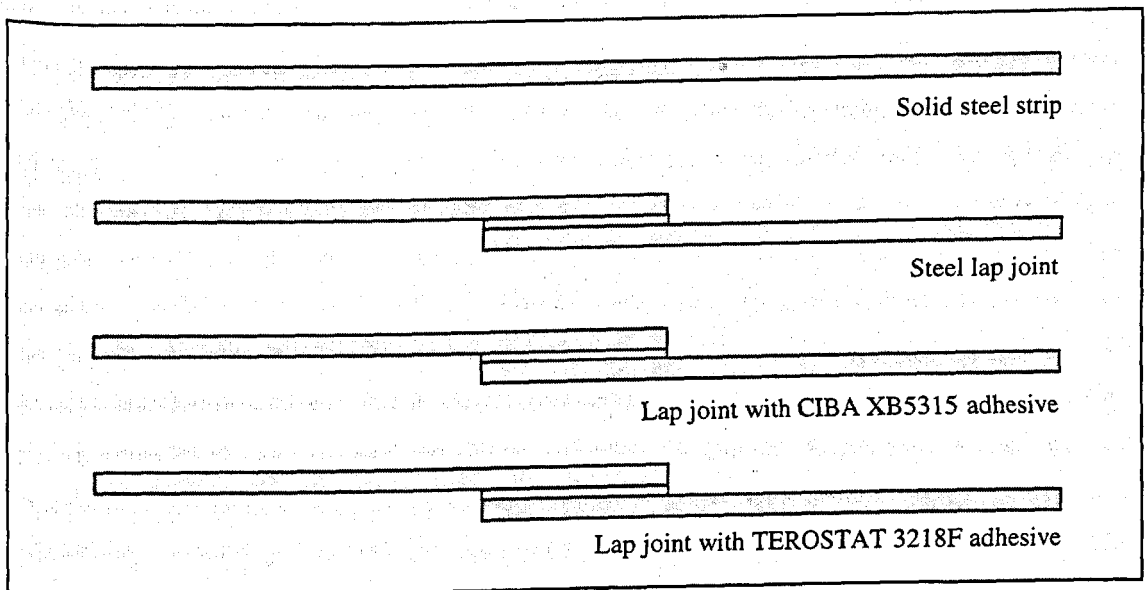


Figure 5.14 Effect of adhesive modulus on joint stiffness of lap joints

For example, if we take the FE model of a lap joint similar to that previously used, and replace the material properties of the adhesive layer with that of the adherends (mild steel), the resultant stiffness is calculated to be 1691 N/mm.mm. This can be compared to 1532 N/mm.mm calculated from an adhesive lap joint using a high modulus epoxy adhesive

(1.8 GPa) and 144 N/mm.mm for a low modulus adhesive. Hence as expected, increasing the modulus of the adhesive will also increase the stiffness of the joint. However, if we take a solid steel sheet of the same sheet thickness and equivalent overall length of the lap joint previously used, the resultant stiffness is 4200 N/mm.mm. The high stiffness of the solid steel sheet is partly due to the overall high modulus of the sheet, but is essentially due to the absence of eccentricity in the load path. Introducing a minimal step, such as a 0.1 mm or 0.2 mm bondline, will result in a dramatic reduction in the overall joint stiffness, as shown in the previous calculations, principally caused by the resultant moments/rotations and non-uniform stresses in the joints.

Figure 5.10 shows the results from the study on the effect of various adhesive materials on joint stiffness. The types of adhesives used in this analysis include extreme values of adhesive modulus; which represent a factor of 300 between highest and lowest moduli. Results from the analyses suggest that the stiffness of the joint, over this wide adhesive range, vary by a factor ranging between 10-20. Hence, the lap joint stiffness is relatively insensitive to changes in modulus particularly for higher modulus adhesives such as structural epoxies of modulus, which may range from 1 GPa and higher. These results are very significant since in actual practice, there is quite a large variability of the adhesive modulus in a product assembly. This may be caused from processing conditions or subsequent service exposures which might range typically from -40°C to $+80^{\circ}\text{C}$. The manufacturers data sheet for CIBA XB5315 quoted modulus values as 2.3 GPa and 1.8 GPa, for -40°C and $+23^{\circ}\text{C}$, respectively. This fourfold change in modulus would result in a change of stiffness from 1350 to 1530 N/mm.mm or $\pm 6.5\%$. However, lower modulus adhesive materials will exhibit a higher sensitivity. The typical range of stiffness, for a similar fourfold change in modulus of an adhesive with a nominal modulus of 0.01 GPa, would be from 150 to 400 N/mm.mm representing a change of $\pm 45\%$.

Further Refinements of Modelling Methods

Combining shell with solid elements, as used in full body vehicle FE models, has caused some concern in the effectiveness of the models and the validity of the results. The initial concern arises from the two different natures of the element types; shell elements have six degrees of freedom (DOF) - three in rotation (δ_x , δ_y , δ_z) and three in translation (u_x , u_y , u_z), while solid elements have only 3 DOF, all in translation. Hence, rotational stiffness

cannot be transferred across the joint between the elements at the shell-solid interface. This problem is usually corrected by embedding the elements or by overlapping them over some distance. Nevertheless, when the two elements are combined in a model, the mismatch at the nodes results in local inaccuracies of displacements and stresses.

The shell-solid element models in this study were used to represent the macro models used in the full body analysis of vehicle structures. In these models, the shell elements represent the adherend plates or panels and the solid elements represent the adhesive layer. To compensate for the thickness in shell elements, the distance between the two plates is calculated by averaging the thicknesses of the plates (equation 5.1). For this study, two 1 mm thick adherends were used and therefore, the adhesive thickness was increased by a factor of 5; consequently, the modulus of the adhesive was also modified by a factor of 5 (equation 5.2). Further modifications of the effective modulus of the bondline, which included the addition of the actual bondline thickness which was given by equation 5.3

Figures 5.13 (a) and (b) show the results from the study on using different modelling techniques; these are also compared with experimental test results. Results show that some correction is required in shell-solid (macro) models in order to predict more accurately joint stiffness. These modifications generally involve adjusting the adhesive modulus to compensate for the bondline thickness in shell-solid models. For single lap joints, such modifications only slightly change the resultant stiffness value; however, it will be shown, in section 5.3, that these adjustments have a larger effect on other joint configurations such as in T-peel or coach joints.

Results of FE analyses were also compared to results obtained from experimental tests. For the low modulus adhesive, all finite element models gave very comparable results to the experimental ones. For the high modulus adhesive, there is rather more variability in the results. Possibly, the main source of error is derived from the experimental tests. Such error might arise from the application and/or curing of the adhesive or maybe due to inaccuracies caused by the experimental set-up such as grip slippage, defects within the joints and/or the overhead movement.

5.3 Coach Joints

Most joints in vehicle body substructures are more complicated in shape and in dimension than basic single lap joints. The flange joint (T-peel), commonly known as the coach joint in the automotive industry, can be considered to be a more representative joint within car substructures primarily due to the flanges which allow joining between different vehicle parts. The geometry of the flange joints allows ease of accessibility for spot-welding and fastening methods and the automotive industry prefers to retain this configuration for adhesive bonding, despite the fundamental limitations of weakness due to peel loading.

Joints within car body structures are subjected to a number of different modes of loading. It is very difficult to determine all the directions and applied loads on an individual joint as these will depend on the loading conditions within the whole structure. In order to evaluate the performance and behaviour of a joint within an automotive structure, it is simple to analyse each joint when subjected to individual specific loading conditions, e.g. tension, compression, bending. By doing so, the effects of each loading condition on the behaviour of the joints can be determined.

The work described in the following section investigates the effects of joint geometry and design parameters on coach joint stiffness for tensile and bending modes of loading. A parametric study was carried out using FE models and these were compared to experimental tests.

5.3.1 Joint Definition

The simple coach joint configuration comprises of two adherends, bent at 90 degrees to each other, and bonded or joined together at the flanges. The coach joint dimensions chosen for this study were selected to represent typical joints found in auto body structures, shown in Figure 5.15. It should be emphasised that in bonded coach joints the extent of the adhesive into the flange bend area may vary, giving rise to a geometric variable which is described as the fillet ratio. This parameter is defined in Figure 5.16. The adhesive fillet ratio has a major influence on joint properties and forms a primary detail in the study.

For the experimental work, test pieces were made from 1 mm thick and 20 mm wide steel strips which were bent to form 14 mm flanges with 6 mm external bend radii (R_o); these dimensions were convenient to form the basis of the numerical models. The dimensions of the standard coach joint configuration are given in Figure 5.15 for the same material properties as those given previously in the study of single lap joints (Table 5.1).

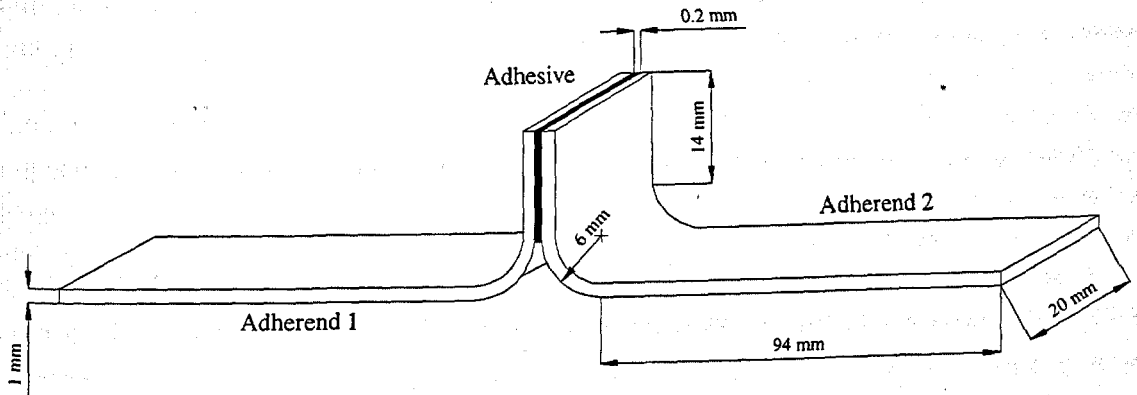


Figure 5.15 Geometry of initial coach (T-peel) joint configuration

Design variables such as the sheet bend radius, adhesive fillet ratio, adhesive bondline and adhesive type were studied in detail in the parametric study and are discussed in section 5.3.3. In most of the work carried out, the bondline thickness was kept constant at 0.2 mm and the sheet thickness at 1.0 mm. The overall length of the coach joint configuration was 200 mm, excluding the bondline thickness. In all cases, an extensometric gauge length of 50 mm was used to calculate and measure the displacements over the joint area (Figure 5.16). From the data obtained, resultant joint stiffness were derived. In the FE analyses, various adhesive properties were used and tensile modulus ranged typically from 3-4000 MPa. However in the experimental tests, the adhesives used were a high modulus (CIBA XB5315) and a low modulus adhesive (TEROSTAT 3218F).

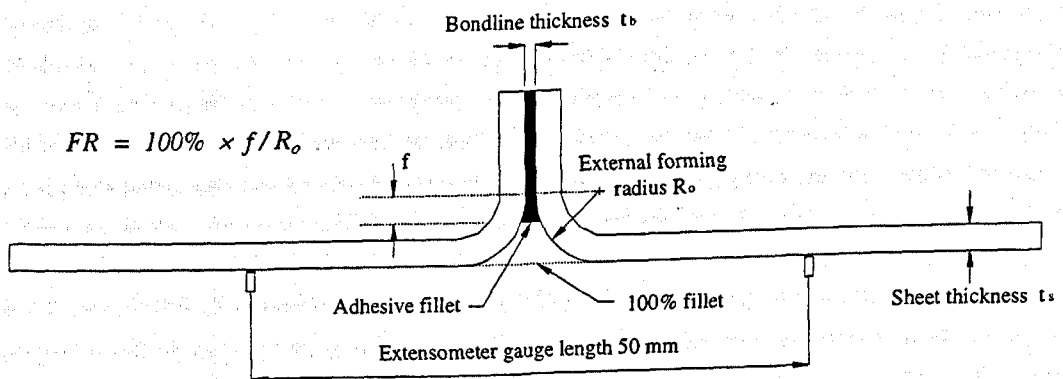


Figure 5.16 Coach (T-peel) joint details and definition of fillet ratio

5.3.2 Experimental Testing

In the experimental part of the study, coach joints were formed for different joint parameters and were tested to validate the results from the numerical analysis. The main study of the experimental tests looked at adhesive bonded joints but a few spot-welded joints were also tested to compare stiffness properties with adhesive bonded joints. Two adhesives were used in the experimental tests, and these represented the extreme ranges of typical adhesives used in car bodies: TEROSTAT 3218F ($E = 0.006$ GPa) and CIBA XB5315 ($E = 1.8$ GPa). The substrate components were primarily formed from mild steel sheets of 1.0 mm thickness, but sheets of 0.8 mm and 1.2 mm thickness were also used.

Joint Preparation

Each of the joining methods used required different surface preparations and treatments. The following section describes the manufacturing procedures that were followed to obtain joints through adhesive bonding and spot-welding joining methods.

a) Adhesive Bonded Joints

Surface treatment was carried out prior to the application of the adhesive. The joint area was first solvent-cleaned with MEK degreasing agent to remove any oils and contaminations from the surface. The sheets were then grit-blasted with Alumina grit-size 60 to create a uniform surface for adhesion and to remove any weak surface layers. The final procedure in the surface preparation involved degreasing the joints again with MEK.

The application of the adhesive involved controlling two main joint parameters: the adhesive bondline thickness and most importantly, the adhesive fillet ratio. To control the bondline, glass beads (ballotini) of appropriate diameters were added to the adhesive at a maximum of 1% by weight ratio, to match the desired thickness.

The adhesive fillet ratio can be considered to be one of the most important factors in the properties of coach joints. Controlling the adhesive fillet ratio is generally very difficult, since the adhesive tends to flow during the curing process, resulting in excess adhesive in the bend radius and greater fillet sizes than the original fillet desired. Fillet ratios of 0%, 50% and 100% were selected for the experimental tests; the ratios were calculated using the expression given in Figure 5.16. Controlling the adhesive fillet ratio was achieved by means of specially shaped templates of appropriate dimensions to the fillet required.

These templates were applied to the joints as soon as they were assembled, prior to curing, and were used to remove any excess adhesive within the joints. Once the joints were assembled and both the bondline thickness and fillet ratio adjusted, the joints were set into spring-clip fixtures and cured at 180°C for 30 minutes.

b) Spot-Welded Joints

Welding conditions were adjusted to form weld nuggets of approximately 5 mm diameter. A special fixture was designed to locate the electrodes on the centre point of the flanges. For a welding current of 8000 Amps, the weld times for various sheet thicknesses were as follows,

22 cycles on 0.8mm thickness adherends

25 cycles on 1.0mm thickness adherends

35 cycles on 1.2mm thickness adherends

Tensile Testing

Static tensile tests were carried out by loading the joints in a Testometric 10kN testing machine. A linear variable differential transformer (LVDT) extensometer, with 4 mm-stroke and 1 μ m resolution, was clipped across the joints and was used to measure the joint deformation under load, as shown in Figure 5.17. The tensile stiffness of the coach joints was calculated over a 50 mm extensometric range (Figure 5.18) based on the slope of the linear part of the load-displacement curves obtained from each test. All joints were loaded until failure.

For each specimen, the outputs from the LVDT and the load cell were processed through the tensile testing machine's computer to generate autographic records. The data was also fed into a separate graphics package for further analysis. Figure 5.19 shows an example of the resultant graphs for a typical coach joint specimen with various fillet ratios. Stiffness values were derived from these graphs by calculating the slope of the linear part of the load-displacement curve, shown in enlargement A.

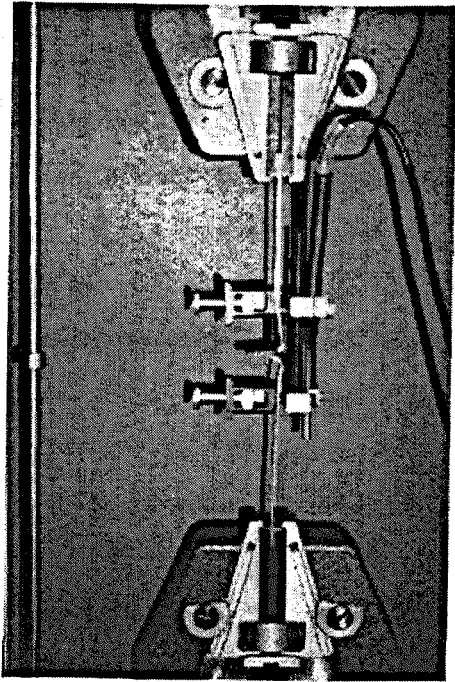


Figure 5.17 Experimental set-up of tensile testing of coach joints

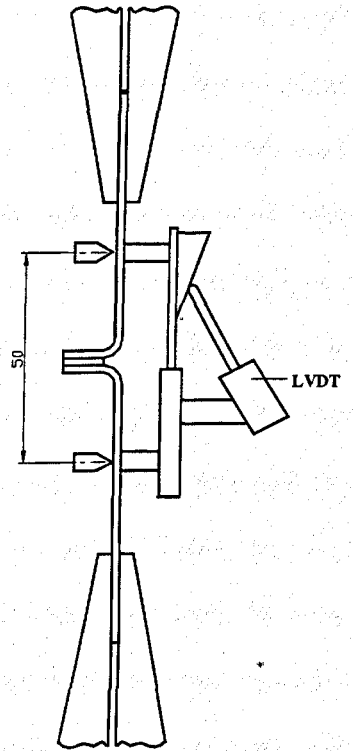


Figure 5.18 Schematic of gauge length

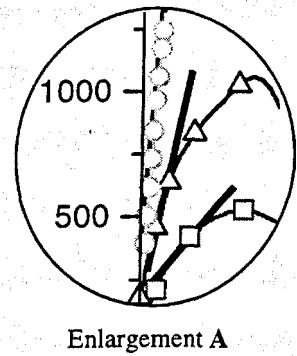
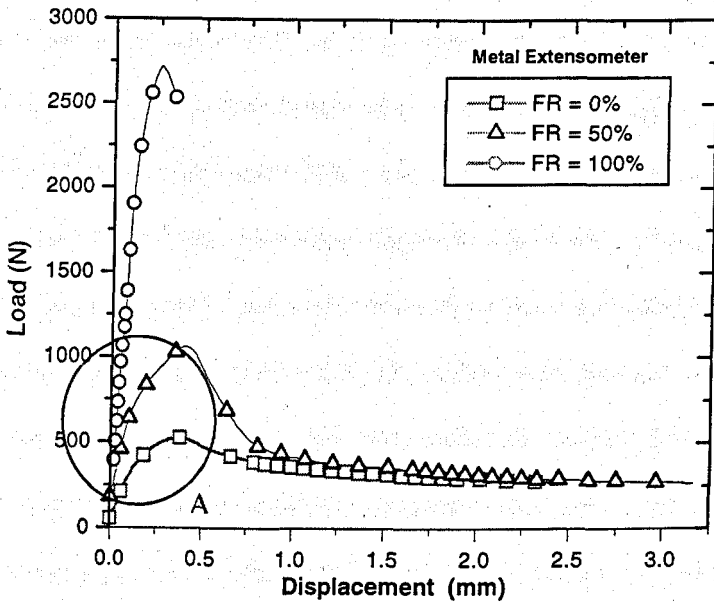


Figure 5.19 Representative load-displacement curves from experimental tests - CIBA XB5315 adhesive

Flexure Testing

A testing jig, shown in Figure 5.20, was constructed to test coach joints subjected to flexure through four-point bending loads. Resultant deflections were measured at different positions of the specimen, e.g. the positions where the loads were applied.

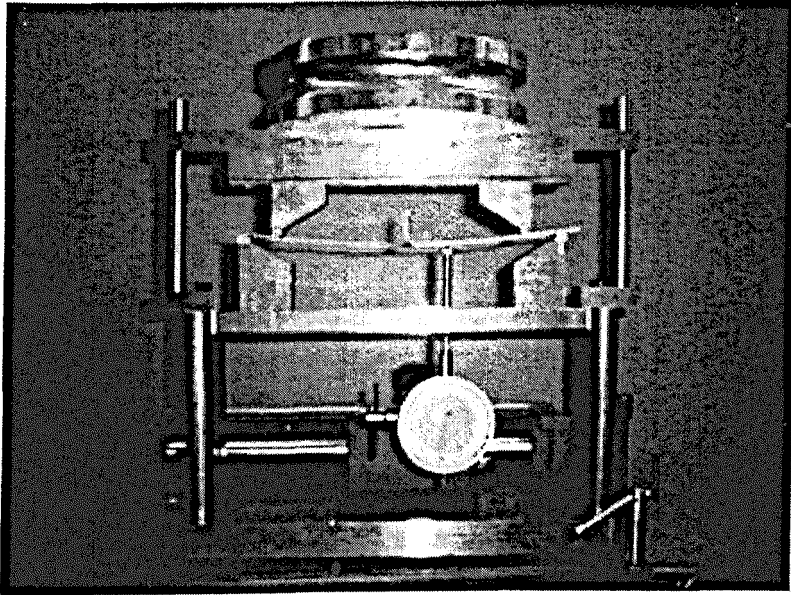


Figure 5.20 Experimental set-up of coach joints in bending mode

The distance between the supports and the loading points were adjustable but for present tests, the supports were set at 180 mm apart and the loading points at 140 mm (Figure 5.21). Weights were placed centrally on the rig so that equal forces were applied at each loading point. It was found that 40 N weights plus the weight of the jig, totalling 53.52 N, gave an acceptable deflection without yielding the specimen; this value was used throughout the experimental tests. A dial gauge was used to measure the deflection of the joint once the load was applied. The gauge was connected to a horizontal sliding vernier gauge, allowing the user to measure the deflection of the specimen and the exact location of its deflection relative to the whole specimen.

All joints were placed horizontally on the jig and subjected to an applied load of 53.52 N, giving a moment load of approximately 0.53 Nm over the central part of the specimen. Only one dial gauge was used to measure the displacements of half the specimen as symmetry could be assumed. The overall deflection profile was then determined by

interpolation of the results. Results from the experimental analysis are shown in section 5.3.4 and compared with FE models of similar joints.

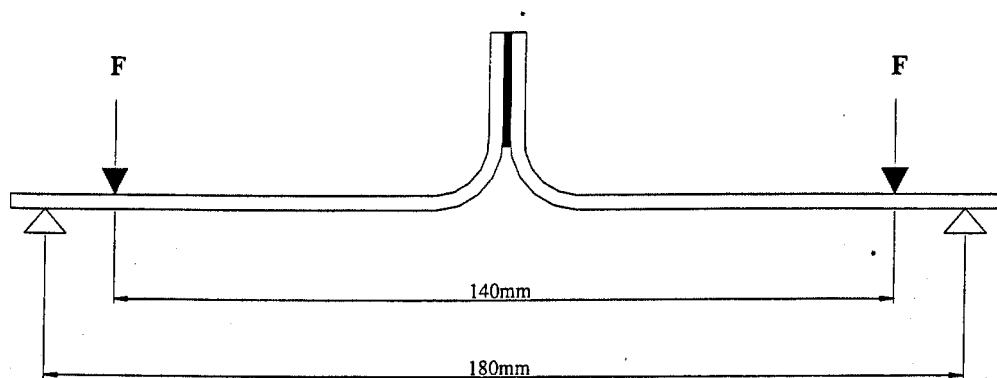


Figure 5.21 Graphical representation of experimental tests showing four-point bending

5.3.3 Numerical Modelling

Coach joints were accurately modelled and subjected to similar loads/constraints as to the actual specimens used in the experimental tests. Initial FE models were carried out using plane 2D solid element models and linear-elastic material properties. The solid element modelling method was used primarily since it allows an accurate representation of the actual joint by defining, through design, all joint geometries and material properties accurately.

To reduce modelling time, size and analysis running capacity, symmetry was used to model only half the joint, as shown in Figures 5.22 (a) and (b) for 0% and 100% adhesive fillet ratio, respectively. Quadrilateral elements were used to provide eight-nodes to each element giving an approximate total of 562 elements and 1921 nodes in each model. To calculate joint stiffness, displacement results were measured at 25 mm from the centre of the joint in the direction of the applied load and perpendicular to the plane. For the tensile loaded configurations, a load of 1620 N was applied to each model. The joint stiffness was calculated per unit width of the joint (N/mm.mm) for various adhesive fillet ratio configurations.

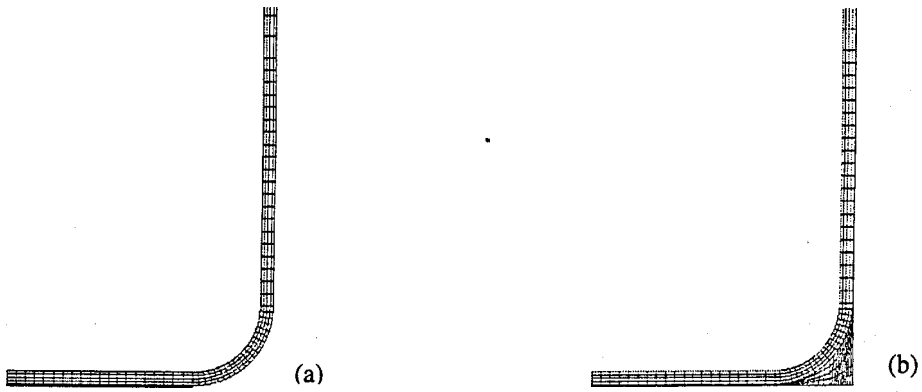


Figure 5.22 Solid half model of coach joint with (a) 0% and (b) 100% adhesive fillet ratios

Parametric Study

An extensive parametric study was carried out to determine the effects of various design variables such as flange bend radius, adhesive fillet ratio and adhesive type, on the stiffness of coach joints. The main body of the work looked at coach joints subjected to tensile loading; further analyses also investigated four-point bending loads. The basic dimensions of the joint and the material properties were kept constant, with the exception of the parameter under investigation. Table 5.3 shows the variables that were investigated in the parametric study of coach joints, for tensile and four-point bending modes of loading.

	Initial Joint Configuration	Variables of Tensile Tests					Variables of Flexural Tests				
Adherend Modulus (GPa)	207 GPa										
Adherend Thickness t_a (mm)	1.0 mm	0.8	1.2								
Adherend Bend Radius (mm)	6 mm	3	8								
Joint Width (mm)	20 mm										
Overlap Length (mm)	15 mm										
Adhesive Thickness t_b (mm)	0.2 mm	0.1	0.5	3							
Adhesive Modulus (GPa)	1.8 GPa	0.003	0.006	0.02	0.1	2.5	3				
Adhesive Fillet Ratio (%)	0%	25	50	75	100			25	50	75	100

Table 5.3 Variables of parametric study on coach joints – tensile and flexural loads

5.3.4 Initial Results

Results from the initial FE analyses of joints in tension are compared with experimental results and are given in Figure 5.23. Parametric studies using finite element methods on variation in bend radius and adhesive modulus are shown in Figures 5.24 and 5.25, respectively.

Tensile Loading

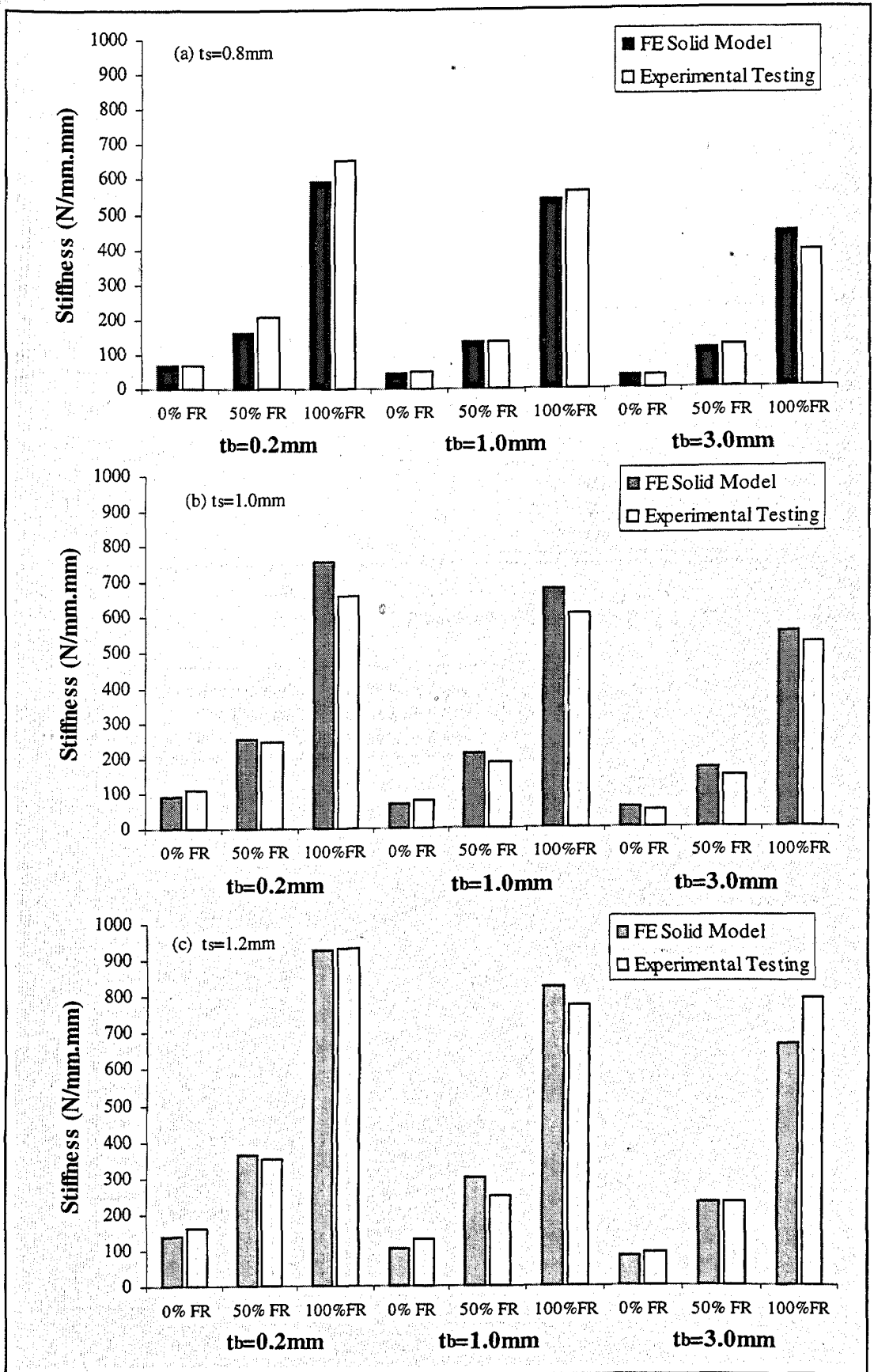


Figure 5.23 Comparison between experimental tests and FE model results using CIBA XB5315 adhesive and for different sheet thicknesses: (a) 0.8mm, (b) 1.0mm and (c) 1.2mm

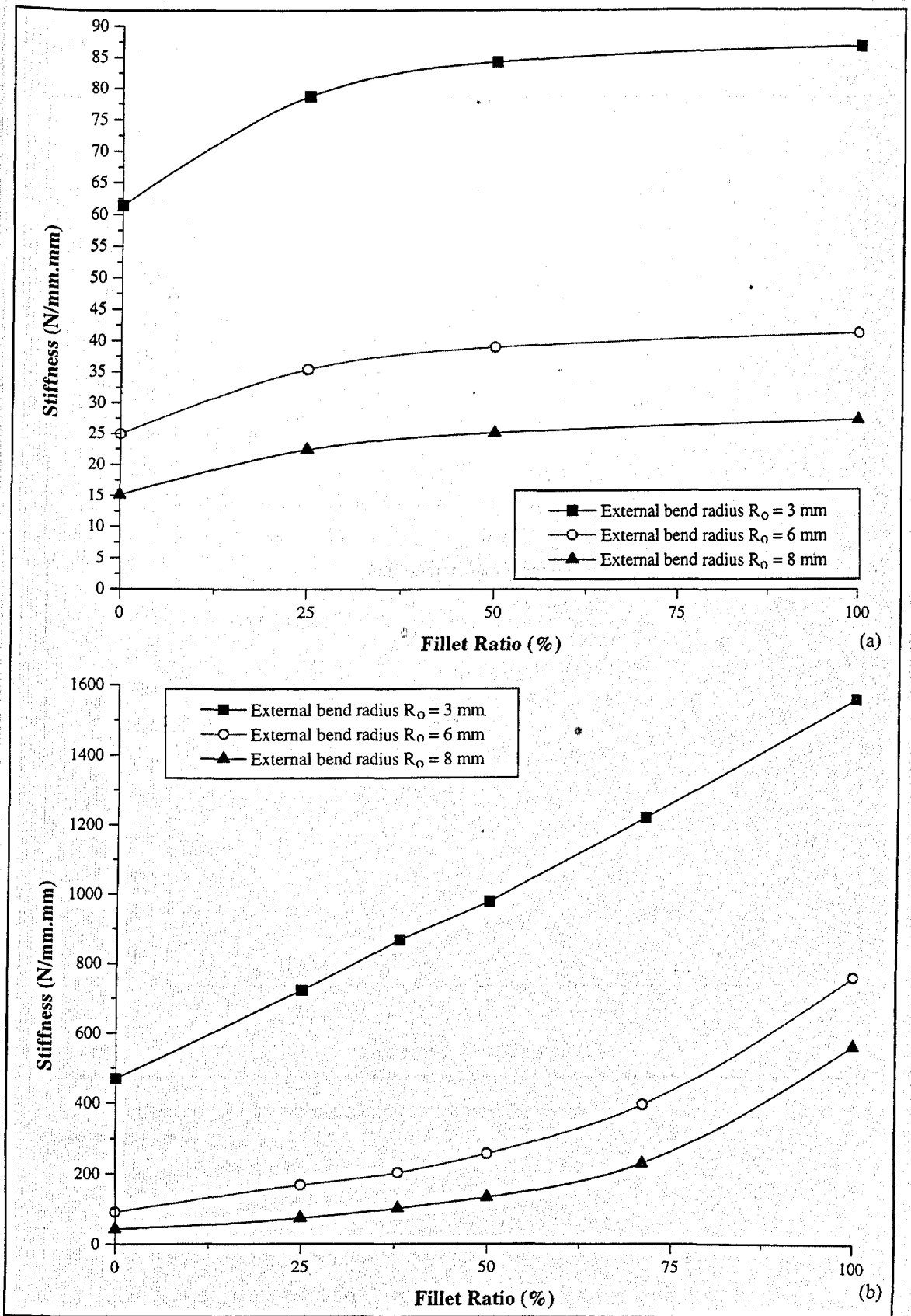


Figure 5.24 Variation of joint stiffness with bend radius and adhesive fillet ratio using (a) TEROSTAT 3218F and (b) CIBA XB5315 adhesives

Figures 5.25 (a) and (b) show the effect of adhesive modulus on joint stiffness for coach joints with 0% and 100% fillet ratio, respectively.

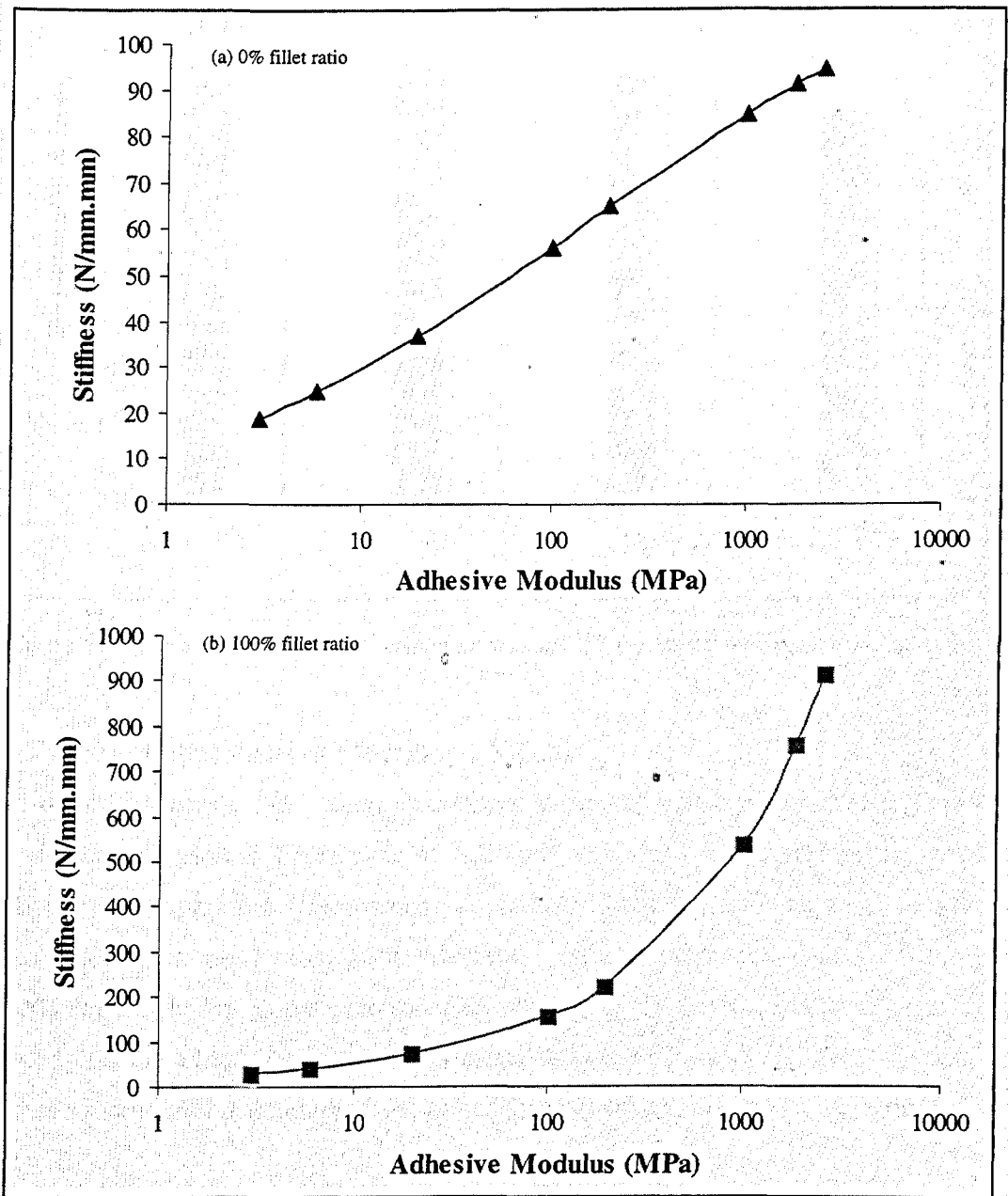


Figure 5.25 Effect of adhesive modulus on joint stiffness for coach joints with (a) 0% and (b) 100% adhesive fillet ratio

Four-Point Bending

Results from the study on four-point bending of coach joints are shown in Figure 5.26. These results are given in terms of a measured displacement over a gauge length of 50 mm, equivalent to the experimental tensile test conditions.

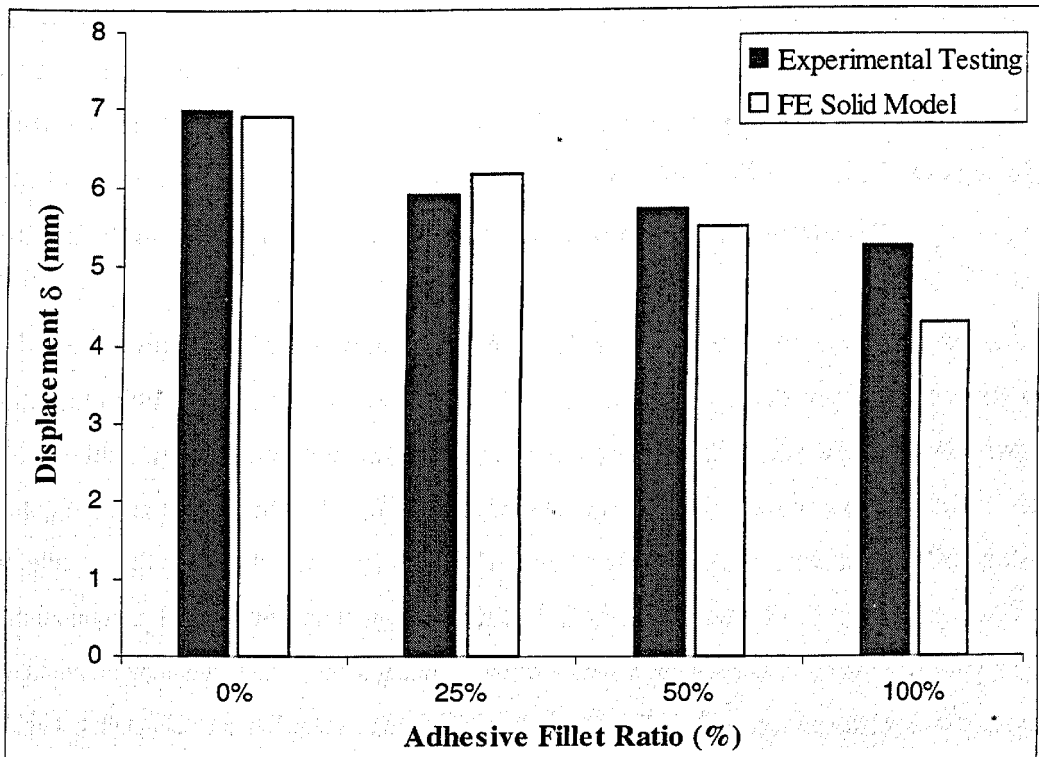


Figure 5.26 Comparison between experimental tests and FE results for four-point bending analysis

5.3.5 Further Refinements of Modelling Methods

As described in section 5.2.5, there is concern about the validity of combining shell with solid elements as used in FE models of full body vehicles. It is therefore the purpose of this study, to compare the effectiveness of shell-solid (macro) models with solid element (micro) models in predicting joint stiffness. Earlier work on shell-solid modelling methods for single lap joints (section 5.2) showed good correlation with solid models provided that the adhesive modulus and distance between the shell plates was modified. The same modification is adopted for coach joints and will be analysed in the following section.

Two different models of coach joints, both using shell with solid elements, are investigated in this study and the results from the analyses are compared with the results from similar solid models, as used in section 5.3.3. The first shell-solid model is based on the method of analysis used primarily by the automotive industry for large-scale structures. The representation of the geometry of the coach joint is very simple and there are many approximations in detail and accuracy. The bend radius of the adherends, for example, is ignored leaving the flanges with 90° edges. Figures 5.27 (a) and (b) show

representations of this 'simple' shell-solid model for cases when the flanges are fully filled (macro model), and when the flanges are representative of a 0% fillet ratio, respectively. The second model is similar to the previous shell-solid models, with the exception that the flange bend radius of the joint is more accurately modelled. Figures 5.28 (a) and (b) show models of representative 100% and 0% adhesive fillet ratios, respectively.

It should be noted that the combination of shell with solid elements in both models necessitates some form of compensation. This is done, as previously described in section 5.2.5, by modifying both the adhesive modulus and the distance between the two shell plates, given in equations 5.1 and 5.2. In this study, since the models are based on half the joint, the bondline thickness will be half of the actual bondline and the modified distance of the bondline for 1 mm thick sheets will be 0.5 mm, instead of 0.1 mm. The modulus of the adhesive will therefore, be adjusted proportionally and for a high modulus epoxy with modulus 1.8 GPa, the effective modulus will be 9 GPa. These corrections are similar to those currently used in full body analyses of vehicle structures; where the adhesive layer is not taken into account. Further corrections to these macro models can be achieved by using equation 5.3; this is valid for up-to-date CAD and FE models which account for a glue-line thickness.

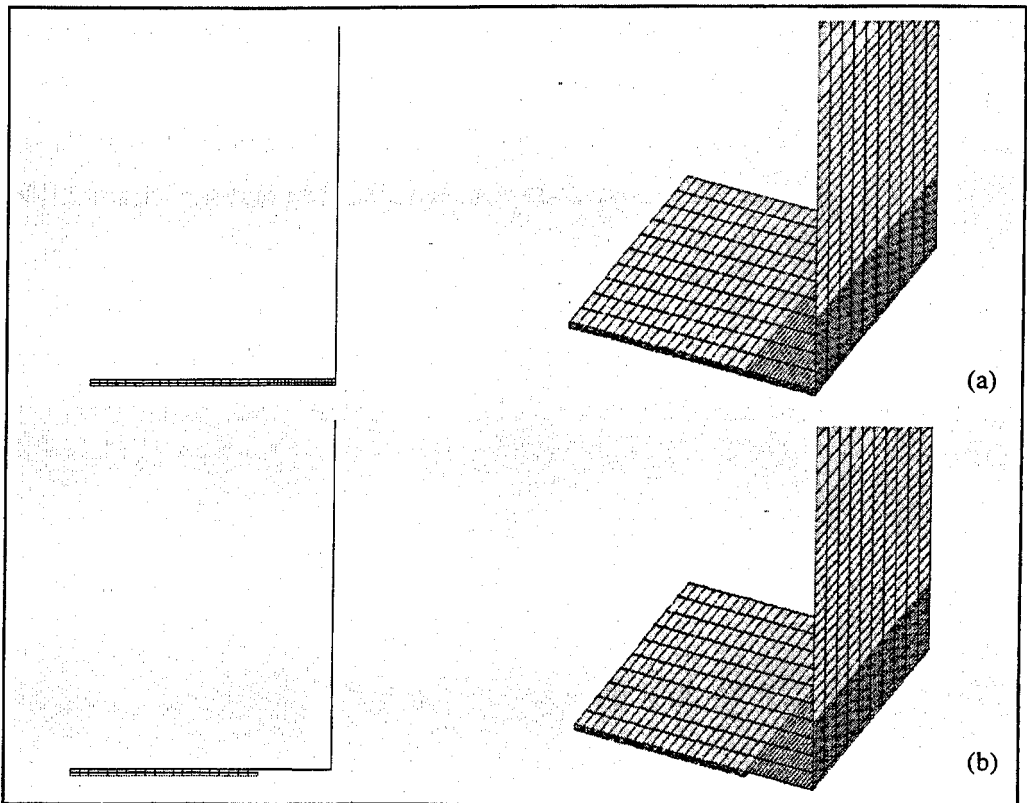


Figure 5.27 Shell-solid models – equivalent (a) 100% (macro model) and (b) 0% fillet ratios

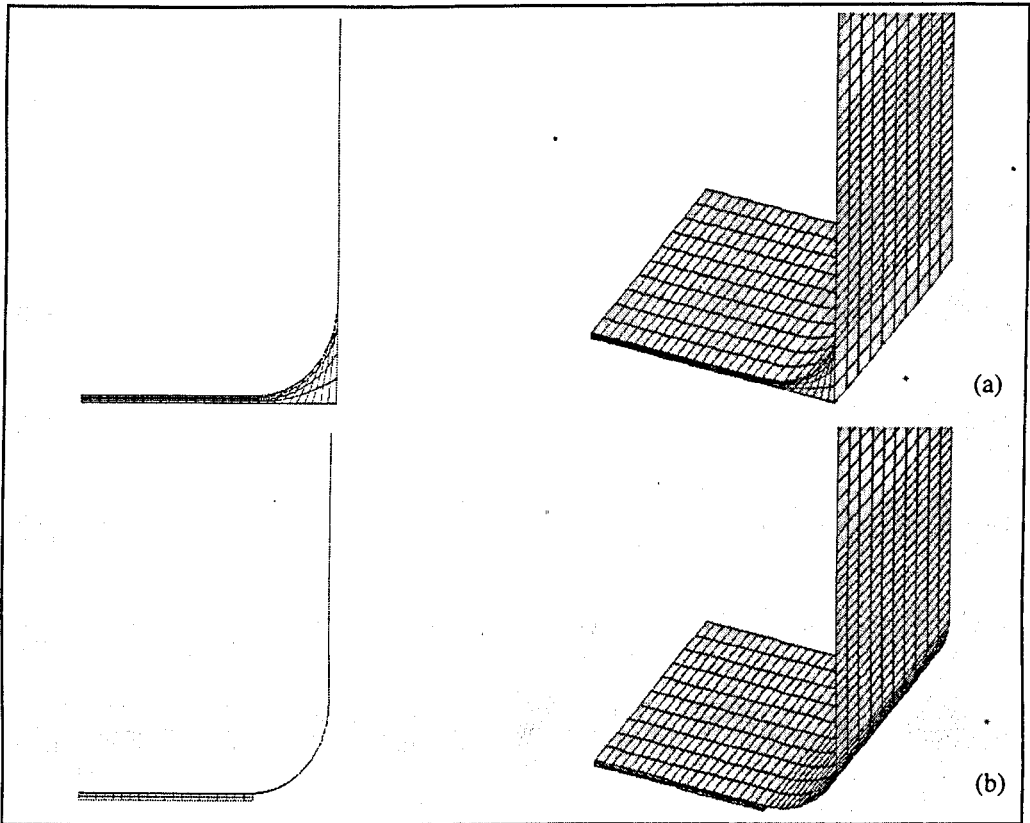


Figure 5.28 Radiused shell-solid models – equivalent (a) 100% and (b) 0% fillet ratios

5.3.6 Further Results of Modelling Methods

Results from the analyses of various modelling methods are given in Figure 5.29 for a CIBA XB5315 adhesive. The graph shows measured stiffness values plotted against various adhesive fillet ratios for three different modelling methods: solid (micro) models, shell-solid (macro) models and radiused shell-solid models.

Figure 5.30 shows the results from the extended numerical analyses of coach joints subject to four-point loading. The results are given in terms of displacement, and these values are also compared to theoretical calculations and FE models of solid steel sheets.

Tensile Loading

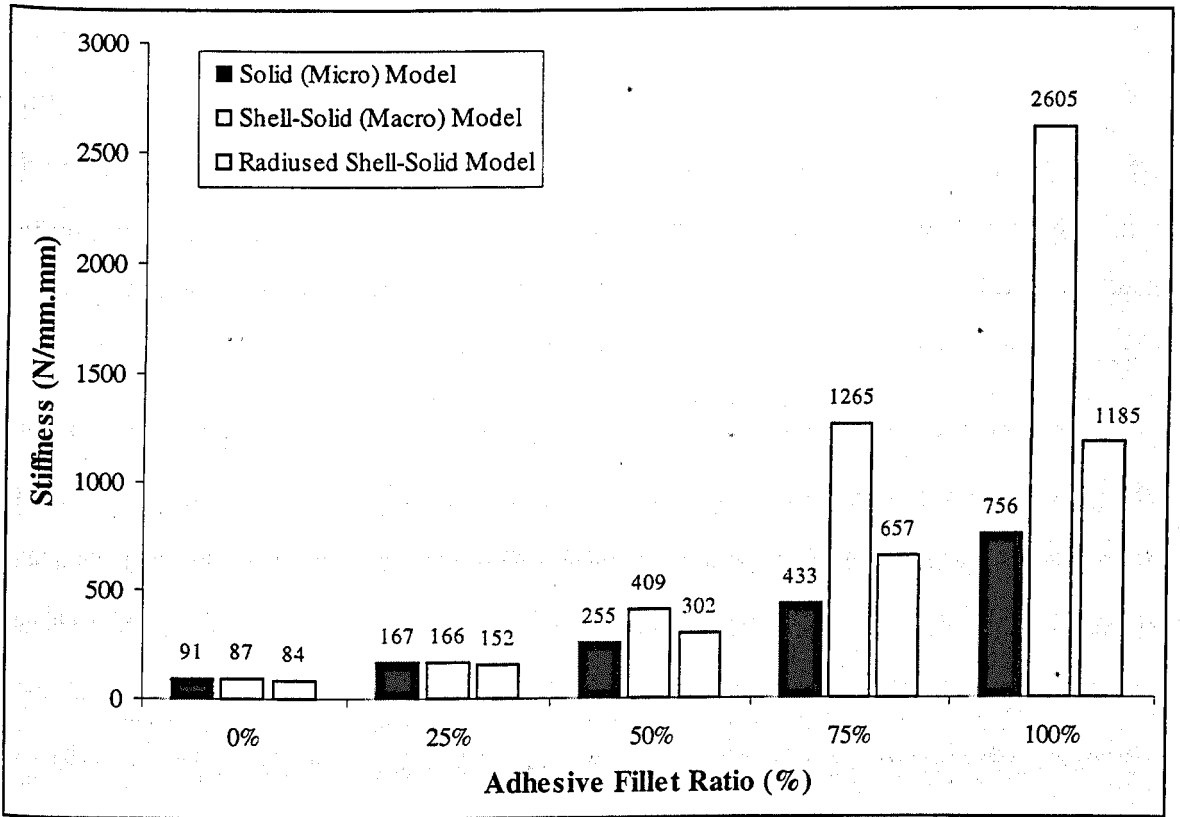


Figure 5.29 Stiffness results from extensive FE modelling of coach joint in tension – CIBA XB5315

Four-Point Bending

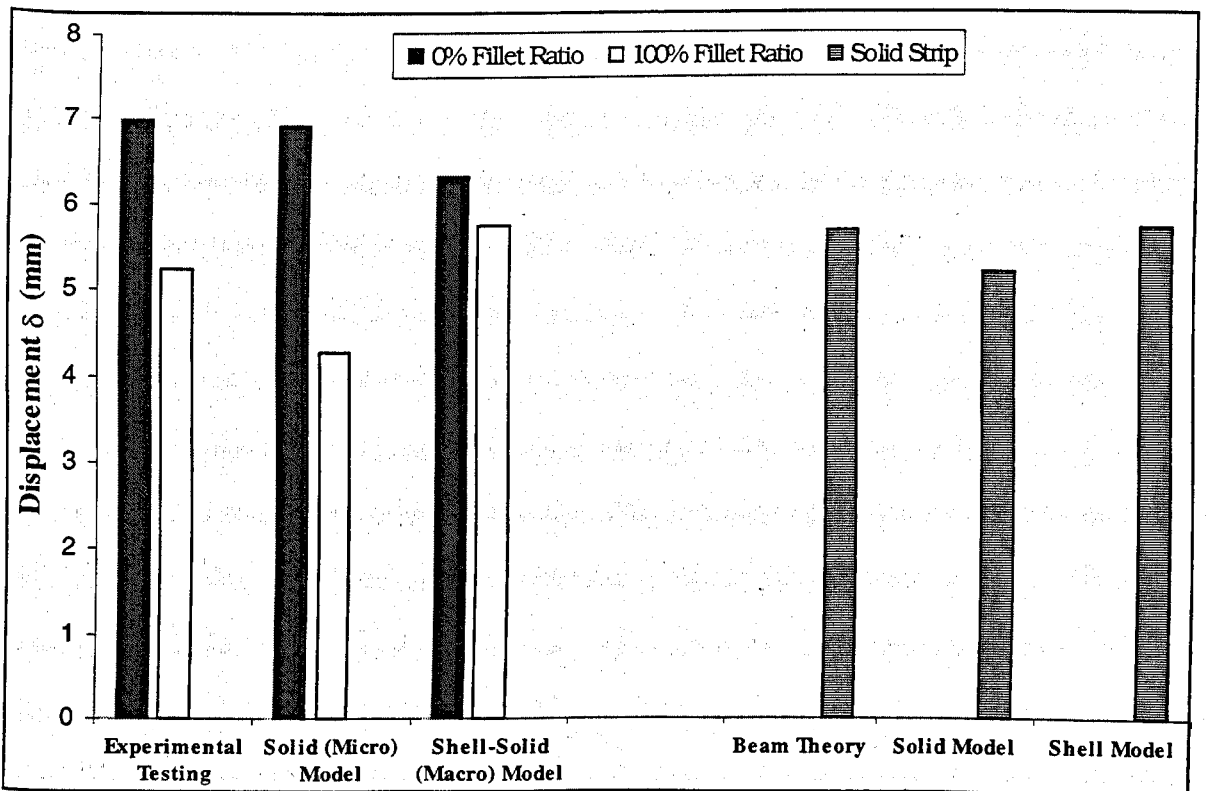


Figure 5.30 Stiffness results from coach joints subjected to four-point bending - CIBA XB5315

5.3.7 Discussion

Tensile Loading

Results from the experimental tests for coach joint in tensile loading are shown in Figures 5.23 (a)-(c) and compared to initial numerical modelling results of similar joints. The graphs show the variation of joint stiffness with adhesive thickness for various grades of sheet thickness. As one might expect, joint stiffness is reduced as the bondline thickness increases. However, the dependency is less critical than the effect of the adhesive fillet ratio; smaller fillet ratios produce significantly less stiff joints. For example, in the case where $t_s = 1$ mm, $t_b = 0.2$ mm and for 0% fillet ratio, increasing the adhesive thickness from 0.2 mm to 3 mm results in an approximate reduction of 55% in joint stiffness. For similar joint configurations, but for 100% fillet ratio, only a 21% reduction in stiffness is measured.

The effect of substrate thickness on joint stiffness is shown in Figure 5.23. Three grades of sheet thickness (0.8 mm, 1.0 mm and 1.2 mm) were used to represent a common range used within car bodies. Results show that increasing the thickness of the substrate will give joints with higher stiffness values. It is shown that coach joints with higher fillet ratios, thicker sheets and thinner bondlines will provide the stiffest joints.

Comparison of experimental and initial FE results show fairly good correlation with the exception of a few of joint specimens. These differences may arise from the fact that the FE models represent an ideal, linear and flawless joint, while the experimental results are derived from real specimens which may contain defects and process variables. Results from the experimental tests will contain some inherent variability and at times, may be inconsistent with expected results. The variability may be due to a number of causes such as measurement error, natural variability in experimental specimens, uncontrolled variation in the external conditions, etc. With careful control of the measurement processes and the environmental conditions, the variability can sometimes be reduced [Chatfield (1992)]. Statistics are sometimes used to measure these experimental errors and variations to provide a better understanding of the results.

The results from the parametric study of coach joints using solid element FE models are given in Figures 5.24 and 5.25. The purpose of the parametric study was to show how

different joint variables, such as adhesive modulus, flange bend radius and adhesive fillet ratio, affected the overall joint stiffness. Results in Figures 5.24 (a) and (b) show that joints with larger bend radii will give greater decreases in joint stiffness for different fillet ratios; in some cases, by a factor of 10 times for the higher modulus adhesive.

As expected, a small bend radius and a high adhesive fillet ratio give the stiffest joints. It is also observed that joints with the structural epoxy adhesive were generally much stiffer than those with the polybutadiene adhesive. However, it should be noted that the modulus of the epoxy is almost 300 times higher than that of the lower modulus adhesive, while the respective effect in joint stiffness is only a factor of 15.

Results showed that for the low modulus adhesive, stiffness is relatively insensitive to changes in adhesive fillet ratio. The graph in Figure 5.24 (a) shows that adhesive fillet ratios exceeding approximately 25-30% fillet give small changes in stiffness, regardless of the bend radius. On the other hand, results for the high modulus epoxy adhesive, given in Figure 5.24 (b), show that changes in fillet ratio result in significant increases in stiffness; and at 100% fillet, stiffness results are approximately 3-10 times higher than for 0% fillet ratios for various sheet bend radii.

Figures 5.25 (a) and (b) show the effect of adhesive modulus on coach joint stiffness for 0% and 100% fillet ratio, respectively. Results are plotted on a logarithmic scale to include the wide range of adhesives used in the study. It is observed that for joints with a minimum adhesive fillet ratio of 0%, stiffness varies almost linearly with changes in modulus. On the other hand, over the same range of adhesives but for a fully filled radius (100%), the variation of joint stiffness with elastic modulus increases more rapidly. Thus, it can be concluded that joint parameters, such as the type of adhesive used and particularly the adhesive fillet ratio, have a significant effect on joint stiffness. Ideally, to obtain stiff joints, a fully filled adhesive flange with a high modulus adhesive and a small sheet bend radius should be used.

Further Refinements of Modelling Methods

Results from the further refinements on modelling methods are given in Figure 5.29. It can be observed that for smaller adhesive fillet ratios, the difference in stiffness between the three FE models is marginal. However, for larger fillet ratios the correlation is not as

good and for a full fillet joint, i.e. 100%, results show that the shell-solid (macro) model with a 90° flange edge will give a stiffness value at least 3 times greater than that of the solid (micro) model. With the detail of the forming sheet radius included in the radiused shell-solid models, the stiffness values drop closer to those obtained in the detailed solid model and experimental results. These results show how modelling certain geometric design parameters, such as the flange radius, are fundamental in order to obtain accurate predictions of joint stiffness. If these details cannot be accommodated for in large-scale (macro) models, then it would be necessary to compensate for them.

The use of shell-solid models with 100% fillet ratio and sharp flange corners (macro models), for example, clearly introduces errors in stiffness prediction, thus requiring some form of correction. This correction could be achieved by translating in some way, the accuracy of the solid model into the shell-solid models, and further work in Chapter 6 describes a novel approach to provide this correction.

Four-Point Bending

Coach joints in vehicle bodies are subjected to many different modes of loading which may affect body stiffness in different ways. In this study, coach joints were subjected to four-point bending and results from the FE modelling and experimental tests are given in Figures 5.26 and 5.30.

Numerical models were developed to represent the experimental arrangement for 0% and 100% adhesive fillet ratios. The analysis was carried out using solid element models and shell-solid element models. Linear elastic material properties were assumed and only half the structure was modelled; constraints were used to represent the symmetry of the structure. From Figure 5.30, it can be seen that both FE models give a reasonable prediction of the flexural displacement of the joint, with the shell-solid model giving slightly higher displacements, i.e. lower stiffnesses, than the equivalent solid models. Both models are also less sensitive to changes in fillet ratio than experimental observations.

During the experimental tests, it was observed that most of the bending displacement was occurring in the strip outside the joint, and it was evident that the coach joint was having relatively little effect on the specimen stiffness. To confirm this observation, a further

series of experiments and models were carried out on simple solid steel strip specimens of the same width and thickness as the joints. The comparison of the coach joint behaviour with the solid strip under four-point bending, confirms that the flexural properties of coach joints are relatively unaffected by the adhesive layer.

Although most experimental tests gave results in similar order of magnitude to the FE results, possible inaccuracies and sources of error might be due to the experimental test procedures such as the reliability and accuracy of the applied loads. For example, the weights were placed manually upon the rig and positioned centrally by eye. Small errors might exist due to the non-central location or initial non-vertical positioning of the load, and the measurements of the readings from the dial gauge. However, the general observation from the experimental tests is consistent with expectations from the model predictions.

5.4 Summary

Results from the study on single lap joints and coach joints have shown that numerical micro modelling methods give good predictions of joint behaviour, particularly in terms of stiffness. The results from the FE analyses were validated with experimental testing of similar joints. However, one of the main concerns in the FE modelling techniques, particularly for large-scale modelling of adhesive joints in car bodies, is the lack of geometric detail in the joint design in macro (shell-solid) models. In single lap joints, results have shown that, because of the simplicity of the structure, the shell-solid models give good correlation with solid (micro) models and experimental tests. However, there are problems in large-scale modelling techniques for more representative joints found in car bodies such as with coach joints; these joints are most frequently used as they provide flange access for spot-welding. Results have shown that the lack of detail and the geometric approximations, made in shell-solid models of adhesive joints, will give large variations from the expected stiffness results. Such approximations limit the accuracy of individual joint behaviour and it is thought that these individual approximations may consequently result in a significant error in the analyses of full bodies.

From these results and observations, it is obvious that some method must be adopted so that joint stiffness is more accurately represented in large-scale models. An initial thought

was to include some form of a substitute element in the shell-solid models which would contain the stiffness parameter of the joints. Substitute elements such as spring elements, joint-line elements and super-elements were investigated in detail, and the advantages and disadvantages of each were discussed in Chapter 4. The main problem involved in adding substitute elements to represent joint stiffness is associated with the limitations due to large model size and computer processing time. A novel approach to overcome this problem in the micro to macro translation of joint stiffness is proposed and discussed in Chapter 6.

6. DEVELOPMENTS OF MICRO TO MACRO MODELLING AND THE UNDERCUT ELEMENT CONCEPT

6.1 Introduction

As discussed in Chapter 5, the typical method used by industry for representing joints in FE models of full car bodies is based on the assumption of square (unradiused) flange corners and fully filled adhesive bondlines (100% fillet ratio). However in reality, the joints have radiused flange corners and the adhesive does not actually extend to the outer limits of the flange. These variations in joint configurations arise from production processing circumstances. For example, the flange bend is formed by press tools which have radiused corners to reduce tool wear, and the adhesive is usually applied as a bead from an extrusion gun. When the parts are assembled, the adhesive bead is squeezed between the flanges but does not usually flow to the edges of the joint.

It is clear that some form of correction is necessary to compensate for the errors introduced when making these assumptions in current full body analyses. Various approaches, described earlier in Chapter 4, have been devised to overcome such problems. Some solutions are based on the inclusion of substitute elements such as super-elements, joint-line elements and spring elements. Each method has its own advantages and disadvantages; for example, the maximum number of super-elements that can be used in NASTRAN is limited to 150 per model in a cold start run, and 100 super-elements in a restart run. The use of the joint-line element method [McGregor et al. (1992), Nardini & Hall (1995)], on the other hand, requires a special pre-processing package and replaces actual joint geometric details with an equivalent element. Part of the equivalencing is achieved through changes to material properties. Apart from the complicated procedures required for pre- and post-processing, the method ignores certain coupled modes of deformation which can occur in a joint, such as bending-stretching coupling. The use of spring elements has also some disadvantages and these have been already highlighted in Chapter 4. Thus, the complications and limitations for the implementation of these existing solutions into full body models require a more applicable solution in order to

obtain improvements in FE macro models. The undercut element method, derived in this chapter, offers a possible alternative to the micro to macro modelling problems and enables more accurate representations of joint characteristics with minimal effort.

6.2 The Undercut Element Concept

The undercut element method has been developed as a tool to improve the accuracy of FE models of large-scale vehicle body structures. It is a method of approximating local joint geometries. The method has been devised through the analyses of joints using micro and macro FE models and experimental methods, obtained in Chapter 5. The effects of different joint configurations, loading and adhesive fillet ratios were also considered.

The analysis and derivation of the undercut element concept was largely based on the coach joint, as this configuration is most representative of the flange joints used in vehicle body assembly, and as it is also most sensitive to bondline conditions. The derivation of the bondline fillet dimensions for solid and shell-solid element models are shown in Figures 6.1-6.3.

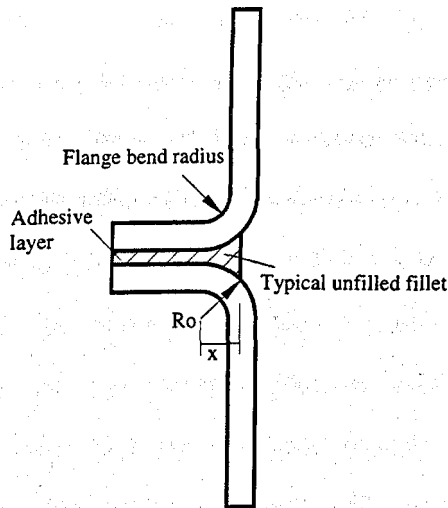


Figure 6.1 Representation of solid element model with all geometric details

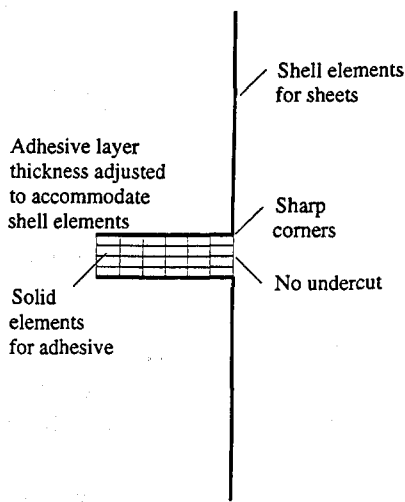


Figure 6.2 Shell-solid element model representing macro model with fully bonded flanges

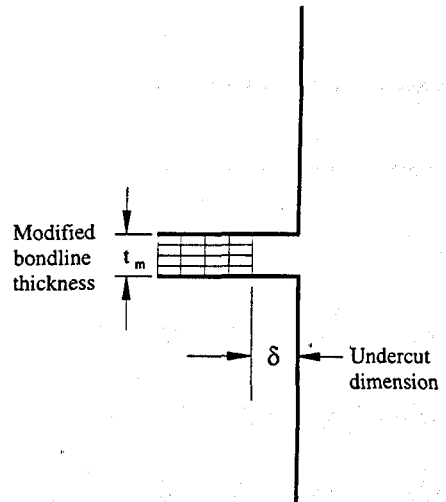


Figure 6.3 Application of the undercut element method in shell-solid models

It should be noted that the bondline thickness t_m in the shell-solid model, is greater than that of the solid model; this is due to the use of the sheet centre-line as the position for the shell elements. To compensate for this, the effective adhesive modulus is modified (equation 5.2) in the same ratio as the change in bondline thickness (equation 5.1), as described previously in section 5.2.5.

Numerical models of coach joints in tensile loading were considered in section 5.3. The results from the micro model (solid model), macro model (shell-solid model) and experimental tests are illustrated graphically in Figure 6.4. The graph compares the joint stiffness calculated by the applied force over the resultant displacement, plotted against the undercut distance/fillet ratio. The fillet ratio scale is used to define the amount of underfill for experimental specimens and FE solid models. The undercut distance scale, on the other hand, identifies the length of the underfill removed from the shell-solid element models. This second scale is essential as the shell-solid models do not include a bend radius which is essential in defining an adhesive fillet ratio.

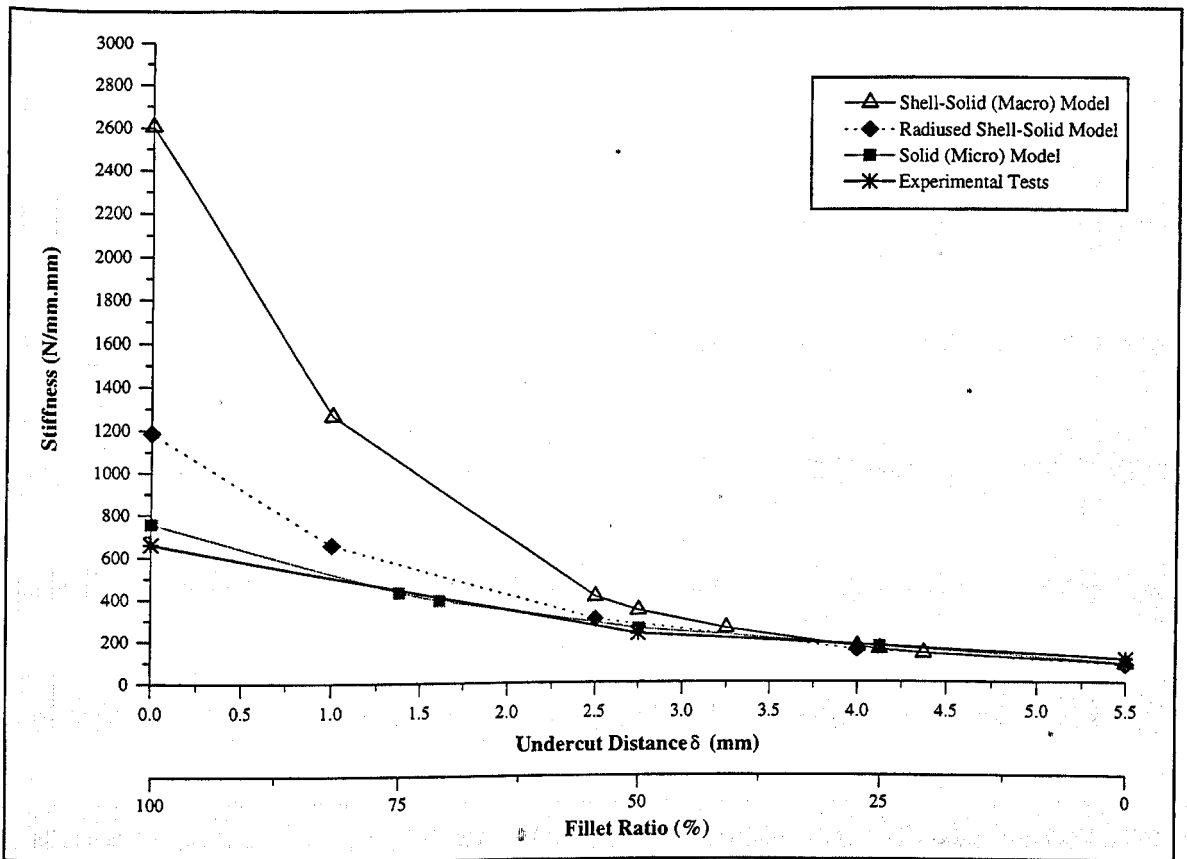


Figure 6.4 Comparison of experimental and FE modeling results with the inclusion of the undercut element

The results from the study show how the stiffness values calculated from the solid (micro) models are very close to those measured from the experimental tests; this is valid over a range of adhesive fillet ratios. Shell-solid (macro) models give extremely high stiffnesses when there is no undercut, but as an undercut of about 3 mm is added, the results converge towards the experimental and FE solid model results.

From an inspection of the characteristic curves in Figure 6.4, it is evident that the stiffness of shell-solid (macro) models can be controlled by the specification of an undercut in the glue-line. The undercut distance δ can be set to a value which will give a joint stiffness equivalent to that of the accurate solid element model. The undercut dimension can be obtained from the correction curve derived from Figure 6.4, and which is illustrated in Figure 6.5.

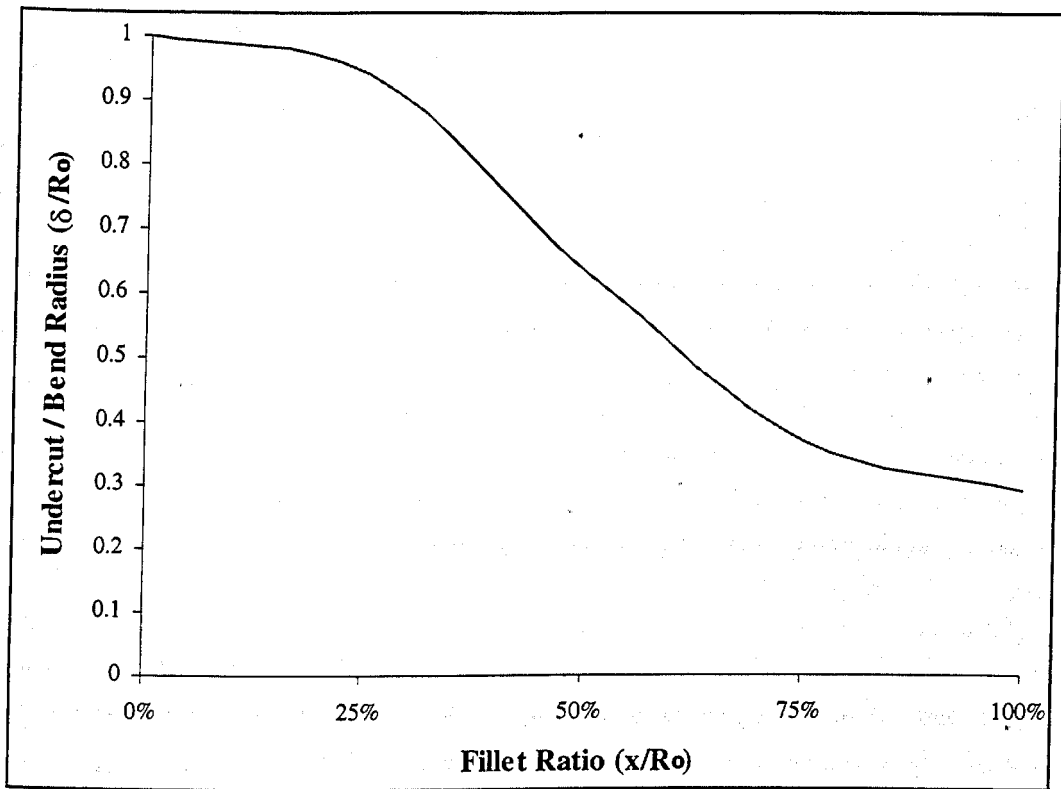


Figure 6.5 Characteristic correction curve for determining the undercut distance for various fillet ratios

For any specific fillet ratio in a micro model, the corresponding value of $\{\delta/R_0\}$ can be obtained from the graph in Figure 6.5. The resultant undercut distance δ can be then calculated from the undercut factor and is given by equation 6.1.

$$\delta = \{\delta/R_0\} \times R_0 \quad (6.1)$$

Where the undercut factor $\{\delta/R_0\}$ is determined from Figure 6.5 for a desired fillet ratio and R_0 is the external bend radius of the adherend

In practice, there is some uncertainty in the real value of the fillet ratio; the adhesive bead in an actual specimen may vary as it is squeezed out during panel assembly. Although some adhesive might be expected to form a partial fillet, in the worst case the fillet ratio may be zero, making it convenient to use this condition to develop a conservative model. Thus for a 0% fillet ratio, i.e. $x/R_0 = 0$, the correction characteristic curve will give an undercut ratio $\{\delta/R_0\}$ equal to 1; where the undercut dimension is equal to the flange bend radius. In typical panel pressings, the press tool is designed to give a 5 mm bend radius, and allowing for the sheet thickness in the shell element model, an equivalent 5.5 mm

adhesive undercut can be used. Although the undercut element principle was derived from tensile loading configurations, it may be noted from Figure 5.30 that the method is equally valid under flexural loading.

It should be noted from Figure 6.5 that for 100% adhesive fillet, $\{\delta/R_o\}$ is still greater than zero. This is because the undercut element compensates for the forming bend radius as well as for the fillet ratio. The summary results from the study on coach joints show that the inclusion of an undercut to shell-solid models (macro) has a significant effect on the overall joint stiffness.

6.3 Validation of the Undercut Element Method for Other Adhesive Joints

In this section, the undercut element technique was implemented in FE models representing other typical joint configurations such as single lap joints and asymmetric joints. Parametric studies were carried out on each joint configuration to determine the characteristics of the joints, and particularly how the undercut would affect the overall joint stiffness. The main objective was to indicate how macro models could be modified through the implementation of the undercut element, so as to reflect the predictions obtained from micro models.

6.3.1 Single Lap Joints

The geometric configurations and numerical methods used in this study are similar to those described previously in section 5.2 for lap joints subject to tensile loading. Typical lap joints with 15 mm overlap length, 1 mm sheet thickness and 0.2 mm bondline were used throughout the FE analysis; the results were compared to similar joints from experimental tests.

This work has been carried out to show how the application of the undercut element method will affect the results of the micro and macro models, with the aim to validate the method. Two implementations were considered; the first was to introduce an undercut length from one side of the overlap and the second, was to remove an undercut of equivalent length from both sides of the overlap. Figure 6.6 illustrates the two implementation techniques used in this investigation.

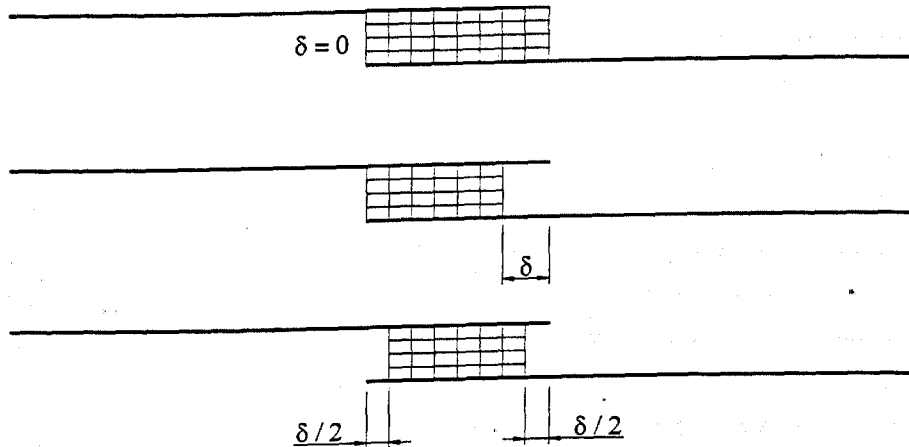


Figure 6.6 Application of the undercut element method to lap joints using different design techniques

Finite element analysis on lap joints with various undercut lengths was carried out and the results obtained were compared with the limited results from the experimental work. All results were calculated in terms of stiffness; this was measured over a central 50 mm gauge length of the joint. Figure 6.7 (a) and (b) show the results for TEROSTAT 3218F and CIBA XB5315 adhesives, respectively.

Results show that the FE shell-solid (macro) models over-predict the stiffness compared with accurate solid (micro) models and experimental test results. With the inclusion of an undercut element in the macro models, the stiffness drops following a similar trend as with the micro models. From the graph in Figure 6.7 (b), to obtain an equivalent stiffness of 1600 N/mm.mm based on the micro model, an approximate undercut length of 6 mm must be introduced into the shell-solid (macro) model. For equivalent stiffnesses, the results also show that the undercut could be removed from one side of the overlap, or an equivalent undercut length could be shared between both sides of the bondline.

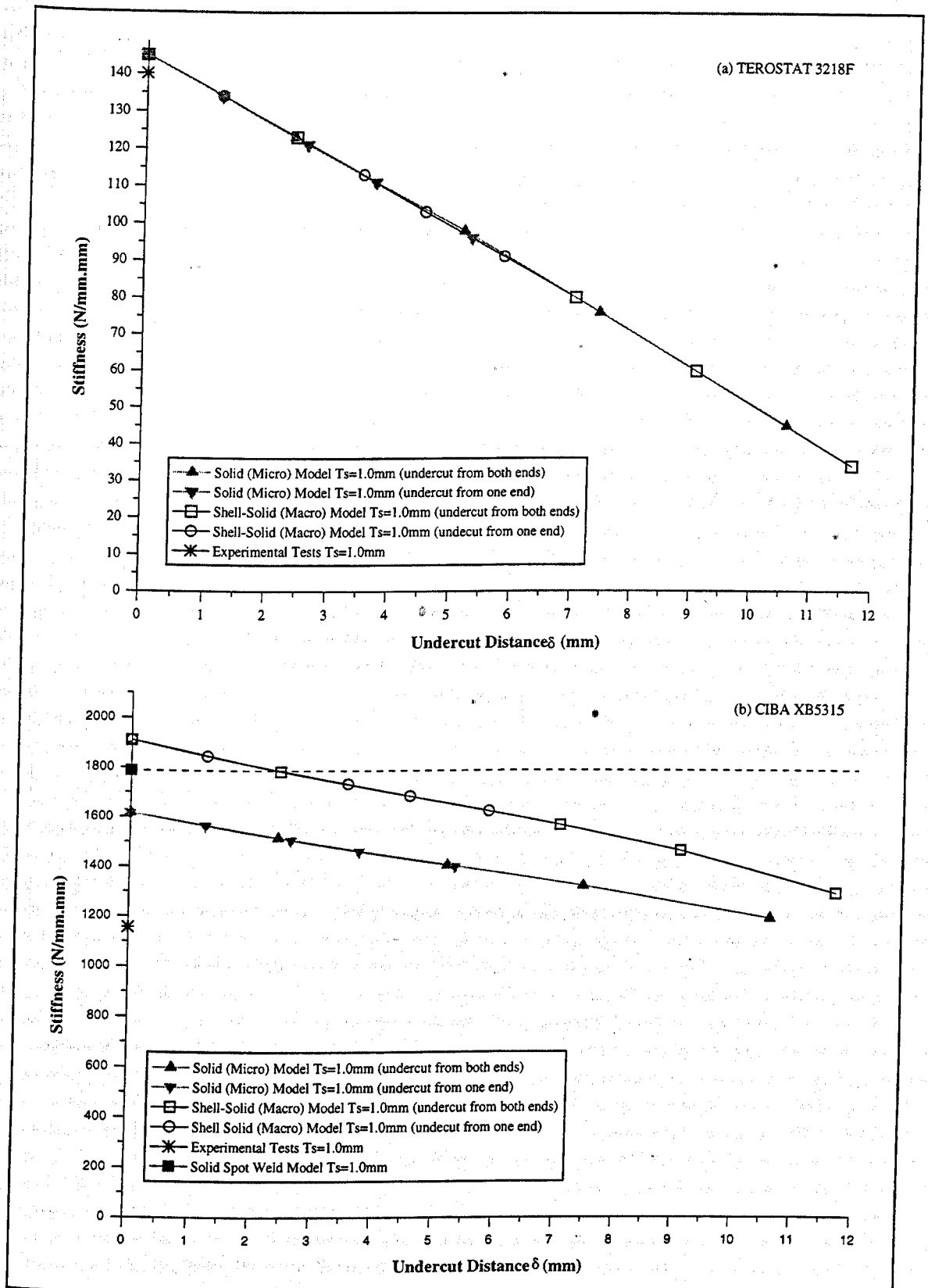


Figure 6.7 Prediction of stiffness using the undercut element method in single lap joints for (a) TEROSTAT 3218F and (b) CIBA XB5315 adhesives

6.3.2 Non-Uniform Geometries

Although the applicability of the undercut element method to 'ideal' flange and lap joints has been demonstrated in section 6.3, many vehicle body joints are geometrically asymmetric and are subjected to a combination of different loading conditions. Four non-uniform geometric joints, shown in Figure 6.8, were selected to represent typical joints found in vehicle structures. These joints were also used to investigate and validate the application of the undercut element method.

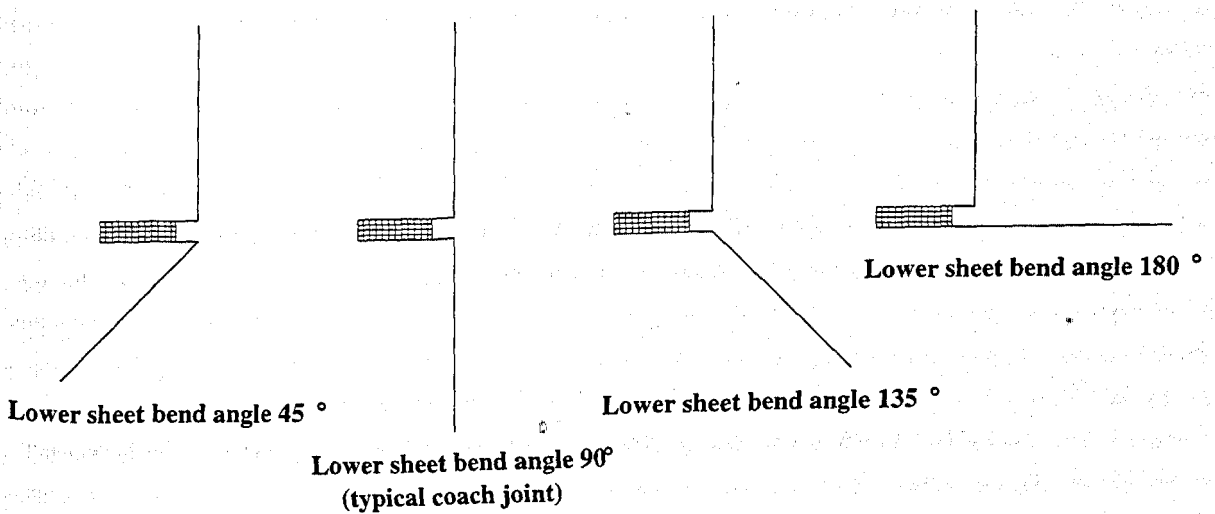


Figure 6.8 Various non-uniform geometric configurations

The dimensions of the joints, the bondline materials and sheet properties used in this investigation were similar to those previously defined in the study of coach joints in section 5.3. The only exception was the inclination of the lower sheet bend angle which was altered for each joint case. Also in the FE models, the length of the upper sheet was equal to the bend radius length used in the solid models, i.e. 5 mm.

Figure 6.9 shows an example of the constraints and the applied loads to a typical non-uniform geometric joint. The figure also shows where the displacements were measured to derive stiffness calculations. A force F was applied at the end of the lower sheet and in the direction of the sheet's length. The top end of the upper sheet was constrained for all degrees of freedom (DOF). The loading and constraint conditions were chosen for simplicity of implementation and they also allowed comparison between the different joints. Resultant displacements were calculated at the ends of the lower sheet where the load was applied and were measured in the direction of the load. Stiffness values were then calculated as a ratio of force over extension per unit width, i.e. N/mm.mm.

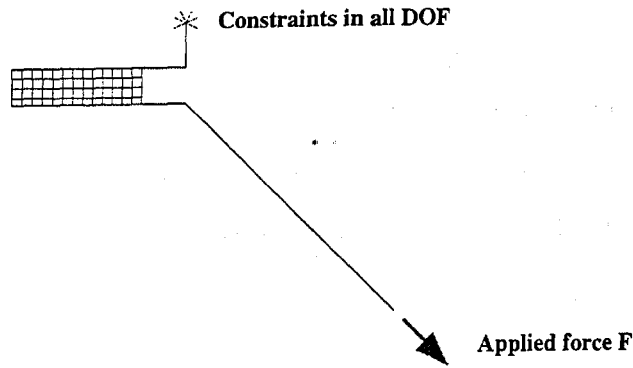


Figure 6.9 Application of loads and constraints to non-uniform geometric joints

Two different finite element methods were used to represent the four different joints; the first method used solid elements to give a detailed micro model, while the second method used shell-solid elements as used in macro model analyses of large-scale body structures. In all cases, an equivalent adhesive fillet ratio of 0%, i.e. 5.5 mm undercut in shell-solid element (macro) models, was used to represent the most critical case which is the lack of adhesive in the flange bend radius area. The comparative results of stiffness, calculated for the shell-solid (macro) and solid (micro) models, are presented in Table 6.1.

Lower Sheet Bend Angle	Solid (Micro) Model	Shell-Solid (Macro) Model
45 Degrees		
Stiffness (N/mm.mm)	2.83	3.15
90 Degrees		
Stiffness (N/mm.mm)	72.67	67.89
135 Degrees		
Stiffness (N/mm.mm)	9.37	11.30
180 Degrees		
Stiffness (N/mm.mm)	137.76	138.70

Table 6.1 Stiffness results from FE analysis on non-uniform geometries with the application of the undercut

The results from the study show very good correlation for all four joints; this is attributed to the equivalent undercut introduced into the shell-solid models. It is expected however, from previous modelling work on coach joints, that for larger fillet ratios, e.g. exceeding 50%, the difference in stiffness between the solid (micro) models and shell-solid (macro) models would be significantly greater, particularly for joints with full adhesive fillet ratios, e.g. 100%.

Although the main purpose of the study was to compare different modelling methods and include the undercut element method into macro models, the results also show how joint stiffness can vary significantly by changing the geometry; in this case the lower bend angle. The stiffest joint was predicted when the lower sheet bend angle was 180° , which is effectively loaded in shear. The second stiffest joint was the typical coach joint configuration, followed by the 135° and 45° lower sheet bend angle joints, which proved to be the least stiff joints.

6.4 Summary

Results from the analyses on small joints have given valuable information with respect to the development of the undercut element concept and its effectiveness towards more accurate predictions of stiffness. Finite element models using shell-solid elements and fully filled adhesive flanges represent the modelling techniques used by the automotive industry for full body analyses (macro models). These have been compared with more accurate micro models based on solid elements. Further validation of the finite element models was achieved through experimental testing of similar joint configurations.

For coach joints, it has been shown that shell-solid (macro) models over-predict stiffness and some form of correction is necessary. This can be achieved by applying an undercut in to the bondline. As a small undercut is introduced into the adhesive layer, the stiffness is significantly reduced. For an approximate 3 mm undercut, the results obtained from the shell-solid models are very similar to those measured from experimental tests and solid (micro) model results. For a typical 5 mm internal bend radius, it is suggested that an undercut of 5.5 mm can be included into the shell-solid (macro) models to provide an acceptable representation of joint stiffness for large-scale models.

Results showed that the inclusion of an undercut element in single lap joints gives similar stiffness trends to those obtained from the solid (micro) models; the more underfill in the adhesive, the less the overall joint stiffness. This variation occurs almost linearly for both shell-solid and solid element models. Hence, an equivalent undercut length can be implemented in the shell-solid models to obtain similar stiffness values to the solid element models.

A further validation of the undercut element method was shown with the analysis of four asymmetric adhesive joints. The study showed that for a 0% adhesive fillet ratio, or equivalent 5.5 mm undercut, the correlation between macro and micro models is very close.

The use of the undercut element concept has been validated for a number of different joint configurations and a design guideline for its application is given in Appendix I. The undercut element method provides a valuable technique for improving the accuracy of joint stiffness predictions in large-scale FE models. The extension of the undercut element method to larger structures, typically found in the vehicle body assemblies, is developed in Chapters 7 and 8.

7. APPLICATION OF THE UNDERCUT ELEMENT METHOD TO IDEALISED BEAM STRUCTURES

7.1 Introduction

Finite element modelling provides an effective way to study the behaviour of automotive structures and to predict characteristics such as vehicle body stiffness. It has been shown that some approximations in FE models may limit the accuracy of large-scale modelling techniques, and the undercut element method has been devised as a potential solution for approximating local joint geometries. The undercut element method has been demonstrated in small joints in Chapter 6 and in this chapter, the validity of the undercut element method is investigated on larger and more representative structures found in vehicle bodies. The applicability of the undercut element method is discussed in detail and the results from various FE modelling techniques are compared with experimental tests of similar structures.

7.2 Idealised Box Structures

Many experimental and analytical studies of vehicle substructures have been based on simple box beams, fabricated from sheet material with flanged corner joints [Beevers & Kho (1983), Eichhorn & Schmitz (1984), Pine et al. (1999)]. Beam dimensions and joint configurations may be selected to represent typical body details such as sills or door pillars, and a commonly used beam section is 60 mm square. The straight, linear beam form provides a simplified structure both for experimental testing and for numerical modelling. This configuration can be conveniently used to investigate the effects of the corner joints such as joining method, flange configuration and as in this study, adhesive properties, on structural behaviour.

In selecting the beam section for this investigation, it was expected that a further extension of the undercut element validation would be applied to the car plenum chamber substructure. The plenum chamber is a transverse box section situated below the car

windscreen and the flange configurations in the idealised box beam were chosen to represent the external joints of this detail from a Jaguar X300 car body.

Various box structure configurations, shown in Figure 7.1, were considered and detailed discussions between industrial partners were carried out to determine which one would best represent a typical substructure found in a vehicle body.

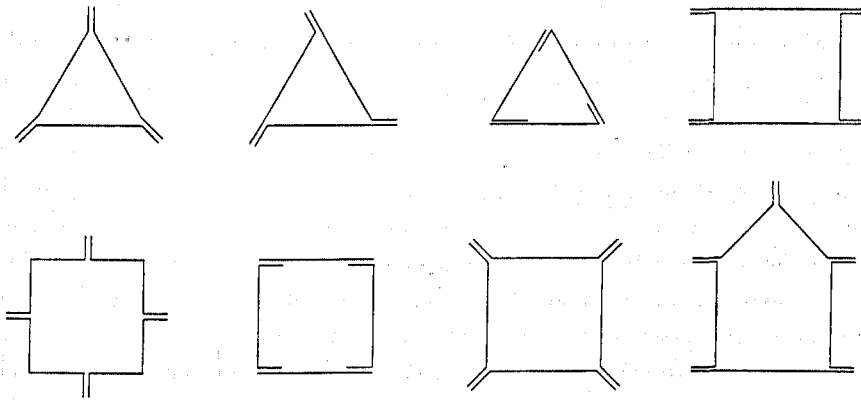


Figure 7.1 Typical box beam configurations

Following an extensive selection process with industrial partners of the LIVEMAN project, it was decided that the box structure to be tested and analysed would be that of an idealised square box with 4 x 45° external flanges, as shown in Figure 7.2.

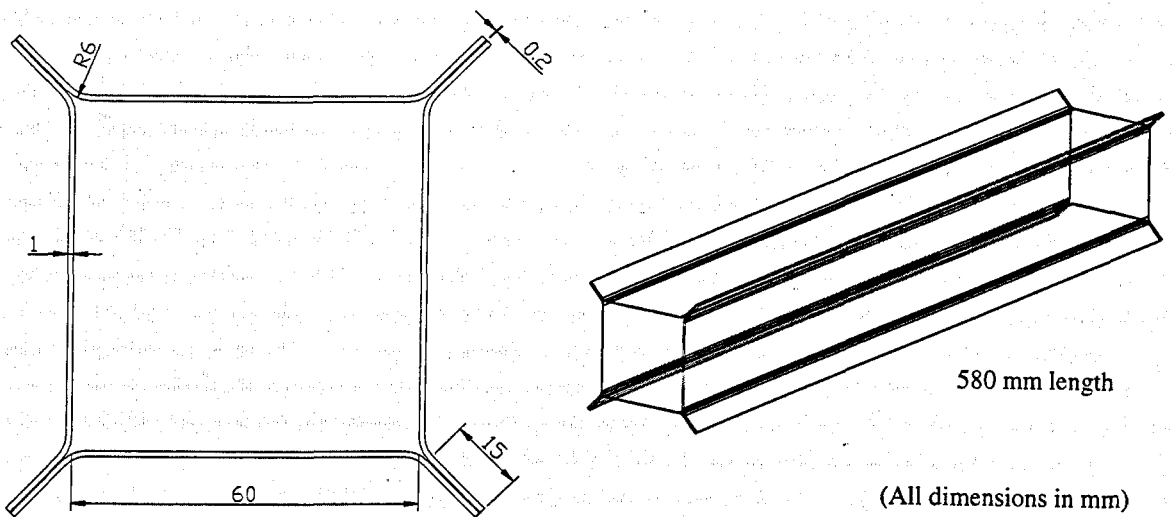


Figure 7.2 Schematic of the idealised box structure

The selection of this box structure was determined by a large number of factors. Firstly, the structure is square and its four 45° flanges make the structure symmetric over two

axes, facilitating both the manufacturing process and the computer modelling of the structure. Another advantage with this configuration is that with four equal angle flanges, the effects of shear deformation in the flange joints could be investigated as well as the sensitivity of the structure to changes in joint details. One of the most important reasons for selecting this structure was the ease of applying loads in bending and torsion to the structure, which with the other beam configurations might have been difficult. The dimensions for the idealised beam were primarily chosen for consistency with other published work [Eichhorn & Schmitz (1984), Pine et al. (1999)] and previous work carried out in Oxford Brookes University [Beevers & Kho (1983)] on similar box structures.

The work described in this chapter involves analysing this idealised box beam structure through experimental tests and using two FE modelling methods: the first using solid elements, and the second combining shell with solid elements. The purpose of this investigation was to verify the effectiveness of the undercut element method and to validate the applicability of the method to larger structures when subjected to various modes of loading, i.e. torsion, transverse tension and bending, represented in Figures 7.3-7.5.

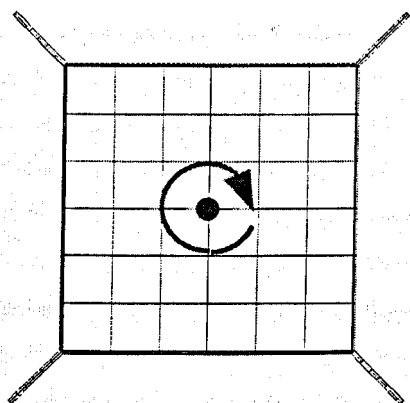


Figure 7.3 Torsional loading

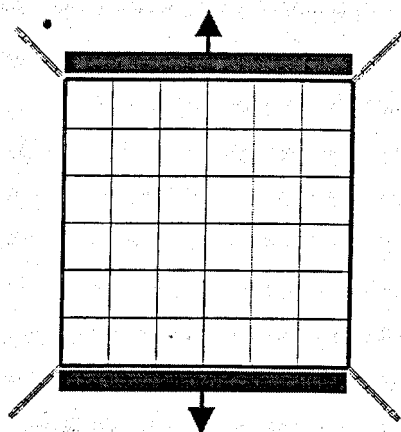


Figure 7.4 Tensile loading

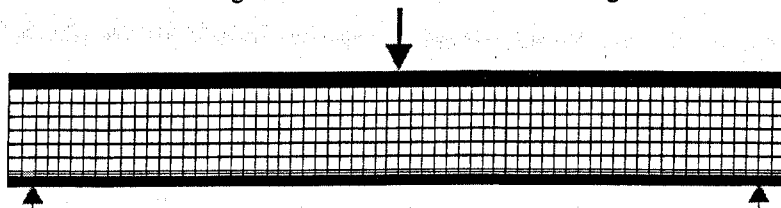


Figure 7.5 Flexural loading

Experimental tests of similar structures and loading conditions were carried out for comparison with FE modelling results. Finite element models of the idealised box

structure also included the required fixtures, such as the aluminium plugs/plates, which were used in the experimental set-up.

Most of the extensive modelling and testing work was carried out on box structures based on torsional tests, as this was also the main testing mode for typical vehicle structures such as the plenum chamber and the full body. Adhesive fillet ratios of 0% and 100% were studied in solid element models and were used to justify the adhesive underfill and the application of undercut elements in shell-solid element models.

7.3 Finite Element Modelling of Beams

Solid Element Modelling

The first FE modelling technique, which was used to predict the stiffness of the idealised box structure, was based on solid elements. These models accurately define and replicate all the essential geometric configurations of the actual structure used in the experimental tests including the bend radius of the flanges, the adhesive fillet ratio and the bondline thickness. The adhesive fillet ratio was one of the most important parameters studied in the numerical analysis. The study on adhesive fill provides a better understanding on the prediction of stiffness and can be used for verification of the undercut element method, discussed previously in Chapter 6. Figures 7.6 (a) and (b) illustrate a schematic representation for the FE solid element definition of a 0% and 100% adhesive fillet ratio, respectively.

For solid element FE models, the definition of the adhesive fillet ratio is primarily dependent on the sheet bend radius used in the idealised beam structure, and the formula to derive the fillet ratio was given previously in Figure 5.16, of section 5.3.1. In practice, a 0% adhesive fillet ratio would define a joint in which adhesive is placed only in the flanges of the joint; this is also the area in which the sheet forming bend radius begins. A 100% fillet ratio defines a fully filled joint, where the adhesive extends over the area up to the point where the forming bend radius ends and where the continuous sheet of the sides of the box structure begins.

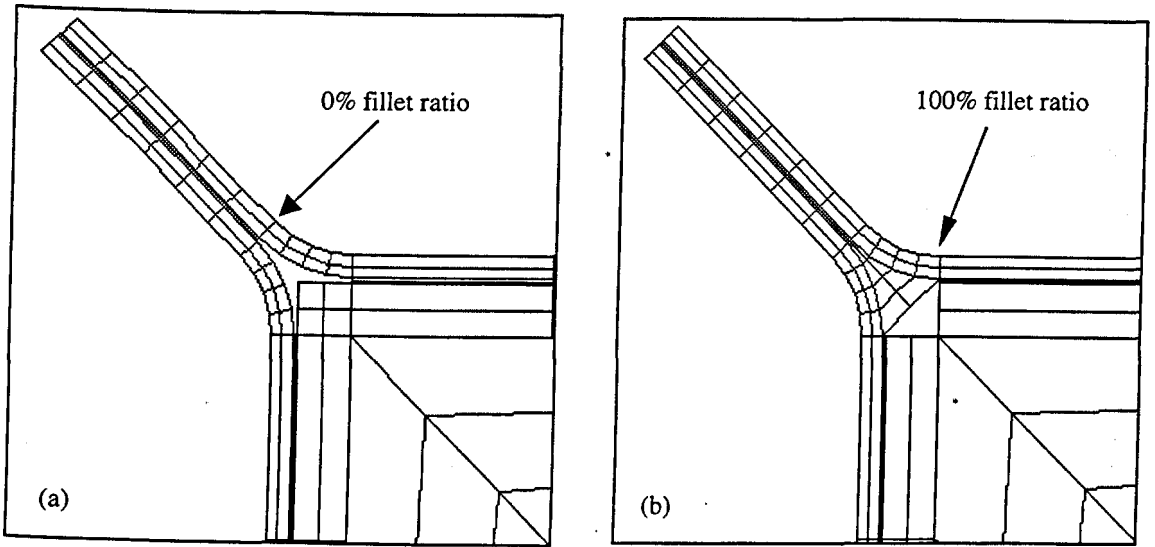


Figure 7.6 FE solid element models with (a) 0% and (b) 100% adhesive fillet ratios

Shell-Solid Element Modelling

The second modelling technique used a combination of shell with solid elements implementing the undercut element method for validation and comparison with accurate solid models and experimental tests. Shell element models lack geometric details of the joints, such as the forming bend radius, which are typically represented with sharp bends. To compensate for the lack of geometric details, undercut elements of various lengths were included in all four flanges of the box structure, and compared with a similar analysis of adhesive fillet ratios in solid models. Figures 7.7 (a) and (b) show schematic representations of the idealised box structure and the application of the undercut element to shell-solid models.

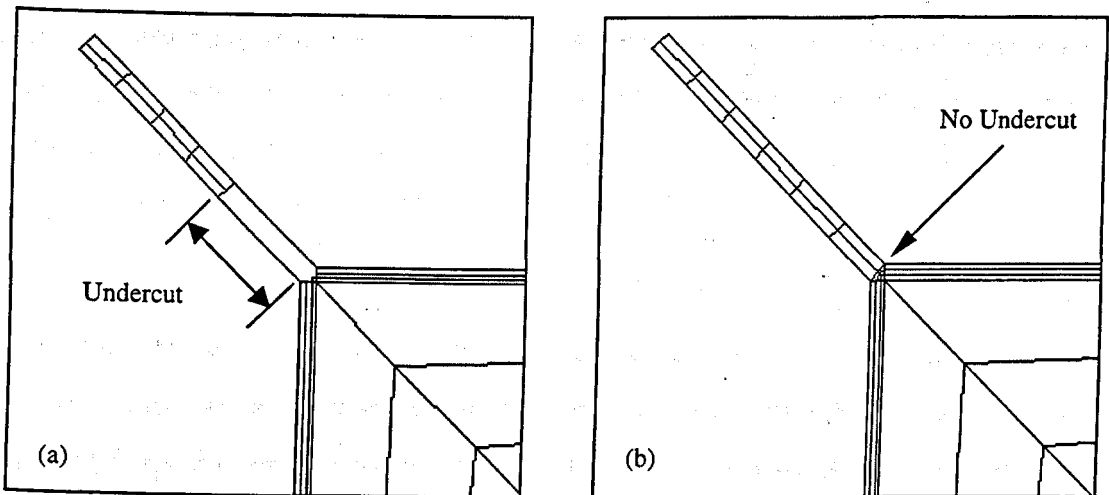


Figure 7.7 Shell-solid element models with (a) the implementation of the undercut element and (b) representing macro models with fully filled adhesive flanges

The interpretation of the adhesive fill for shell-solid element models is primarily based on the development of the undercut element method. From previous work carried out on coach joints, an equivalent 0% adhesive fillet ratio for a coach joint with 6 mm external bend radius would be obtained by introducing an equivalent undercut of 5.5 mm into the correspondent shell-solid models. In this study, the same undercut length of 5.5 mm was used since the forming bend radius was also 6 mm; the results obtained were compared with equivalent solid models.

7.4 Torsional Loading of Box Structures

The main study of box structures investigated beams when subjected to torsional loading. In the experimental work, two 20 mm thick aluminium plugs were inserted and bonded into the ends of the box structure to minimise local deformations which might occur when a uniform load is applied to a thin-gauge sheet structure. These were also replicated in the FE models. Angular rotation of the structure was achieved by introducing a rotational displacement to the centre of one of the aluminium plugs while the remote end was constrained. Figure 7.8 shows the resultant box structure when a rotation is applied to create torsional loading.

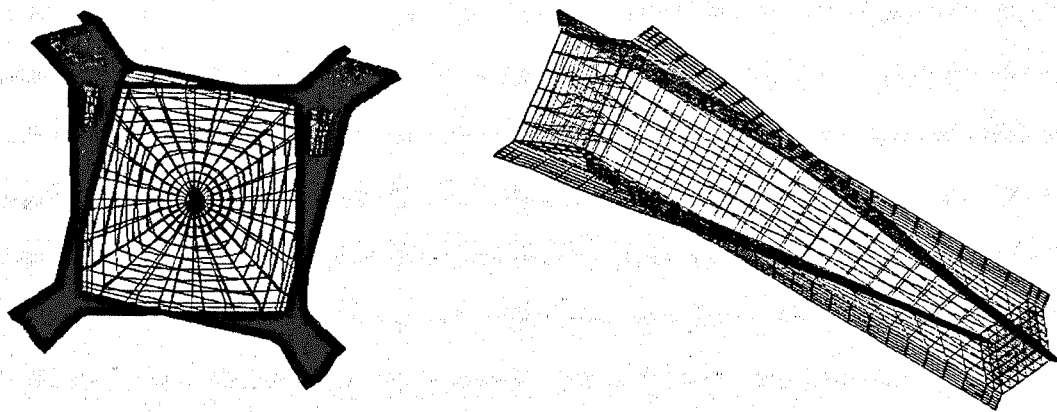


Figure 7.8 Resultant box structure with the application of torsional loading through nodal displacements

An extensive study was carried out on the accuracy of the mesh used to model the structure. Initial results with lower mesh densities proved to give inaccurate results compared to those with larger mesh densities. A number of FE tests were carried out on models with different mesh sizes in order to determine the mesh limits for convergence to be reached. Quarter models and half models of the box structure were also modelled and

compared to full model results. There was some concern in the results obtained from the quarter and half models as it was believed they did not accurately represent the loading and constraining conditions specified in the experimental tests. Further work was carried out on full models which provided the closest replicate of the loading and boundary conditions used in the experimental testing work. This was eventually achieved by increasing the area of the specific rotation and by applying a nodal displacement around a circular path. Detailed refinements of the modelling method eventually resulted in a model which gave comparable results to other published work, shown in Table 7.1, and which provided a more confident comparison with experimental test results.

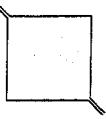
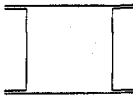

Published Work	Box Structure	Torsional Stiffness (Nm/degree.m)
[Eichorn and Schmitz (1984)] Spot-welding (25 & 50mm weld pitch) Weld-bonding (PVC & epoxy adhesives)		150 - 185 240 - 265
[Kho and Beevers (1983)] Spot-welding (25, 35 & 45mm weld pitch) Adhesive bonding (epoxies & toughened acrylic adhesives) Weld-bonding (epoxy adhesive & 35/45mm weld pitch)		62-124 140-200 100-135
Closed-Form Analysis $\theta = \frac{TL}{4 A^2 G t}$		300

Table 7.1 Comparison of numerical modelling methods with other published work on box structures in torsional loading

7.4.1 Validation with Experimental Work

To justify the finite element analysis results and the undercut element method, experimental tests were carried out parallel to the FE work. Other researchers in the Joining Technology Research Centre at Oxford Brookes University undertook the experimental testing on various box structures for three loading conditions: torsion, flexure and tension. In all loading cases, the adhesive fillet ratio was the most significant parameter investigated; this was needed to compare with finite element models and the efficiency of the undercut element method.

The main bulk of the experimental work on box structures was in torsional loading. In the testing set-up, square aluminium alloy plugs of 20 mm width were inserted into the ends of the beams and bonded so that the load could be distributed evenly and thus minimise

local plastic deformations. These plugs were designed specifically for torsional tests, where the loads were transferred by means of specially designed drive/adaptor plates which were fitted into an Avery-Denison torsion testing machine. One of the adaptor plates was located onto the testing machine by a centralising chuck, and the other plate was designed to fit into the $\frac{3}{4}$ " drive of the torque transducer, shown schematically in Figure 7.9. The experimental set-up is shown in Figure 7.10.

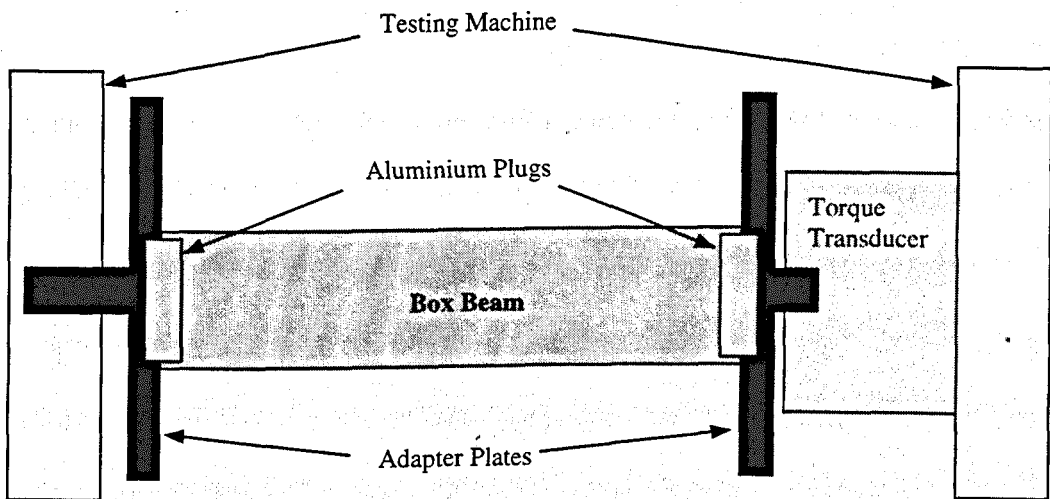


Figure 7.9 Schematic representation showing the arrangement of the box beams in the testing machine

Small mild steel brackets were attached through self-tapping screws to one side of the beam plates to provide gauge points for the location of the LVDT displacement transducers. The transducers measured the twisting movement of the box structure through the measurement of the displacement of the brackets. The brackets were located at approximately 90 mm from the centre line of the beam, giving 1.57 mm of movement for every 1 degree rotation. The applied torque was measured by means of a strain gauge torque transducer. Outputs from the LVDT displacement transducers and load cell were recorded onto a data logger. The results from initial tests showed that the beams exhibited non-linearity below 20 Nm applied torque, possibly due to embedding of the driving surfaces. Therefore, all structures were pre-loaded three times before any results were actually taken and recorded. Care was taken to ensure that the loading conditions did not introduce significant yield into the beams and that the torque/displacement recordings were essentially linear. Early experiments identified the upper torque limits as 30 Nm for the TEROSTAT 3218F adhesive and 100 Nm for the CIBA XB5315 adhesive. The actual stiffness analysis was determined from the slope of the torque/displacement curves

between 20 and 30 Nm for the TEROSTAT 3218F beam and between 50 and 100 Nm for the CIBA XB5315 beams.

For each test, the beam was carefully positioned in the machine, the instrumentation calibrated and the structure pre-loaded. During the full loading cycle, the outputs from the transducers were recorded and through the signal processing software were inserted into a spreadsheet package. Graphs showing torque against rotation per metre length were derived. The resultant torsional stiffness was determined by calculating the slope or gradient of the best-fit line obtained from the test results. Figure 7.10a shows the experimental set-up of the box structure during torsion testing and Figure 7.10b shows a representative autographic recording from the instrumentation.

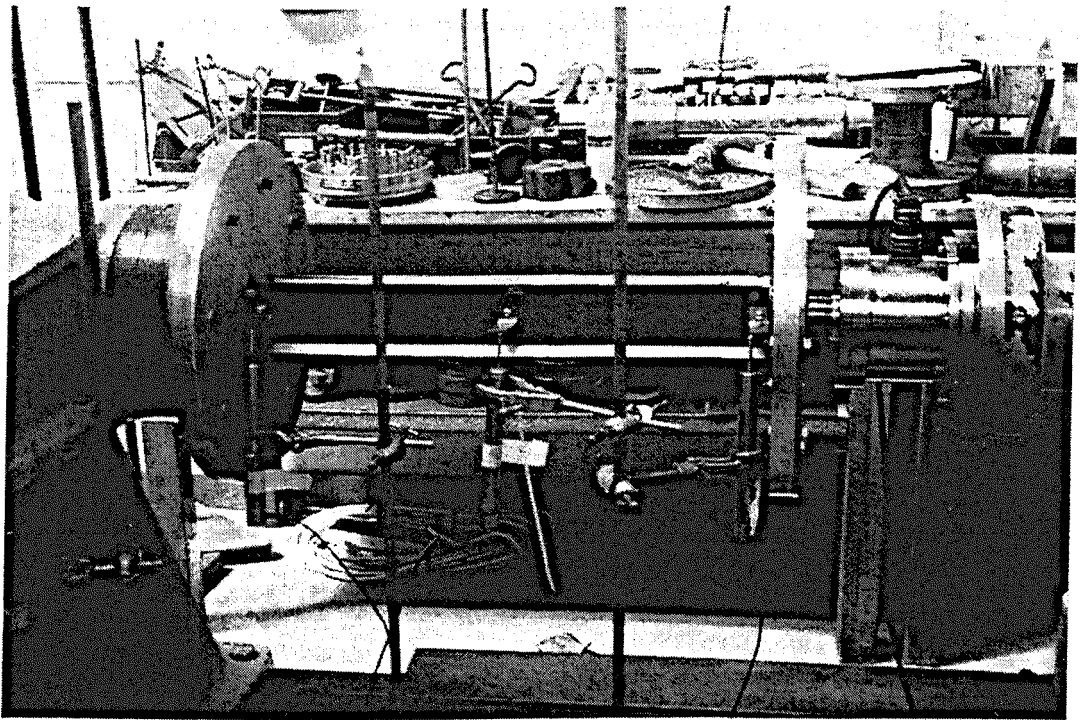


Figure 7.10a Experimental set-up of the box beams in the Avery-Denison torsion testing machine

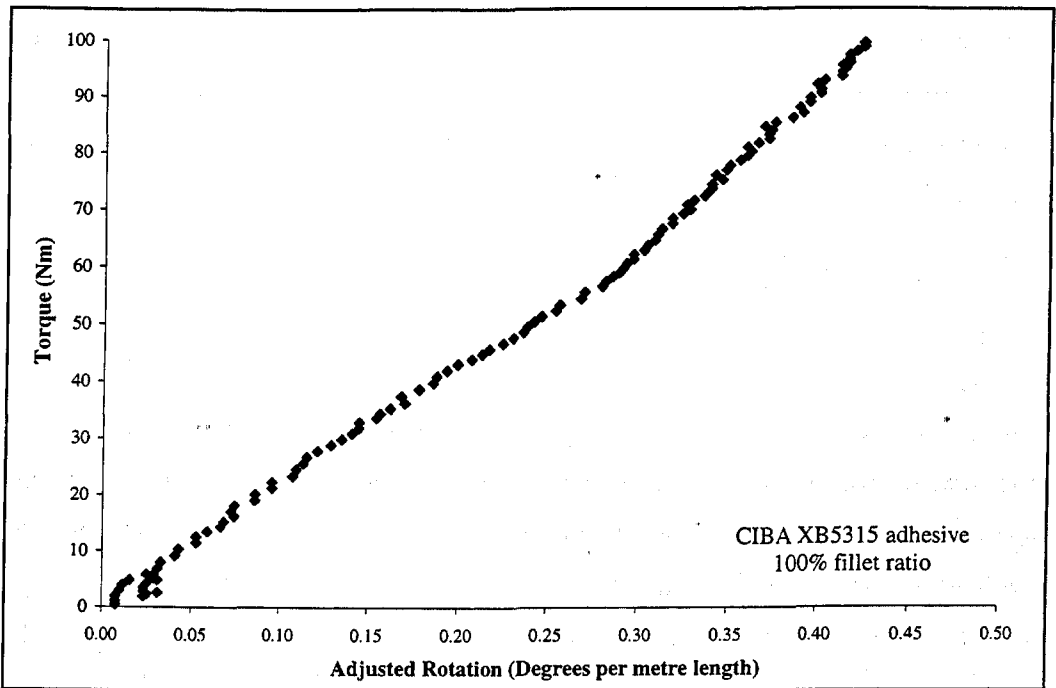


Figure 7.10b Typical torque-rotation curve obtained from experimental tests

The results from the experimental tests are presented in Table 7.2 and compared to the predicted stiffness values from the FE models.

Adhesive Type	Adhesive Fillet Ratio	Torsional Stiffness (Nm/degree.m)		
		Experimental Tests	FE Solid (Micro) Model	FE Shell-Solid (Macro) Model
CIBA XB5315	100%	276	327	316
	0%	270	314	276
TEROSTAT 3218F	100%	26	37	37
	0%	26	37	36

Table 7.2 Comparison of torsional stiffness values from experimental tests and FE modelling methods

Results from the experimental tests and numerical modelling analyses show that generally, the adhesive fillet ratio has little effect on torsional stiffness. The largest variation in stiffness between 0% and 100% fillet ratio was of approximately 15%. Generally, the values calculated from the FE analyses gave slightly higher predictions than those obtained from the experimental tests; this was possibly due to uncertainties in adhesive modulus. Another observation from the results was that there was significant difference of torsional stiffness between the beams bonded with CIBA XB5315 and TEROSTAT 3218F adhesives. However, this is expected considering that the higher modulus adhesive (CIBA XB5315) has a modulus about 300 times greater than that of the lower adhesive (TEROSTAT 3218F), while the resultant stiffness is about 10 times higher. Similar experimental tests of spot-welded beams were also carried out and the resultant stiffnesses

were approximately 240 Nm/degree.m, compared to 270-276 Nm/degree.m measured from the CIBA XB5315 bonded beams. These results show how with the use of selected adhesives, stiffer structures than comparable spot-welded beams can be obtained. Also, the results from the shell-solid models which included the undercut element, gave stiffness values which were closer to the experimental results; this validates the use of the undercut element method.

7.4.2 Effects of Apertures in Beam Walls

The box beam structure was chosen to represent a structure which would be most typically found within a car body. However, most vehicle substructures, such as the plenum chamber, are not continuous sheet forms as in the idealised box structure. On inspection of vehicle structures, the presence of many holes and apertures of different sizes and various locations were noted. To better represent car substructures, a single aperture was introduced in the FE models along the mid-span of the side of the beam, as shown in Figure 7.11.

The effects of various sized apertures on the stiffness of the box structure was investigated in experimental tests, as well as for both solid element and shell-solid FE models. The sizes of the apertures were primarily dependent on the sizes of the elements defined along and across the sheet surface. The largest aperture, shown in Figure 7.11, was limited by the width of the structure's flanges and was equivalent to approximately 26% of the total upper sheet area. Figure 7.12 shows the experimental set-up of the box beam with a large central aperture when subjected to torsional loading.

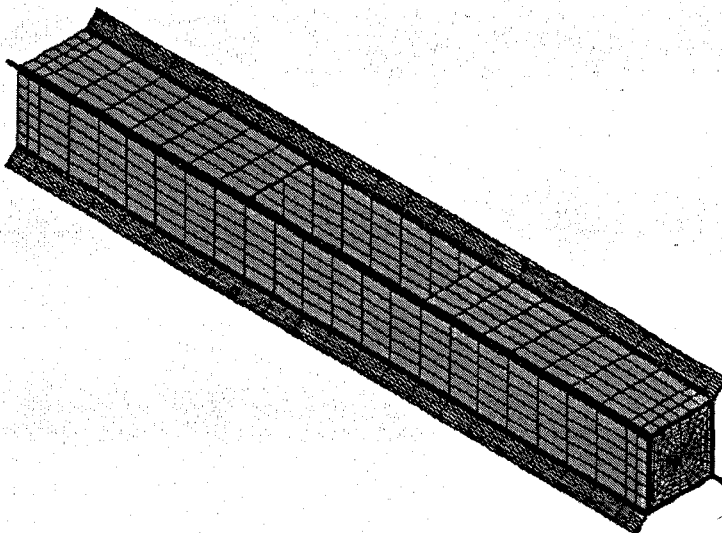


Figure 7.11 FE model of box structure with a central aperture

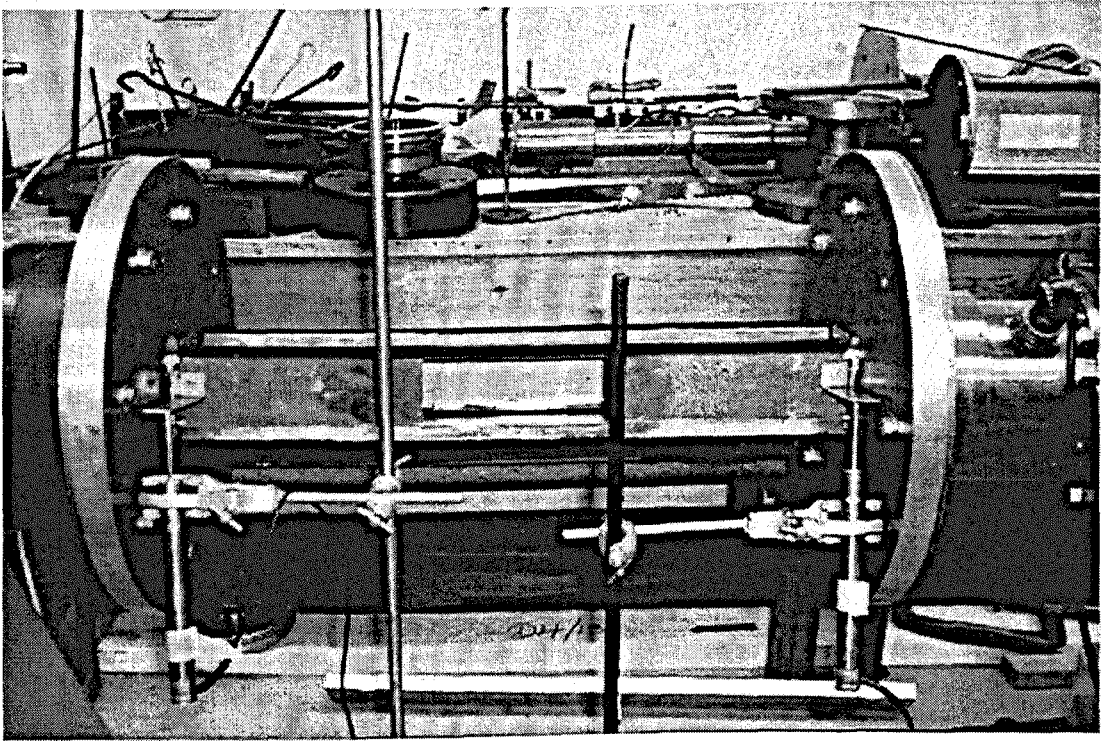


Figure 7.12 Experimental set-up of box beams with a central aperture for torsional loading

Results from the FE analyses on box beam structures subject to torsional loading and for various aperture sizes are given in Table 7.3 and are compared with experimental tests in Table 7.4. CIBA XB5315 and TEROSTAT 3218F adhesives were primarily used in the study as these represent the extreme ranges of typical automotive adhesives.

Adhesive Type	FE Modelling Method	Effective Fillet Ratio	Torsional Stiffness (Nmm/degree.m)				
			0% Aperture	3% Aperture	6% Aperture	12% Aperture	26% Aperture
TEROSTAT 3218F	Solid Model	100%	37	37	36	35	28
		0%	37	37	36	35	28
	Shell-Solid Model	100%	37	37	36	33	19
		0%	26	26	25	24	15
CIBA XB5315	Solid Model	100%	327	316	300	235	116
		0%	314	303	287	226	110
	Shell-Solid Model	100%	316	293	259	169	59
		0%	276	259	214	176	51
All Steel Box	Solid Model	100%	375	368	345	269	143
		0%	334	330	312	242	118
	Shell-Solid Model	100%	355	337	315	238	130
		0%	304	287	248	214	83

Table 7.3 Torsional stiffness results of box structure for various size apertures

A significant observation of the investigation is the effect of apertures on the overall stiffness of the structure. As the size of the aperture increases, the torsional stiffness of the box structure decreases significantly, particularly for higher modulus adhesives. However,

there is some concern regarding the departure of the prediction between solid and shell-solid models in beams with larger apertures, e.g. 26%. Experimental tests were carried out to investigate the effect of large apertures on stiffness and how these compare with predictions from the FE models. These results are given in Table 7.4.

Beam Aperture	Adhesive Type	Adhesive Fillet Ratio	Torsional Stiffness (Nm/degree.m)		
			Experimental Tests	FE Solid (Micro) Model	FE Shell-Solid (Macro) Model
26% Aperture	CIBA XB5315	100%	42	116	59
		0%	36	110	51
	TEROSTAT 3218F	100%	17	28	19
		0%	17	28	15

Table 7.4 Comparison of torsional stiffness results from experimental and FE modelling methods for box beams with a large central aperture (26%)

The divergence of correlation with FE solid models, particularly for larger apertures, may be due to the local buckling which occurs at the corners of the apertures in the experimental tests, and which is not accounted for or included in linear elastic FE models. Nevertheless, both experimental and numerical modelling results show how the presence of an aperture will contribute significantly to loss in stiffness of the beam. It is expected that for larger vehicle substructures, which include a number of various sized apertures, such as the plenum chamber, the overall stiffness results will be significantly lower. Sakurai and Kamada (1988) also investigated the effects of apertures in vehicle structures and found that both the size and positioning of apertures affected the overall stiffness.

7.5 Transverse Tensile Loading of Box Structures

The second loading condition investigated was transverse tensile loading. Similar FE models of the structures were used as in torsional models however, the overall lengths of the beams were modified to 100 mm compared to the original 580 mm length. In order for the FE models to accurately represent and simulate experimental test procedures, two 10 mm steel plates (40x10x100mm) were placed on either side of the top and bottom beam walls, as shown in Figure 7.13. The top plates were then subjected to a vertical displacement of 1 mm, while the bottom plates were constrained in all directions.

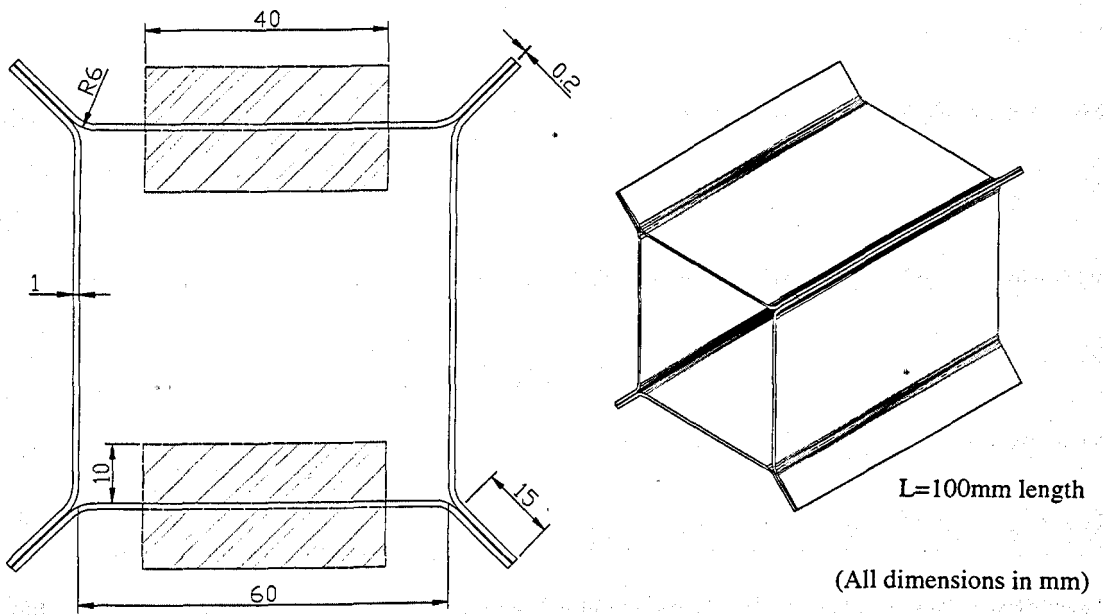


Figure 7.13 Dimensions of box structure in transverse tensile loading

The main purpose of this study was to investigate the behaviour of the box structures when subjected to transverse tensile loading and in particular, the effect of the adhesive fillet on stiffness. By using solid models and shell-solid models in the FE analysis, the effectiveness of the undercut element method and its applicability to large FE models of structures subjected to tensile loading conditions could be verified. Figures 7.14 and 7.15 show examples of the two FE modelling techniques used in the analysis; the first one represents a solid element model with a 0% adhesive fillet ratio, and the second one represents an equivalent shell-solid element model with the inclusion of a 5.5 mm undercut.

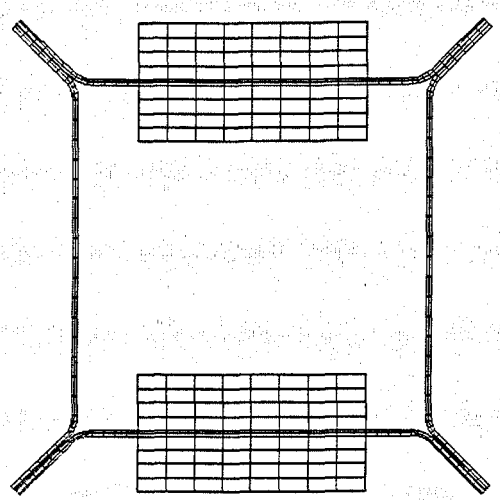


Figure 7.14 Solid element (micro) model with 0% adhesive fillet ratio

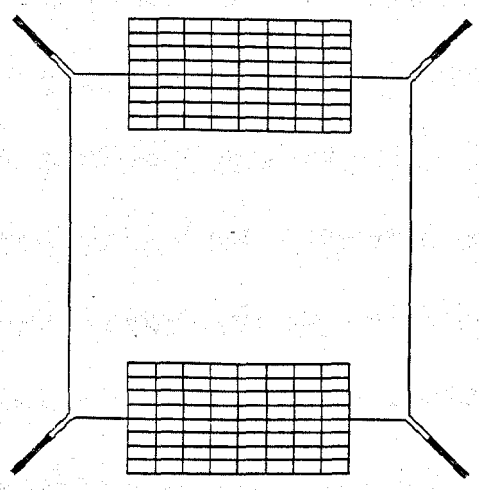


Figure 7.15 Shell-solid (macro) element model with 5.5mm adhesive undercut

Initial results from the FE analyses showed large variations between the solid and shell-solid element models for a range of adhesive fillet ratios and undercut lengths. Further analysis work confirmed the need to improve the mesh density of these models. This was probably due to the nature of the solid elements which do not take into account any rotational movements; which are present at the edges of the steel plates. After an extensive mesh convergence analysis, results from both solid and shell-solid models could be compared to one another; the results from these refined models are compared with experimental test results and are given in Table 7.5.

7.5.1 Validation with Experimental Tests

The manufacturing of the 100 mm long box beam structures was carried out in a similar manner as the procedures used in the torsion beam tests. In order to provide a transverse tensile load to the beams, two steel plates (40x10x100mm) were clamped about the top and bottom steel sheets, as shown in Figure 7.16.

Six beam specimens were manufactured and tested for each beam configuration. The structures were clamped into a jig and pulled at a speed of 0.5 mm/min, until a 1 kN load was reached or a 1 mm displacement measured. Because of the possible geometric variations in the manufactured box structures, the beams were tested in two orientations. An average of these results was used to calculate the resultant stiffness of the structure. The stiffness of the test jig was also assessed and accounted for in the resultant data. A comparison between the experimental test results and the FE results is given in Table 7.5.

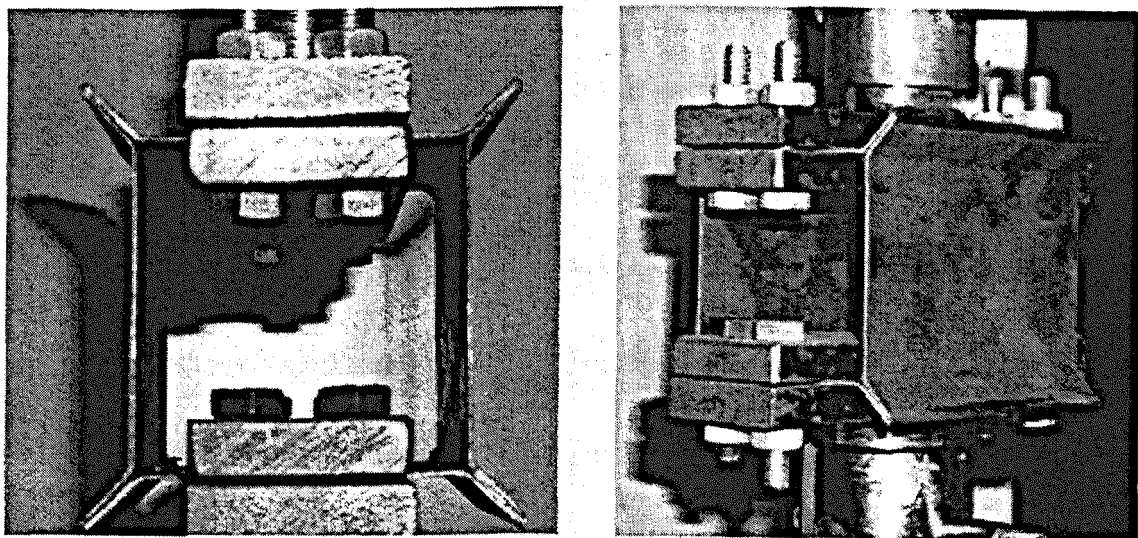


Figure 7.16 Experimental set-up of box beams for transverse tensile tests

Adhesive Type	Effective Fillet Ratio	Tensile Stiffness (N/mm.m)		
		Experimental Tests	FE Solid (Micro) Models	FE Shell-Solid (Macro) Models
CIBA XB5315	100%	15475 ± 5435	48,980	48,650
	0%	13344 ± 5054	44,930	34,890
TEROSTAT 3218F	100%	11560 ± 1334	33,190	34,510
	0%	9923 ± 1299	29,020	18,960

Table 7.5 Comparison between FE and experimental test results for box structure in tension

Results from the FE analyses show good comparison between the two different modelling methods for high fillet ratios/low undercut lengths. However, shell-solid models with 0 mm undercut gave significantly lower stiffness values compared with equivalent solid models of 100% adhesive fillet ratio. From this observation it is evident that the undercut element method might give a conservative estimate of transverse tensile stiffness.

Another observation was the variation of the experimental test results from the modelling results. The experimental results exhibit large scatter of stiffness values, particularly for the high modulus adhesive. On further inspection of the manufactured box structures, it was noticed that some of the beams were not true square sections and one example of this can be seen in Figure 7.17. Such variations in geometric orientations probably occurred as a result of manufacturing misalignment and these inaccuracies may account for the larger variations in the experimental results. The high scatter of the experimental results caused difficulties in correlation with results from the 'ideal' geometric box structure, represented by the FE models. Further FE modelling analysed the 'out-of-square' box structure, shown in Figure 7.17.

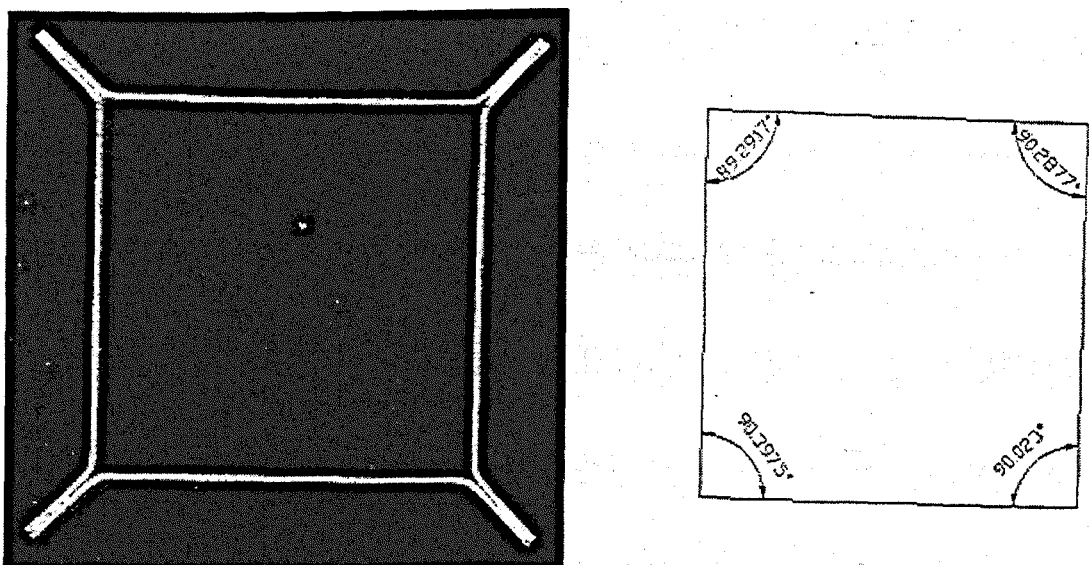


Figure 7.17 Cross-section of experimental box structure and measurements of angles

Results showed that when a box structure is manufactured with angular errors, the overall stiffness of the box structure is considerably lower than the stiffness measured from the idealised beam models. Table 7.6 shows the results from the FE analysis on out-of-square box structures when subjected to transverse tensile loading.

Adhesive Type	Effective Fillet Ratio	Tensile Stiffness (N/mm.m)		
		Square Solid Model	Square Shell-Solid Model	Out-of-Square Shell-Solid Model
CIBA XB5315	0%	45,170	34,890	30,540
	100%	49,250	48,650	41,400
TEROSTAT 3218F	0%	29,130	18,960	16,010
	100%	33,330	34,510	28,930

Table 7.6 FE results from analysis on out-of-square box beams in tensile loading

By comparing the results from the shell-solid element models, it can be observed that the stiffness of the structure drops by approximately 15% when the corners of the box are modelled to include small angular errors. Although this does not fully account for the lack of correlation between the experimental results and the analytical models, it is evident that out-of-squareness contributes significantly to loss of stiffness. Other sources of error may be due to the deflections of the fixtures in the experimental tests.

7.6 Flexural Loading of Box Structures

The third loading condition that was investigated was flexure loading, through three-point bending. The testing was carried out using similar FE models of box beams as used in the torsion tests, with the exception of a minor modification to the models. This was the insertion of an additional 20 mm aluminium plug positioned at the mid-span of the beam length, as shown in Figure 7.18.

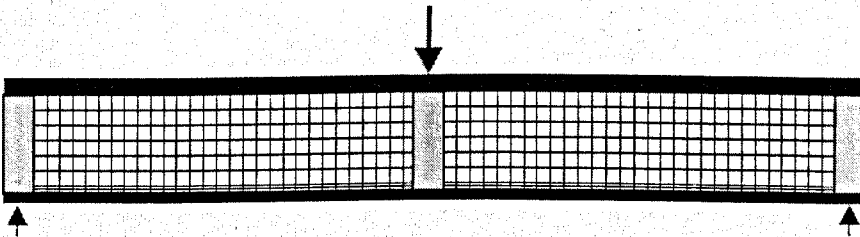


Figure 7.18 FE model of box structure for flexure loading with the inclusion of a central plug

The additional plug was used to accommodate the centre-point load used in the experimental work. Solid and shell-solid element models were modelled for various adhesive fillet ratios/undercut lengths using two extreme ranges of adhesives: TEROSTAT

3218F and CIBA XB5315. These models were used to validate the effectiveness and applicability of the undercut element in structures subject to flexural loading. An additional solid element model was designed to represent a spot-welded box structure; this was used to provide a further comparison with a different joining method.

Three-point loads were applied along the centre-line of each plug width. The two outer plugs were constrained in the vertical direction, while a 1 mm vertical deflection was applied in the opposite direction to the centre-line of the middle plug. Flexural stiffness values were calculated by measuring the reaction forces resultant of the 1 mm applied deflection, along the centre-line of the mid-span plug. Various adhesive fillet ratios and undercut lengths were applied to the solid and shell-solid FE models of the box structures, in order to determine the effectiveness of the undercut element method in flexure. Results from the FE analysis are given in Figure 7.19, for beams joined through adhesive bonding and through spot-welding.

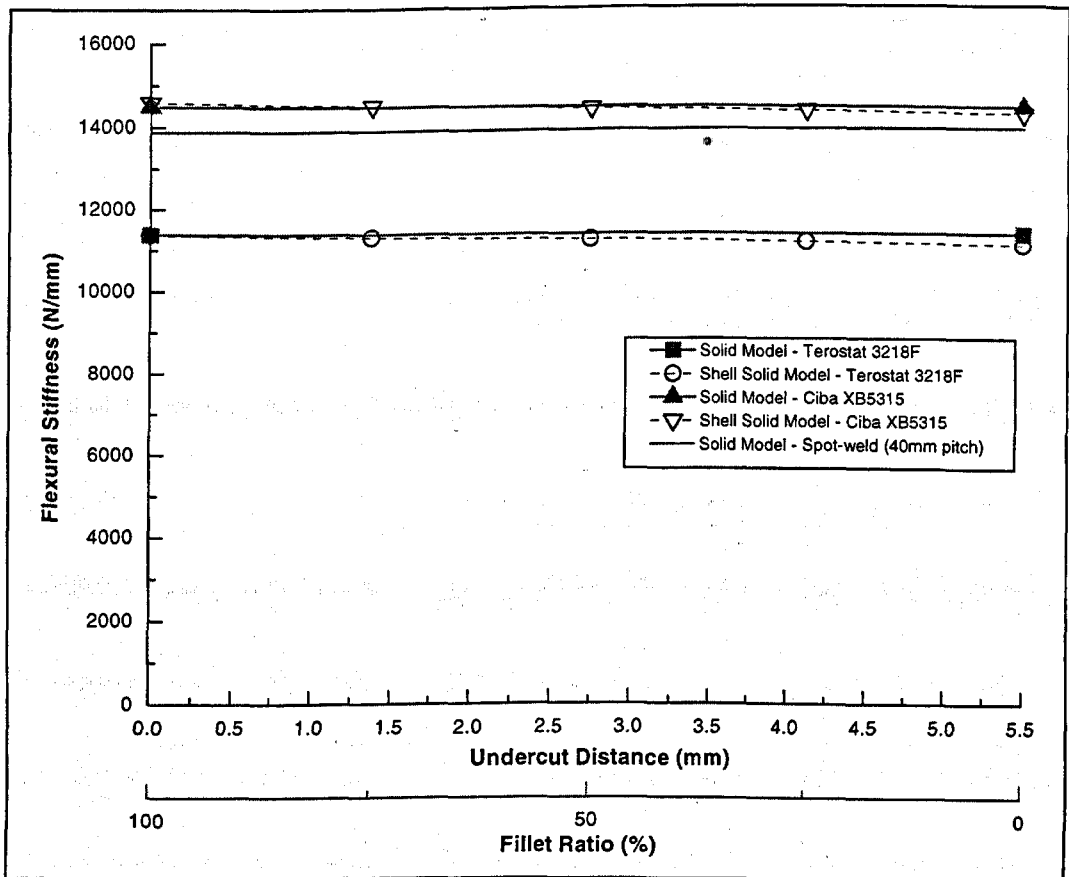


Figure 7.19 FE results of box structures in flexure with the application of the undercut element

Results from the graph show that both solid and shell-solid FE analyses are in close agreement when the undercut element is included. Another observation is that the actual box stiffness does not change significantly when increasing the adhesive fillet ratio, i.e. when the undercut length approaches 0 mm. For flexural loading, it can be concluded that box beam stiffness is relatively insensitive to changes in fillet ratio. It is evident that the application of the undercut element method is still valid for translating joint details into FE models of larger structures. Further validation of the FE work is obtained through the comparison of the results with experimental testing of similar box structures.

The results from the analyses also show the effectiveness of different joining techniques and adhesives. For example, the high modulus adhesive gives stiffness values which are approximately 27% higher than the results calculated from the lower modulus adhesive. It is also observed that the high modulus adhesive is slightly stiffer by approximately 4%, than the spot-welded structure.

7.6.1 Validation with Experimental Work

The manufacturing process of the box beams for flexural testing was similar to previous beams assembled for torsional tests. To allow for three-point loading, an additional 20 mm aluminium plug was inserted and bonded along the mid-span of the box structure. Two beams were made for each testing configuration, i.e. fillet ratio and adhesive type. Each beam was placed onto the testing machine and tested in two orientations, and an average of the two test results was taken in order to calculate the resultant flexural stiffness of the beam. Results from the experimental tests are compared with previous FE results and are given in Table 7.7 for various joining methods.

Joining Method	Effective Fillet Ratio	Flexural Stiffness (N/mm)		
		Experimental Tests	Solid (Micro) Models	Shell-Solid (Macro) Models
TEROSTAT 3218F	100%	5413 ± 3295	11,383	11,369
	0%	3995 ± 647	11,307	11,045
CIBA XB5315	100%	5429 ± 1587	14,478	14,578
	0%	11622 ± 4906	14,376	14,223
Spot-welding	(40mm pitch)	9089 ± 2243	13,876	-

Table 7.7 Comparison between FE and experimental results with the undercut element method - flexural loading

Unfortunately, large variability in the results from the experimental tests prevents any realistic correlation. The cause of the wide variability is uncertain but the lack of

squareness, as observed in the transverse tensile tests (section 7.5.1), undoubtedly contributes to the scattered results. Also, despite the central plug reinforcements, some local deformations of the beam under the central loading point occurred. This also varied across the beam width and between beams, perhaps reflecting the geometric asymmetry. The local deformations and indentations in effect contribute to a greater measured displacement of the loading point and this would give a lower effective stiffness. It is noted that all the experimental stiffness values are lower than the FE predictions. Despite the inadequacy of the correlation between the experimental test and the FE model results, it is evident that the application of the undercut element method is still acceptable.

7.7 Summary

In this chapter, modelling methods have been developed and extended from the earlier work on joint details into more representative large-scale structures. An idealised box beam structure was modelled and tested experimentally, and stiffness characteristics of the beams have been analysed under three different modes of loading: torsion, tension and flexure.

It has been observed that for torsion and flexure loading conditions, the stiffness of the box beam is relatively insensitive to adhesive fillet ratios. However, box structures subjected to transverse tensile loading exhibit a greater effect of fillet ratio on stiffness. In all cases, the FE models give the right order of magnitude and ranking of stiffness predictions although experimental inaccuracies prevent a reliable correlation between FE prediction and experimental test results.

The application of the undercut element method is valid on structures such as box beams, and in Chapter 8 the method will be applied to FE models of large vehicle structures, such as the plenum chamber and the full vehicle body.

8. APPLICATION OF THE UNDERCUT ELEMENT METHOD TO VEHICLE STRUCTURES

8.1 Introduction

Vehicle rigidity is influenced by the design of many substructure details located at various strategic positions within the body. One important substructure is the plenum chamber which is in effect a transverse box situated below the windscreen. The plenum chamber for the Jaguar X300 model series consists of four irregular thin sheet panels joined into a nominal kite-shaped section with flange joints. A finite element model of the plenum chamber is shown in Figures 8.1 and 8.3, and the actual component for experimental tests is shown in Figure 8.9. This structure was the subject of investigation in a related project within the collaborative programme, and produced a convenient case study for the application of the undercut element method.

8.2 Application of the Undercut Element Method to a X300 Plenum Chamber

Initial finite element work on the plenum chambers was carried out by Hawtal Whiting, one of the collaborating partners in the LIVEMAN project. Jaguar Cars, another project partner, supplied CAD models of the X300 plenum chamber. The main finite element work was investigated using the *Hypermesh* finite element modelling package.

The FE diagram in Figure 8.1 shows the complexity of the structure, and the possible areas for bonding are noted in Figure 8.2. Figure 8.3 shows the FE model of the plenum chamber which also includes the projecting end bars; these represent the torsional loading attachments used in early experimental tests, but the configurations were changed in later tests.

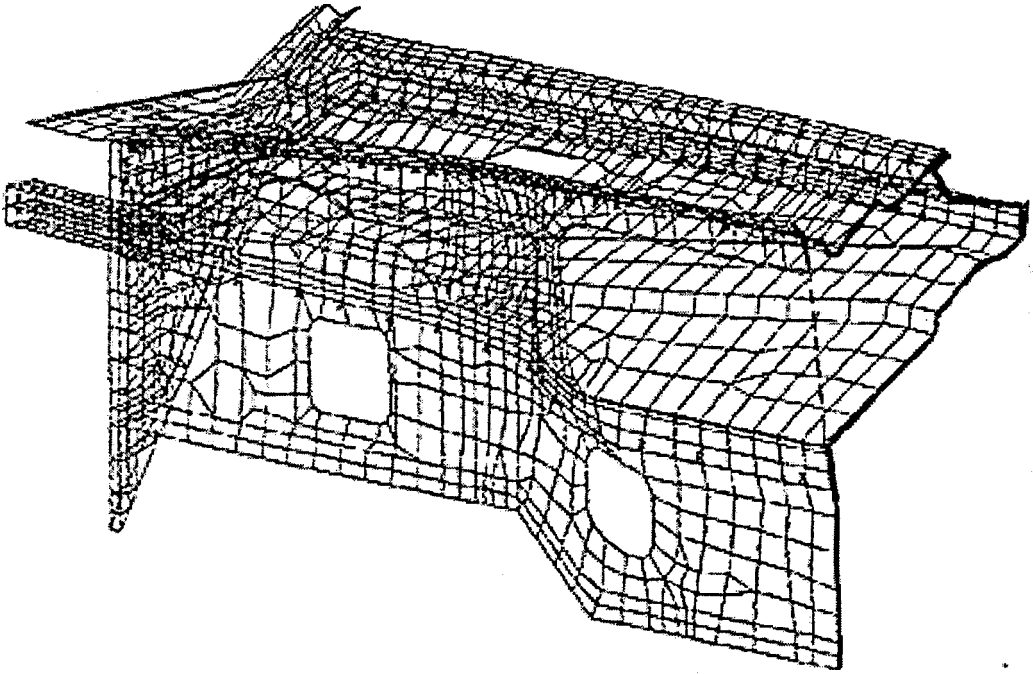


Figure 8.1 FE model of half the Jaguar X300 plenum chamber

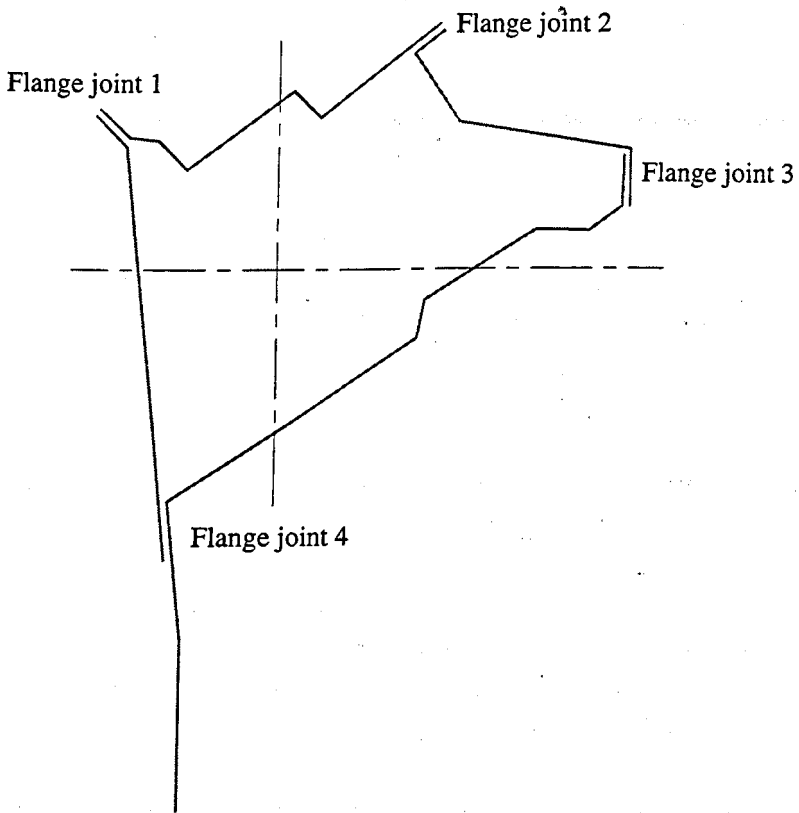


Figure 8.2 Schematic representation of the plenum chamber cross section showing the flange joints

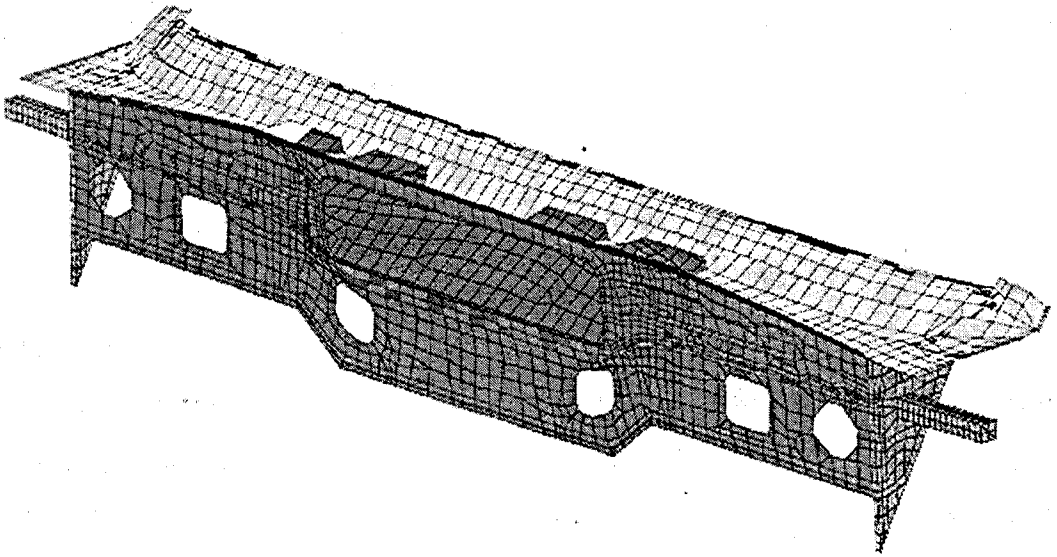


Figure 8.3 Full FE model of the Jaguar X300 plenum chamber

The FE model of the plenum chamber is composed of shell elements representing the metal sheet panels, and solid elements which are used to represent the adhesive bondline in the flange joints. In the initial analysis, the bondline extended over the whole flange area, as shown in Figure 8.4, and was designed using 2 elements across the flange length. Through minor modifications of the CAD drawings and element dimensions, it was possible to reconfigure the bondline elements to introduce undercuts, as shown in Figure 8.5. The elements in the bondline were modified to 3 elements along the flange, of which the outer elements represented the length of the desired undercut ($\delta = 5.5$ mm); these outer elements were then removed. This modified model was implemented by Hawtal Whiting, and the torsional stiffness results from the analysis provided comparison with the original unmodified model.

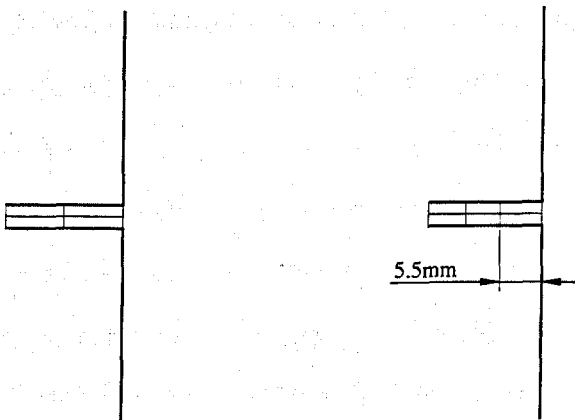


Figure 8.4 Original FE macro model with a two-element bondline

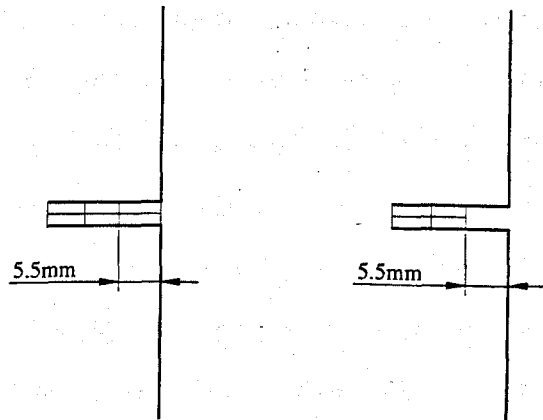


Figure 8.5 Modified FE model with a three-element bondline and a 5.5 mm undercut

The original CAD models of the plenum chamber were designed for spot-welded flanges. The FE models used 2 shell elements along the flange width so that the centre nodes could be joined with a rigid link to represent the spot-weld (Figure 8.6). However, with the introduction of adhesive bonding and weld-bonding into vehicle substructures, more accurate representations of the joints were required and the model developments are shown in Figures 8.7 and 8.8. Initial stiffness results from the FE analysis of the plenum chamber are carried out using original FE modelling techniques of unbonded (spot-welded) structures and are shown in Table 8.1. The results are compared to two FE models of weld-bonded joints.

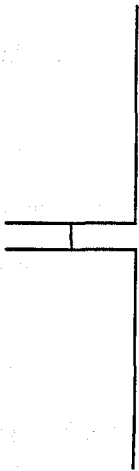


Figure 8.6 Original FE model of a spot-welded joint

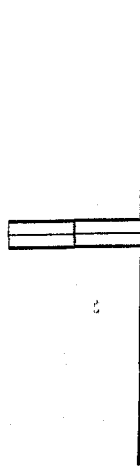


Figure 8.7 Original FE model of a weld-bonded joint

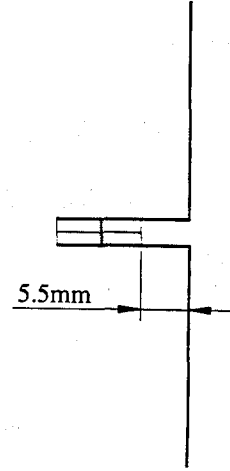


Figure 8.8 Modified FE model of a weld-bonded joint and a 5.5mm undercut

The first model is based on the original, unmodified method used to represent the bondline, i.e. two elements along the flange length with no undercut; while in the second modified model, an undercut element of 5.5 mm length is introduced in the joint line to represent more accurately the adhesive bondline. It should be noted that the end fittings and constraints in these first models of the plenum chamber are different from those used in the second FE analyses, results of which are given in Table 8.2. By comparing the FE results for different joining techniques, it can be seen that the weld-bonded model is approximately 30% stiffer than a similar spot-welded structure. This result is significant as it shows how adhesives can be used to enhance the stiffness of vehicle structures.

	Torsional Stiffness (Nm/degree)	Percentage Increase Compared with Spot-Welded Structure using Original FE Model
Spot-Welded Structure using Original FE Model (Unbonded)	8.21	-
Weld-Bonded Structure using Original FE Model	10.70	30.3
Weld-Bonded Structure with Undercut Element in FE Model	10.06	22.5

Table 8.1 Torsional stiffness results from the FE analysis of a Jaguar X300 plenum chamber

The results in Table 8.1 also show how the undercut element method affects the prediction of the overall stiffness of the structure, when compared to the original FE model. The FE model with a 5.5 mm undercut is only 23% stiffer than the spot-welded structure. It can be observed from these results that FE model representation of the large-scale structures give an over-estimation or over-prediction of the stiffness of bonded structures. With the inclusion of the undercut element, the resultant stiffness values are more representative of the actual structure.

8.2.1 Validation with Experimental Work

An initial experimental test programme was undertaken by Jaguar Cars to measure stiffness characteristics of plenum chambers [Cotton (1998)]. However, there was considerable variability in the results which was primarily attributed to the supports and the end fittings for the test fixture. The Joining Technology Research Centre at Oxford Brookes University, therefore, undertook a further test series on the plenum chamber with refined mountings and test procedures, shown in Figure 8.9.

Plenum chambers were prepared by project partners TWI and Ford with different flange joint conditions. These included a simple spot-welded structure and weld-bonded chambers using three different adhesives; CIBA XB5315 and TEROSTAT 3218F as used in previous studies, and also another high modulus epoxy adhesive, TEROKAL 4500 ($E = 4$ GPa). During assembly of the chambers, it was not possible to control the adhesive fillet ratio, but inspection of the completed units indicated an excess of adhesive on most joints, with full fillets giving 100% fillet ratios.

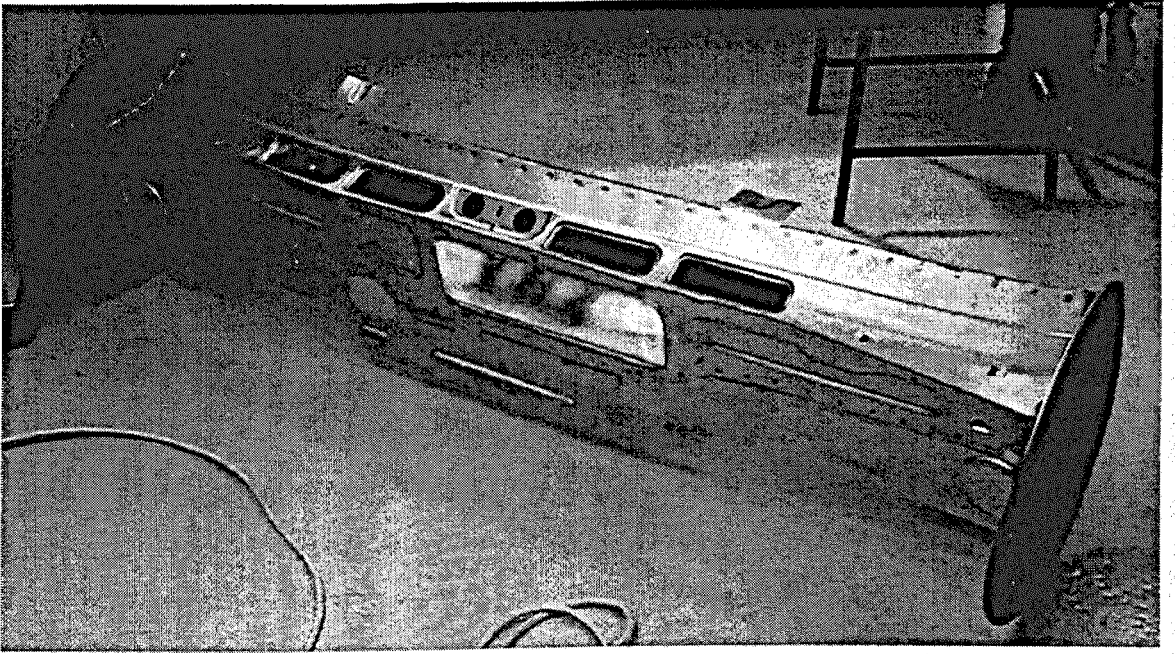


Figure 8.9 Jaguar X300 plenum chamber used in experimental tests

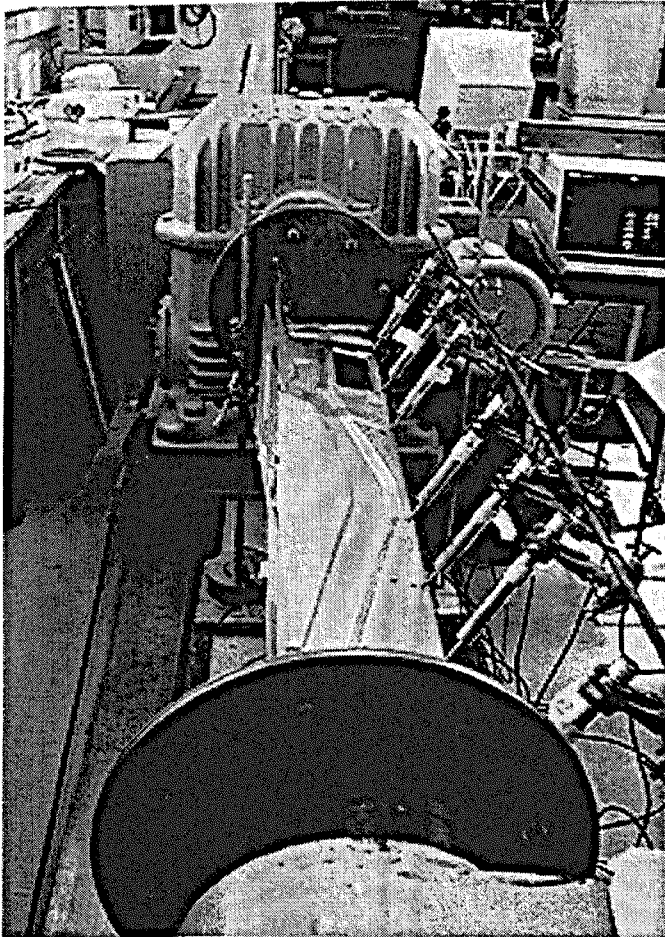


Figure 8.10 Experimental set-up of plenum chamber showing the position of the LVDT transducers

The experimental procedure for testing the plenum chambers was similar to that of the box structures in torsional loading. The plenum chambers were mounted on to an Avery-Denison torsion testing machine using specially manufactured adapter plates which were welded onto the structures, as shown in Figure 8.10.

Nine LVDT displacement transducers were used to measure the angular displacements, while a torque transducer measured the twisting moment of the structure. Seven of these LVDT transducers were distributed uniformly along the flanges, while the other two transducers were used to record the movement of the end plates which were welded to the ends of the plenum chamber. Stiffness measurements were calculated based on the movement of the end plates recorded from these two transducers.

The initial undercut of 5.5 mm introduced in the FE models was based on the assumed worst case condition of 0% adhesive fillet ratio. However, as the experimental plenum chambers were seen to have 100% fillet ratio, the large undercut was expected to over-compensate. Nevertheless, as observed in the derivation of the undercut element method in Chapter 6, some correction is still necessary for the effect of the flange bend radius. A more accurate undercut value was derived from the graph in Figure 6.5 and this was calculated to be approximately 2 mm.

Results from the experimental tests are shown in Table 8.2 and compared with the results from the modified finite element models. These plenum chamber FE models were modified to include a 2 mm undercut element so that they could accurately represent the adhesive bondline in the experimental specimens. The position of the spot-welds, shown earlier in Figures 8.6-8.8, were also modified in each model so that they could be directly compared to one another. However, it has been noticed that generally the positions of the spot-welds in automotive structures do vary and therefore, this change should not significantly affect the results.

The results show a fairly good correlation between experimental tests and modified FE models when introducing the undercut element method. Results for the spot-welded plenum chambers and the low modulus adhesive (TEROSTAT 3218F) give very good correlation (3-6% difference) while there is a slightly larger variation (8-10%) between the experimental and FE results for weld-bonded structures using the high modulus adhesives.

Causes for such variations could be attributed either to the experimental techniques, i.e. poor joint manufacturing, imperfect bondlines, test set-up procedures, or possibly due to some errors in the FE models. The precision of the constraints, loading positions and alignment of the central axis may introduce some uncertainty. Also, the apertures may cause local buckling effects which are not accommodated for in the FE models. Despite these differences, it is clear that adhesive bonding does give a significant increase in stiffness to plenum chambers.

	Torsional Stiffness (Nm/degree)	
	Finite Element Models	Experimental Tests
Spot-Welded Structure with Original FE Model (40 mm pitch)	37.12	39.39
Weld-Bonded Structure with Undercut Element (TEROSTAT 3218F)	41.08	42.12
Weld-Bonded Structure with Undercut Element (CIBA XB 5315)	47.47	42.96
Weld-Bonded Structure with Undercut Element (TEROKAL 4500)	47.74	43.72

Table 8.2 Comparison of torsional stiffness results from FE and experimental testing of the plenum chamber

Both experimental test and FE results show that weld-bonded structures will increase the torsional stiffness of the plenum chamber; FE results show an increase by approximately 10% for a low modulus adhesive and up to 30% for a high modulus adhesive. Considering the plenum chamber is only one structure within a car body, this 10-30% improvement obtained with weld-bonding is regarded as a significant enhancement for stiffer vehicle bodies. As a further design observation, it is suggested that there is scope for improvement in the layout, position and size of apertures, to optimise the stiffness of vehicle structures.

8.3 Application of the Undercut Element Method to a X300 Body-In-White

The body-in-white represents the main frame of a vehicle. In this interpretation the doors, bonnet and boot are excluded from the FE models; it is clear that the overall vehicle

stiffness is dependent on the body-in-white properties. Finite element work of the body-in-white was carried out by Hawtal Whiting using *Hypermesh* and *Nastran* as the pre- and post- processing packages. The finite element model of the X300 vehicle body is shown in Figure 8.11. Summary results from the FE analysis by Hawtal Whiting [Harpham (1999)] are given in Table 8.3, where the torsional stiffness is calculated for spot-welded and weld-bonded vehicle body frames. The undercut length that was removed in this model was of 5.5 mm.

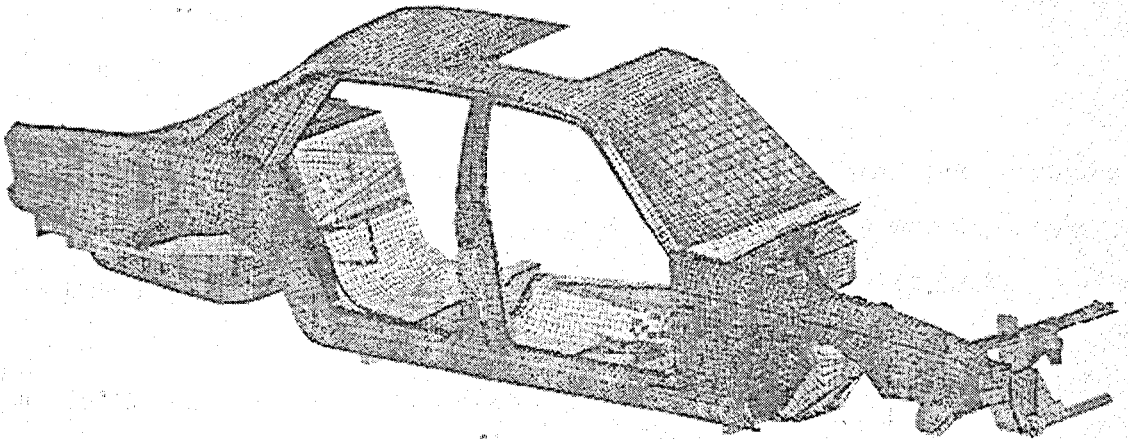


Figure 8.11 FE model of half the Jaguar X300 body-in-white

	Torsional Stiffness (Nm/degree)	Percentage Increase Compared with Spot-Welded Structure using Original FE Model
Spot-Welded Structure using Original FE Model (Unbonded)	11.88	-
Weld-Bonded Structure using Original FE Model	17.95	51.1
Weld-Bonded Structure with Undercut Element in FE Model	16.23	36.6

Table 8.3 Torsional stiffness results from the FE analysis of the Jaguar X300 body-in-white

Initial comparisons with the original FE models indicate that a 51% enhancement of stiffness might be achieved by using adhesive in the joints during body assembly. The introduction of the undercut element method in the FE models reduces the predicted stiffness by about 15%. The initial, higher prediction is perhaps optimistic compared with observations from the plenum chamber experiments. Nevertheless, it is evident that adhesive bonding should give significant improvements in stiffness. Also, the undercut element method should give a more accurate prediction.

8.4 Summary

In this chapter, the application of the undercut element method to larger vehicle structures was investigated. Experimental test results were compared to extensive finite element analyses of original and modified models to include an undercut. The key observations can be summarised as following.

- The application of the undercut element has been demonstrated to be effective in real vehicle details.
- For structures such as the plenum chamber, FE model predictions with the inclusion of the undercut element gives fairly good agreement with experimental tests, in particular for lower modulus adhesives and spot-welded structures.
- The dimension of the undercut element to be implemented into the FE models can be determined from experimental tests to derive a more accurate calibration.
- The ease of use of the undercut element method has been demonstrated in the application to a full vehicle body analysis.
- An improvement in the weld-bonding techniques for vehicle structures has been found to be in the order of 10-30% for plenum chambers (2mm undercut) and 37% for full vehicle bodies (5.5mm undercut) compared to the original FE methods for spot-welded structures.

9. DISCUSSION

9.1 Introduction

The automotive industry is aiming to improve the overall performance of cars through the development of light-weight vehicles. Vehicle weight reduction leads to lower fuel consumption and hence reduced emissions, making them more environmentally friendly and cost effective. New technologies such as steel/aluminium welded tailored blanks for car doors, for example, have been shown to significantly reduce the overall weight of a vehicle and increase the stiffness of the structure. Materials, such as high strength steels, aluminium alloys and composites are also being introduced to reduce vehicle weight. Associated with the use of dissimilar and new materials, advanced joining methods are being devised in order to assemble and join such light-weight materials.

Traditional joining methods, such as spot-welding, have been typically used to join thin sheet steel material in vehicle structures, particularly in areas such as the body frame where enhanced stiffness is required. However, there are some restrictions with the use of spot-welding, particularly when joining new and dissimilar materials such as aluminium and polymer composites. Therefore, other joining methods are being considered to connect these load bearing structures.

Adhesive bonding is one of the preferred joining methods as it offers considerable potential for joining dissimilar and light-weight materials. One of the advantages of bonding is that with the structural continuity of the joint line, the overall performance and strength of the structure are improved. A range of different adhesives, from polybutadienes to structural epoxies, is being used to join structures within vehicles. The selection of the adhesive to be used primarily depends on the specific performance requirements for that structure. However, as a general observation, the stiffness of an adhesive joint is considerably higher than joints made with other traditional joining methods, such as mechanical fastening or spot-welding techniques.

9.2 Requirements for Stiffness

One of the major requirements in vehicle body construction is the structural stiffness of the body. Noise, vibration, passenger comfort and performance are some factors which are determined by the integrity and stiffness of the body frame. Steel frames have been widely used, and steel is still a preferred material for body shells primarily because of its relatively high strength properties and ease of fabrication. Research on the stiffness of body shells has shown that by using adhesive within the body, it is possible to reduce the thickness of the steel sheet without loss of stiffness performance. This provides an important route to possible weight reduction.

The potential of adhesive bonding is not only as an advanced joining method for new and light materials, but also as a method for improving the stiffness of the vehicle body. Further work has shown that a combination of spot-welding and adhesive bonding methods to form weld-bonds can further enhance the stiffness and reduce the weight of a structure. Weld-bonding methods have been shown to improve the stiffness of the structure typically by 25% compared with a spot-welded equivalent [Fenton (1998)].

9.3 Numerical Modelling of Adhesive Bonded Joints

Numerical modelling methods are now used extensively to predict body characteristics, such as stiffness and strength, and to analyse the overall performance of a vehicle. However, with the demand for light-weight vehicles, new and advanced joining technologies are being implemented into vehicle structures, and it has been found that joint details are not being accurately represented in the FE models.

In the automotive industry, current FE modelling techniques have been developed for spot-welded structures but with new joining techniques, such as adhesive bonding and weld-bonding, these methods must be reconsidered. This is primarily due to additional geometric details in adhesive bonded joints, e.g. bend radius, fillet ratio and adhesive type, which in spot-welded macro models are unaccounted for. To effectively predict the stiffness of vehicle structures which involve bonding techniques, current FE macro models require better representations of such joints.

FE analysis and experimental testing of typical adhesive joints, such as the single lap joint and the coach/T-peel joint, were carried out to understand the behaviour of the joints and to compare the effectiveness of the different FE modelling techniques used: the 'micro' and the 'macro' modelling methods. The 'micro' modelling method represents a FE model made out of solid elements and where all the geometric details, such as the flange bend radius, the bondline thickness, the sheet thickness, the adhesive fillet ratio, etc., are accurately represented. The 'macro' method, on the other hand, describes the modelling technique used primarily by the automotive industry where large-scale structures are modelled. 'Macro' models use a combination of shell elements with solid elements; the solid elements represent the adhesive bondline and the shell elements represent the sheet metal. The main problem with 'macro' modelling methods is the uncertainty of the validity of combining shell with solid elements, particularly in terms of the adhesive fill and the lack of geometric details such as the sheet bend radius. In previous 'macro' or large-scale models, where spot-welding was principally used as the joining technique, these geometric approximations were not noticed. However, with the introduction of adhesive bonding as a joining technique, these geometric inaccuracies have a significant influence on the prediction of the performance of the structure.

Modelling smaller joints, using 'micro' and 'macro' modelling techniques, showed that a method of translating the results of joint details into the 'macro' models was required. Different approaches of accounting for micro details were reviewed in order to try solve the problems associated with micro to macro modelling. These included the joint-line element method, the super-element method and the spring element method. The main function of these substitute elements was to improve joint details which were not accurately represented in large-scale models. This was done by implementing elements that would define joint properties to improve the prediction of joint stiffness of the macro-models. However, there were some limitations and drawbacks associated with each models, and these have been previously identified in section 4.5.1.

The undercut element method was developed as a tool for including joint details, to obtain more accurate predictions of the structural behaviour and stiffness performance of adhesive bonded structures. The ease and applicability of the method to FE models, proved to be an effective way to correct 'macro' models and predict more accurately the actual behaviour of the joint. The undercut element method was applied to typical smaller

joint configurations and to larger structures such as the idealised box beam structure, the plenum chamber and the body-in-white of a Jaguar X300 series vehicle.

As a general outcome from the study, the FE models of the bonded structures which incorporated the undercut element method, gave stiffness values which were considerably lower than the original models. The original FE models used in the automotive industry give an over-prediction of the actual stiffness of bonded structures. With the inclusion of the undercut element method in these models, a closer and more accurate prediction of the joint behaviour and of the overall performance of the structure can be determined.

9.4 Problems Encountered with FE Modelling Methods

The primary requirement of the analytical studies was prediction of structural stiffness, and it was therefore considered acceptable to use linear FE models for most of the investigation. During the study, there were several issues pertaining to FE modelling methods which caused some concerns, and these will be addressed in this section.

9.4.1 Mesh Convergence

One of the most important aspects related to accurate modelling is the mesh size used to define a structure. Before each joint or structure was analysed, an extensive mesh validation process was carried out to determine the minimum number of elements required for convergence of an accurate model. This process also helped to identify the minimum mesh density necessary for fast and efficient analysis, needed particularly in the analysis of larger structures.

For lap and coach joints, the meshes were denser at the edges of the overlaps and across the bondline thickness, as these were critical areas. In the analysis of the idealised box structures, it was also found necessary to increase the mesh density at selected regions over the cross-sectional area of the structure, to provide accuracy and convergence of the results.

9.4.2 Geometric Representations

Accurate representations of the geometry of a structure in FE models is an important factor for good predictions of structural behaviour. Most of the simpler geometric joints

such as single lap or coach joints, for example, are easy to design and model. However, there may be some difficulties when designing some of the more complicated structures such as the idealised box beam and the plenum chamber. The main sources of error arise from the adjustment of the adhesive bondline in the shell-solid FE models. One example of inaccurate geometric representations can be demonstrated in the idealised box beam structure, illustrated in Figure 9.1.

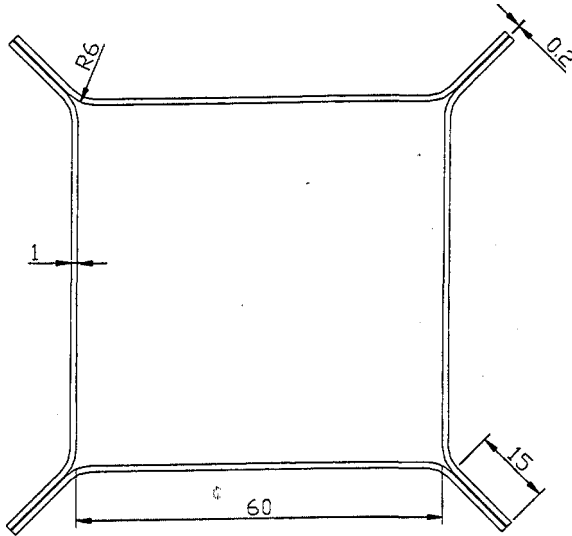


Figure 9.1 Basic configuration of the idealised box structure

To satisfy the dimension specifications, that is that the structure has an internal area of 60x60 mm, the FE models must be designed accordingly. With spot-welded structures this was not a problem since each of the four plates making up the structure were joined together giving the closest match to that of the required area. However, with the introduction of adhesive bonding, the joining of the plates will also include an additional 0.2 mm adhesive thickness hence, increasing the area. The accuracy of the FE models will depend primarily on the initial design methodology. The solid element models can be easily replicated from the manufacturing dimensions, as shown in Figure 9.2. However, there are various ways to represent the sheet in shell element models. The first method is to use the centre-lines of the solid metal sheets or CAD models to design the shell surfaces. If these models include the bondline thickness, then the resultant shell element models will have dimensions, as in Figure 9.3, which is equivalent to a 60x60 mm box. However, generally industrial CAD drawings are designed for spot-welded structures and therefore, do not include the additional bondline. If the design specification was to

maintain a 60x60 mm cross sectional area, then extensive time and manipulation of the model would be required.

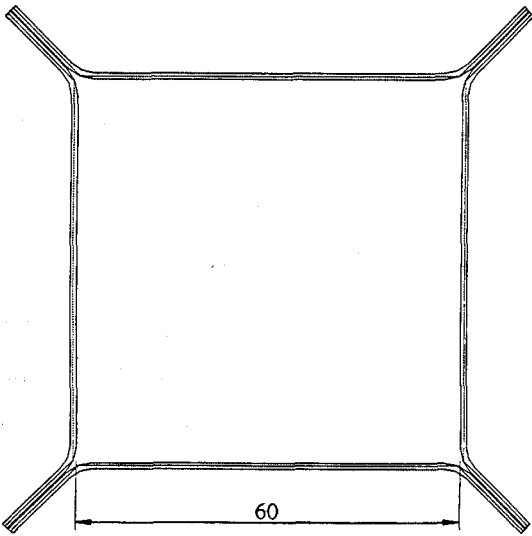


Figure 9.2 Solid element model of a box structure with 0.2 mm bondline thickness

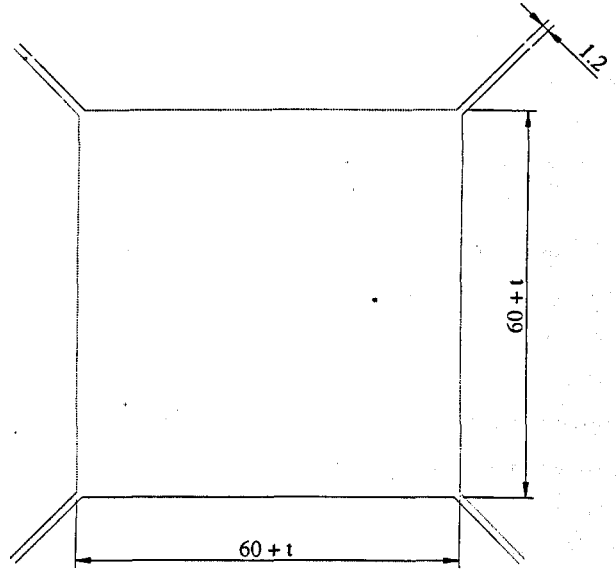


Figure 9.3 Shell model derived from centre-lines of solid structure taking into account the bondline

Approximations were also made at the corners of the plug in order to accommodate 100% adhesive fillet ratios in solid element models, and shown in Figures 9.4 and 9.5. On further analyses however, it was shown that removing the corners of the plug to accommodate an exact 100% adhesive fillet ratio did not affect the overall results.

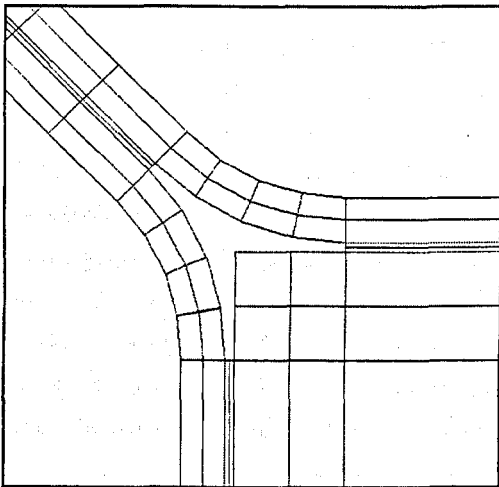


Figure 9.4 FE solid element model with a 0% adhesive fillet ratio

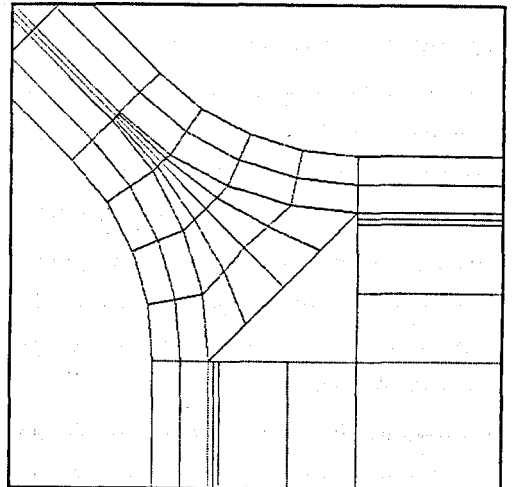


Figure 9.5 Approximation of the plug in solid models to accommodate a 100% adhesive fillet

The sources of modelling errors are primarily associated with the lack of accurate geometric representation. It is essential for good, accurate and comparative results to replicate the geometric details of the actual specimen through FE modelling methods.

9.4.3 Application of Boundary and Loading Conditions

Another problem associated with modelling adhesive joint structures, particularly larger ones such as the box structures, was to accurately represent the experimental loading conditions. For a direct comparison between FE models and experimental tests, the material properties, constraints and loading conditions must be similar in both cases. Because the experimental set-up involved more complicated issues, the FE models were designed at a later date to represent the existent experimental conditions as closely as possible.

For the idealised box beam structure, this proved to be a problem particularly for the application of the torsional displacement through the aluminium end plugs. Because it is quite difficult to represent exactly what occurs during the experimental tests, a series of methods was used to represent the applied loading conditions in the FE models. Initially, the displacements were applied at four nodes, equidistant from the centre axis of rotation, as shown in Figure 9.6. Results showed that the angular displacements of the inner nodes during torsional loading were higher than the angular displacements at the outer edge of the plug. In another model, displacements were applied at the four nodes on the mid-span of the sides of the plug, at the interface with the adhesive layer, as shown in Figure 9.7. Although this model adequately transmitted nominal angular displacement to the box, it was thought that the application of the load to only 4 nodes did not offer adequate uniform application of the torque applied. The rotational displacements were therefore applied over a uniform and wider area in a third model, illustrated in Figure 9.8.

The rotational displacements in the third model, were applied along circular paths. All nodes within the outer path were subjected to displacements, and these were calculated based on the distance of the nodes from the centre of the box. For example, if the desired torsional displacement was 1 mm over a circular path of 10 mm diameter, then the outer nodes would rotate by 1 mm, the inner ones of a 7.5mm diameter by 0.75 mm, the 3rd path by 0.5 mm, the 4th by 0.25 mm, the 5th by 0.125 mm, and so on, depending on the mesh produced; the innermost node represents the centre of rotation. Figure 9.8 shows a

schematic representation of the application of rotational displacement used in the FE models to replicate the experimental test procedures. At each node, the angular displacement was calculated and defined by a horizontal (x) and vertical (y) movement. The representation of applied rotation in this model, gave stiffness values which were in good agreement with experimental results.

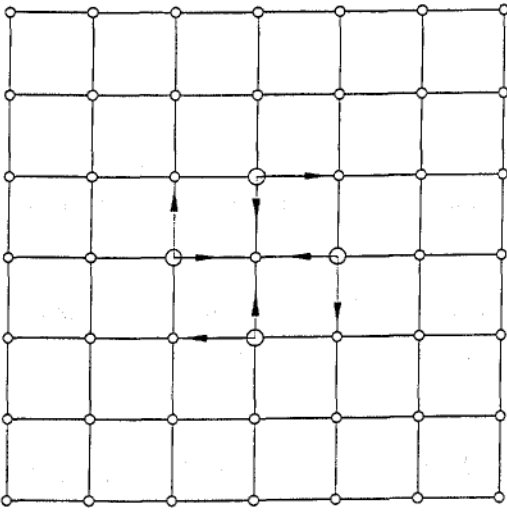


Figure 9.6 Applied displacements at inner 4 nodes

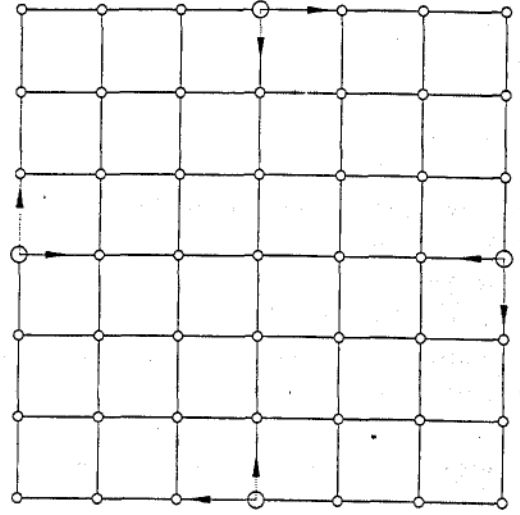


Figure 9.7 Applied displacements at outer 4 nodes

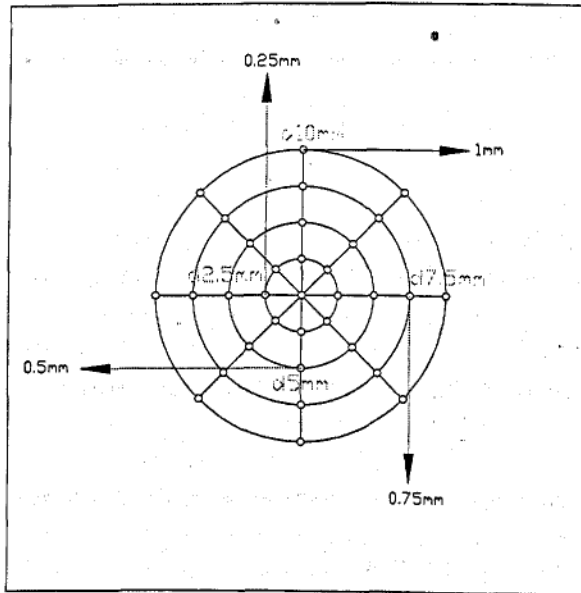


Figure 9.8 Application of rotational displacements on all nodes around a circular path

Eventually, it was found that all three models could be used to predict stiffness, provided that the relative displacements of the front and back edges of the box were used to calculate the actual angular rotation.

Correct application of all loading and boundary conditions is a fundamental and important issue when using numerical modelling methods. FE models should accurately represent, to the closest extent, the experimental models in order to obtain good and comparable results. There are however, some unaccounted factors in the experimental tests such as local deformations and distortions across the plug-structure interface; such factors are difficult to accurately represent in FE models, and may result as small sources of error which have to be accepted.

9.4.4 Other Sources of Inaccuracies

Apart from the accuracy of representation of geometry and loading conditions, the FE models cannot fully accommodate the inherent variability in adhesive joints. Sources of variability include voids and defects, non-uniformity in fillet dimensions and mechanical properties of the adhesives, which can arise through differences in curing conditions, humidity, etc. To better assess these possible sources of error in experimental tests, parametric analyses using FE methods were carried out to determine how different design factors affected the sensitivity of the joint, in terms of stiffness. The main parameters investigated were the adhesive fillet ratios and different adhesive materials. Characteristic curves obtained from the results of the analyses, showed the variation of stiffness to these parameters. The resultant curves would also allow one to understand the sensitivity of the joint to such uncontrollable variables, existent in experimental tests.

For example, the adhesive fillet ratio in experimental specimens will contain some inaccuracies. Although special scrapers were used to control the adhesive fillet of the joint prior to curing, the measurements of the adhesive fillet ratios after curing were generally larger. The main cause of fillet variability is associated with the flow of the adhesive during the curing process, resulting in a slightly larger fillet. From an observation of the fillet ratios of the experimental specimens prior to and after curing, it was noted that generally, the adhesive fillet ratio might increase typically by 10%. One solution to obtain comparable FE models to the experimental specimens, which include such errors, is to measure the fillet ratio of the experimental specimens after they have been cured. Additionally, FE parametric studies of changes in adhesive fillet ratio on joint stiffness, can also provide a better understanding of the sensitivity of the joint. Results from the parametric study on coach joints, given previously in Figure 6.4, showed that say, for a 50% fillet ratio, a 10% increase in fillet size would give a stiffness change of

approximately 11%. A greater variation in stiffness is noted at higher fillet ratios and hence, the percentage error for such joints is greater.

A similar parametric study was also carried out to determine the sensitivity of joint stiffness with respect to changes in adhesive modulus. The variability of the adhesive modulus in experimental tests is generally caused by different curing conditions such as under-curing or over-curing and moisture uptake, both of which can alter the adhesive modulus. It is expected that in worst cases, the errors for experimental joints caused by changes in adhesive modulus, are in the range of $\pm 30\%$. Figure 9.9 shows the results from the parametric study on the variability of adhesive modulus, for lap joints and coach joints in tension.

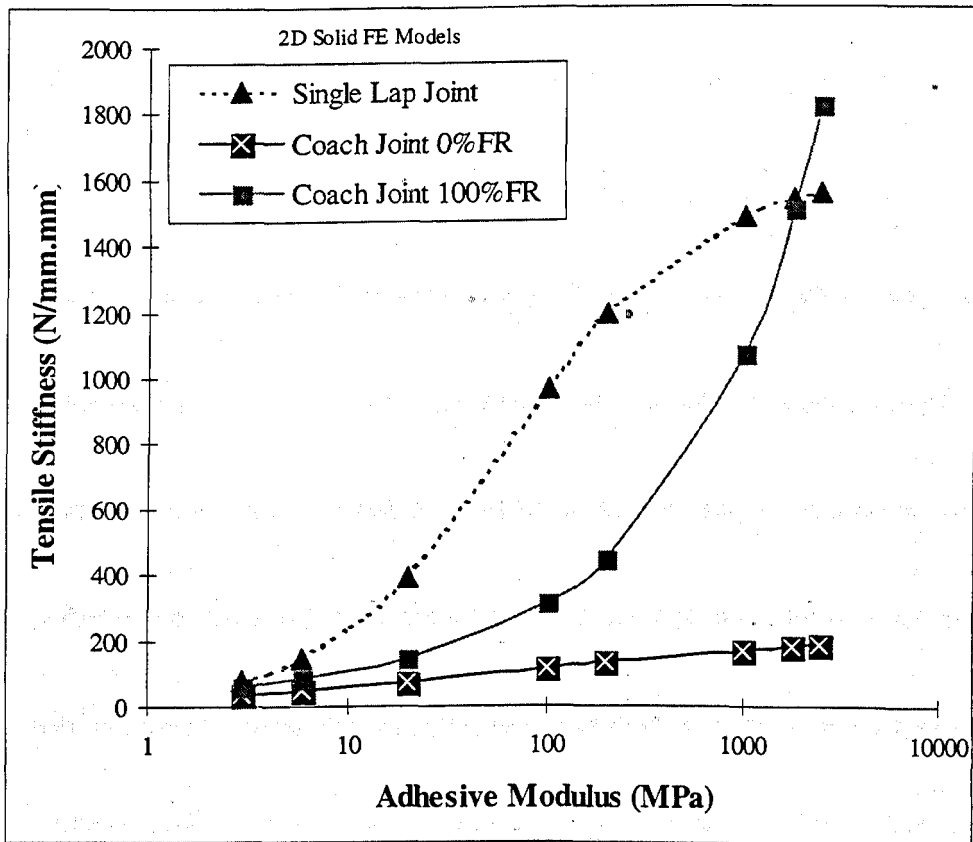


Figure 9.9 Variation of tensile stiffness with adhesive modulus for typical joint configurations

For a lap joint with a 1.0 GPa epoxy adhesive, a change in adhesive modulus by say, +30% would give stiffness results in the order of 1% greater; for a -30% reduction in modulus, there would be a resultant 5% change in stiffness. Similar studies on coach

joints for 0% and 100% adhesive fillet ratios showed that for similar variations in adhesive modulus, i.e. $\pm 30\%$, would result in changes in stiffness values by $\pm 5\%$ and $\pm 16\%$, respectively. From the results, it can be observed that coach joints with 100% fillet ratio are most sensitive to variability in adhesive modulus. The general observation from these results is that errors caused by experimental variability can make direct comparison with FE models quite difficult. However, parametric studies of joint design parameters can provide better understanding of the sensitivity of the joint.

Other sources of error caused by experimental variability are due to bondline defects, such as debonds or voids within the adhesive layer. The presence of such imperfections may cause significant losses in joint stiffness. FE parametric analyses of various sizes, positions and shapes of these defects can provide a better understanding of the sensitivity of the experimental joints. Also, to try reduce the experimental error, careful attention should be given to precise procedures during the manufacturing of the joints.

9.4.5 Introduction of Apertures into FE Models

During initial analysis of plenum chamber sections, it was found that their torsional stiffness was significantly lower than expected from the idealised beam studies. This was attributed to apertures in the panels of the plenum chambers. To check this hypothesis, further studies were made on idealised beams with various aperture configurations. While the FE analyses did demonstrate the substantial reduction in torsional stiffness, which would explain the low values of torsional stiffness of the plenum chambers, there was some concern as to the validity of the modelling results for box structures with large central apertures, i.e. 26% of sheet area. Results showed a departure between solid element models and shell-solid element models as the size of the aperture increased. Experimental results showed a closer similarity with the shell-solid element models. This variation is assumed to be due to the inability of solid elements to represent the response of thin sheet shell-like structures, correctly.

Nevertheless, it has been shown from the study on box structures, that large apertures, such as those found in the plenum chamber sections, contribute significantly to loss of stiffness. Whilst the objective of the automotive industry is to try to reduce the weight of vehicles through the use of apertures, there remains much scope for their optimisation. An

investigation should be carried out to determine how apertures with various sizes, shapes and positioning along a structure can contribute to loss of stiffness, with respect to weight saving in vehicle structures.

9.5 The Undercut Element Method

The use of adhesive bonding in main vehicle structures is increasing and there is a need for better representations of joints in FE models. Many studies on typical adhesive joints have shown the importance of joint details for accurate predictions of joint behaviour. In large-scale or macro models, joint details such as the adhesive fillet ratio and the forming bend radius, are not accounted for and certain approximations are made instead. Consequently, the overall stiffness prediction of full vehicle bodies is not accurately represented. The undercut element method provides a tool for improving joint details in large-scale models of vehicle structures. The implementation of the undercut in FE macro models accounts for the approximations made both to adhesive fillet ratio and those made for the sheet forming bend radius. The method is applicable to all types of adhesive joints. The undercut element method is a method of approximation of the local joint geometries, to obtain improved predictions of stiffness in vehicle body structures.

10. CONCLUSIONS

The aims and objectives set out at the beginning of the project have been accomplished.

The work presented in this thesis has shown that current methods of representation of adhesive joints in large-scale finite element models, for the analysis of vehicle structures, have some limitations. Finite element analyses were carried out using micro and macro modelling techniques and results were also validated with experimental tests. The general observation from the study showed the need for some form of refinements in macro models, to represent adhesive joint details more accurately. The undercut element method has been proposed as a method for including joint details in large-scale models to provide more accurate and representative predictions of stiffness in vehicle bodies.

10.1 Finite Element Analysis

In order to derive the undercut concept, some of the key observations of numerical methods must be highlighted and these are summarised in this section.

Finite element analysis is a powerful tool for predicting the behaviour and performance of a large variety of structures. FE methods have been used extensively in the modelling of car bodies and give accurate predictions of spot-welded structures. However, for adhesive bonded joints, extra attention is required in defining joint details such as the forming bend radius, adhesive fillet ratio and adhesive material properties.

Because of the large size of FE vehicle structure models, the accuracy of geometric details of adhesive joints is limited. Shell-solid (macro) modelling, used by the automotive industry, is a valid method of analysis but some form of refinement is necessary if adhesive joints are introduced in the structure. This study has resulted in the development of a novel approach for compensation of adhesive joint details in vehicles, based on an undercut element concept.

10.2 The Undercut Element Method

The undercut element method is a tool for providing joint details which are unaccounted for in large-scale models. By incorporating an undercut element in current FE macro models, it is possible to obtain more accurate predictions of the performance of vehicle structures. The application of the undercut element is simple and there are no specific limitations to its use.

The principle behind the undercut element method has been derived through the analysis of typical small-scale adhesive joints. An extension of these micro modelling techniques has been carried out using the undercut element method on more representative structures, such as box beams, plenum chambers and a full vehicle body. Generally, results from the industrial application of the undercut element into vehicle structures gave stiffness values which were significantly lower than the initial predictions. This suggests that modelling techniques used in unmodified macro models overestimate the stiffness behaviour of vehicle structures. The undercut element method has been proposed as a technique to enhance full body analysis methods.

10.3 Experimental Tests

Testing of small-scale joints was used to validate initial FE models which led to the undercut element concept. Experimental procedures provided an acceptable degree of reproducibility for a confident comparison with FE predictions. On larger-scale structures, experimental variability became more significant due to dimensional and geometric inaccuracies and other cumulative effects such as adhesive cure. As a result, direct correlation was less visible although trends and effects followed predicted patterns. The large-scale tests demonstrate that the undercut element correction should give improved predictions of stiffness in full vehicle body structures.

10.4 Further Findings

An important observation arose from studies on actual vehicle body substructures which demonstrated that apertures in sheet components have a significant, and potentially over-

riding, effect on stiffness. Holes are cut in panels for various reasons including weight reduction, ducting, cabling and mechanical linkages. Analyses on the effects of apertures suggest significant losses in stiffness even for structures with small, single apertures. The results from the study show a potential for enhancing the structural behaviour of vehicle structures; this can be obtained through optimisation in the size, shape and distribution of apertures in vehicle structures.

10.5 Recommendations for Future Work

The undercut element method derived from this study has been developed primarily in the context of vehicle bodies constructed from steel sheet. The extension of its application to other body materials will require further refinement and validation. In the case of aluminium alloys, simple substitution of modulus values may accommodate material stiffness effects, but sheet thicknesses and joint geometries may require further analysis. Composite materials will also introduce additional complications because of their directional properties.

All the stiffness studies carried out were for static loading. While this condition provides a good measure of the structural behaviour of the car body, which affects aspects such as handleability, dynamic analysis would be desirable to investigate the effectiveness of numerical models on predicting modal responses which determine noise and vibration.

There is still a confidence gap in the use of adhesives in structural automotive assembly due to uncertainties in long term integrity. Because of this, manufacturers favour hybrid joining methods such as weld-bonding. The corrective effects of the undercut element method generally relate to the adhesive fillet and flange bend radius, and the method should be equally applicable to bonded and weld-bonded joints. However, further qualifications of this assumption would be desirable.

Consideration of joint integrity aspects also raises the issue of strength prediction. Although the numerical models used in this study could be extended for analyses of stresses, it would be necessary to use non-linear material properties. Many investigators are addressing problems related to the prediction of strength of bonded structures and further work is necessary to extend this research into vehicle bodies. Specific problems

include impact behaviour, environmental degradation and other time-dependent mechanisms such as creep and fatigue.

The experimental studies in this project identified the important effect of apertures on the behaviour of sheet metal structures. Future work should address design optimisation of apertures on representative substructure details such those found in the plenum chamber.

REFERENCES

- ABAQUS User's Manual (1998)**, Version 5.8, Hibbitt, Karlsson & Sorensen Inc., USA
- Adams RD, Chambers SH, Del Strother PJA & Peppiatt NA (1973)**, 'Rubber model for adhesive lap joints', *Journal of Strain Analysis*, Vol.8, No.1
- Adams RD, Comyn J & Wake WC (1997)**, 'Structural adhesive joints in engineering', Second Edition, Chapman & Hall, United Kingdom
- Adams RD, Coppendale J & Peppiatt NA (1978)**, 'Failure analysis of aluminium - aluminium bonded joints', *Adhesion 2* edited by Allen K, Applied Science Publishers, London, United Kingdom
- Adams RD & Davies RGH (1995)**, 'Numerical modelling of the influence of temperature on the mechanical behaviour of single lap joints', *SAE IV Conference Proceedings*, Institute of Materials, Bristol, United Kingdom
- Adams RD & Peppiatt NA (1973)**, 'Effect of Poisson's ratio strains in adherends on stresses of an idealised lap joint,' *Journal of Strain Analysis*, Vol.8, No. 2
- Adams Rd & Harris JA (1987)**, 'Influence of local geometry on the strength of adhesive joints', *International Journal of Adhesion and Adhesives*, Vol.7, No.2
- Adams RD & Wake WC (1984)**, 'Structural adhesive joints in engineering', Elsevier Applied Science Publishers Ltd, United Kingdom
- Aivazzadeh S, Babi N & Verchery G (1987)**, 'Assessment and comparison of classical, mixed, and interface elements for the stress analysis in adhesive joints', *EUROMECH Colloquium 277: Mechanical Behaviour of Adhesive Joints*, Saint-Etienne, France
- Allen K (1992a)**, 'Diffusion theory of adhesion', *Handbook of Adhesion* edited by Packham DE, Longman Group Ltd, Great Britain
- Allen K (1992b)**, 'Theories of adhesion', *Handbook of Adhesion* edited by Packham DE, Longman Group Ltd, Great Britain
- Allman DJ (1977)**, 'A theory for the elastic stresses in adhesive bonded joints', *Quarterly Journal of Mechanics and Applied Maths*, Vol.30
- Anon (1985)**, 'High-strength laminates for concept and race cars', *Automotive Engineer*, October/November
- Anon (1987)**, 'Welding Handbook', 8th Edition, Vol.1: *Welding Technology*, American Welding Society, Florida, USA
- Anon (1990a)**, 'Making it with plastics', *British Plastics & Rubber*, January

Anon (1990b), 'The Ford tests car structure produced by RTM', Advanced Composite Engineering, March

Anon (1994a), 'Light-weight construction', Materials World, February/March

Anon (1994b), 'Holistic design with steel for vehicle weight reduction', AISI Report

Anon (1994c), 'Steelmakers point to weight savings with HSS alloys', Materials World, February/March

Anon (1994d), 'Processing demand for future', ULSAB brochure, British Steel Publications

Anon (1995a), 'Ultra Light Steel Auto Body Consortium', Porsche Engineering Services, Final Report, August

Anon (1995b), 'The Aluminium Car', Aluminium Extruders Association, Second Edition, January

Anon (1995c), 'The Challenge – The Response', ULSAB brochure, British Steel Publications

Anon (1995d), 'Steel Evolution', ULSAB brochure, British Steel Publications

Anon (1995e), 'The Styling – Challenge', ULSAB brochure, British Steel Publications

Anon (1996a), 'Weight loss programs helping steel to take on a new look', USCAR, URL site: <http://www.uscar.org/techno/lw-steel.htm> (19/04/2000)

Anon (1996b), 'Advanced processes aimed at needs for both steel and aluminium', USCAR, URL site: <http://www.uscar.org/techno/steel-alum.htm> (19/04/2000)

Anon (1996c), 'Carbon fibre composite structures; very light, very strong, very costly', USCAR, URL site: <http://www.uscar.org/techno/carbonfib.htm> (19/04/2000)

Anon (1996d), 'Costs must come down dramatically if composites are to compete', USCAR, URL site: <http://www.uscar.org/techno/compcost.htm> (19/04/2000)

Anon (1997), 'Ultra Light Steel Auto Body', URL site: <http://www.ulsab.org> (19/04/2000)

Anon (1998), 'Ultra Light Steel Auto Body: lower weight, lower cost', USCAR, URL site: <http://www.uscar.org/techno/ulsab2.htm> (19/04/2000)

Anon (1999), 'World steel industry forms new consortium to develop advanced automotive concepts', USCAR, URL site: <http://www.uscar.org/public/news/ulsab-avc.htm> (19/04/2000)

Anon (2000a), 'About PNGV', USCAR, URL site: <http://www.uscar.org/pngv/index.htm> (19/04/2000)

Anon (2000b) 'Ford, GM unveil partnership for a new generation of vehicle concepts', USCAR, URL site: <http://www.uscar.org/techno/unveil.htm> (19/04/2000)

Anon (2000c), 'Body structure/material alternative project', USCAR, URL site: <http://www.uscar.org/pngv/technical/body.htm> (19/04/2000)

Anon (2000d), 'Encyclopaedia Britannica', URL site: <http://www.britannica.com> (03/04/2000)

Anon (2000e), 'Aluminium: a high tech material for the automotive future', URL site: http://www.audi.com/java/models/stage/technic/alu/e_alu.html (25/05/2000)

Apalek MK, & Davies R (1993), 'Analysis and design of adhesively bonded corner joints, International Journal of Adhesion and Adhesives, Vol.13, No.4

Basu D & Ghosh KK (1993), 'Experimental validation of a generalised shell formulation by mixed finite element approach', Computers & Structures, Vol.48, No.1

Beardmore P (1988), 'Automobile materials of the future', Chemtech, Vol.18, No.10

Beer G (1985), 'An isoparametric joint/interface element for finite element analysis', International Journal for Numerical Methods in Engineering, Vol.21, No.4

Beer G (1986), 'A comparison of the boundary element and superposition methods', Computers and Structures, Vol.23, No.3

Beermann HJ (1989), 'The analysis of commercial vehicle structures', Mechanical Engineering Publications Ltd, United Kingdom

Beevers A & Kho ACP (1983), 'The performance of adhesive bonded thin-gauge sheet-metal structures with particular reference to box-section beams', International Journal of Adhesion and Adhesives, January

Beevers A & Kho ACP (1984), 'The performance of adhesive bonded thin-gauge sheet-metal structures with particular reference to box-section beams', Adhesive Joints edited by Mittal KC, Plenum Press, New York, USA

Bigwood DA and Crocombe AD (1989), 'Elastic analysis and engineering design formulae for bonded joints', International Journal of Adhesion and Adhesives, Vol.9, No.4

Bigwood DA & Crocombe AD (1990), 'Non-linear adhesive bonded joint design analyses', International Journal of Adhesion and Adhesives, Vol.10, No.1

Birch S (1999), 'A2 arrives in aluminium', SAE Automotive Engineering International, November

Chatfield C (1992), 'Statistics', Handbook of Adhesion edited by Packham DE, Longman Group Ltd, Great Britain

- Chen D & Cheng S (1983)**, 'An analysis of adhesive-bonded single lap joints', Mechanical Engineering, Vol.105, No.7
- Chiu WK & Jones R (1992)**, 'A numerical study of adhesively bonded lap joints', International Journal of Adhesion and Adhesives, Vol. 12, No.4
- Clark JD & McGregor IJ (1993)**, 'Ultimate tensile stress over a zone: a new failure criterion for adhesive joints', Journal of Adhesion, Vol. 42
- Cofer WF & Will KM (1991)**, 'A 3-dimensional, shell-solid transition element for general non-linear analysis', Computers & Structures, Vol.38, No.4
- Cofer WF & Will KM (1992)**, 'A finite element technique for the ultimate strength analysis of tubular joints', Engineering Computations, Vol.9
- Cole GS & Sherman AM (1995)**, 'Lightweight materials for automotive applications', Materials Characterization, Vol. 35, No.1
- Comyn J (1992)**, 'Compatibility', Handbook of Adhesion edited by Packham DE, Longman Group Limited, Great Britain
- Cooper PA & Sawyer JW (1979)**, 'Critical examination of stresses in an elastic single lap joint', NASA Technical Paper No. 1507, USA
- Cotton B (1998)**, 'X300 98MY front bulk head torsional tests', Jaguar Technical Report - JA1A100901
- Crocombe AD (1989)**, 'Global yielding as a failure criterion for bonded joints', International Journal of Adhesion and Adhesives, Vol.9, No.3
- Crocombe AD & Adams RD (1981)**, 'Peel analysis using the finite element method', Journal of Adhesion, Vol.12, No.2
- Crocombe AD & Moulton AC (1988)**, 'The effect of the adhesive thickness on the strength of a bonded joint', Adhesion 12 edited by Allen K, Elsevier Applied Science, United Kingdom
- Crookes MJ & Miner RE (1996)**, 'The Ultra Light Steel Auto Body program completes phase I', Journal of Materials, Vol. 48, No.7
- Demarkles LR (1955)**, 'Investigation of the use of a rubber analog in the study of stress distribution in riveted and cemented joints', Technical Note 3413, Nat. Advisory Cttee Aeronautics, Washington D.C., USA
- Dickson JN, Hsu TM & McKinney JM (1972)**, 'Development of an understanding of the fatigue phenomena of bonded and bolted joints in advanced filamentary, composite materials', Volume 1 - Analysis methods, Technical Report AFFDL No. TR-72-64

Dieffenbach JR (1996), 'Body-in-white materials', JOM-Journal of the Minerals & Materials Society, Vol.48, No.4

Dieffenbach JR (1997), 'Challenging today's stamped steel unibody: assessing prospects for steel, aluminium and polymer composites', IBEC '97 Advanced Body Concept & Development, SAE Conference, Detroit, USA

Drake R (1997), 'Structural adhesive technology: two decades of enduring progress', Adhesives Age, Vol.40, No.13

Drewes EJ, Engl B & Tenhaven U (1994), 'Potential for lightweight car-body construction using steel', Technische Mittellungen Krupp, Vol.1

Eichhorn F & Schmitz BH (1984), 'Comparative testing of standardized spot-welded hollow sections of sheet steel with and without additional bonding of the groove', Schweißen und Schneiden, Vol.36, Institute of Welding Techniques, Aachen, Germany

Elinck JP, Halleux P & Winand A (1987), 'The behaviour of bolted and adhesive bonded joints in structural steelwork', EUROMECH Colloquium 277: Mechanical Behaviour of Adhesive Joints, Saint-Etienne (France)

Fenton J (1998), 'Handbook of automotive body construction and design analysis', Professional Engineering Publishing Ltd., Great Britain

Fernlund G, Chaaya R & Spelt JK (1995), 'Mode I fracture load predictions of adhesive T-joints', Journal of Adhesion, Vol.50

Findlater D (1987), 'A design approach for adhesively bonded joints', EUROMECH Colloquium 277: Mechanical Behaviour of Adhesive Joints, Saint-Etienne (France)

Frielink RJ (1997), 'New solutions for lightweight bodies', IBEC '97 Advanced Body Concept & Development, SAE Conference, Detroit, USA

Froes FH (1994), 'Advanced metals for aerospace and automotive use', Materials Science and Engineering - AA184

Garg A (1995), '2-D finite element analysis of engineering components', ASME Symposium

Gilchrist MD (1993), 'Fatigue growth of cohesive defects in t-peel joints', Journal of Adhesion, Vol. 42, 1993

Gilchrist MD & Smith RA (1993), 'Development of cohesive fatigue cracks in T-Peel joints', International Journal of Adhesion and Adhesives, Vol.13, No.1

Gmür TC & Schorderet AM (1993), 'A set of three dimensional solid to shell transition elements for structural dynamics', Computers & Structures, Vol.46, No.4

Goland M & Reissner E (1944), 'The stresses in cemented joints', Journal of Applied Mechanics, Tran. ASME, Vol. 66, A17

Grant L (1994), 'The characteristics of adhesive joints found typically in the automotive industry', PhD Thesis at Bristol University, April

Grant P & Taig IC (1976), 'Strength and stress analysis of bonded joints', BAC Report No. 109, SOR(P)

Gugisch K (1993), 'The manufacturing technology of the Audi aluminium body', Auditorium, Aluminium-Technologie im Karosseriebau, Germany

Gumpinger J, Hahn O, Horte M, Kudrnac P, Singh S & Unger B (1997), 'Computer simulated estimation of the fatigue behaviour and stiffness of spot joints in automotive structures', IBEC '97 Advanced Body Concept & Development, SAE Conference, Detroit, USA

Hadavinia H, Steidler S, Durodola J & Beevers A (1998), 'Stiffness sensitivity of adhesive bonded coach joints in automotive structures', SAE V - International Conference, Institute of Materials, Bristol, United Kingdom

Hamn L (1997), 'The body of the new Porsche 911', IBEC '97 Advanced Body Concept & Development, SAE Conference, Detroit, USA

Han HN & Clark JP (1995), 'Lifetime costing of the body-in white: steel vs. aluminium', JOM - Journal of the Minerals, Metals and Materials Society, Vol.47, No.5

Harpham I (1999), 'Comparison of weld bonding analysis methods in a full size car', Hawtal Whiting Report HWT5796 - Executive Summary

Harris JA & Adams RD (1984), 'Strength prediction of bonded single lap joints by non-linear element method', International Journal of Adhesion and Adhesives, Vol.4, No.2

Hart-Smith LJ (1973), 'Adhesive bonded single lap joints', NASA Technical Report CR-112236, Langley Research Centre, Virginia

Hart-Smith LJ (1981), 'Further developments in the design and analysis of adhesive bonded structural joints, ASTM Special Technical Publication, Minneapolis, USA

Hart-Smith LJ (1985), 'Designing to minimise peel stresses in adhesive bonded joints', ASTM Special Technical Publication, California, USA

Hart-Smith LJ (1994), 'The key to designing durable adhesively bonded joints', Composites, Vo.25, No.9

Hildebrand M (1994a), 'Non-linear analysis and optimisation of adhesively bonded single lap joints between fibre-reinforced plastics and metals', International Journal of Adhesion and Adhesives, Vol.14, No.4

Hildebrand M (1994b), 'The strength of adhesive-bonded joints between fibre-reinforced plastics and metals', VTT Publications, Finland

Hinopoulos G & Broughton WR (1999), 'Evaluation of the T-peel joint using the finite element method', NPL Report CMMT(A) 207

Hunter JA & Wiseman CR (1998), 'The application of adhesive bonding to the repair of aluminium automotive structures', International Conference of Joints in Aluminium (INALCO), TWI, Cambridge, United Kingdom

Hunter JA, Nardini D, Gao Y & Ricks RA (1998), 'Design and production of adhesively bonded aluminium automotive structures', ISATA 31, Düsseldorf, Germany

Hutchinson AR (1996), 'Principles of adhesive bonding for engineers', Mechanical Engineer's Reference Book, 12th edition, Butterworth-Heinemann

Ikegami K & Sugibayashi T (1986), 'Adhesive bonded joints of metals', Adhesives in Japan, DTI Report, December

Irving B (1995), 'Building tomorrows automobiles', Welding Journal, Vol.74, No.8

Jeandrau JP (1987), 'Analysis and design of adhesive-bonded structural joints: new tools for engineers', EUROMECH Colloquium 277: Mechanical Behaviour of Adhesive Joints, Saint-Etienne (France)

Jeandrau JP (1991), 'Analysis and design data for adhesively bonded joints', International Journal of Adhesion and Adhesives, Vol. 11, No. 2

Jiang W, Bao G & Roberts JC (1997), 'Finite element modelling of stiffened and unstiffened orthotropic plates', Computers & Structures, Vol.63, No.1

Jindal UC (1983), 'Adhesives and stress distribution of a plate with reinforced hole', Adhesives Age, Vol.26, No.8

Kewley D, Campell IG & Wheatley JE (1987), 'Manufacturing feasibility of adhesively bonded aluminium for volume car production', SAE Technical Paper Series - 870150, USA

Kho ACP (1983), 'The performance of adhesive bonded thin gauge sheet metal structures with particular reference to box-section beams', MPhil Thesis, Oxford Polytechnic, May

Kim YY, Yim HJ, Kang JH & Kim JH (1995), 'Reconsideration of the joint modelling technique: in a box-beam T-joint', SAE Technical Paper Series - 951108, USA

Kinloch AJ (1986), 'Structural adhesives', Elsevier Applied Science Publishers, United Kingdom

Kochan A (1996), 'Lotus: aluminium extrusions and adhesives', Assembly Automation, Vol. 16, No. 4

Kochan A (1997), 'ISATA highlights trends in automotive assembly techniques', Assembly Automotion, Vol.17, No.4

Koehr R (1997), 'Ultra Light Steel Auto Body: from concept to hardware', IBEC '97 Advanced Body Concept & Development, SAE Conference, Detroit, USA

Kornmann M, Genet M & Anderson E (1987), 'Durability testing of adhesives for automotive application', EUROMECH Colloquium 277: Mechanical Behaviour of Adhesive Joints, Saint-Etienne (France)

Krenk S, Jonsson J & Hansen LP (1996), 'Fatigue analysis and testing of adhesive joints', Engineering Fracture Mechanics, Vol. 53, No.6

Kurihara Y (1995), 'Vehicle weight reduction obtained with lightweight materials', JSME International, Series A, Vol. 38, No.4

Lancaster J (1992), 'Handbook of structural welding', Abington Publishing, Great Britain

Lang TP & Mallick PK (1998), 'Effect of spew geometry on stresses in single lap adhesive joints', International Journal of Adhesion and Adhesives, Vol. 18, No.3

Lang TP & Mallick PK (1999), 'The effect of recessing on the stresses in adhesively bonded single-lap joints', International Journal of Adhesion and Adhesives, Vol. 19, No.4

Langerak NAJ (1997), 'The use of steel and aluminium in the next generation auto bodies', IBEC '97 Advanced Body Concept & Development, SAE Conference, Detroit, USA

Lee YW, Kwon YW, Kwon SY & Cho WS (1997), 'A study on the improvement of the structural joint stiffness for aluminium BIW', Society of Automotive Engineers Inc., SAE Special Publications – 970583, USA

Lees WA (1984), 'Adhesives in engineering design', The Design Council, Bath (UK)

Li W, Blunt L & Stout HJ (1997), 'Analysis and design of adhesive-bonded tee joints', International Journal of Adhesion and Adhesives, Vol.17, No.4

Liniecki A, Hsu TR & Li W (1995), 'Fatigue strength of adhesive bonded aluminium joints', Journal of Testing and Evaluation, Vol.23, No.6

Liu SC & Hu SJ (1995), 'An offset finite element model and its applications in predicting sheet metal assembly variation', International Journal of Machine Tools Manufacturing, Vol.35, No.11

Lowe K (1994), 'How steel is responding to the new materials challenge', Materials World, November

Lowe K (1997), 'Slimline cars are more healthy', Materials World, Vol.5, No.5

Lucas W (1990), 'TIG and plasma welding', Woodhead Publishing, Cambridge, United Kingdom

- Lucas W (1995)**, 'Design and manufacture of components for lightweight vehicles', DTI Report No. 88253, TWI, Cambridge, United Kingdom
- Mallick V (1989)**, 'Stress analysis of metal/CFRP adhesive joint subject to the effects of thermal stress', PhD Thesis, University of Bristol
- Marwick WF & Sheasby OG (1987)**, 'Evaluation of adhesives for aluminium structured vehicles', SAE Technical Paper Series - 870151, USA
- Matthews AE & Davies GM (1997)**, 'Precoated steel development for the automotive industry', Proceedings of the Institution of Mechanical Engineers, Vol.211, Part D
- McGregor IJ, Seeds AD & Nardini D (1990)**, 'The design of impact absorbing members for aluminium structured vehicles', SAE Technical Paper Series - 900796, USA
- McGregor IJ, Nardini D, Gao Y & Meadows DJ (1992)**, 'The development of a joint design approach for aluminium automotive structures', SAE Technical Paper Series - 922112, USA
- McGregor IJ, Nardini D, Gao Y & Meadows DJ (1993)**, 'A joint-design approach for aluminium structures', Automotive Engineering, August
- McGregor IJ, Gao Y, Sheasby OG & Wilson I (1994)**, 'Weld-bonding: a joining technology for aluminium structured vehicles', IBEC '94 Automotive Body Materials, SAE Conference, Detroit, USA
- Messler RW (1993)**, 'Joining of advanced materials', Butterworth-Heinemann, USA
- Nardini D & Hall RW (1995)**, 'Analysis of joints for stiffness, strength and fatigue in vehicle structures using a specially developed FE software', ISATA '95, Paper Series - 95ME053
- Nardini D, McGregor IJ, Seeds AD (1990)**, 'Analysis and testing of adhesively bonded aluminium structural components', SAE Technical Paper Series - 900795, USA
- Norrish J (1992)**, 'Advanced welding processes', Institute of Physics Publishing, Bristol, United Kingdom
- Ojalvo IU & Eidinoff HL (1978)**, 'Bond thickness effects upon stresses in single-lap adhesive joints', AIAA Journal, Vol. 16, No.3
- Olia M & Rossettos JN (1996)**, 'Analysis of adhesively bonded joints with gaps subjected to bending', International Journal of Solids Structures, Vol.33, No.18
- Oplinger DW (1994)**, 'Effects of adherend deflections in single lap joints', International Journal of Solids Structures, Vol.31, No.18
- Ostermann F et al. (1993)**, 'Aluminium materials technology for automobile construction', Mechanical Engineering Publication Ltd, United Kingdom

- Pearson IT (1993)**, 'Adhesive bonding of vehicle structures', MSc Thesis, University of Warwick, January
- Pennington JN (1998)**, 'Extruded frame stiffens prototype sports car', *Modern Metals*, January
- Peterson PT (1997)**, 'Holistic design as a tool for environmental improvement – the ULSAB example', ENCOSTEEL for Sustainable Development, Sweden, June
- Pine T, Lee MMK & Jones TB (1998)**, 'Factors affecting torsional properties of box sections', *Ironmaking and Steelmaking*, Vol.25, No.3
- Pine T, Lee MMK & Jones TB (1999)**, 'Weight reduction in automotive structures – an experimental study on torsional stiffness of box sections', *Proceedings of the Institution of Mechanical Engineers*, Vol.213, Part D
- Pinefold M & Chapman C (1999)**, 'The application of knowledge based engineering techniques to the finite element mesh generation of an automotive body-in-white structure', *Journal of Engineering Design*, Vol.10, No.4
- Powell JH (1994)**, 'Structural bonding of aluminium in automotive applications', *Vide-Science Technique et Applications*, No.272 (SS)
- Renton WJ & Vinson JR (1975)**, 'Efficient design of adhesively bonded joints', *Journal of Adhesion*, Vol.7, No.3
- Richardson G, Crocombe AD & Smith PA (1993)**, 'A comparison of two- and three-dimensional finite element analyses of adhesive joints', *International Journal of Adhesion and Adhesives*, Vol.13, No.3
- Robinson A (1993)**, 'The repair of vehicle bodies', 3rd edition, Butterworth-Heinemann Ltd., Great Britain
- Sakurai T & Kamada Y (1988)**, 'Structural stiffness of automotive body', Society of Automotive Engineers Inc., SAE Technical Paper - 880550
- Sancaktar E (1987)**, 'Elastoplastic fracture behaviour of structural adhesives', *EUROMECH Colloquium 277: Mechanical Behaviour of Adhesive Joints*, Saint-Etienne, France
- Saunders FI & Wagoner RH (1996)**, 'Forming of tailored-welded blanks', *Metallurgical and Materials Transactions A - Physics Metallurgy and Materials Science*, Vol.27, No.9
- Seal MR, Kutz J & Corriveau G (1981)**, 'Development of an advanced composite monocoque chassis for a limited production sports car', SAE, Vehicle Research Institute Western Washington University (SAE)
- Seeds A, Nardini D & Cassese F (1989)**, 'The development of a centre cell structure in bonded aluminium for the Ferrari 408 research vehicle', SAE Technical Paper Series - 890717, USA

- Selwood PG, Law FJ, Sheasby PG & Wheeler MJ (1987)**, 'The evaluation of an adhesively bonded structure in an Austin-Rover Metro vehicle', SAE Technical Paper Series - 870149, USA
- Semerdjiev S (1970)**, 'Metal to metal adhesive bonding', Business Books Limited, Great Britain
- Sheppard A, Kelly D & Tong LY (1998)**, 'A damage zone model for the failure analysis of adhesively bonded joints', International Journal of Adhesion and Adhesives, Vol.18, No.6
- Sharman PW & Al-Hammoud A (1987)**, 'The effect of local details on the stiffness of car body joints', International Journal of Vehicle Design, Vol.8, No.4/5/6
- Sigman DR, Buechel JH & Ervin PR (1983)**, 'Evaluation of the Ford GrFRP lightweight car', International Journal of Vehicle Design, Vol.4, No.6
- Simon JG (1988)**, 'Directions in automotive materials', Advanced Materials & Processes, Vol.133, No.1
- Sneddon IN (1961)**, 'The distribution of stress in adhesive joints', Adhesion edited by Eley DD, Oxford
- Steidler S, Hadavinia H, Durodola J & Beevers A (1997)**, 'Stiffness characteristics of adhesive joints in vehicle body structures: a comparison between FE models and experimental measurements', EUROMECH Colloquium 358: Mechanical Behaviour of Joints, Nevers, France
- Steidler S, Durodola J & Beevers A (1998)**, 'Modelling of adhesive bonded joints', Automotive Seminar: Design and Manufacture of Lightweight Steel Vehicles, TWI, Cambridge, United Kingdom
- Steidler S, Durodola J & Beevers A (1999)**, 'Modelling of adhesive bonded joints in vehicle structures', International Journal of Materials & Product Technology, Vol.14, No.5-6, Inderscience Enterprises Limited, Great Britain
- Stuart TP & Crouch IG (1992)**, 'The design, testing and evaluation of adhesively bonded, interlocking, tapered joints between thick aluminium alloy plates', International Journal of Adhesion and Adhesives, Vol. 12, No.1
- Surana KS (1986)**, 'A generalised geometrically nonlinear formulation with large rotations for finite elements with rotational degrees of freedom', Computers & Structures, Vol.24, No.1
- Surana KS (1980a)**, 'Transition finite elements for axisymmetric stress analysis', International Journal for Numerical Methods in Engineering, Vol.15
- Surana KS (1980b)**, 'Transition finite elements for three-dimensional stress analysis', International Journal for Numerical Methods in Engineering, Vol.15

- Tong, L, Sheppard A & Kelly D (1996)**, 'The effect of adherend alignment on the behaviour of adhesively bonded double lap joints', *International Journal of Adhesion and Adhesives*, Vol. 16, No.4
- Tsai MY & Morton J (1994a)**, 'Three-dimensional deformations in a single lap joint', *Journal of Strain Analysis*, Vol.29, No.1
- Tsai MY & Morton J (1994b)**, 'A note on peel stresses in single-lap adhesive joints', *Journal of Applied Mechanics, Transactions of ASME*, Vol. 61, No.3
- Tsai MY, Morton J & Matthews FL (1995)**, 'Experimental and numerical studies of a laminated composite single-lap adhesive joint', *Journal of Composite Materials*, Vol.29, No.9
- Turner MJ, Clough RW, Martin HC & Topp LJ (1956)**, 'Stiffness and deflection analysis of complex structures', *Journal of Aero. Science*, Vol.23
- Van Schaik MAM (1997)**, 'The Ultra Light Steel Auto Body – marketing tool for steel', *Steel Times*, April
- Valente F, Li X, Messina A, Properzi M & Menin R (1998)**, 'A new methodology for improving accuracy of structural analysis of car body parts', *IBEC' 98, SAE Conference*, Detroit, USA, September
- Volkersen O (1938)**, 'Rivet strength distribution in tensile-stressed rivet joints with constant cross section', *Luftfahrtforschung*, 5
- Wang SS, Mandell JF, Christensen TH & McGarry FJ (1976)**, 'Analysis of lap shear adhesive joints with and without short edge cracks', *Massachusetts Institute of Technology Research Report R76-2*
- Wang PC & Ewing W (1991)**, 'Fracture mechanics analysis of fatigue resistance of spot welded coach – peel joints', *Fatigue Fracture Material Structures*, Vol. 14, No.9
- Wang CH & Rose LRF (1997)**, 'Determination of triaxial stresses in bonded joints', *International Journal of Adhesion and Adhesives*, Vol. 17, No.1
- Wang CH & Rose LRF (2000)**, 'Compact solutions for the corner singularity in bonded lap joints', *International Journal of Adhesion and Adhesives*, Vol. 20, No.2
- Warren AS, Wheatley JE, Marwick WF & Meadows DJ (1989)**, 'The building and test-track evaluation of an aluminium structured Bertone X1/9 replica vehicle', *SAE Technical Paper Series - 890718, USA*
- Watson C (1992a)**, 'Advantages of use of adhesives: specific examples of improved design', *Handbook of Adhesion* edited by Packham DE, Longman Group Ltd, Great Britain
- Watson C (1992b)**, 'Industrial applications of adhesives', *Handbook of Adhesion* edited by Packham DE, Longman Group Ltd, Great Britain

Watts JF (1992), 'Primary bonding at the interface', Handbook of Adhesion edited by Packham DE, Longman Group Ltd, Great Britain

Wells P & Rawlinson M (1997), 'ULSAB – a critical appraisal', IBEC '97 Advanced Body Concept & Development, Detroit, USA

Wheeler MJ (1997), 'Trip the light aluminium', Materials World, Vol.5, No.6

Wheeler MJ, Sheasby PG & Kewley (1987), 'Aluminium structured vehicle technology – a comprehensive approach to vehicle design and manufacturing in aluminium', SAE Technical Paper Series - 870146, USA

Wooley GR & Carver DR (1971), 'Stress concentration factors for bonded joints', Journal of Aircraft, Vol.8, No.10

Wu G & Crocombe AD (1996), 'Simplified finite element modelling of structural adhesive joints', Computers & Structures, Vol.61, No.2

Zhao X (1991), 'Stress and failure analysis of adhesively bonded joints', PhD Thesis, University of Bristol

Zienkiewicz OC (1971), 'The finite element method in engineering science', McGraw Hill, New York, USA

APPENDIX I

DESIGN GUIDELINES FOR APPLICATION OF THE UNDERCUT ELEMENT METHOD IN FE MODELLING OF ADHESIVE JOINTS IN CAR BODY STRUCTURES

DESIGN GUIDELINE FOR APPLICATION OF THE UNDERCUT ELEMENT METHOD IN FE MODELLING OF ADHESIVE JOINTS IN CAR BODY STRUCTURES

1. Introduction

The modelling of body shells for the prediction of stiffness characteristics essentially involves approximations of some structural details, particularly relating to the joints. Generally, numerical modelling approaches are based on shell elements and various assumptions are made to accommodate joint characteristics. More detailed analysis of joints has shown that these approximations can introduce inaccuracies in prediction of stiffness in adhesive bonded structures. For example in modelling a plenum chamber substructure the predicted torsional stiffness is 16% higher than experimental measurement. A semi-empirical approach has been developed to compensate for these errors.

This guideline defines procedures for the inclusion of an undercut element detail to give more accurate representation of adhesive joints in FE models.

2. Schematic Representations of Coach Joints

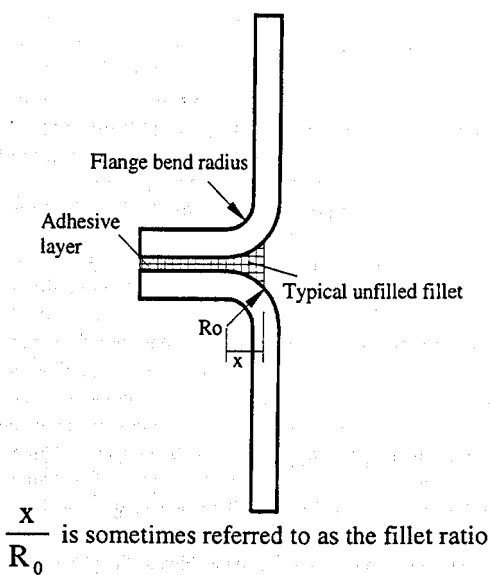


Figure 1a. Actual joint configuration

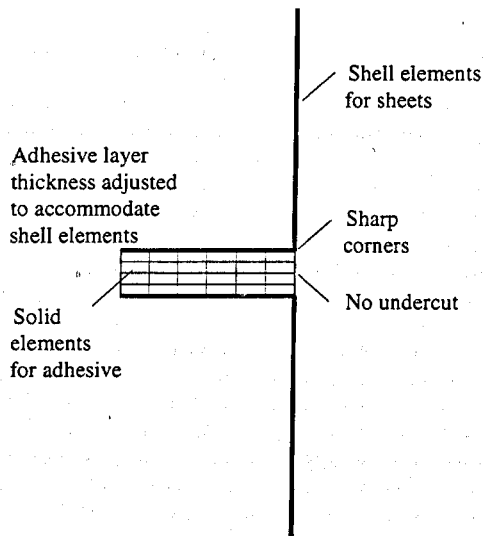


Figure 1b. Simple FE model representation

3. Inaccuracies in Simple Models

- The bondline thickness with the shell element model is greater than in practice, as the shell elements are modelled to act on the centre line of the panel. The adhesive layer is therefore increased by the average of the sheet thicknesses. This geometric difference may be compensated for by increasing the adhesive modulus in the same proportion as the change in thickness.
- The adhesive is assumed to fill the entire flange area in the shell element model. In practice the adhesive does not extend to the edge of the flange.
- The simple shell element model assumes a 90° corner at the flange edge. In practice there is a flange bend radius typically of 5mm internal radius on most flanges.

4. The Undercut Element Correction

The undercut element method is applicable to shell element models in which the adhesive bondline is represented by solid elements. The correction to the adhesive modulus to compensate for the thicker bondline is still applied. The undercut dimension δ , shown in figure 2, is selected to compensate both for the partially filled joint AND the flange bend radius.

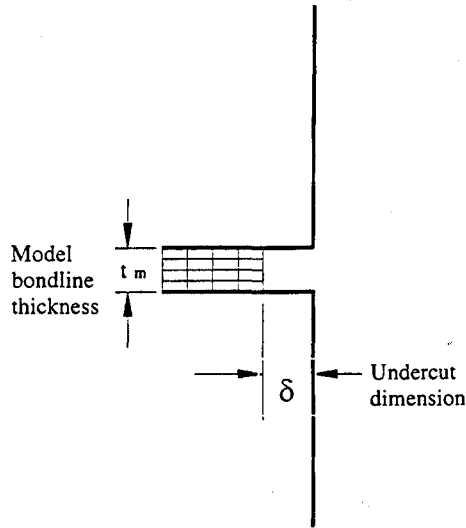


Figure 2. Undercut element configuration

The important parameters to be included in the modified model are as follows:

- bondline thickness
- adhesive modulus
- undercut dimension

4.1 Calculation of Bondline Thickness for Model (t_m)

$$t_m = (t_s) + \frac{1}{2} (t_1 + t_2)$$

Where t_s is the separation distance of the sheets, and t_1 , t_2 are the upper and lower sheet thicknesses, respectively, as defined in the CAD model.

Note: the separation distance in the CAD model should ideally match the adhesive bondline thickness used in manufacture. If the adhesive thickness has not been included in the CAD model, i.e. $t_s = 0$, some inaccuracy may arise.

4.2 Calculation of Adhesive Modulus for Model (E_m)

$$E_m = (E_a) \times \frac{t_m}{t_a}$$

Where E_a and t_a are the actual adhesive modulus and adhesive thickness in manufacture.

4.3 Calculation of Undercut Dimension

In principle the dimension of the undercut in the model should reflect the actual fillet ratio in the joint. As this is rather indeterminate, it is advisable to base the model on a 'worst-case' condition of a zero fillet ratio in which the undercut distance is equal to the flange bend radius. Thus for a simple approximation, $\delta = R_o$.

5. Validation

The application of this undercut element correction has been tested on various joint configurations, modes of loading and structural details, and results have been compared with experimental tests and more refined solid-element models. In all cases the undercut element correction gives a more accurate prediction of stiffness than the simple shell-element model.

6. Refinements to Undercut Element Method

Typical flange dimensions for coach joints in car bodies are 15mm flange width and 5mm bend radius. A 5mm undercut in the shell-solid model provides an acceptable conservative approximation of the joint characteristic assuming a 0% fillet ratio. If the design is to be based on the provision of an adhesive fillet, a more accurate undercut dimension can be derived from graphs such as figure 3, which has been determined from coach joint analyses.

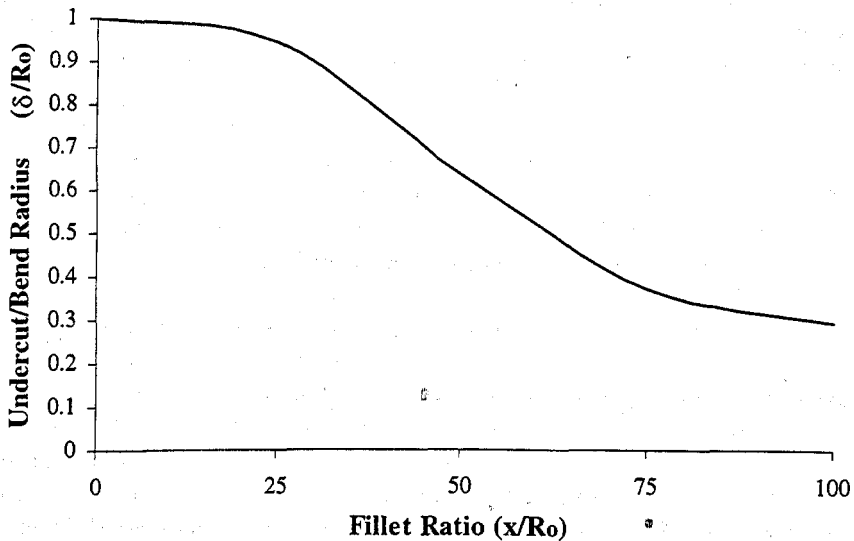


Figure 3. Determination of undercut for different fillet ratios

An exact geometric representation translation from the radiused sheet to a sharp-cornered model may introduce an uncertainty in interpretation in some configurations. However, the illustrations in figure 4 provide a guideline for including undercut dimensions in different joint geometries. The shell elements represent the mid-planes of the sheets. It should be noted that the coach joint is the most sensitive configuration to the undercut element correction.

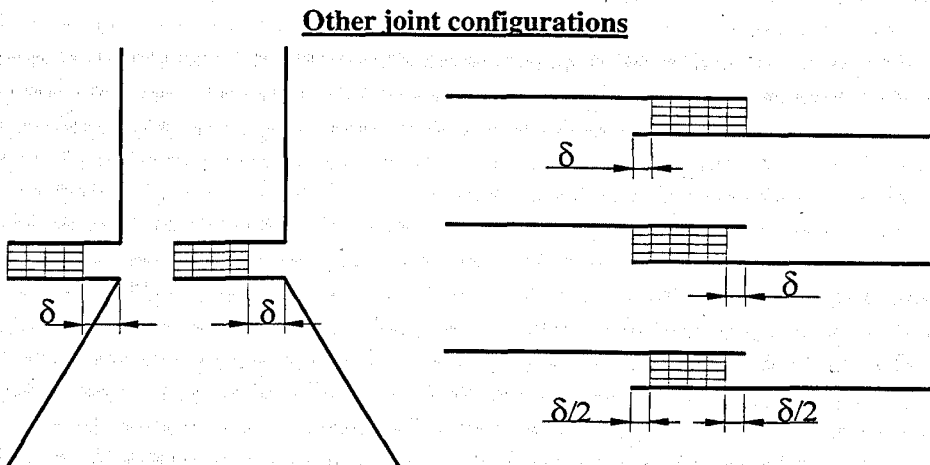


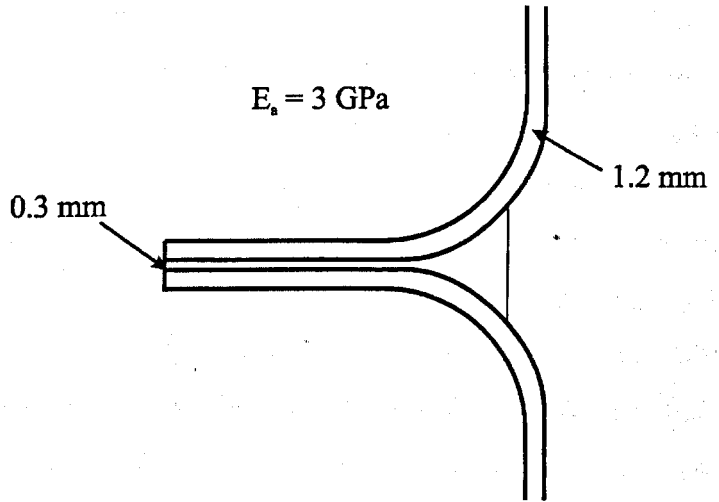
Figure 4. Application of undercut to different joint configurations

7. Undercut Application Examples

7.1 Coach Joint

Joint Definition

Flange 15mm long
Bend radius 5mm
Upper sheet thickness 1.2 mm
Lower sheet thickness 1.2 mm
Adhesive thickness 0.3mm
Adhesive modulus 3 GPa
Fillet ratio = 50 %



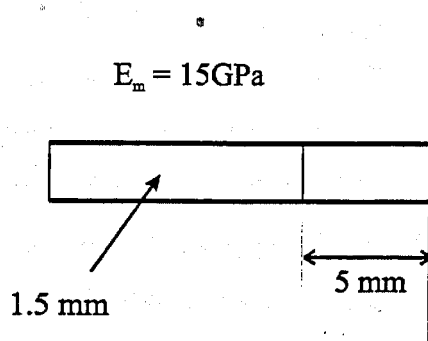
Modelling of Joint

From section 4.1, the bondline thickness t_m is given by,

$$\begin{aligned} t_m &= \text{CAD model separation distance } (t_s) + \frac{1}{2} (\text{upper sheet thickness} + \text{lower sheet thickness}) \\ &= 0.3 + \frac{1}{2} (1.2 + 1.2) \\ &= 1.5 \text{ mm} \end{aligned}$$

And the adhesive modulus by,

$$\begin{aligned} E_m &= \text{Actual adhesive modulus } (E_a) \times \frac{t_m}{t_a} \\ &= 3 \times \frac{1.5}{0.3} \\ &= 15 \text{ GPa} \end{aligned}$$



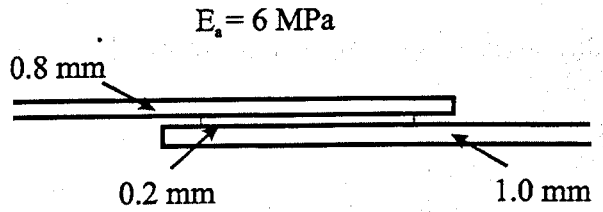
The appropriate undercut for this joint can be found from figure 3 which gives a value of approximately 3.5mm. In the model it is convenient to use a 5mm undercut as this models a 0% fillet ratio which allows for variations in the fillet ratio achieved in manufacture.

Undercut applied – 5mm

7.2 Single Lap Joint

Joint Definition

Overlap Length 15 mm
Upper sheet thickness 0.8 mm
Lower sheet thickness 1.0 mm
Adhesive thickness 0.2 mm
Adhesive modulus 0.006 GPa
2 mm unfilled from each edge



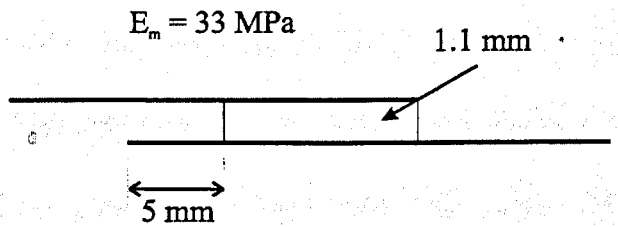
Modelling of Joint

From section 4.1, the bondline thickness t_m is given by,

$$\begin{aligned} t_m &= \text{CAD model separation distance } (t_s) + \frac{1}{2} (\text{upper sheet thickness} + \text{lower sheet thickness}) \\ &= 0.2 + \frac{1}{2} (0.8 + 1.0) \\ &= 1.1 \text{ mm} \end{aligned}$$

And the adhesive modulus by,

$$\begin{aligned} E_m &= \text{Actual adhesive modulus } (E_a) \times \frac{t_m}{t_a} \\ &= 0.006 \times \frac{1.1}{0.2} \\ &= 0.033 \text{ GPa} \end{aligned}$$



As lap joint stiffness is relatively insensitive to undercut it is convenient to use the undercut values as used in the coach joint. In this case a 5 mm undercut from one edge gives conservative design.

Undercut applied – 5 mm from one edge